Universidade de Aveiro Departamento de Geociências
2009

Leonardo Azevedo Guerra Raposo Pereira

Atributos Sísmicos na Caracterização de Reservatórios de Hidrocarbonetos

Seismic Attributes in Hydrocarbon Reservoirs Characterization

Universidade de Aveiro Departamento de Geociências
2009

Leonardo Azevedo Guerra Raposo Pereira

Atributos Sísmicos na Caracterização de Reservatórios de Hidrocarbonetos

Seismic Attributes in Hydrocarbon Reservoirs Characterization

Dissertação apresentada à Universidade de Aveiro para cumprimento dos requisitos necessários à obtenção do grau de Mestre em Engenharia Geológica, realizada sob a orientação científica do Prof. Doutor Luís Menezes Pinheiro, Professor Associado do Departamento de Geociências da Universidade de Aveiro. Este trabalho incluiu um estágio na empresa *Schlumberger* sob orientação do Dr. Hamid Abbassi, geólogo sénior.

o júri

presidente

Prof. Dra. Beatriz Valle Aguado
Professora Auxiliar do Departamento de Geociências da Universidade de Aveiro

Dr. António Kaschaka
Geólogo Sénior da *Schlumberger*

Prof. Dr. Luís Filipe Fuentefria Menezes Pinheiro
Professor Associado do Departamento de Geociências da Universidade de Aveiro

agradecimentos

Este trabalho representa o fim de mais uma etapa. É a concretização de um desejo e o apoio incondicional dos meus pais. É o exemplo e os conselhos do meu irmão. Obrigado!

Um obrigado especial à Adriana pela sua infinita paciência e compreensão, mesmo em momentos em que a razão parecia não existir.

Um verdadeiro obrigado ao Prof. Luís Menezes Pinheiro pela sua orientação científica durante a preparação desta tese e pelas ideias que propôs para o enriquecimento deste trabalho. Este obrigado incluí também a enorme paciência demonstrada na correcção do meu inglês e a sua sempre disponibilidade para ajudar. A minha gratidão incluí ainda o último ano e meio, durante o qual me introduziu ao "misterioso" mundo da ciência, à geologia marinha e ao método sísmico, assim como toda a confiança depositada em mim e todas as oportunidades que cria de maneira a corresponder aos meus desejos futuros.

Uma palavra de agradecimento muito especial ao Dr. António Kaschaka que me possibilitou um fantástico estágio na Schlumberger, em Paris. Sem ele esta tese não existiria desta forma. Um gigante obrigado a todos os "colegas" da *Schlumberger Information Solutions* com quem tive o privilégio de partilhar quatro meses de uma experiência indescritível. Aos meus supervisores na empresa, Hamid Abbassi e Andreia Mandiuc, e a todos os outros colegas que aos poucos se foram tornando amigos tendo me apoiado e ajudado em diversas ocasiões e por diversas razões: Míchel Remy, Caroline Martinez, Marianne Lenormand Berthome, Ludovic Guenoux, Julie Latoille, Lauriane Petit, Estella Pimenta, François Avril, Anna Bui Xuan Hy, Stephane Martine e Isabelle Jacquemin. A este grupo juntam-se ainda todos os colegas que nunca me deixaram almoçar sozinho e aqueles que me proporcionaram grandes momentos de futebol.

Existe um grupo de pessoas muito especiais que todos os dias me ajuda a crescer. Os amigos do LGGM/DGEO a quem gostaria de deixar um obrigado cheio de carinho. À madrinha Catarina pelo seu apoio como amiga e colega de trabalho, e às suas sempre justas chamadas de atenção que me tornam numa pessoa melhor e ajudam a evitar erros futuros; Ao Ro pela sua maturidade e conselhos em tantos momentos difíceis. As suas respostas são as certas no momento certo!; à Daniela por termos atravessado esta etapa juntos sempre com um sorriso nos lábios, construindo alicerces mútuos para que o trabalho fosse bem concluído; To Mr. Kamran the seismic processing expert; ao Francisco e ao Vitor, por serem um exemplo para jovens investigadores; à Sandra; ao Tiago; à Diana e à boa disposição da Ana M.. Um obrigado ainda às companheiras de "gabinete" Ana Antunes e Martha que não sendo parte oficial da equipa são como se fossem.

agradecimentos

Aos amigos que transformaram uma dura caminhada em passeio, OBRIGADO! Não querendo destacar ninguém, porque cada um deve tirar o seu próprio crédito, agradeço: aos MECs pela partilha das primeiras experiências; aos que pertencem à melhor colheita, que pela união fizemos a força; ao MAL e às perdas de tinta nas respectivas canetas; aos que nunca deixaram o 2º ano, e que me ensinaram a jogar PES; e aos que a altas horas nocturnas trocam abraços e lições de vida.

Obrigado “à galera” do surf por me terem levado, ensinado e pelas boas vibrações que vou trazendo comigo.

O Departamento de Geociências da Universidade de Aveiro é sem dúvida um local especial. Este prazer de estar por aqui só existe porque há pessoas que trabalham e se esforçam todos os dias para dele fazerem o melhor! Um obrigado especial à D. Paula, à D. Graça e ao Sr. Graça por toda a ajuda que sempre me deram ao longo deste cinco anos.

Um último agradecimento para todos aqueles que não tendo sido referidos, se foram cruzando comigo nestes curtos cinco anos e me ajudaram a ser aquilo que hoje sou.

palavras-chave

Atributos Sísmicos, Sísmica 3D, Caracterização de Reservatórios de Hidrocarbonetos, Sistemas de Canais, *Deep-offshore*, *Petrel* 2008.1.

Resumo

No presente trabalho apresentam-se as vantagens da utilização de atributos sísmicos na interpretação de dados de sísmica de reflexão 3D e na identificação e caracterização de reservatórios de hidrocarbonetos. O trabalho prático necessário para a elaboração desta tese foi realizado durante um estágio de quatro meses na empresa de serviços para a indústria petrolífera, *Schlumberger*, em Paris, utilizando o *software* de interpretação sísmica e de modelação de reservatórios de hidrocarbonetos, *Petrel* 2008.1. Os atributos sísmicos podem ser considerados formas alternativas de visualizar os dados de sísmica de reflexão, que normalmente são representados em amplitude. A sua utilização facilita o processo de interpretação sísmica, uma vez que permite aumentar a razão sinal-ruído, detectar descontinuidades, reforçar a continuidade dos reflectores sísmicos e evidenciar indicadores directos de hidrocarbonetos nos dados sísmicos originais. Os atributos sísmicos podem ainda ser usados para treinar processos de auto-aprendizagem utilizados em redes neuronais na predição da distribuição de facies numa área em estudo. De uma forma geral, a utilização de atributos sísmicos facilita a correlação entre os dados provenientes do método sísmico, dados de poços e a geologia da área em estudo. Neste trabalho foi utilizado um bloco migrado de sísmica de reflexão 3D, com aproximadamente 6000 km^2, adquirido no *deep-offshore* da costa Oeste Africana. Para além de um teste individual dos atributos sísmicos disponíveis no *Petrel* 2008.1, esta tese incluí uma avaliação preliminar do potencial em hidrocarbonetos de um sistema de canais amalgamados identificado na área em estudo. A sua identificação, interpretação e caracterização foi possível com o recurso a atributos sísmicos que evidenciam a presença de falhas, ou outras descontinuidades, e de atributos sísmicos sensíveis a pequenas variações na litologia e à presença de fluídos nos poros das formações litológicas.

acknowledgments

This works is the end of a step. It is also the conclusion of a dream of my parents. Thanks for their unconditional support and the example and guidance of my brother. Thank you!

A special thank to my dear Adriana, for her help, support and understanding even in moments that were difficult to understand. During these five years our paths are inextricably linked.

I deeply thank to my supervisor Prof. Luís Menezes Pinheiro for his scientific orientation during the preparation of this thesis. I would specially like to thank his all time availability and his enthusiastic ideas, making this thesis a much better work. This thank includes his huge patient in correcting my English. During the last year and a half he introduced me to the scientific research world, the marine geology and the seismic method, always placing great confidence on me and trying to open the opportunity door which best fits my hopes. For these reasons, and many other which are impossible to write in here, I am extremely grateful.

I am indebted to Dr. António Kaschaka who gave me the opportunity to do an internship, at *Schlumberger*, in Paris. Without him this thesis would not be like it is today. Thanks also for the good suggestion to complement my work. Huge thanks to all my colleagues and friends from *Schlumberger Information Solutions* which I had the privilege to share four wounderful months of work. Very special thanks to my both supervisors Hamid Abbassi and Andreia Mandiuc, and all the people who helped, supported and guided me in so many ways and situations: Míchel Remy, Caroline Martinez, Marianne Lenormand Berthome, Julie Latoille, Lauriane Petit, Estella Pimenta, François Avril, Anna Bui Xuan Hy, Ludovic Guenoux, Stephane Martine and Isabelle Jacquemin. Thanks also to everybody who shared his lunch time with me and the colleagues allowed me to have lots of fun during the football on Mondays.

There is a special working team which makes me grow everyday. Very special thanks to my friends from LGGM/DGEO. Thanks to my “godmother”, Catarina, for her support as a friend and work colleague. Thanks also for her useful advices in order to prevent me to commit further errors in the future and help me to be a better person. Thanks to Ro, the maturity, for his support and advice in special key moments with the right words. Thanks to Daniela for her support during this hard time writing. Together we built foundations between both in order to achieve our common goal. Thanks also to Mr. Kamran, I already said something about him in the Portuguese version, to Franscisco and Vitor, for being an example to younger student researchers, to Sandra, Tiago, Diana and Ana M.. I also thank to my colleagues and friends of “office” Ana Antunes e Martha which do not belong to the official team but is as if they are.

acknowledgments

To those friends who changed this hard climbing in a nice walk, a very special THANKS! Since everyone knows of who I am talking about, I do not need to identify anyone in particular. I would like to thanks to: the MECs for the share and support of the first experiences and steps; those who belong to the best produce, the union made us stronger; To MAL, and the loss of paint in our pens; to those who will always be in the 2nd year, and that taught me to play PES; and to those which at improper hours of the night share their philosophical thoughts and hugs of respect and truly friendship with me!

Thanks to "*galera do surf*" for your friendship, taught and the good vibes that now I carry inside of me.

The Department of Geoscienses of the University of Aveiro is a special place. The pleasure of spending time in it, working, chatting or studying only exists because there are extremely hard working people who work to make every day a new and better day! A special thank to Mrs. Paula Cruz, Mrs. Graça Marques and Mr. João Graça.

Finally, thanks to all those who have crossed my life during this last five years and although not being referred here helped in the process of what I am today.

Key words

Seismic Attributes, 3D Seismic, Channel Systems, Deep-water, Hydrocarbon Reservoir Characterization, *Petrel* 2008.1.

abstract

In this work the advantages related to the use of seismic attributes in the interpretation of 3D seismic data and in the characterization of hydrocarbon reservoirs are discussed. A four months internship at *Schlumberger*, in Paris, using the *Petrel* 2008.1 "*seismic-to-simulation"* software provided the necessary data to perform the work described in this thesis. Seismic attributes are different ways to look at the original seismic data, which normally is displayed in amplitudes. Using seismic attributes during the seismic interpretation process allow a significant improvement in the signal-to-noise ratio, the automatic detection of discontinuities, the enhancement of seismic reflectors continuity and the enhancement of direct hydrocarbon indicators. In the self-learning process for neural networks, seismic attributes can be used as training data to predict facies distribution in the study area. Generally, seismic attributes provide a better correlation between the data provided by the seismic reflection method, well log data and the geology of the study area. In this work, a 3D migrated seismic cube was used, with an approximate area of 6000km^2, acquired in the deep-water of West Africa. Besides an individual test of each attribute available in *Petrel* 2008.1, this thesis also includes a preliminary evaluation of the oil and gas potential of a system of stacked channels identified within the study area. The identification, interpretation and characterization of this potential hydrocarbon reservoir was possible using seismic attributes to enhance faults and other discontinuities, and by using seismic attributes sensitive to subtle lithological variations and the presence of fluids in the pore spaces of the lithological formations.

Contents

Table of Figures

List of Tables

Chapter I. Introduction

I.1. Nature and scope of this work

The current thesis reports the main results of the work carried out as a trainee at *Schlumberger Information Solutions* (SIS), Paris, France, for four months, under the supervision of Senior Support Engineer Hamid Abbassi and Support Engineer Andreia Mandiuc, and co-supervised by Prof. Luís Menezes Pinheiro from the University of Aveiro. This internship was carried out in the scope of the Dissertation/Final Project/Internship course from the final year of the Master Course in Geological Engineering, Geological Resources branch, from the Department of Geosciences of the University of Aveiro, Portugal.

I.2. Schlumberger Limited

Schlumberger Limited is the world's biggest company providing oilfield services on technology, information solutions and integrated project management to costumers working worldwide in the oil and gas industry (www.slb.com (a)).

The very beginning of *Schlumberger* was in 1912 when Conrad Schlumberger had the first *avant-garde* idea to map the land subsurface using electrical methods; this is currently considered the beginning of the electrical geophysics. 14 years later, in 1926, and after his brother Marcel joined the business, they founded the *Société de Prospection Electrique*, the starting point for what is nowadays *Schlumberger*. They recorded the first electrical resistivity well log one year later, in France, and in 1929 the Schlumberger brothers logged the first well in the USA. 1934 represents the beginning of *Schlumberger Well Services*, the antecedent of what is nowadays *Schlumberger Well Surveying Corporation*. In 1962, *Schlumberger Limited* entered in the New York Stock Exchange under the title of SLB and today

it is spread over several stock exchanges markets such as New York Stock Exchange, Euronext Paris, Euronext Amsterdam, London and SWX Swiss (www.slb.com (b)).

At present, *Schlumberger Limited* is headed by Andrew Gould (Chairman and CEO[1]) and operates in nine oilfield segments (Figure 1): Artificial Lift, Schlumberger Completations, Data & Consulting Services, Drilling and Measurements, Integrated Project Management, Schlumberger Information Solutions, Well Services, Wireline and Testing Services. It and also offers solutions on high quality seismic acquisition and processing through *WesternGeco*. These segments are organized under *Reservoir Characterization*, *Reservoir Production* and *Reservoir Management* groups (Figure 1; www.slb.com (a); (c)).

Since Conrad Schlumberger until present *Schlumberger* grew up and now is spread in more than 80 countries with more than 84 000 employees of over 140 different nationalities, reflecting the company's belief that "*diversity spurs creativity and understanding of customers' needs*". Schlumberger also built 23 research and engineering facilities all over the world to develop cutting-edge technology in oil and gas industry leading to a better and faster response to customers' wishes (www.slb.com (a)).

Schlumberger Information Solutions, is one of the several segments of *Schlumberger Limited*, and provides services in software, information management and information technology infrastructure. Its main aim is to help the oil and gas companies to reduce exploration risks and costs, implementing effective and safety workflows from exploration to production phases (www.slb.com (c)).

SIS includes several technical teams formed by geologists, geophysicists, reservoir engineers, data management engineers and networks engineers, who

[1] CEO: Chief Executive Officer

work together in order to give the best response and support to the costumers' needs (www.slb.com (c)).

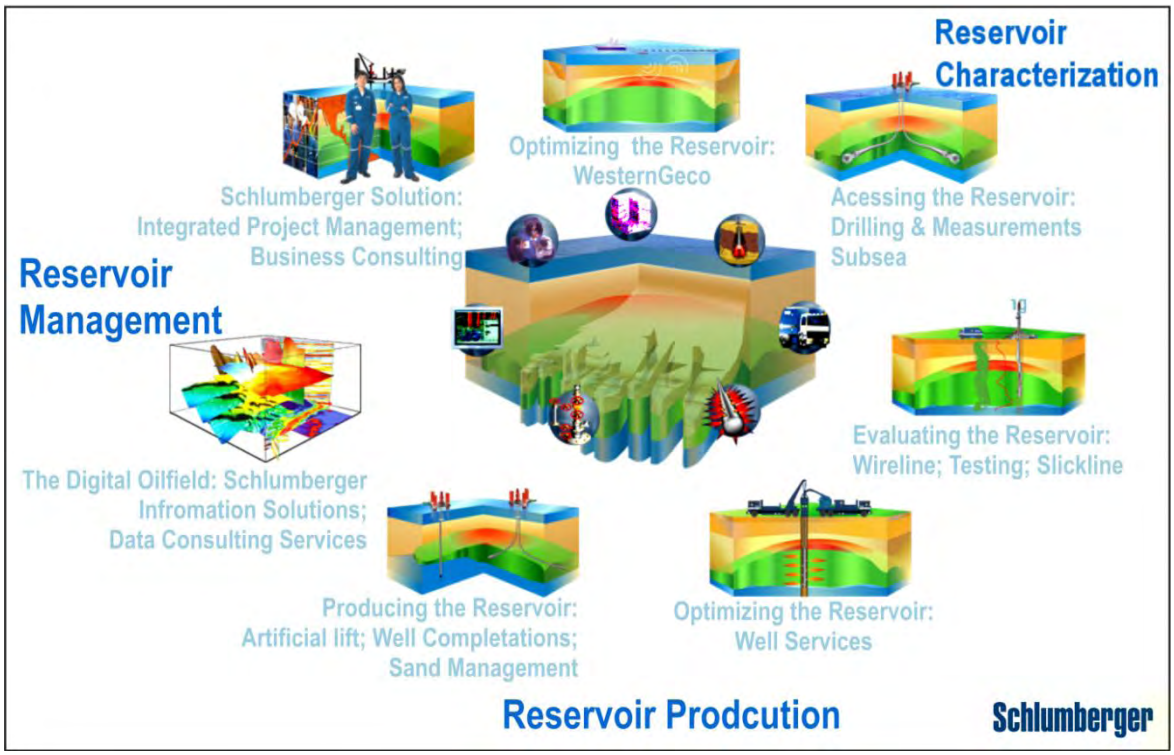

Figure 1 - Schlumberger's oilfield segments and groups division (hub.slb.com).

I.3. Objectives of this thesis

During the four months as a trainee at SIS, several main objectives, related with both scientific and professional/personal experiences were accomplished.

During this period the author became familiar with the daily routine of an employee in a support team from a service company for the oil and gas industry, learned how to use the seismic interpretation and hydrocarbon reservoir modeling software, *Petrel* 2008.1 and applied it to a case study. The introduction to new concepts related to seismic data processing, seismic attributes, seismic interpretation of key seismic reflectors and the characterization and identification of potential hydrocarbon reservoirs were also initially proposed and these goals were achieved.

The starting point for this work was to learn how to use the basics of *Petrel* 2008.1. To achieve this objective and as a basis for further studies, the author attended two *Petrel* training courses: *Petrel Introduction Course,* taught by *Petrel* Support Engineer Caroline Martinez, and *Petrel Seismic Visualization and Interpretation Course*, taught by *Petrel* Support Engineer Marianne Lenormand Berthome.

After an introduction to the latest version of the software and to the new seismic related concepts, the main research work carried out concentrated, on the potential use of seismic attributes in *Petrel* 2008.1, for the recognition and characterization of hydrocarbon reservoirs areas, fracture patterns and seismic classification using artificial neural networks (ANN). These studies were performed on a previously processed 3D seismic cube (see Section I.4).

I.4. Dataset and Methodology

The dataset used for this work consisted of a 3D processed seismic cube acquired by *WesternGeco* in the ultra-deep offshore of the West African Margin. This seismic volume corresponds to an area of approximately 6000 km^2, originally recorded in SEG-D format, with a record length of 9 seconds and a sampling interval of 2ms. The data processing flow included basic filtering, amplitude correction and pre-stack Kirchhoff migration. The processed 3D seismic cube was reformatted to SEG-Y format, the conventional file standard for data exchange between oil companies, resampled at 4ms, to reduce the SEG-Y file size, and cropped vertically at 2.3 seconds (Schlumberger, personal communication).

From the resampled 3D seismic volume, a quick interpretation of the seabed (Figure 2) was performed, using *Petrel*'s 3D autotracking function over a coarse interpretation grid of inlines/crosslines. Various *variance* attribute volumes (see IV.3.3.5) with different parameters were also computed for the entire 6000 km^2 seismic survey, with the purpose to define potential hydrocarbon accumulations in the study area.

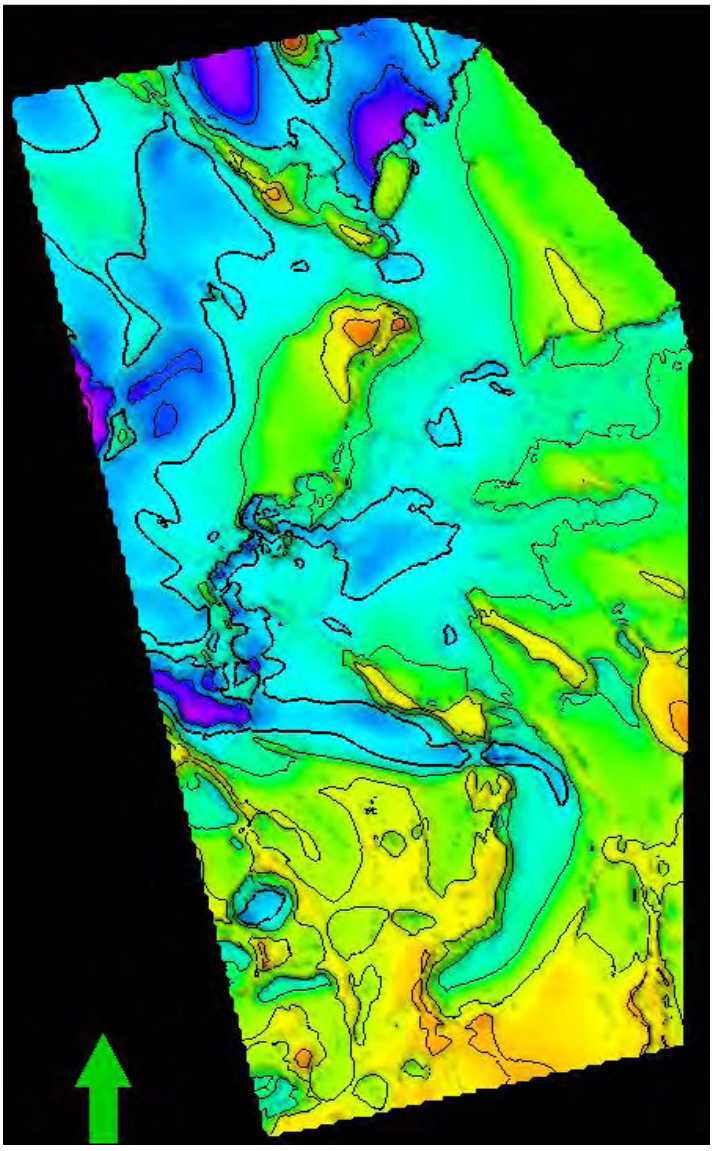

Figure 2 – *Petrel's* 3D view from above of the interpreted seabed for the entire survey. Colour scale ranges from red, for minimum depth values, to purple, for maximum depth values.

In order to reduce the time consumption for computing the various seismic attributes investigated, and also for an easier manipulation of the data and to liberate some of the system memory, the resampled seismic cube was cropped around an area of interest identified in several time-slices from the variance attribute volume (Figure 3).

The delineated area has approximately 2450km^2, with 2327 inlines and 3362 crosslines (Figure 4) and it was the work base to test the application of various seismic attributes and to perform the *prospect generation* and *advanced interpretation* stages (see V.1 and V.2).

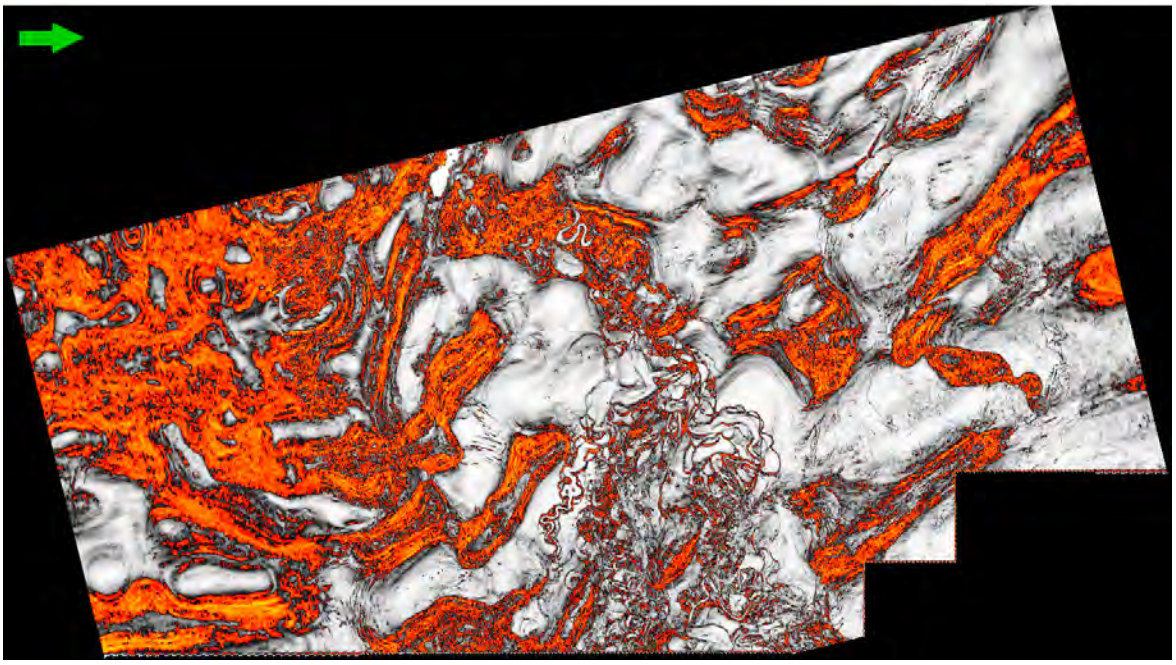

Figure 3 - Example of a variance time slice at 1000 ms showing a complex pattern of deep-sea channels and salt bodies. This variance time slice was, among other purposes, used to define the limits for the new cropped volume (see basemap on Figure 4). For a detailed discussion, see Chapter IV.

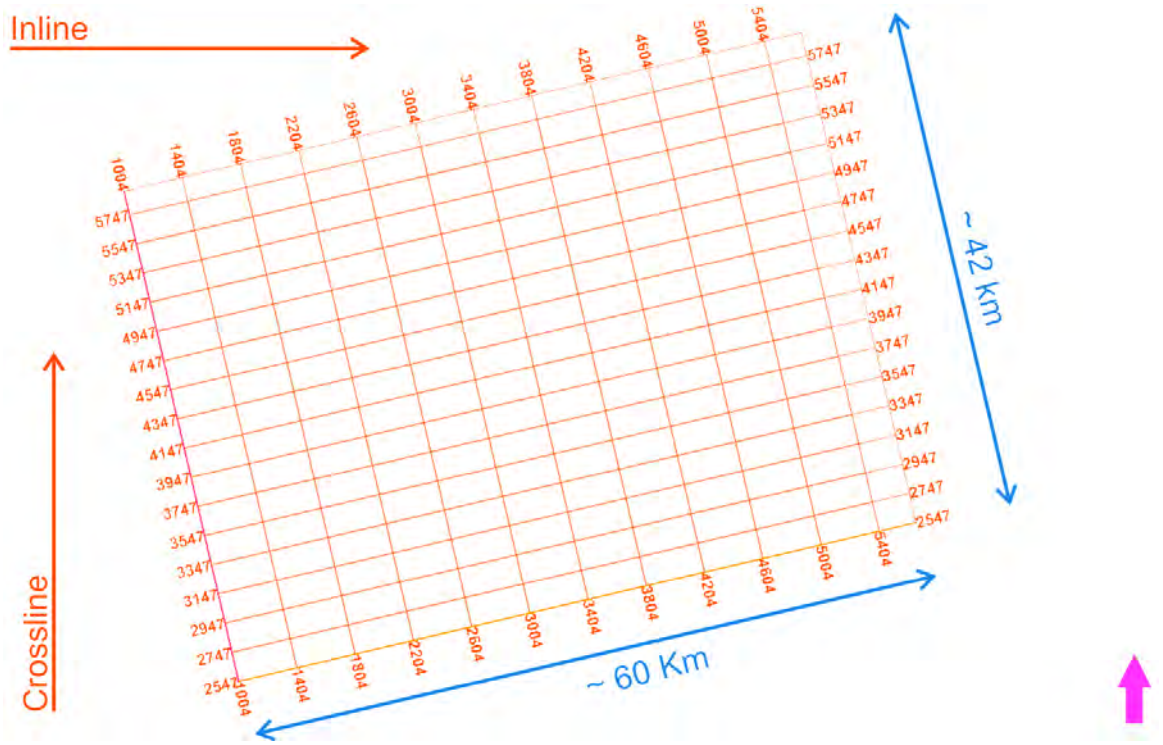

Figure 4 – Grid of inlines/crosslines of the new cropped seismic cube used as a work base to compute the seismic attributes.

The study area is intensely affected by salt tectonics and deep-sea turbidite complexes (Figure 5) characteristic of this region of the globe. Tertiary

channelized sands represent most of the known hydrocarbon reservoirs above the evaporite salt sequence in areas surrounding the survey area (Figure 5; Evans, 2002).

The adopted methodology for this work were: (1) to test the seismic attributes available in *Petrel* 2008.1, showing examples from different areas of the cropped cube that best characterize each of the attributes (Chapter IV); (2) to select and apply the best combination of seismic attributes for the identification and characterization of potential hydrocarbon plays (Chapter V).

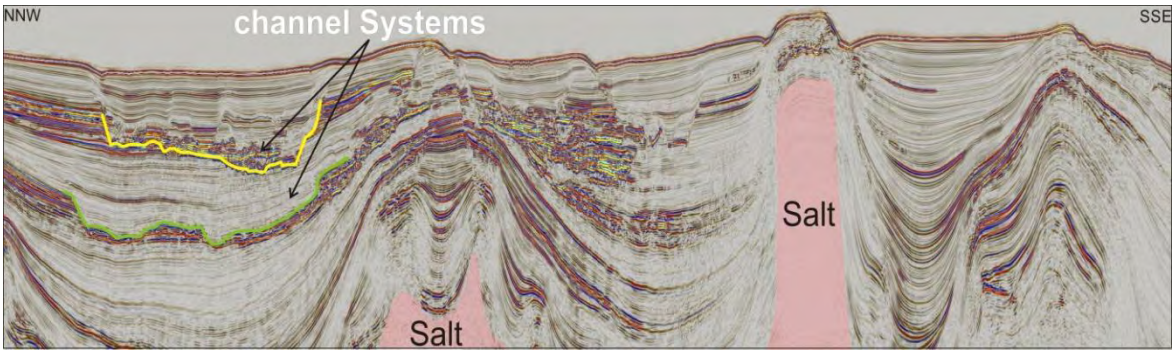

Figure 5 – Seismic inline showing an area intensely affected by salt diapirs and channelized sands originated from a turbiditic system.

I.5. Structure of this thesis

The present thesis is divided into six main parts. The first chapter introduces the scope and objectives of this thesis, the dataset and methodology used and a small reference to *Schlumberger Limited* and *Schlumberger Information Solutions*.

In the second chapter the seismic reflection method is briefly introduced, highlighting the importance of using 3D seismic data versus 2D seismic data. Basic seismic data processing steps and different methods for 3D seismic acquisition are also presented.

Chapter three describes briefly available commercial software for seismic interpretation and geological modeling, in particular *Petrel* 2008.1.

Chapter four discusses the theory behind seismic attributes and their use in *Petrel* 2008.1. It starts with a small introductory text about seismic attributes and an historical overview of classification of seismic attributes. Finally, the available seismic attributes in *Petrel* 2008.1 are shown with examples from real data, complemented with the respective theoretical explanation.

The fifth chapter reports the application of seismic attributes to a case study from the Western African margin. They are used to identify and characterize a potential hydrocarbon reservoir and define the associated fault pattern: this is normally designated in industry as *prospect generation*. Seismic attributes are then used as part of an *advanced interpretation* workflow which includes the interpretation of key seismic reflectors and their respective seismic attributes and seismic classification, based in artificial neural networks trained with computed seismic cubes from the original dataset.

The final chapter consists of the presentation and discussion of the results obtained, and the main conclusions that can be drawn from this work, followed by a short description of future work.

Chapter II. 3D Seismic Reflection Data

Seismic reflection data results from acquisition surveys carried out both onshore (on land) and offshore (in marine environments). Taking into account the recent discoveries of giant hydrocarbon reservoirs in particular off West Africa and Brazil, it is believed that most of the largest hydrocarbon plays yet to be found are located in the offshore and particular in the deep-offshore. As such, the seismic reflection method and acquisition survey geometries described in this chapter will be dealing only with marine acquisition. For a more comprehensive overview of the seismic method, the reader is referred to Sheriff and Geldart (1995) and Yilmaz (2001).

II.1. The Seismic Reflection Method

The seismic reflection method is, without doubt, the most used geophysical technique in the oil and gas industry, as a tool for looking for hydrocarbon reservoirs, due to its high resolution even for great depths (Gomes and Alves, 2007). In fact, it can be considered that the success of oil and gas exploration and production industry is what it is nowadays due to the high quality of the seismic data acquired presently and its more accurate and better constrained interpretation (Alfaro *et al*., 2007).

The seismic reflection method (or exploration seismology) is a remote-sensing technique which allows recording a "*picture*" of the subsurface with great accuracy, high resolution and great penetration, that can be used to map geologic features associated with a petroleum system (Mcquillin *et al*., 1984; Telford *et al*., 1990; Chopra and Marfurt, 2005).

Exploration seismology is a descendent branch of earthquake seismology since both techniques are used to understand and infer the geology inside the Earth by applying the same wave propagation principles at different scales. In earthquake

seismology the propagation of seismic energy originated from earthquakes (uncontrolled sources with unknown characteristics), to receivers spread all over the Earth, is investigated to determine the large scale Earth's structure and assess the risks for populations associated with those events. Exploration seismology uses the same principles of wave propagation, mainly for compressional p-waves, which travel inside Earth's layers, produced by an artificial controlled source of energy using short source-receivers offsets. Depending on the survey target, sources and receivers acquisition geometries are previously planned to maximize the imaging capacity of the seismic method for the targets under investigation (Telford *et al*., 1990).

In seismic reflection data, the information about the subsurface geology, physical rock properties and layers attitude, is inferred from the reflected wave travel-time between the source and its arrival at the receivers. The two-way travel-time (TWT) is defined by the time taken for the seismic waves to travel down from the source until they meet a boundary between layers with a different seismic velocity (*V*), density (*ρ*) and acoustic impedance (*Z*; Equation (1)) where they are reflected and then return to the surface. The contrast between acoustic impedance is called reflection coefficient (*RC*; Equation (2)).

$$Z = \rho V \qquad \text{Eq. (1)}$$

$$RC = \frac{Z_2 - Z_1}{Z_2 + Z_1} \qquad \text{Eq. (2)}$$

At such interfaces, the seismic rays are partially refracted, partially transmitted and partially reflected back to the surface where they are detected by a group of receivers (Figure 6). The arrival of reflected seismic waves produces systematic variations from trace to trace. These variations are called seismic *events*, and if they are consistent in the recorded seismic data, they can probably be interpreted as real geological interfaces between layers with different reflection coefficients. Measuring the travel-time of the events allow to determine the attitude and location of the geological interfaces which gave rise to each reflection event. The interpretation process also takes into account amplitude, frequency, phase and wave shape variations. Besides trying to identify direct hydrocarbon indicators,

seismic data is most often used to identify potential structures for hydrocarbon accumulation - traps[2] (Telford *et al*., 1990; Gomes and Alves, 1997).

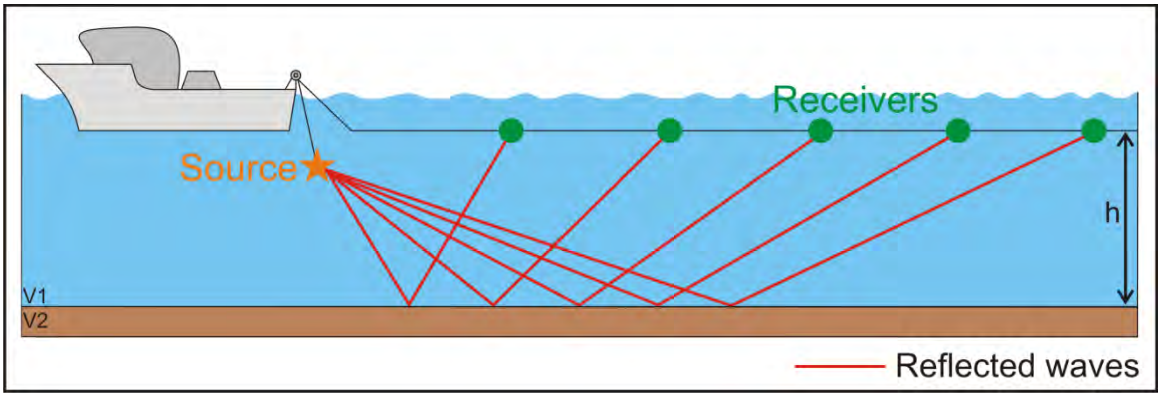

Figure 6 – Diagram showing the path of the reflected seismic energy in one dimension as it travels from the source to the receivers and it is reflected from the interface between two layers with different acoustic impedances.

Despite of the planned geometry, the acquisition environment and the type of seismic acquisition (2D or 3D), receivers are disposed along a line, or along parallel lines with more than one receiver line acquiring at the same time. A seismic acquisition survey is always composed of: (a) an input source; (b) groups of receivers, which detect the reflected seismic energy (the output of the Earth) and transform it into an electrical signal. Depending on the type of acquisition, receivers are disposed along a line (2D) or along parallel lines with more than one receiver line acquiring at the same time (3D); (c) amplifiers, (d) filters (e) an analog-digital-converter (ADC) which converts the signal from analytical to digital, for recording (Figure 7; Telford *et al*., 1990, McQuillin *et al*., 1984).

The input source produces a previously designed pulse of energy which meets, as close as possible, certain predefined requirements such as total energy, duration, frequency content and maximum amplitude. These parameters should be set respecting the commitment of enough Earth's penetration, resolution, and good signal-to-noise ratio (McQuillin *et al*., 1984). Receivers should be precise enough to detect very small ground motion, due to wave propagation, and preserve the signal without adding noise.

[2] A trap is a component of a petroleum system described as a geologic feature appropriate for hydrocarbon accumulations and sealed by a relatively impermeable formation. Traps can be structural or stratigraphic (e.g. faults or reefs, respectively) (glossary.oilfield.slb.com (a))

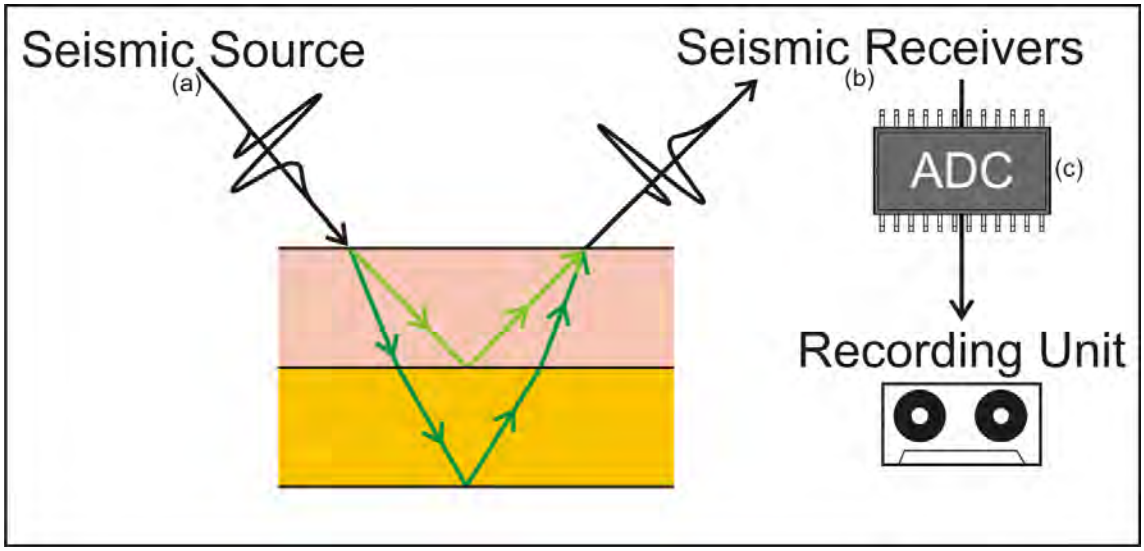

Figure 7 - Schematic representation of a general seismic acquisition system. The signal is originated by the source, travels through the Earth and is received at the surface by a group of receivers. Then, the signal is sent to a digital recording system after being transformed by an analog-digital-converter.

In marine surveys the most widely used seismic sources are airguns and the receivers are piezoelectric sensors designated hydrophones, which are distributed inside a tube filled with kerosene, called a streamer. All the acquisition equipment (sources and receivers) used in marine surveys is towed behind the seismic vessel (Sheriff and Geldart, 1995).

II.1.1. Seismic Sources

Airguns are impulsive methods that create seismic energy. An airgun is a cylindrical device which is filled with high pressured air that is suddenly released into the water generating a pressure pulse. Using an array of variable size airguns (Figure 8) rather than using a single airgun is nowadays the standard procedure in the oil and gas exploration industry; this method allows producing a signal that matches as close as possible the theoretical desired characteristics of the input source.

An airgun is divided into four principal components, a solenoid valve, the upper and lower chamber, which determine the size of the gun, and a double ended piston (Figure 9). The power of the airgun depends on the amount of high

pressured air stored in the lower chamber which is released into the water when the gun is shot.

Figure 8 - An array of airguns with different sizes (commons.wikimedia.org).

The air is injected in the upper chamber, flows through the axial opening of the piston and is kept inside the lower chamber (Figure 9, on the left). When the gun is fired an electrical signal opens the solenoid valve, the high pressured air reaches the underside of the piston producing an upward force on it. This upward movement will open the lower chamber, and release the air into the water forming a bubble (Figure 9, right). The charging cycle starts again with the introduction of new high pressured air inside the upper chamber which will force the piston to move downward and restart the steps described above (McQuillin *et al*., 1984; Sheriff and Geldart, 1995, Telford *et al*., 1990).

The biggest challenge in airguns is producing a seismic pulse as close as possible to a spike, because after the first bubble pulse, an undesired train of waves is normally created (McQuillin *et al*., 1984). This effect is called “bubble effect” and its origin is related to alternately moments of expansion and contraction of the air bubble formed by the shoot. This phenomenon will depend on the relationship between the pressured gas, the hydrostatic pressure of the surrounding water and the net force which accelerates the water outwards the bubble. When the hydrostatic pressure becomes larger than the gas pressure, the bubble originated from the shoot collapses and reduces its radius until the gas pressure inside the bubble reaches the water pressure, when the bubble starts to expand again. This

oscillatory cycle will keep working until the bubble reaches the water surface. Every time a bubble collapses or expands it will produce new energy, interfering with the first and well designed source pulse, creating an oscillatory signal (Figure 10; Telford *et al*., 1990).

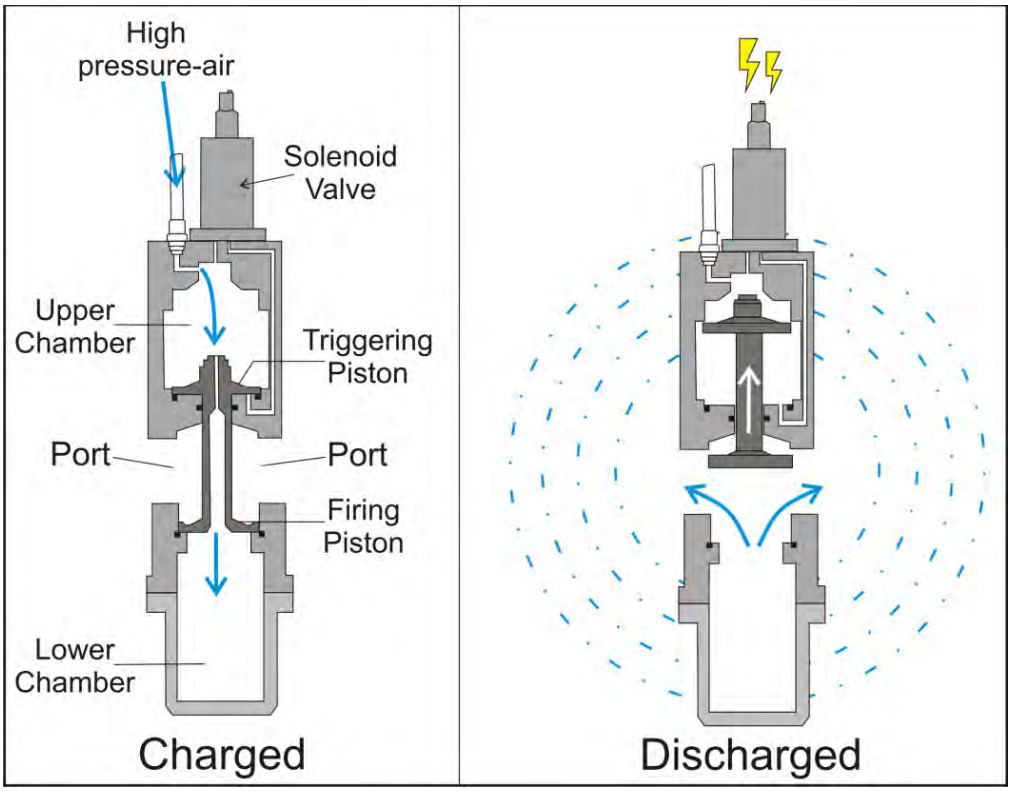

Figure 9 - Schematic representation of an airgun operation. When the gun is charged the lower chamber is filled with high pressured air (on the left). The airgun is then discharged by an electrical signal which opens the solenoid valve, allowing air to be released into the water while the piston moves upward producing a bubble of air (on the right) (modified from woodshole.er.usgs.gov).

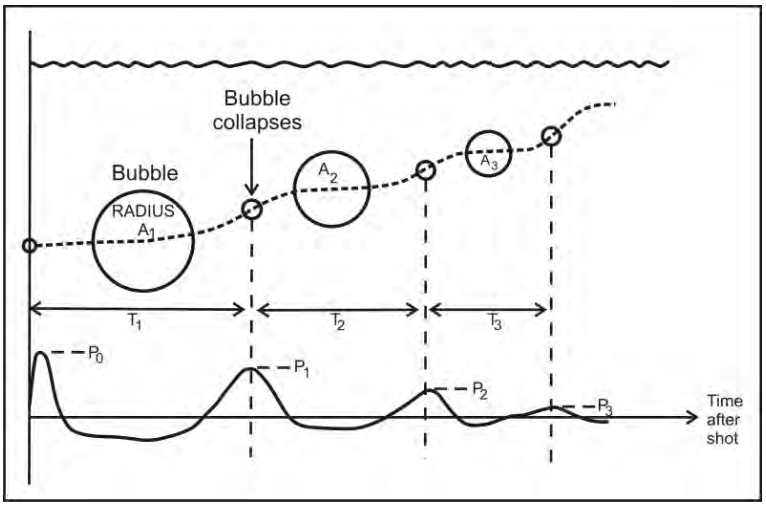

Figure 10 – Representation of the bubble effect. The radius of the produced bubble when the airgun is fired is continuously expanding and collapsing until it reaches the surface creating an undesired oscillatory signal (www.aug.geophys.ethz.ch).

Many of the acquisition seismic surveys use arrays of variable size airguns disposed in a special geometry and fired at different intervals to minimize the bubble effect. Synchronizing the firing time to align the first pressure peak will produce a cancelation of the oscillatory signal, producing a signal with frequency as close as possible to a spike pulse. Special types of airguns, called GI-guns were especially designed to minimize this effect (Sheriff and Geldart, 1995).

II.1.2. Seismic Receivers

Depending if the survey is carried on land or at sea, the receivers used are geophones or hydrophones, respectively. Standard hydrophones are piezoelectric sensors towed inside a streamer and transform the compressional p-waves into an electrical signal. Onshore, different kinds of geophones are used to detect p-waves or s-waves, depending on the survey purpose, and are normally coupled to the ground along straight lines (McQuillin *et al*., 1984).

A streamer (Figure 11) is a neoprene tube where hydrophones are placed by groups in regular intervals with a total length from 6 to 8km (Alfaro *et al*., 2007; Telford *et al*., 1989). The streamer is filled with a liquid lighter-than-water (e.g. kerosene) to turn it neutrally buoyant. Connection wires in between hydrophones and from the receiver to the recording system are also included inside the streamer (Sheriff and Geldart, 1995).

A streamer is divided in several functional parts (Figure 12). The first component is a lead-in section which connects the vessel and the first group of hydrophones. This ensures the minimum interference from the vessel's movement in the streamer. Hydrophones are arranged in sections called "live sections" and in each section there are twenty or more hydrophones spaced approximately 1m. In terms of seismic processing the signal received at each hydrophone inside a section is summed up and is considered just one receiver group (or channel). This technique improves the signal-to-noise ratio but when there is a great component of noise acquired with the signal, it can damage the quality of the data (Alfaro *et al*., 2007). "Dead sections" (Figure 12), i.e. sections without hydrophones, are placed

between live sections to give the desired length and configuration to the streamer. The last section is followed by a tail buoy equipped with positioning tools that communicate with the vessel (Figure 12). The buoy is used both to calculate the positioning of the streamer and to reduce the drift of the streamer due to water currents.

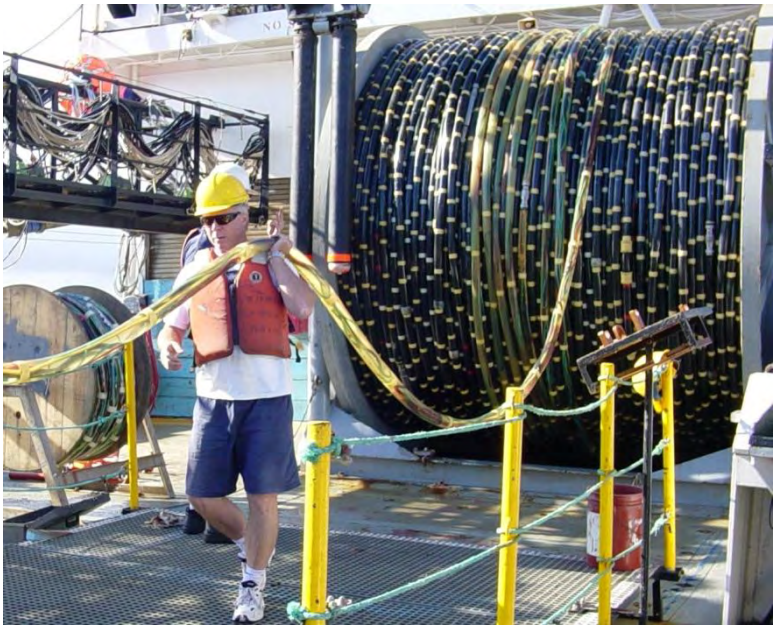

Figure 11 – A streamer being deployed into the water. When the vessel is not acquiring seismics, the streamer is kept onboard coiled on a reel (www.ig.utexas.edu).

In intervals between channels hydrostatic pressure-based depth controllers, normally designated as “birds” are placed. These devices will induce a compensation against the upward or downward movements of the streamer to maintain it at a constant depth (Sheriff and Geldart, 1995; McQuillin, 1984).

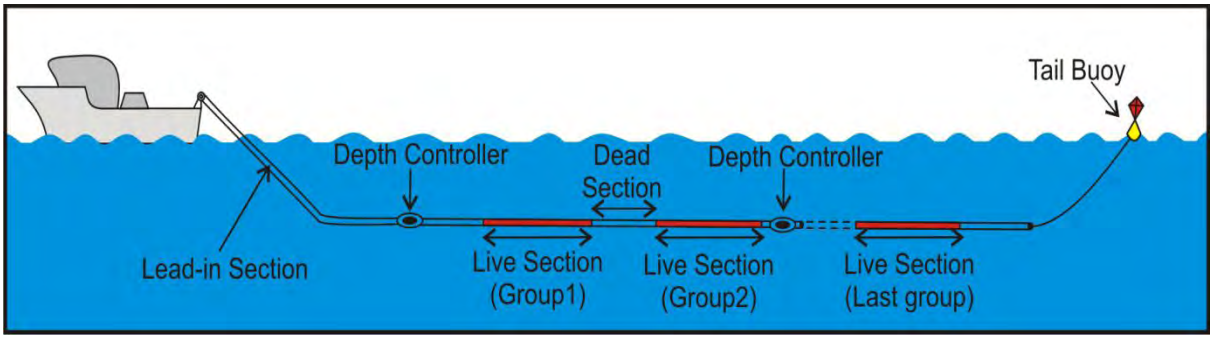

Figure 12 - Schematic representation of a streamer configuration (Modified from Sheriff and Geldart, 1995).

A stabilized streamer will reduce the noise content of the data and will ensure the right positioning of the group of channels, in depth and space, to be later corrected in the definition of the acquisition geometry, during the seismic data preprocessing stage (see Section II.4). In addition, the towing depth will also determine the frequency component of the received signal; if a streamer is towed at less than 8m depth than the sea surface, it will better preserve the high-frequency content of the signal but it will also increase the noise derived from weather and sea conditions. Increasing the towing depth value will preserve the low-frequency content of the signal and it will also increase the depth penetration. Traditional towing depths are from 8 to 12m (Alfaro *et al*., 2007).

II.2. 2D Seismic Data *versus* 3D Seismic Data

2D Seismic Data

Two-dimensional seismic data is normally acquired along spaced straight lines at distances from each other that normally range from hundred of meters to several kilometers. In marine seismic surveys, a single seismic vessel is used with one airgun array and a single streamer. Theoretically the content of the 2D seismic data has only information about the subsurface vertically below the acquisition path. However, the received signal has contributions of reflections from points outside the acquisition path. In terms of comparison, two-dimensional seismic sections can be considered as cross-section of a seismic volume (Yilmaz, 2001b).

In the current days and due to their low acquisition costs, 2D seismic surveys are the first exploration method used in oil and gas industry, where not enough knowledge about the subsurface exists. Regional surveys are carried out to identify potential large scale hydrocarbon accumulation sites and decide about further 3D surveys parameters (McQuillin *et al*., 1984).

In order to improve the signal content of the data a redundant sampling of the same reflection point is used, based on the common midpoint (CMP) reflection method (Figure 13; Sheriff and Geldart, 1995). The recorded seismic trace is a time-series associated with a source-receiver pair; for processing purposes this

geometry needs to be transformed into common midpoint (CMP) coordinates. For a horizontal interface, a CMP is a point at the surface located at half-offset between the source and the receiver, that is common to several source-receivers pairs (Figure 13). The number of times a CMP is sampled represents the *fold* of the data. A CMP gather (Figure 13, below) is a collection of traces that share the same midpoint. This method provides enhanced data quality, suppression of multiple reflections and improved general signal-to-noise ratio, especially after stack (glossary.oilfield.slb.com (c); Robinson *et al*., 1986; Yilmaz, 1997a).

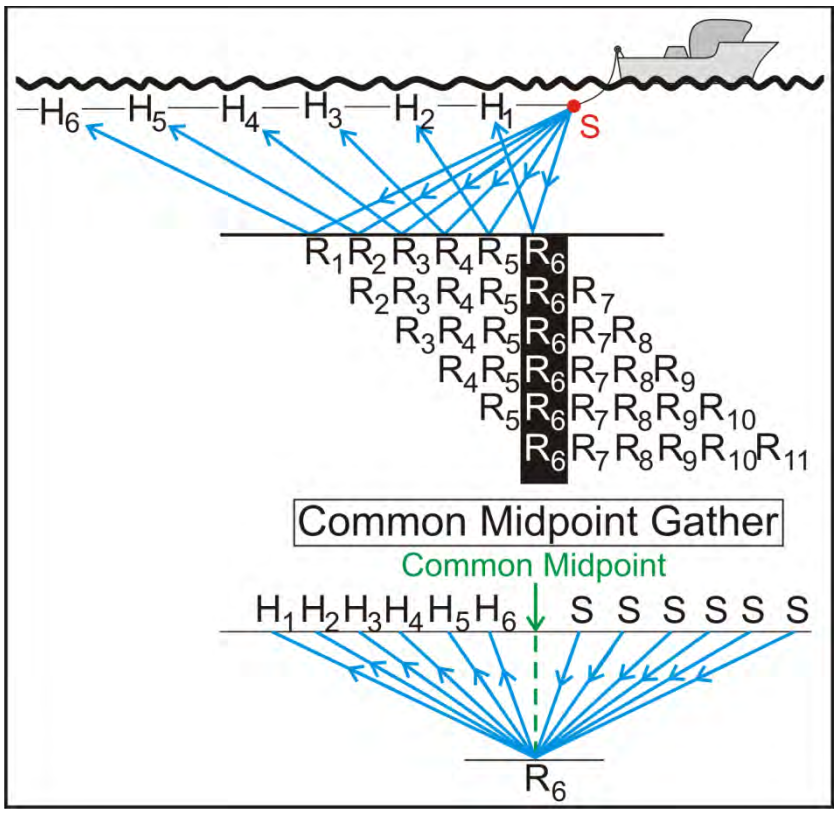

Figure 13 – Seismic data acquisition is done in shot-receiver coordinates (on the top) which is processed as a CMP gather. The lower part of the figure shows a six-fold coverage for one CMP location (modified from glossary.oilfield.slb.com (c)).

3D Seismic Data

The acquisition of three-dimensional seismic data started in 1976 (Sheriff and Geldart, 1995) and rapidly increased its importance for the petroleum industry due to its high vertical and lateral resolution even for great depths (Gomes and Alves, 2007).

Unlike traditional two-dimensional surveys which only provide information in depth along a straight line, three-dimensional seismics provides a cube with seismic data relative to three dimensions of the space (X,Y and time/depth) organized in inlines (with the same direction as the acquisition track) and crosslines (in a perpendicular direction of the acquisition path). Depending on the quality of the data in the 3D seismic volumes, the interpreter is able to map horizons and follow seismic events along the entire acquisition survey area and build a reliable geological model of a hydrocarbon reservoir.

3D seismic surveys have probably done more than any other modern technology to increase the likelihood of success of exploration drilling (Buia *et al*., 2008). In fact, interpretation of 3D seismic data benefits both exploratory wells (wildcats[3]) and development wells. The number of successful wildcats has increased in the last decades with the introduction of new acquisition and processing techniques. Development wells have also benefited, since the interpretation of three-dimensional seismic data allows a better knowledge of the subsurface and the possibility to develop new solutions to improve wells productivity (Alfaro *et al*., 2007).

In three-dimensional seismic acquisition surveys, four to ten streamers separated by 50 to 150m and airguns arrays of 12 to 18 guns that can be fired every 10 to 20 seconds at different times, are normally used (Figure 14; Alfaro *et al*., 2007).

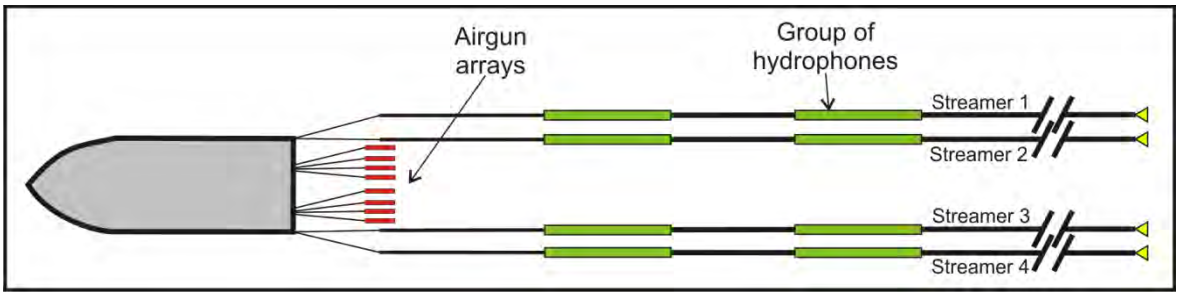

Figure 14 - Schematic representation of a 3D seismic vessel configuration with 2 arrays of 4 airguns each and 4 streamers.

[3] A wildcat is an exploratory well in an area where there are few geological knowledge of the subsurface (glossary.oilfield.slb.com (b)).

Since three-dimensional seismic acquisition is a multi-coverage method there is an immediate improvement in the signal-to-noise ratio and multiples attenuation, by sampling the same reflection, or bin[4], several times from different positions. In addition, the resulting dense sampling grid and data quality makes it possible to map not only hydrocarbon reservoirs but in some cases also assess the quality and the distribution of the oil and gas within a reservoir (Alfaro *et al*., 2007).

II.3. 3D Seismic Marine Acquisition Surveys

A marine acquisition survey requires that the water column is deep enough (more than 10m deep) to allow freedom of movements for seismic vessels with lengths between 30 to 70m. Marine seismic acquisition is faster and consequently cheaper when compared to land surveys, since there are less non-productive time[5] (Telford *et al*., 1990; Sheriff and Geldart, 1995).

The concept of seismic imaging is inextricably linked with the way in which the data is acquired (Amundsen and Landon, 2009). Subsurface imaging using 3D seismic surveys (Figure 15) is particularly successful in areas with clastic sediments. However, problems arise, particularly in the deep-water, when imaging sediments beneath hard seafloors, salt, basalts and carbonate layers. These limitations are caused by ray bending on the highly reflective and folded layers leading to portions of the subsurface remaining unsampled. This effect can be particularly important for seismic data acquired in just one direction. The key for a representative "*picture*" of the subsurface is a successful data acquisition with a 360º azimuth-offset illumination of the target area, only possible to achieve with the introduction of new acquisition geometries which consider more than one track direction (Buia *et al*., 2008).

[4] Bins are small square areas (normally 25 m by 25 m) that are treated as reflection points for the purpose of 3D data processing (Alfaro *et al*., 2007).

[5] Non-productive time is the time spend not acquiring data due to field operations. In the marine seismic acquisition sense means the amount of time a seismic vessel spends in transit from the end of one seismic line to the beginning of the next one.

In the oil and gas industry new proposed approaches for seismic data acquisition pretend to face the great challenge of today, imaging correctly the subsalt and reduce the number of dry holes in exploratory wells (Alfaro *et al*., 2007).

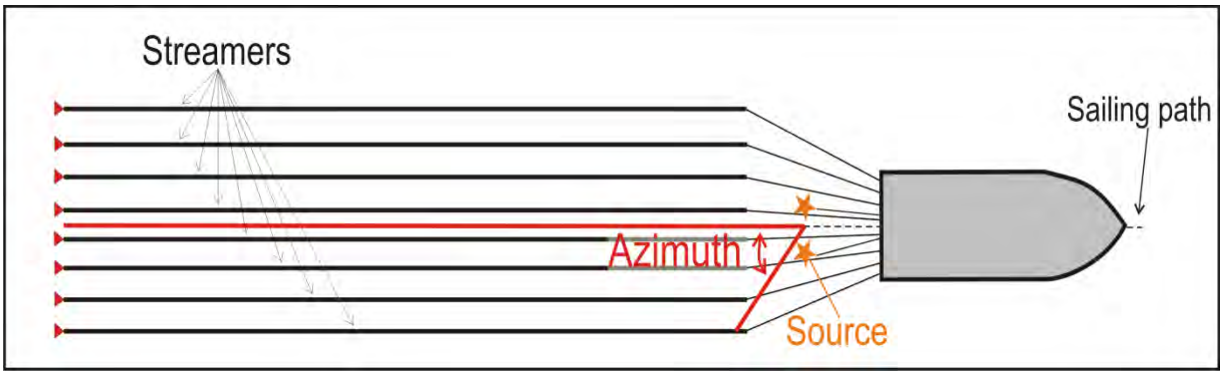

Figure 15 – Schematic representation of a seismic vessel acquiring 3D seismic data, sailing in a straight path. Azimuth is the angle, at the source array, between the sail path and the considered receiver (Modified from Alfaro *et al*., 2007.

Typical Marine Seismic Surveys

In conventional seismic acquisition surveys, the data is acquired by a single seismic vessel sailing in straight parallel lines, with opposite directions providing a coverage of about every 12.5m, with multiple streamers, over a target area (Figure 16). The seismic vessel is normally equipped with eight to ten streamers and a variable number of airguns and source arrays, depending on the target depth (Alfaro *et al*., 2008).

This kind of survey has a high percentage of non-productive time represented by curved path between the end of one line and the beginning of the next. In total, non-productive time can reach 50% of the total duration of the survey, therefore increasing acquisition costs (Buia *et al*., 2008).

If well planned, this acquisition geometry is enough to obtain a reasonable imaging of the subsurface for almost all geological environments. Moreover, since it is a standard oil industry acquisition scheme, seismic processing flows are well known and easily applied with high effectiveness in noise reduction and improvement of the data quality. However, there are imaging limitations related to some geological contexts which cause ray bending (e.g. areas affected by intense salt tectonics)

and when there are infrastructures that obstruct the acquisition path creating coverage gaps (Alfaro *et al*., 2007).

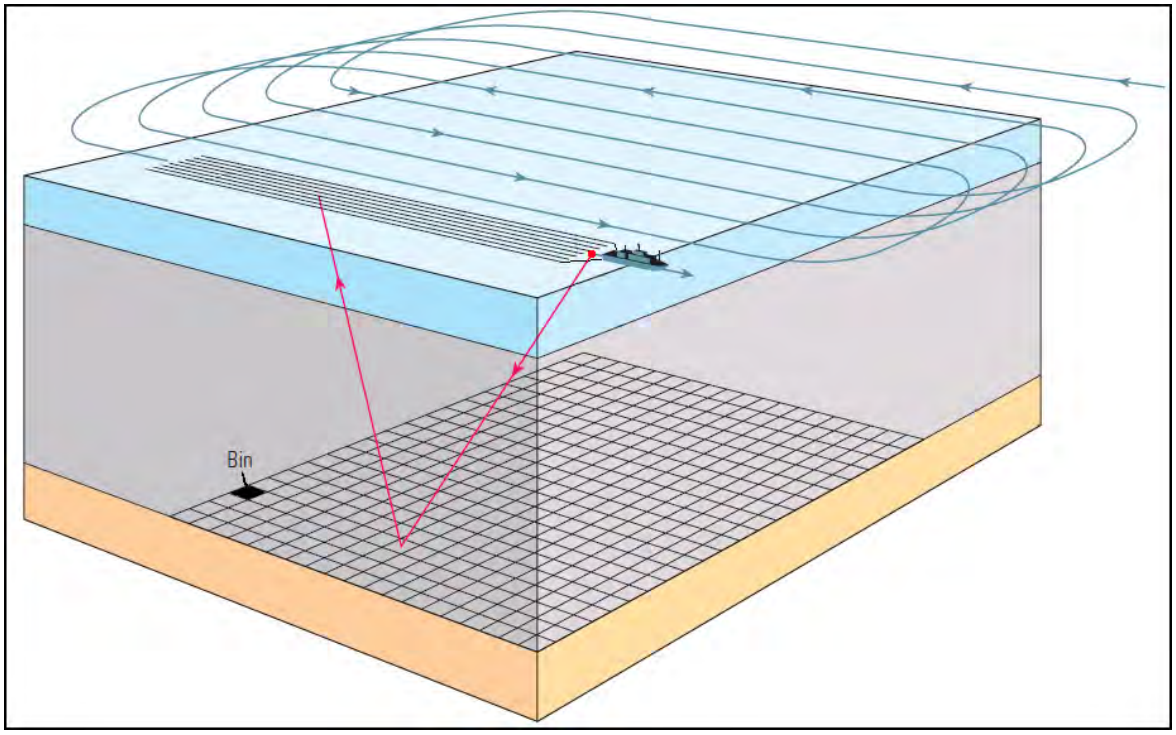

Figure 16 - Schematic representation of a traditional seismic survey. The vessel sails in parallel lines with opposite directions, curved paths represent non-productive time because the acquisition system is switched off. The target area is divided in bins for the purpose of processing the data (Buia *et al*., 2008).

Typical marine seismic acquisition surveys have narrow azimuth-offset coverage, just +/- 10º azimuths for far offsets (Figure 19a), since the illumination is just in one direction and the direction of the reflected ray path will be close to the vessel track. In order to attenuate the lack of azimuth-offset illumination of this acquisition geometry, it should be carried out ensuring the maximum possible trace coverage per bin (Alfaro *et al*., 2007; Buia *et al*., 2008).

This conventional acquisition geometry is the mostly used acquisition method to acquire 3D seismic data worldwide. However, seismic data can easily have low quality, making the interpretation process very difficult, leading to possible incorrect reservoir prediction and characterization. Alternative seismic acquisitions geometries based on more than one sailing direction have been more recently developed to obtain more consistent and reliable 3D seismic data (Alfaro *et al*., 2007).

Wide-Azimuth Seismic Surveys

Wide-azimuth surveys (WAZ) were first introduced in the oil and gas exploration industry by BP and PGS[6] in 2001 with a testing acquisition survey in the Norwegian Sea (Alfaro *et al*., 2007).

WAZ is a multi-vessel based method which follows the same acquisition pattern as a typical survey, in straight and parallel lines, but at least two source seismic vessels are used. The source vessels follow the recording vessel (typically with ten streamers), one behind and the other besides the streamer (Figure 17). Other geometries using additional seismic receiver vessels can also be applied depending on the complexity of the subsurface target (Alfaro *et al*., 2007; Buia *et al.,* 2008).

This method has proven improvements for large surveys in areas with great complexity and in subsalt imaging. For an effective seismic data quality, the survey should be designed taking into account the greatest possible distance between the source and the receiver, in a perpendicular direction to the acquisition path (crossline direction) and between consecutive acquisition lines depending on the number of involved vessels and the size of the survey area (Alfaro *et al*., 2007).

The wide-azimuth acquisition technique provides a general increase in coverage for all azimuths-offsets when compared to the traditional acquisition system. In fact, for near offsets it provides a full azimuth range, the optimal situation, and +/- 30º for far-offsets (Figure 19b).

Lastly, processing flows for data acquired by WAZ geometries are derived from those applied to data supplied by conventional seismic acquisition surveys, but after several basic processing steps. When compared with conventional 3D data, WAZ seismic data shows less coherent noise, higher resolution, improved multiple attenuation and much better seismic reflectors continuity and interpretability, especially for those beneath salt bodies (Alfaro *et al*., 2007).

[6] Petroleum Geo-Services.

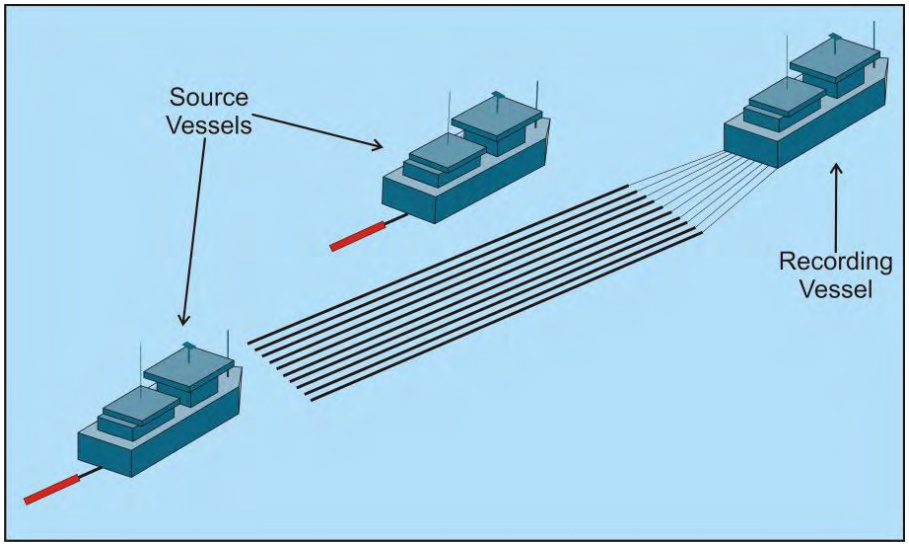

Figure 17 - Schematic representation of a wide-azimuth survey. A seismic receiver vessel sails along a straight path, above the target area, followed by two source vessels sailing one behind the towed-streamer and the other besides the receivers.

Coil Shooting Seismic Surveys

A new revolutionary technique for seismic acquisition – Coil Shooting[7] – has been recently introduced by *WesternGeco*, first tested in 2006 in the Gulf of Mexico, to solve the limited range of azimuth-offset fold from traditional and multi-vessel acquisition surveys (Buia *et al*., 2008). Coil Shooting (Figure 18) is a single-vessel method, with one powerful source and ten streamers, to acquire high-quality 3D seismic reflection data in large and continuous linked circles (with 5 to 7km of radius) (Buia *et al*., 2008; Amundsen and Landro, 2009).

Like many other breakthrough technical developments, the idea to acquire seismic data along a circular pattern is not recent. In fact, it remounts to the 1980's but only in the last years, with the development of new seismic sources and receivers and the arising of new tools for precise receiver positioning, did it became possible the real implementation of this method (Buia *et al*., 2008).

The acquisition survey is planned in order that the target area is covered by an overlapping circular pattern in which the seismic vessel sails, shooting and recording continuously (Figure 18), reducing in this way the typical non-productive time of a seismic marine survey and consequently costs and survey duration.

[7] Coil Shooting is a trademark of *Schlumberger*.

The result is high quality of three-dimensional seismic data with improved signal-to-noise ratio, multiple attenuation and enhanced reflectors continuity and consistency in every geological environment and even below highly reflective layers. It is an extremely powerful method for subsurface imaging since it guarantees a full azimuth-offset illumination (Figure 19c).

The potential noise produced by the circular trajectory of the vessel and the streamers is compensated with the introduction of new steering devices, used for the receivers, that precisely control the depth, the lateral position of the streamers and ensure a constant streamer separation. Most of the noise content within the data is from cross-currents perpendicular to the streamer direction which can be effectively reduced with new processing techniques (Amundsen and Landon, 2009).

Additionally, the Coil Shooting technique implies lower costs for small to medium surveys, when compared to the two methods previously discussed. Being a single-vessel method makes it also attractive for acquisition surveys in remote areas where it is difficult and very expensive to sail with more than one vessel (Buia *et al*., 2009).

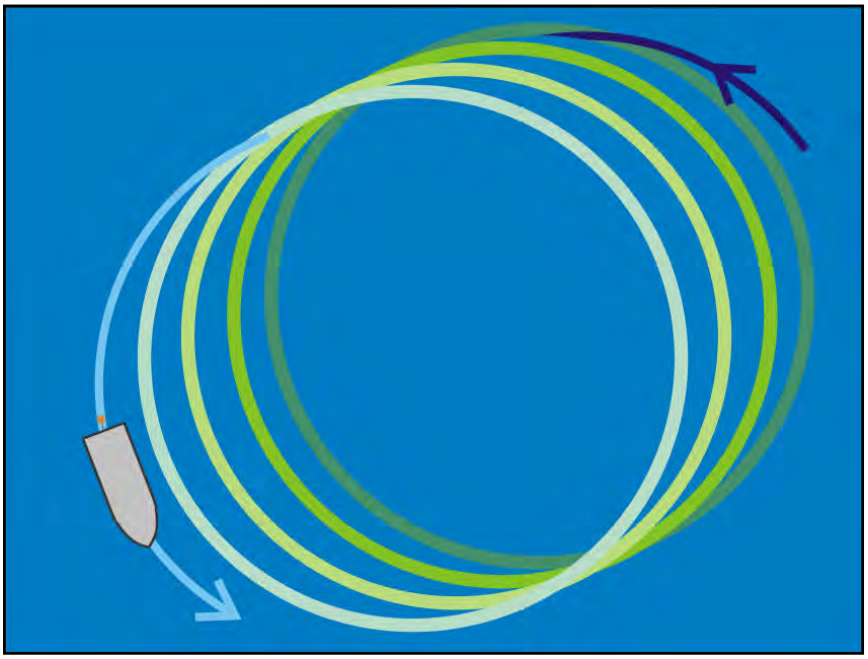

Figure 18 – Schematic representation of the Coil Shooting acquisition technique. The acquisition is done by one single seismic vessel (source and receiver) continuously following a pre-defined circular pattern over the target area to provide full azimuth illumination of the subsurface.

From the economical point of view and taking into account the huge amount of non-productive time for a conventional seismic acquisition survey, it is recommended to acquire seismic by the WAZ method for large seismic surveys in non remote places and by the Coil Shooting technique for small and medium surveys or for surveys realized in remote areas (Buia *et al*., 2008).

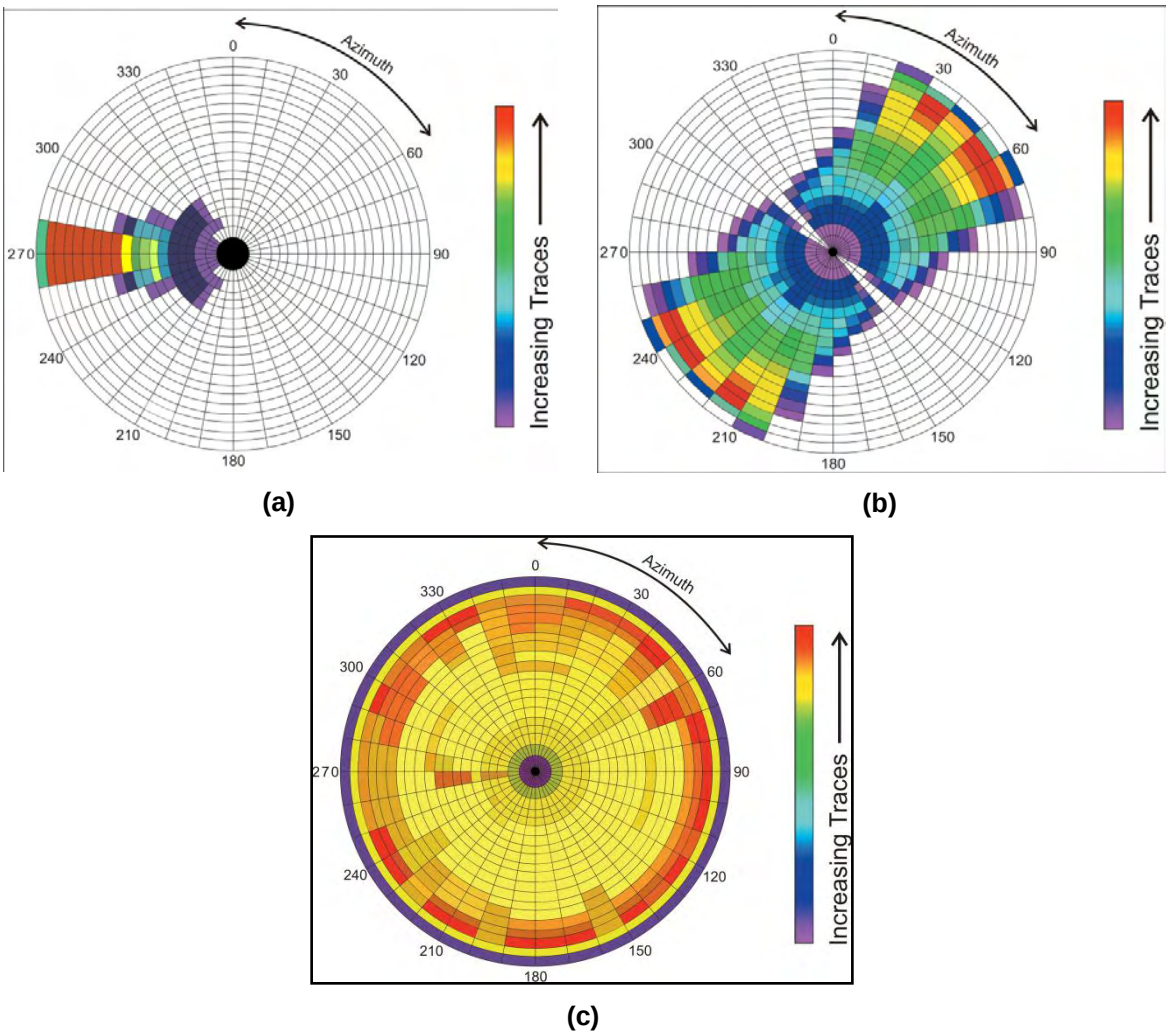

Figure 19 - Rose diagram of average azimuth-offset coverage for: **(a)** a traditional 3D seismic acquisition survey; **(b)** a Wide-azimuth survey; **(c)** a Coil Shooting survey. The number of traces recorded at an azimuth-offset pair is plotted in colour. Offset is the distance between the center and the considered azimuth (modified from Buia *et al*., 2008).

II.4. Basic Seismic Data Processing

Standard seismic processing flows are fully implemented and well known in the industry with the ultimate goal to increase the vertical resolution, to improve the

signal-to-noise ratio of the data, and to display the seismic events in their correct spatial position (McQuillin *et al*., 1984).

A typical simple processing flow for a 2D survey is composed of a *preprocessing stage*, which includes: demultiplexing, trace editing, spherical divergence and geometry corrections, and a *processing flow* which normally includes: deconvolution, CMP sorting, velocity analysis, normal moveout correction, CMP stack and migration. The processing concepts and algorithms applied in 3D seismic data processing are almost the same as those applied to 2D data. The main differences concern: quality control, statics correction, velocity analysis, migration and the way in which reflective points are considered for seismic processing purposes. In 3D seismic data, reflection points are designated as “bins” instead of common midpoints (CMP; Yilmaz, 2001a).

The seismic data is sometimes recorded in a multiplexed way in which samples from the same time interval from different shots are recorded consecutively. In such cases, the first step of the preprocessing stage consists of demultiplexing, to convert the data into a suitable and organized file format for processing purposes. In oil industry, the conventional standard for seismic files exchange is SEG-Y (Yilmaz, 1997a).

The data is then edited in order to detect and correct abnormal traces with high noise content or inverted polarity. If basic filtering is not enough to repair the noisy trace they should be eliminated since their contribution will decrease the signal-to-noise ratio. Basic filtering is also applied to all data in order to reduce the characteristic low-frequency noise originated from bad weather and/or sea conditions and by undesired movements of the streamer (Yilmaz, 2001a).

The spherical divergence correction applied next is a gain correction function to compensate the amplitude effects of spherical wavefront divergence. Finally, the data is corrected for the acquisition geometry with the positioning of shots and receivers inserted into the trace headers. This simple step is one of the most important in the processing flow and many of the problems that arise at later stages are originated by geometry definitions errors (Yilmaz, 2001a).

Deconvolution is then applied to compress the wavelet shape in the data, recover high-frequencies, attenuate reverberations and short-period multiples, increasing the vertical resolution of the reflectors and normalizing the frequency spectrum of the data (Yilmaz, 1997a).

Ideally, the recorded seismic trace is a convolution of the seismic wavelet, which travels from the source through the subsurface, with the reflection coefficient series, derived from the properties (in particular density and seismic velocity) of the different rock layers crossed by the seismic energy. Deconvolution tries to undo this natural convolution process, by eliminating the source signature and derived multiples, obtaining the reflection coefficient series. However, the received signal does not contain only information about the wavelet signature and the Earth's impulse response. In fact, there many other components such as noise and limitation on sources and receivers that make it impossible to obtain the real impulse response of the Earth (Yilmaz, 2001a).

The Normal Moveout (NMO) correction is then applied to data sorted by CMP (a CMP gather) using a previously created velocity field. This correction removes the source-receiver offset effect in a non-dipping seismic reflector, assuming that the reflection travel-time, which is a function of offset, follows a hyperbolic trajectory. Since reflections arrive first at nearest offsets and later at far offsets, the greater the source-receiver offset the larger the delay observed. In the NMO correction, seismic events corresponding to seismic reflections are flattened across the offset range in order to remove the previously described effect (Figure 20; Yilmaz, 1997a).

NMO is a dynamic correction since corrections will decrease with the increase in two-way-time and the increase in sound speed of rocks (Robinson *et al*., 1986).

After a detailed velocity analysis, the resulting velocity field is applied for NMO correction and to stack the data. Stacking consists of summing the traces which belong to a CMP location into just one trace after NMO correction (Figure 21). The output data will have reinforced reflections, since noise is theoretically random and

when summed tends to cancel, increasing the signal-to-noise ratio (glossary.oilfield.slb.com (e)).

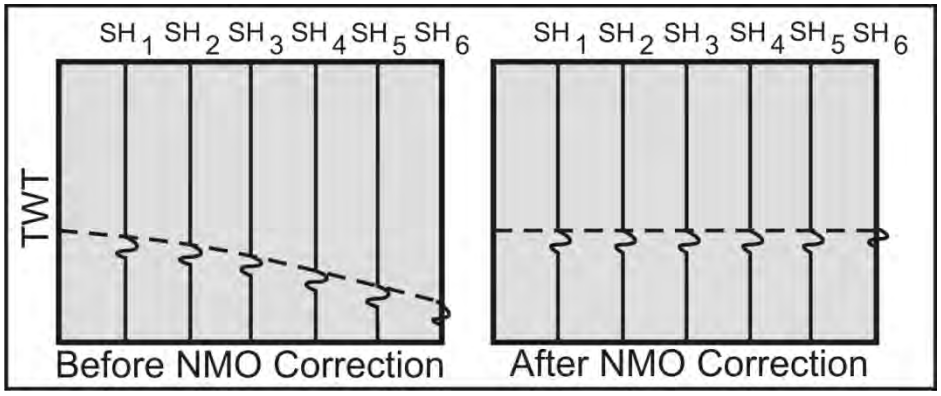

Figure 20 – Diagram of six traces displayed before and after normal moveout correction (from glossary.oilfield.slb.com).

The classic processing flow normally finishes with a migration algorithm. This process attempts the repositioning of the seismic reflections in their supposedly true subsurface position in depth.

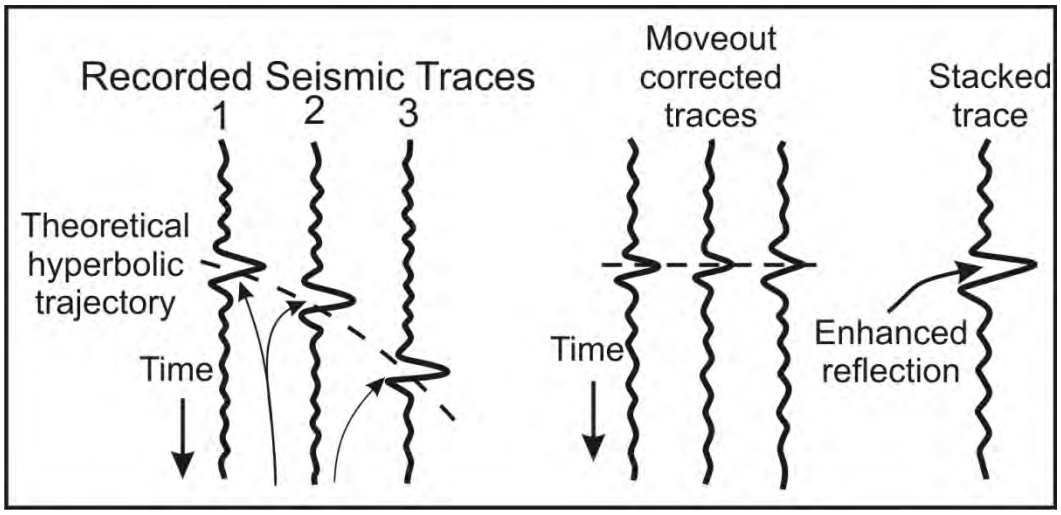

Figure 21 – Data is organized by CMP which are corrected for the normal moveout effect and finally stacked to improve data quality (glossary.oilfield.slb.com (e)).

With a proper migration, based on a realistic velocity model, most of the diffractions within the data are collapsed. Migration has proven results for improving seismic interpretability and mapping of complex structural areas intensely folded and faulted. This processing algorithm also increases the spatial resolution of the data. For three-dimensional seismic data, 3D-migration algorithms are used (Yilmaz, 1997a).

Another way of applying a migration algorithm is before stack (pre-stack migration). Pre-stack migration is an intensive time-consuming and a heavy computation process which allows to imaging reflectors with abrupt variations of lateral velocities, with non-hyperbolic reflection events, conflict dips, and steep discontinuities. The algorithm is applied trace to trace at each CMP location, instead of being applied to the stacked data. Pre-stack migration will solve seismic imaging below salt bodies which is especially important in hydrocarbon migration and accumulation detection (Yilmaz, 1997a).

All the processing steps should be quality controlled through seismic cross-sections displays in order to ensure that the quality of the data is not diminishing (Yilmaz, 2001b).

II.5. Interpretation of 3D Seismic Data

Seismic interpretation is the last stage in the oil and gas industry to prospect and correctly identify hydrocarbon reservoirs on properly migrated seismic cubes. Without a consistent interpretation, the seismic data itself is useless (Robinson *et al*., 1986).

Seismic data interpretation is an exhaustive data analysis process. Nowadays there is a lot of geological information associated with a seismic volume, which should be taken into account. This large amount of information increases the time consumption but, if well correlated, reduces the uncertainty to build a reliable geological model (Yilmaz, 2001b).

The interpreter must combine the various components of the dataset (e.g. 3D seismic cube, 2D lines and well log data) in order to recognize seismic patterns that can give clues about potential hydrocarbon accumulations sites, depositional environments and the structural geology of the area. This recognition is often based on comparisons between the data and a mental database created by the interpreter's experience. As such many people consider the interpretation process as something in between a science and art (Chopra and Marfurt, 2005).

The interpretation is done visually and interactively, in powerful workstations, over vertical seismic sections, in *inline* and *crossline* directions, and in horizontal seismic sections called horizontal time slices. Available interpretation software (Chapter III) allows the manipulation and visualization of seismic data together with well log data and allows correcting possible mis-ties. This combined visualization allows associating seismic reflectors to boundaries of known lithological layers (Robinson *et al*., 1986). Identified features such as faults and key seismic reflectors (called horizons), are interpreted based not only in the travel-time but also in the amplitude content, with the objective of building a reliable geologic model (Yilmaz, 2001b).

Direct hydrocarbon indicators (DHI) in seismic data are not as common as often assumed. Only in few datasets show reflections which can be unequivocally interpreted as DHIs. The interpreter will therefore mainly be looking for structures, both tectonic and stratigraphic, that can potentially hold hydrocarbon accumulations (e.g. faults and antiforms; Gomes and Alves, 2007).

From seismic data alone it is not possible to unambiguously identify lithologic sequences or the fluid content filling the pore spaces. This information is normally achieved with the use of modeling algorithms, well log data and more recently (Robinson *et al*., 1986) using seismic attributes (Chopra and Marfurt, 2005). In fact, seismic attributes are used as a starting point or complement in the interpretation process.

A careful interpretation of 3D seismic data allows accurately mapping geological features, defining the structural geology and infering about lithological variations and their distributions, thereby characterizing the respective depositional systems in the survey area. A fully understanding of the study area is the key for success in oil and gas exploration and production industries.

Chapter III. 3D Seismic Interpretation in *Petrel*

The development of new technology and the growth of 3D seismic data with lower costs, particularly after the 1980s, propelled the emergence of powerful interpretation workstations, leaving behind hardware limitations to deal with large datasets. Today, innovative commercial software for seismic interpretation and analysis can run in ordinary personal computers and easily handle interpretation tasks for medium-large datasets.

Available interpretation software tends to be easy-to-use providing several automatic algorithms to help the geoscientist in the geophysical interpretation process. Automatic tools, when properly supervised by a user, execute a more consistent seismic reflectors interpretation based not only in the visual continuity of the reflector but also in its consistency in terms of amplitude. Interpreted well log data and geological information are easily displayed and correlated with the seismic data and other geophysical datasets, reducing the number of mis-ties[8] and allowing the identification within the seismic data of known and important lithologic formations. In the seismic attributes domain (see Chapter IV), new software solutions have large attributes libraries being able to compute and display them, on-the-fly, even for large amounts of three-dimensional seismic data.

These combined factors introduced a new paradigm in seismic interpretation: the possibility of creating different geological models, in a faster and reliable way, which associated with the increase in quality of seismic data, led to optimized well design and location (Chopra and Marfurt, 2005).

[8] When interpretation from the seismic data does not match well log data or when two seismic lines cross and the interpreted seismic reflectors do no match.

There are many seismic interpretation software but the three most used in the oil and gas industry are: *SeisWorks*, *Kingdom Suite* and *Petrel*.

SeisWorks is the *Landmark UNIX* based software suite solution for 2D and 3D seismic interpretation and analysis taking into account the existing geological data (www.halliburton.com).

The *Kindgom Suite* software, developed by *Seismic Micro-Technology*, is a basic software package to perform seismic interpretation, 2D and/or 3D, integrated with geological and log data with the purpose of building a geological model with less time consumption and reduced uncertainty (www.seismicmicro.com).

Petrel is mark of *Schlumberger* and is a unique "*Seismic-to-Simulation Software*". It enables the possibility of geologists, geophysicists and reservoir engineers to work together as one, in the same work base. The last step in *Petrel* is creating a completely and fully detailed reservoir model: from the interpretation of seismic data, through the integration of geological log data and testing of different geological scenarios with the aim of modeling and simulating a hydrocarbon reservoir (Schlumberger, 2008).

III.1. Seismic – to – Simulation software, Petrel 2008.1

Petrel has been developed by *Schlumberger* since 1996 and many upgrades have been done from version to version in order to improve algorithms and give an effective response to the customers' needs. It unites geosciences and reservoir engineering domains to work together allowing to "*think critically and in a creative way*" about the modeled hydrocarbon reservoir. Companies can increase profits by reducing the uncertainty and time consumption of data analysis, interpretation and modeling, while experiencing the different *Petrel* modules (Figure 22; Schlumberger, 2008; www.slb.com (d)).

Geophysical data can be interpreted, often with automatic picking, either in a 2D view or directly from a 3D display of the seismic volume. Automatic interpretation

tools are quality controlled, constrained and validated by a user supported by previously computed seismic attributes and/or by other geological well log data.

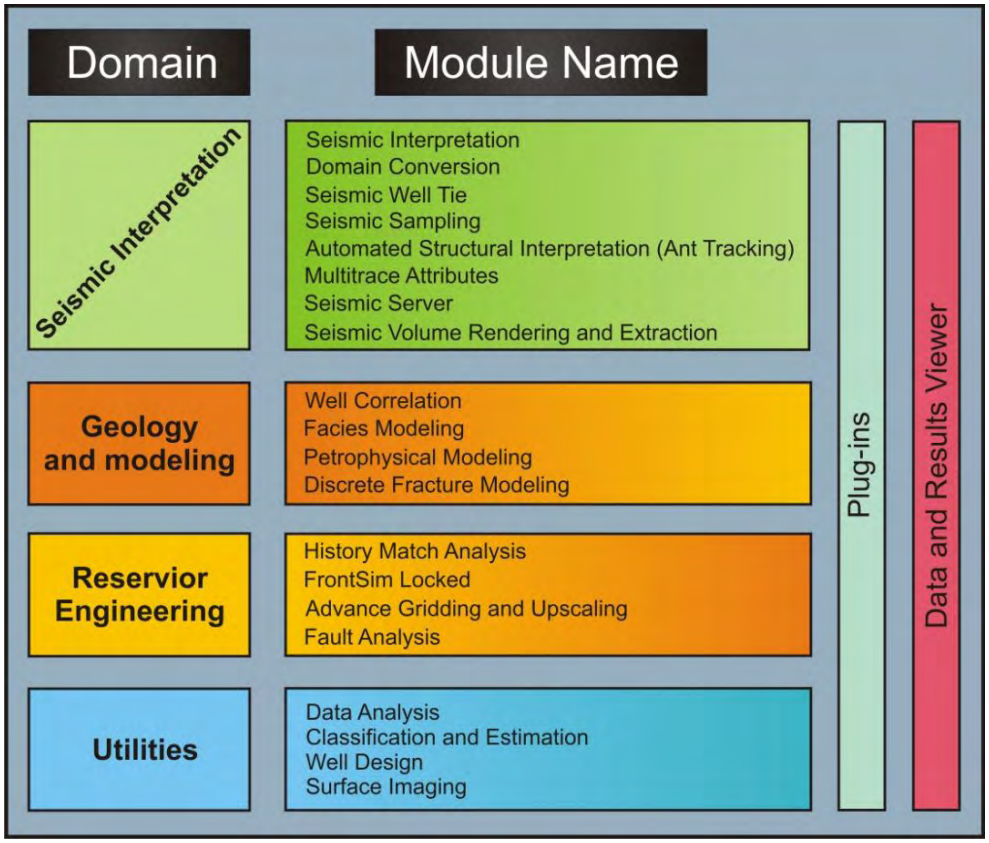

Figure 22 - Petrel 2008.1 module dependency map (modified from www.slb.com (d)).

The correlation between geological and geophysical domains can be done through synthetic seismograms or by depth-time conversion using an adequate velocity model. With a validated structural geology model of the hydrocarbon reservoir, this can be populated with facies and properties distributions based in geostatistic analysis (www.slb.com (d)).

Reservoir engineers can easily simulate reservoir flows by exporting the reservoir model to *Eclipse*[9]. The output results are imported back to *Petrel* where they can be displayed and analyzed. Potential wells can be visually designed and used as a guide for successful real-time perforation. All of these data and results are interactively displayed in proper windows within *Petrel*'s user interface (see Section III.1.1; www.slb.com (d)).

[9] *Eclipse* is the reservoir simulation solution of *Schlumberger*.

III.1.1. *Petrel* 2008.1 User Interface

Petrel 2008.1 has a *Windows* based, user friendly, interface divided in different customized areas, as shown in the figure below.

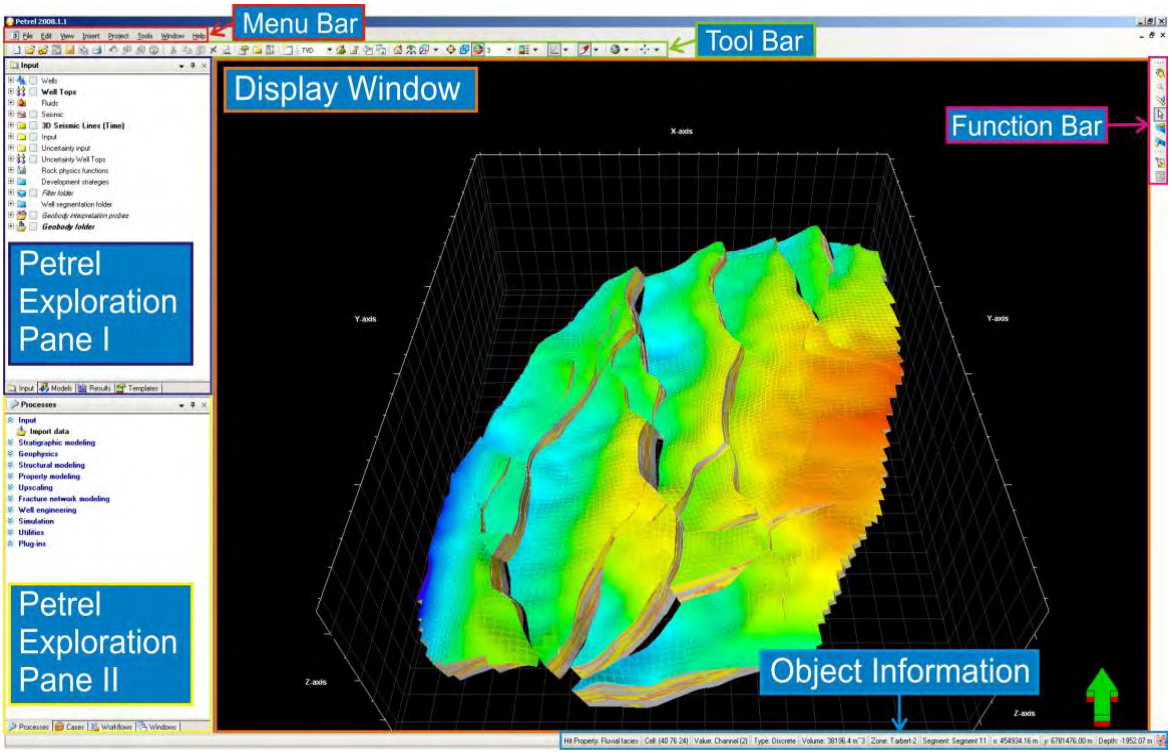

Figure 23 - Petrel 2008.1 user interface.

The display window allows the user to visualize different types of data, considered as objects. The different data are displayed in the correspondent type of window (Figure 24) depending on their type. Seismic data can be displayed in a 3D, 2D or in an interpretation window.

Petrel Exploration Pane I (PE-1; Figure 25a) contains all the data within the project organized in a tree structure. All data not related to a 3D grid is stored in the *Input pane,* while data related to a 3D grid is located in the *Models pane*. The *Results pane* stores the numerical results of volume calculations and simulation computed from the modeled reservoir. *Petrel* uses templates to display data and data properties. Those templates, or colour scale bars, are saved inside the *Template pane* catalogued in folders by type. More information about templates can be found in the following section.

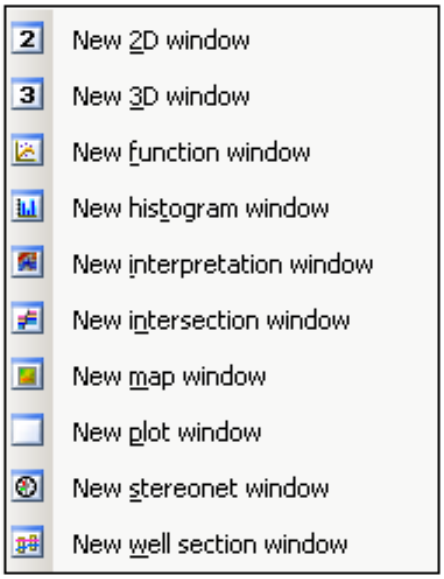

Figure 24 – Example of available windows in *Petrel* 2008.1.

Exploration Pane II (PE-2; Figure 25b) is located below PE-1 and contains the *Processes diagram pane*, where all available processes are stored by the order they should be performed to build a reservoir model. The *Workflows pane* is where workflows, a sequence of pre-designated tasks created by the *Process Manager* are saved. The *Cases pane* is used when a volume calculation is performed. Finally, the *Windows pane* has information about all the opened windows within the project.

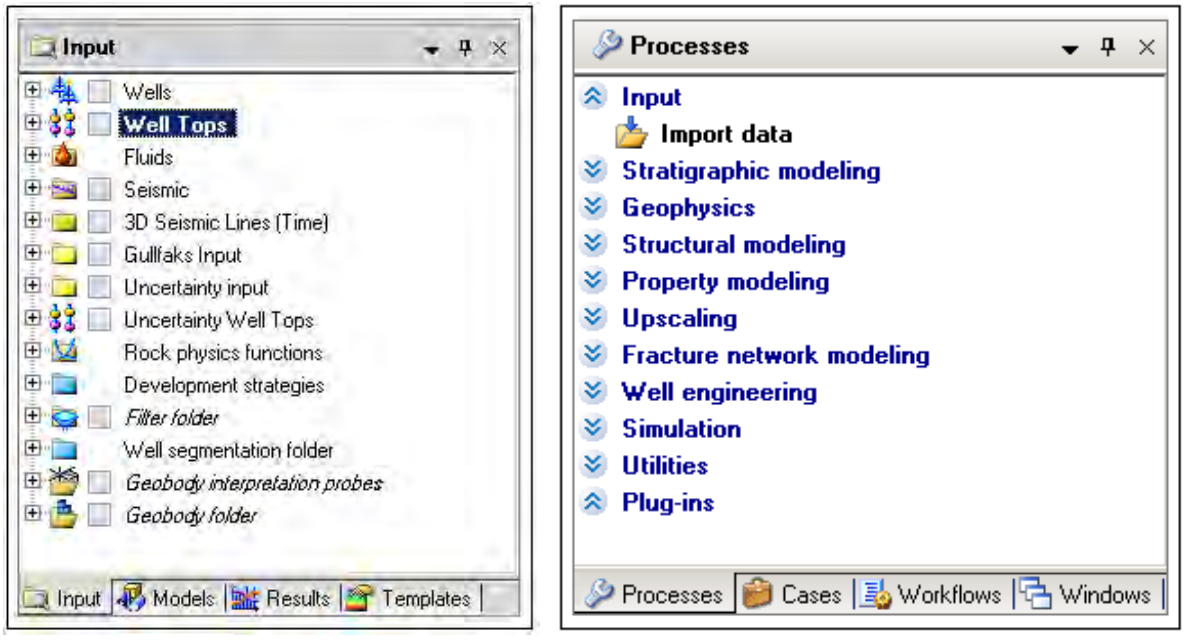

(a) **(b)**

Figure 25 – (a) *Petrel* Exploration Pane I; **(b)** *Petrel* Exploration Pane II.

The *Function bar* is placed by default on the right side of the display window and is related to the Processes diagram pane. When a process is active (highlighted) available tools to accomplish the process will be shown in *Function bar*.

III.1.2. Templates in *Petrel* 2008.1

The way how Petrel displays objects and object properties is through templates (Figure 26a). Templates are defined as objects which contain information about the colour table settings and the correspondent opacity curve common to groups of similar data.

Each template is by default already connected to a group of data and is organized inside the *Templates pane* by folders (Figure 26b). To display an object correctly, the template can be visually tuned by to the user in two ways: by accessing templates properties through clicking the right mouse button (RMB) on a template, or by selecting the desired object and accessing its settings. In both cases it should be kept in mind that templates are assigned to groups of similar data objects. If a template is changed for one object, this modification will affect the display of all the objects under the same template. To edit the template in a specific object the user should click on the padlock, inside objects settings, (Figure 26a, top) or make a copy of the template, edit it and assign it to the desired object (Schlumberger, 2008).

The user is free to create a totally new colour range scale, transform continuous templates into discrete ones and vice-versa. For example, constraining the maximum and minimum values displayed or adjusting the colour scale range, can be useful to enhance hidden features. This method is widely applied in seismic attributes analysis to withdraw the maximum information from the data.

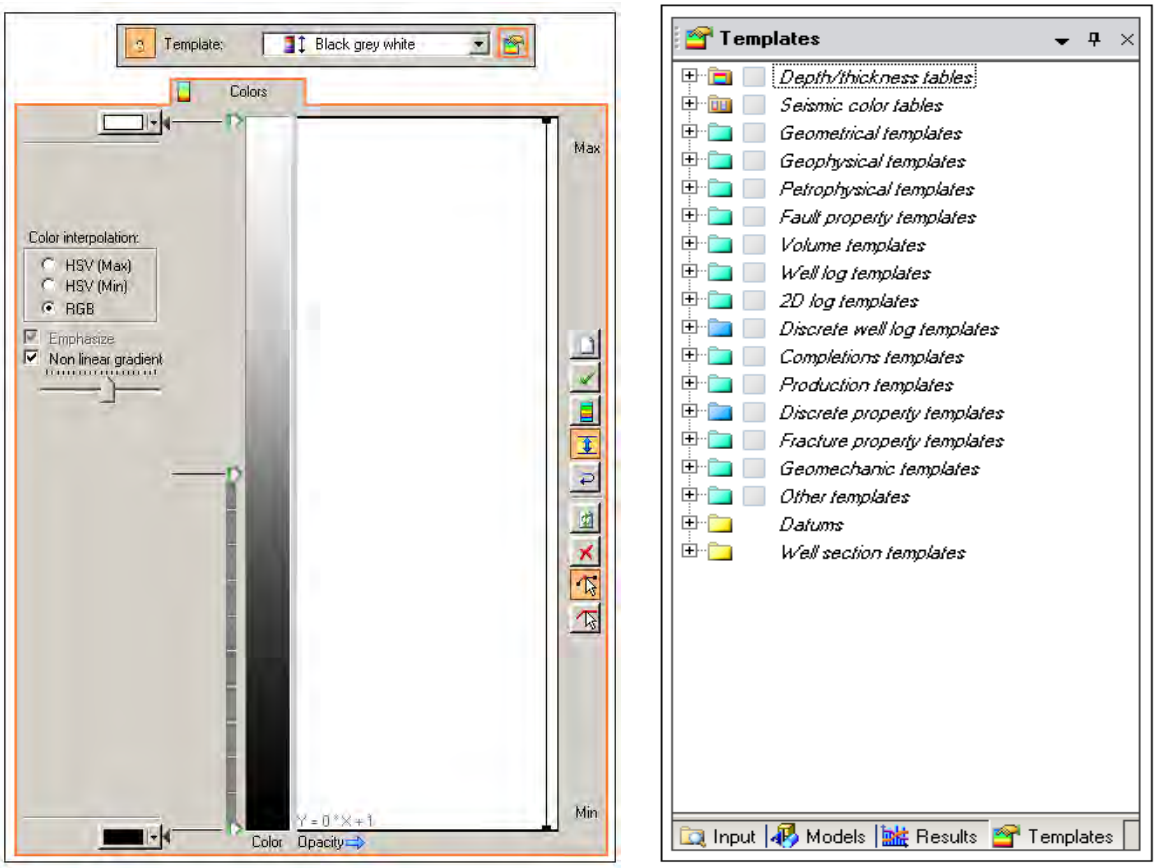

(a) **(b)**

Figure 26 - (a) Colour scale bar and opacity curve inside templates properties. To change a template for just one object, the padlock, on objects setting, should be activated. **(b)** Several templates, divided by folders, can be found under the *Templates pane* in PE-1.

III.1.3. Importing Seismic Data

Seismic attributes, which are the main topic of this thesis, are computed from previously loaded seismic data in *Petrel*. This section discusses how seismic data is imported into a project and what kind of seismic files formats are supported by *Petrel* 2008.1.

Both 2D and 3D seismic data can be loaded into *Petrel* 2008.1, in standard SEG-Y format or in ZGY (internal) bricked format.

SEG-Y is a standard binary format, created by the Society of Exploration Geophysicists (SEG) in 1973. This format was created with the purpose to become a standard between the seismic data from different oil companies which in

the past used proprietary formats (Barry *et al*., 1975). Nowadays, most of the seismic data exchanged between oil companies is recorded in SEG-Y format (Gaillot jr., 1994).

The original SEG-Y format has a *reel identification header* which consists of 3600 bytes, divided into two parts: *the EBCDIC header*, with 3200 bytes, where information about the survey and about the acquisition parameters are recorded, and one *Binary header* with 400 bytes. Within these 400 bytes, 60 are assigned to seismic data information and the rest 340 bytes can be user-assigned to additional information. The rest of the SEG-Y file is filled with "n" *Trace Data Blocks*, corresponding one for each recorded trace. 240-bytes are saved for each *Trace header*, where information about the position of the trace is recorded. The rest is kept free to record the seismic signal. For detailed information about the SEG-Y format it is suggested reading the "*SEG Technical Standards*" (Barry *et al*., 1975).

SEG-Y files can be loaded into *Petrel* in two different ways. If the user is sure that the data is saved in the right byte position according to the standard SEG-Y file format, the seismic data should be loaded as "*SEG-Y seismic data*". If the user is not sure about how the data is organized, seismic data should be imported as "*SEG-Y import with present parameters*". In this way the user can specify the correct byte location for each acquisition parameter. Byte locations within the file can be checked in the "*SEGY headers from first file*" (Figure 27).

With the correct byte positions defined, before finishing the loading process, it is preferable to do a scan of the first "*n*" traces to quality control the imported data (Figure 28). This last step is very important and the final result should match the acquisition parameters such as inline/crossline relative positions and separation.

ZGY extension is a *Petrel* internal *bricked* format for 3D cubes or binary format for 2D seismic data. In this format the seismic data is stored under *bricks* (instead of being stored in the traditional trace format) which allow big datasets to be easily accessed and manipulated. Big *bricks* with low resolution are loaded first into memory, after which the program will start loading smaller bricks with higher resolution. Using this method, large volumes can be loaded and rendered in a 3D

view, allowing the user to interact with the data at any time, since the loading of smaller bricks is stopped if the user moves the view (Schlumberger, 2007b).

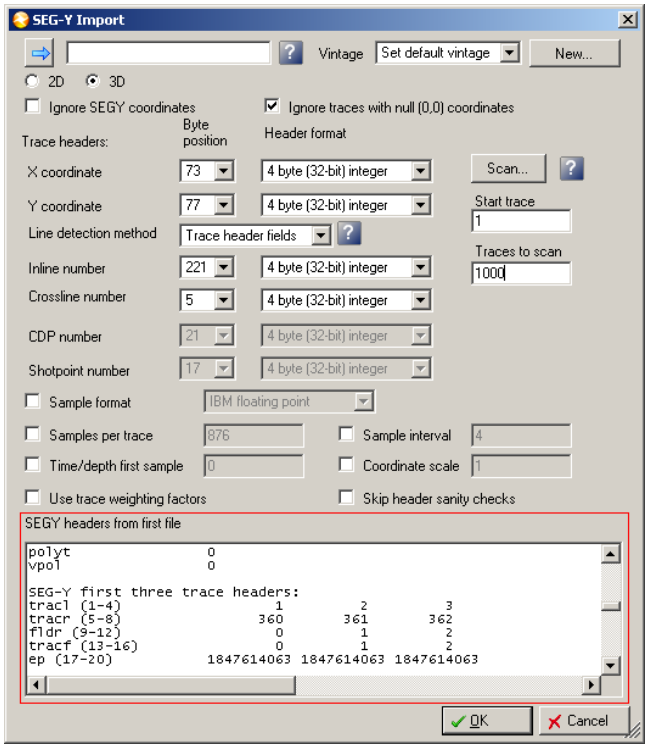

Figure 27 - Dialog box to import SEG-Y files in *Petrel* 2008.1.

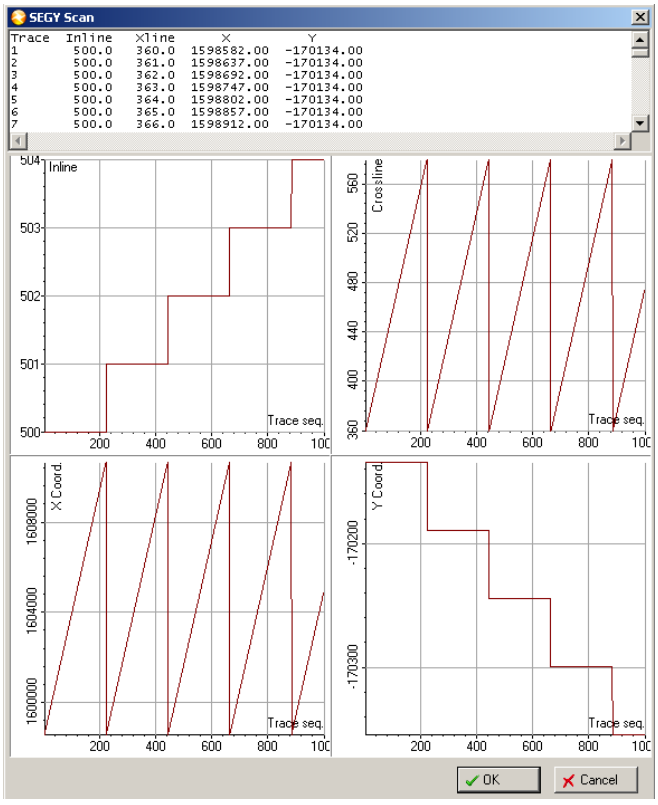

Figure 28 - Scan of the first 1000 traces to quality control the imported SEG-Y file.

It is preferable to use ZGY format within *Petrel* rather than standard SEG-Y format, especially for big datasets with high resolution. ZGY files can be exported into SEG-Y to be used in other applications. SEG-Y files can be internally converted in ZGY files using the *Realize function* (see Section III.1.4).

III.1.4. Realize Seismic Cube

The process within *Petrel* which allows the user to create a physical copy of a seismic volume or a 2D seismic line is called *Realization*. *Realization* is mainly done for three purposes: (1) to allow the user to create a physical copy from virtual seismic data; (2) to permit to change data resolution; (3) to convert SEG-Y files into ZGY format (Schlumberger, 2007b).

Creating virtual cropped seismic data or seismic attributes cubes is a solution in order to save disk space and test different parameters without wasting time. Virtual data is efficient to display 2D seismic lines or vertical seismic section of a seismic cube. In contrast, to perform quick slicing (on time) or to render a volume it is necessary to use a physical copy of the data; this will increase the access time to the data but will also create a new ZGY file, with large size, on the hard disk (Schlumberger, 2007b).

Petrel also allows changing the seismic data from 32-bytes floating point to 16-bytes or 8-bytes, which represents, respectively, a file size smaller 50% or 70% than the original. Changing the resolution is not critical for many operations; however, seismic data should always have 32-bytes resolution if it will be used in the automatic interpretation processes. If lower resolution is chosen, the volume will not have enough dynamic range[10] to perform a quality event tracking (Barnes, 2000; Schlumberger, 2008).

[10] Dynamic Range is the ratio of the largest measurable amplitude to the smallest. It can be mathematically defined as: $20*\log_{10}(A_1/A_2)$.

Finally, the last purpose is simply to create a ZGY file format from a SEG-Y file. The advantages of using this kind of data in *Petrel* have already been discussed in the previous section.

To access the *realization operation* the user has to choose the settings menu for the respective seismic data object and select the *Operations* tab (Figure 29) followed by a click in "*Set from source as shown above*" and finally the "*Scan"* button. This first sequence of steps will perform a scan of the values within the data and display the result in one histogram. The *Filter Bins* option should then be selected to exclude the maximum spike, often related with null values, in the histogram. Removing this effect has special importance when the realization process is being done for a seismic attribute volume (Schlumberger, 2007b).

Realization can be very time-consuming and heavy, in terms of computation, and may need a large amount of free disk space, although it runs in background allowing the user to continue using *Petrel* for other tasks.

It should be kept in mind that *realization* should always be done for large seismic volumes for an easier manipulation and visualization. The output resolution will depend on the purpose of the data.

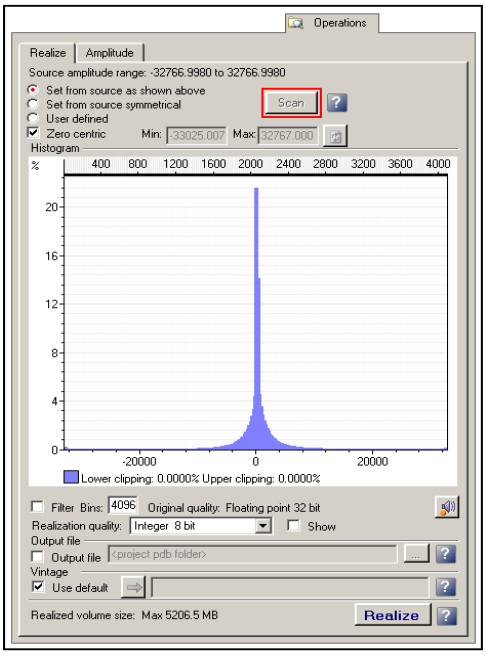

Figure 29 - Realization process dialog box.

III.1.5. Computing Seismic Attributes in *Petrel* 2008.1

There are two processes to compute seismic attributes in *Petrel* 2008.1 and they can be found in PE-2, under the *Processes pane* inside the *Geophysics* family (Figure 30). The available seismic attributes are divided into *volume* and *surface* attributes. Each process has the available attributes organized by several libraries (Figure 31) which attempt to group attributes with similar outputs.

Volume attributes are those computed from an entire 3D seismic cube resulting in a new seismic cube containing the attribute information. Surface attributes are the value of the computed attribute from a seismic cube in one surface, created from seismic interpretation, or in between two surfaces, or between a surface and a constant time window.

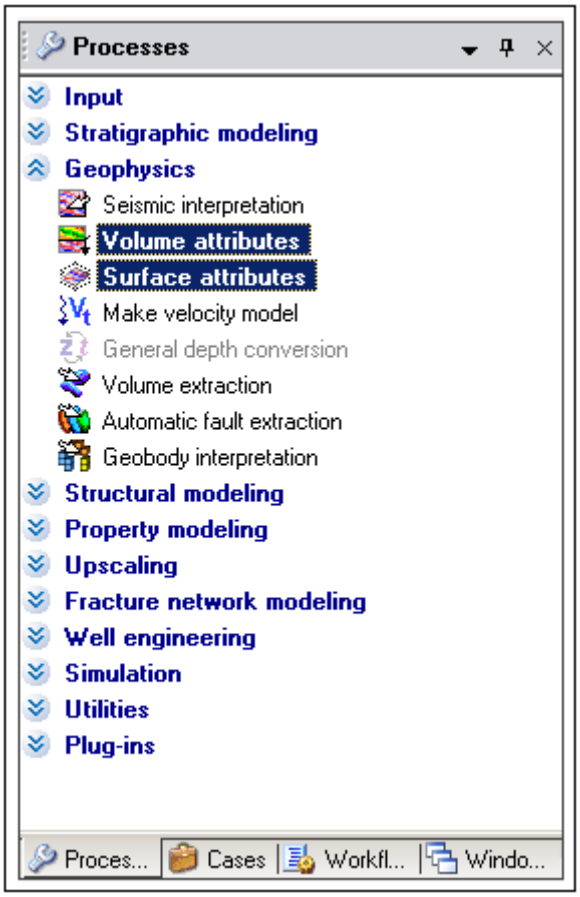

Figure 30 - Volume and Surface attributes processes that can be found under the *processes pane*, in PE-2.

Volume attributes are divided into five libraries and within each library several attributes can be chosen in a total of 29 (Figure 31, left). *Surface Attributes* have an extensive list of 50 attributes which are categorized into four libraries depending on how they are computed: *Amplitude*, *Statistical*, *Signal Shape* and *Measurable Interval* (Figure 31, right).

Depending on the algorithm for their calculations, seismic attributes may have, or not, user-defined parameters which will be taken into account when the algorithm is applied, in order to achieve the desired output data with the best quality possible. In all user-defined parameters *Petrel* always suggests a value by default which in many cases is suitable for the expected result.

Apart from the catalogued attributes, a myriad of attributes can also be calculated with *Petrel*'s *Seismic Calculator*. This tool allows the user to create new versions of seismic cubes by user-defined formulas. The new attributes seismic cubes are generated based on already existing and realized cubes.

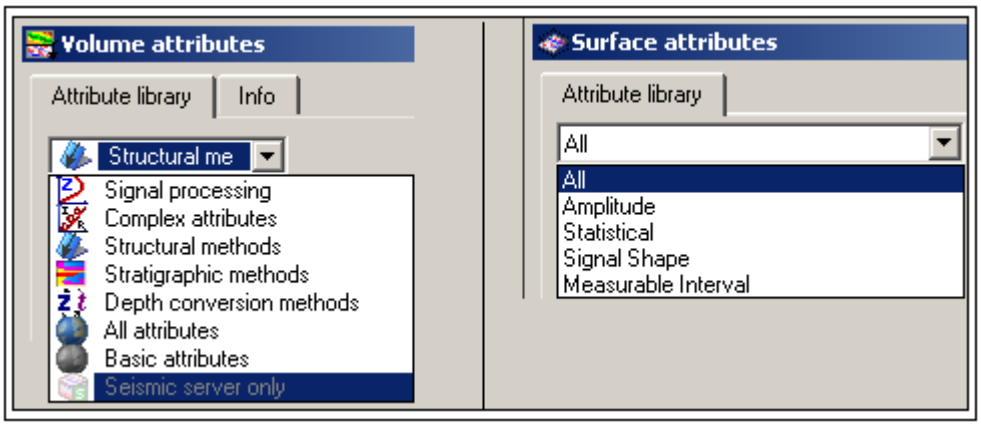

Figure 31 - Volume attributes libraries (left) and Surface attributes libraries (right).

Chapter IV. Seismic Attributes in *Petrel* 2008.1

The use of seismic attributes has passed through periods of great proliferation and enthusiasm contrasting with moments of disuse and lost in credibility (Figure 32). These oscillations are closely dependent on the technological development and what geophysicists think about them (Chopra and Marfurt, 2005). This chapter reflects how seismic attributes, in particular the available in *Petrel* 2008.1, are understood today.

To answer the needs of the exploration and production industry intensive studies in seismic attributes have been carried out, mainly due to their potential for hydrocarbon reservoir prediction, characterization and monitoring (Chen and Sidney, 1997). Interpretation workflows for structural geology, stratigraphy analysis and rock/pore fluid properties based on attributes derived from processed seismic data, are now daily routines in oil and gas companies (Chopra and Marfurt, 2005). Recent developments in multi-attributes analysis, combined with self-learning processes (e.g. artificial neural networks) can transform large amounts of data into one single seismic volume with valuable geological information content (Cooper, 2008), shortcutting the heavy interpretation process.

Petrel 2008.1 provides a comprehensive package of both *surface* and *volume* seismic attributes that can be used in every stage of the hydrocarbon reservoir modeling process to reduce uncertainty and complement the available data. In this chapter a small introduction to the most important available attributes in *Petrel* 2008.1 is presented, followed by the application to a case study (Chapter V). The detailed mathematical derivations of the methods are however beyond the scope of this work.

When possible, some best practice, to use in *Petrel* 2008.1, which combine more than one attribute are proposed, in order to achieve a better final result. The order in which the attributes are presented in this thesis tries to combine them into families, depending on the final result of each attribute. Therefore, attributes from the same library with similar results will be introduced one after another with examples from real data.

The described algorithms and theoretical background are based on Schlumberger's booklet *Interpreter's Guide to Seismic Attributes* (Schlumberger, 2007a).

IV.1. Introduction to Seismic Attributes

With the proliferation of many seismic attributes it becomes a challenge to strictly define what seismic attributes are, when they should be applied and how to classify them. These questions remain not totally answered, even for the many authors who dedicated part of their work to solve the disordered situation in seismic attributes classification (e.g. Chen and Sidney, 1997; Taner, 2000; 2001). Nowadays, a consensus has not yet been reached (Barnes 2001).

The definition of seismic attributes given next is a blend of, more or less, accepted concepts present first by Taner (1997; 2000; 2001), Barnes (2001), Chopra and Marfurt, (2005). An attribute, as the name indicates is an intrinsic quality of an object or person (www.priberam.pt). Therefore in the geophysical context, "seismic attributes" are a way to describe and quantify a characteristic content of the seismic data. Quantified characteristics can be directly computed and/or measured from the original data or implied from logical or personal experiences of the user. Attributes are also the rate of change of any of these quantities with respect to time or space, both from pre- and post-stack seismic data. In a nutshell, seismic attributes are new ways to look at the seismic data which conventionally is plotted in amplitudes (www-sst.unil.ch).

Seismic attributes emerged to transform the subjective and experience based interpretation process into something less tedious, and more objective. They try to mimic the interpreter's expertise, by automatically identifying and correlating seismic events with real geological features (Chopra and Marfurt, 2005). Today, seismic attributes are added values for structural, stratigraphic and texture analysis, and in facies and hydrocarbon reservoir properties prediction, when correctly used by an expert user (e.g. Taner, 2001; Barnes, 2001; Sheline, 2005; Chopra and Marfurt, 2005). Seismic attributes analyses are not a new concept in the seismic world; in fact, attributes derived from seismic data are around since the beginning of exploration seismology, in the 1950s (Chopra and Marfurt, 2005). So, why was it just in the last few decades that attributes saw their importance grow? Cooper (2008) attributes this late development to the traditional resistance in the oil and gas industry to the introduction of new concepts and methods.

The enormous number of different seismic attributes has mainly proliferated since the 1970s (Figure 32). This "*boom*" of attributes came about especially after the introduction of coloured seismic sections by Balch (1971), following the work of Taner *et al.* (1979) on complex seismic trace analysis (see IV.3.2), and lastly by the generalization of 3D seismic data and interpretation workstations (Barnes, 2001; Chopra and Marfurt, 2005; Cooper, 2008).

Nowadays, with the advances in seismic interpretation technology, seismic attributes analysis has became vulgarized, leading in some cases to the abuse and wrong use of this valuable tool (Sheline, 2005). The seismic interpreter should not stop searching through the suite of available attributes in his interpretation workstation after finding one attribute that shows the feature he wants to see. The user should use one attribute for each property or feature of interest and combine them through geostatistics or other multi-attribute analysis tool, to check the correlation between the different attributes (Chopra and Marfurt, 2005).

Historically, attributes are divided depending from where they are derived, how sensitive they are to the geological background of the data and if they are direct

hydrocarbon indicators (DHIs, e.g. a *Bright Spot*[11]; Chen and Sidney, 1997).

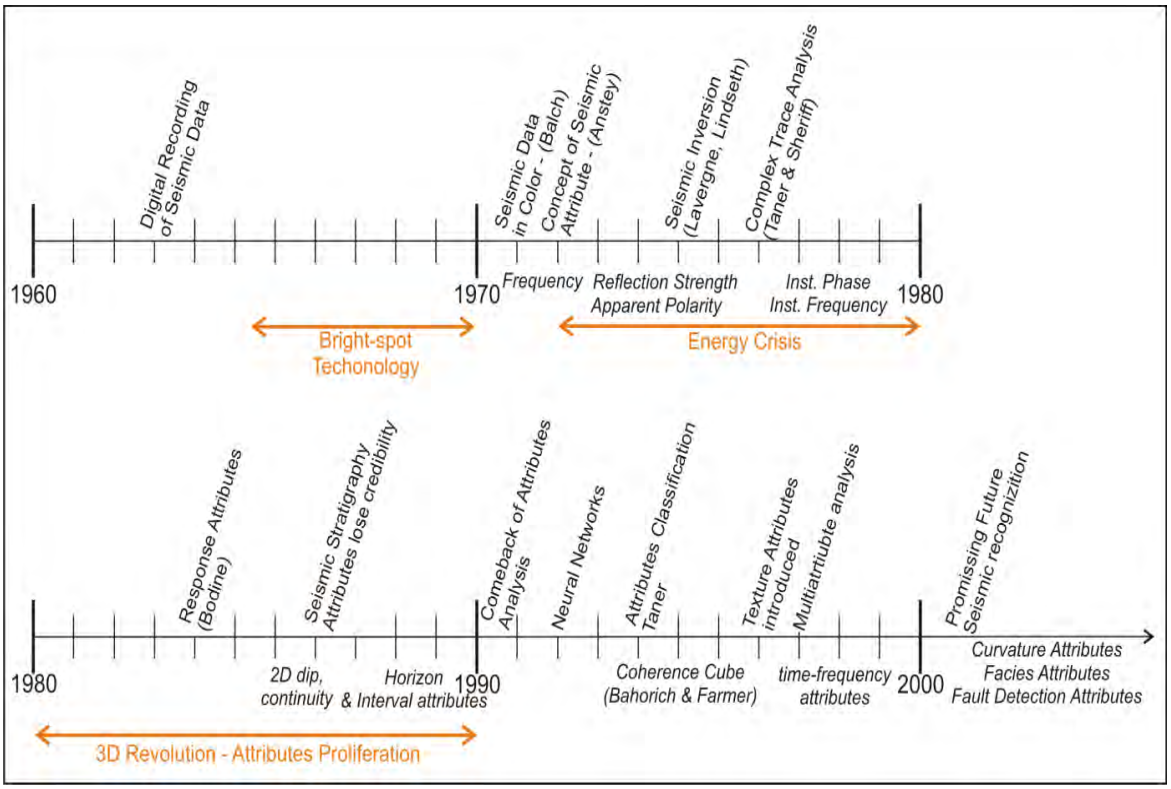

Figure 32 – Time line of seismic attributes development (in italic) and their relation with advances in seismic exploration technology, from 1960 to the present. Key works are represented by their authors' name (Modified from Barnes, 2001).

Attributes with the most predictive results are those derived from the various seismic wavelet components. The amplitude content within the data effectively provides physical parameters about the subsurface such as acoustic impedance, reflection coefficients, velocities and absorption effects which supply structural detail or act as DHIs. Phase content is used to determine the shape and geometry of reflectors and it is an important attribute to improve seismic reflectors continuity and for the interpretation of seismic stratigraphy and depositional regimes (Taner, 2001; Brown, 2001; Chopra and Marfurt, 2005). Frequency derived attributes are useful in stratigraphic events, fault interpretation due to absorption effects, as DHIs, in forecast of reservoir properties, and when combined with amplitude-based attributes, they may help in the interpretation of additional geologic layering (Brown, 2001).

[11] A bright spot is an amplitude anomaly within the seismic data that can indicate the presence of hydrocarbons.

A real implementation of multi-attribute analysis is the next step in the seismic attributes domain. With multi-attribute analysis, improved spatial coherence of depositional events, such as ancient channels systems, is just the beginning of what can be reliably predicted (Cooper, 2008). The ultimate step, especially for areas where well log data is unavailable, is a real and effective estimation of facies distribution and prediction of hydrocarbon reservoirs properties based mostly on seismic patterns recognition and correlation (Barnes, 2001; Chen and Sidney, 1997).

In exploration seismology, seismic attributes can be considered a turning point in seismic interpretation. Seismic attributes allow obtaining accurate detailed information on structural, stratigraphic and lithological parameters of the seismic prospect (Taner, 2001) as an integrated solution (Cooper, 2008) for hydrocarbon reservoir identification, modeling and characterization with reduced uncertainty (Sheline, 2005). At the limit, the main issue is not the attributes themselves but their application, which should be carefully chosen. The desired geologic features to be enhanced should be first clearly defined by the interpreter. An attribute should not be used just because it is available as a software tool. In multi-attribute analysis, attributes should be first correlated to detect if different attributes will not enhance the same result. For instance, using too many attributes can generate geostatiscal errors in hydrocarbon reservoir properties prediction (Sheline, 2005).

Lastly, apart from a careful and adequate attribute choice, with the right user-defined parameters, the associated colour scale range with which they will be displayed is also a very important aspect (see Section III.1.2). The quality of one attribute will be dependent not only on the quality of the original seismic data but also in the colour scale bar used to display the attribute. The correct display allows the human eye to detect and distinguish subtle changes which may be associated with interesting features (Lynch and Lines, 2004). As a last concern, seismic attributes should not be applied as recipe, expecting the same result to be always achieved independently of the input data and the geological background. Indeed, it is necessary to first understand the data and realize first which features will be potentially enhanced by the seismic attribute.

IV.2. Classification of Seismic Attributes

With the increasing interest on seismic attributes and their large number and diversity it now becomes necessary to catalogue them into different classes. Many proposals have been put forward with the aim of classify seismic attributes in a tight, strict and intuitive way, based on both the input and the expected result. Unfortunately, new attributes appear every day and algorithms of well known attributes can be improved since sometimes they give unexpected results. The proposed classifications are constantly changing, depending on the understanding of the seismic attribute today (Taner, 2000).

Taner *et al*. (1994) were the first to introduce a coherent and real classification for seismic attributes. They created two general categories for seismic attributes: *geometrical* and *physical*. *Geometrical attributes* enhance geometrical characteristics of the input data such as: dip, azimuth and continuity. *Physical attributes* are related to physical properties of the subsurface which are inextricably connected to the lithology. This family of attributes corresponds to attributes derived from amplitude, frequency and phase components of the trace. These two categories can further be divided into prestack and poststack, depending on the data processing step from which they have been computed.

Brown (2004), in Chopra and Marfurt (2005), proposed to classify attributes using a tree structure with branches for time, amplitude, frequency and attenuation, with each branch being further divided in prestack and poststack attributes. Time attributes provide information about structural geology while amplitude attribute give information on stratigraphy and reservoir properties.

The Chen and Sidney (1997) classification divides attributes in two main groups: one based on wave kinematic/dynamics, and the second group based on geologic reservoir features; further sub-divisions depend on where the attribute is extracted and on the expected output.

More recently, Chopra and Marfurt (2005) based on classifications from other authors, proposed a new classification for seismic attributes. The classification divides attributes into: *general*, *specific* and *composite*. *General attributes* comprises seismic attributes which measure geometric, kinematic, dynamic or statistical features derived from seismic data. They are related either to the physical or morphological character of the data since they represent the response of a specific lithology. Therefore they can be generally applicable to different geological environments with expected similar outputs. *Specific attributes* are less correlated to the lithological character of the input data and therefore cannot be extrapolated to similar geological environments, since their response is intrinsic of specific hydrocarbon reservoir properties. *Composite attributes* include sums, products or other combinations of more fundamental general attributes.

Petrel 2008.1 does not follow any of these classification schemes, as discussed before. It uses a new and more user-friendly classification for seismic attributes. Attributes are first divided into *volume* and *surface* attributes, depending on the input data, and then into *libraries* (Figure 31). Each library groups attributes which will enhance similar features.

IV.3. Volume Attributes

Volume attributes are computed from processed seismic cubes or from previously computed attribute volumes which are extracted, depending on the mathematical algorithm, trace by trace or considering a group of traces (multi-traces). The extraction is performed over a user-defined fixed window, where two horizontal time slices are defined as upper and lower boundaries.

The single-trace method is applied when the computation algorithm operates in each trace separately between a vertical fixed window. Attribute extraction is done within the user-defined window length in a random position, inside the seismic volume. The extracted attribute is then saved in one time slice, which will be placed in a central position inside the window interval. The final attribute volume is the result from repeating the attribute extraction, with the same vertical range, for

different times and spatial positions, and then stacking the resultant slices (Figure 33a; Chen and Sidney, 1997).

Multi-trace seismic attributes are also computed inside a fixed vertical window with user-defined limits. In this case, besides the vertical range, the user has to define a bound in the number of traces that will be used to the attribute extraction, according to a mathematical algorithm. Like in the single-trace method, the output volume is the result of stacking all the time slices were the attribute computation was kept from each window position in space and time (Figure 33b; Chen and Sidney, 1997).

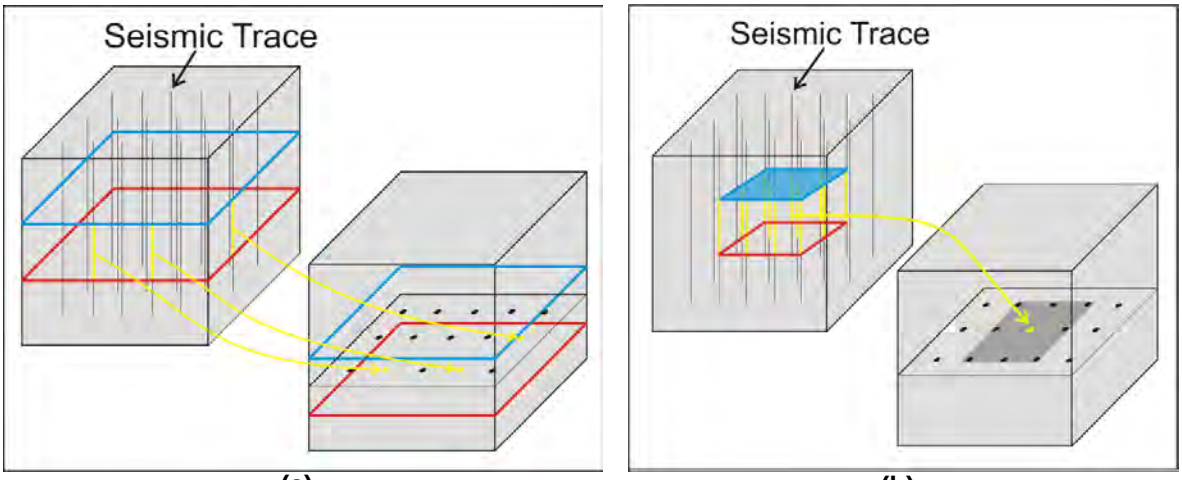

Figure 33 - Seismic attributes can be generated **(a)** trace by trace or **(b)** using a collection of multi-traces. Blue and red squares represent the upper and lower time slice boundary respectively. Traces from where the attributes were extracted are represented in yellow and will be saved in a time slice placed in a central position in the computation window (modified from Chen and Sidney, 1997).

IV.3.1. Seismic Signal Processing Library

In this section a generalized concept of attribute will be used following the definition used in *Petrel* software. As such, frequency filtering and amplitude corrections are considered as seismic data attributes.

Petrel's *Seismic Signal Processing* library includes attributes related to seismic data processing and data display. Attributes within this library are computed according to the chosen method on each seismic trace separately.

Seismic Signal Processing attributes execute small seismic processing steps to help the interpreter, who is not an expert in seismic signal theory, to improve data quality and consistency without the need to re-process the entire seismic data in a special processing software. Available seismic attributes permit the user to improve data quality in certain areas of interest, resulting in enhanced data coherency by modifying the gain in amplitudes, applying basic filtering and through performing phase shifts on the data.

A total of eight seismic attributes are included in *Seismic Signal Processing* library. Three perform phase shifts to the data, useful to match different vintages of seismic data and to improve reflectors sharpness; three other are related to filtering and amplitude tuning; the last two operate in the energy content of the seismic trace.

In all the theoretical description and when describing the mathematical algorithms which are used to extract each seismic attribute, the original seismic trace, also called original amplitude, will be from now on designated by *f*(t).

IV.3.1.1. First Derivative

The *first derivative* attribute is defined as the time rate change of the input trace, or the derivative of *f*(t) with time.

$$FirstDerivative\ (t) = \frac{df(t)}{dt} \qquad \text{Eq. (3)}$$

The *first derivative* of a digitized seismic trace can be approximately calculated by:

$$\frac{df(t)}{dt} = \frac{[f(t-2) - f(t+2)] * 1}{12} - \frac{[f(t-1) - f(t+1)] * 8}{12} \qquad \text{Eq. (4)}$$

Visually, applying the *first derivative* attribute to a collection of seismic traces is the same as computing a phase shift of 90º for those traces. As such, no user-defined parameter is required for this step. *First derivative* can, first, be useful to quality check the signal consistency, since positive or negative picks should produce zero crossings, to improve reflector sharpness, match different versions of seismic data

and improve the correlation between seismic data and lithology-indicative well log data (Zeng, 2005a; b).

Nowadays most of the seismic data is acquired, or processed, to have a constant nearly zero-phase wavelet (Figure 34), which historically is the best type of wavelet to use in seismic interpretation. Indeed a zero-phase wavelet resolves better the top and the bottom of a bed, separated from more than 1/4 of the dominant wavelength, for simple layered models (1/4 of the wavelength is traditionally defined as the maximum value for seismic vertical resolution).

If a 90º-phase wavelet, shifted from nearly zero-phase seismic data (Figure 34), is used, the vertical resolution increases with a decrease in thin-bed interference. In addition, the output volume will have significantly improvements for lithologic, stratigraphic and depositional facies interpretation. Thin layers analysis also become easier because reflectors have increased consistency and sharpness, leading to a better amplitude-lithology correlation (Zeng, 2005a; b).

This method is also effective in thin-bed hydrocarbon reservoirs, which most times are unresolved in zero-phase data, since the fluid anomaly signal is better detected with stronger amplitude and higher stratigraphic resolution; although the original seismic data should have a high signal-to-noise ratio and an original wavelet with small side lobes (Zeng, 2005b).

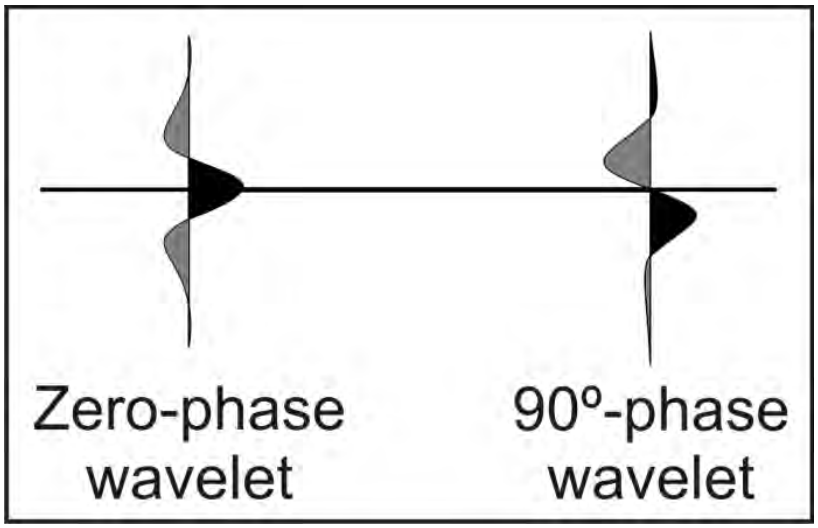

Figure 34 - Zero-phase wavelet (on the left) and 90º-phase wavelet (on the right). Both wavelets are with SEG polarity inverted, black is positive amplitude (modified from Zeng, 2005a).

Visually, comparing 90º-phase (Figure 35b) with nearly zero-phase seismic data (Figure 35a), an increased vertical resolution and sharpness of seismic reflectors can be observed, which are two pre-requisites for thin-bed interpretation. The use of *first derivate* attribute volumes, calculated from a zero-phase seismic data, has proven improved interpretability and can be used as seismic conditioning for automatic picking tools in seismic reflector interpretation, working as an added value to reduce interpretation time-consumption.

Typically the correlation between the seismic and well log data is poor due to the different nature of these two techniques. Well log data is acquired with high frequency sources while seismic data is normally acquired with low frequency[12]. Seismic data processed to have a 90º-phase wavelet better mimics the acoustic log signal, increasing the correlation between the seismic data and lithology-indicative well log data, particularly for acoustic impedance and porosity logs (Figure 36; Zeng, 2005b).

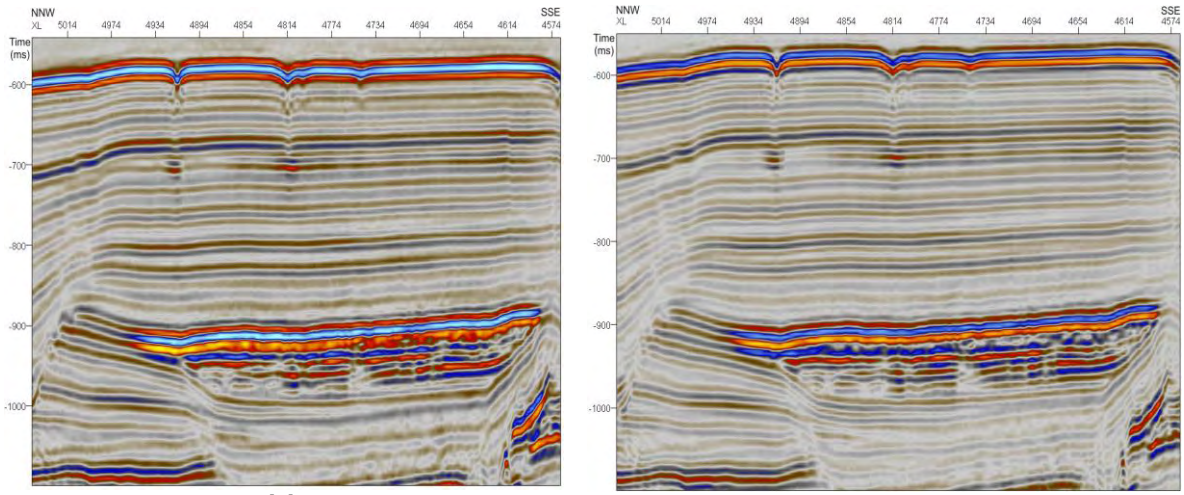

Figure 35 – (a) Original seismic line and correspondent **(b)** *first derivative* attribute. The *first derivative* attribute data shows higher vertical resolution, with enhanced reflectors continuity and sharpness. Peaks in amplitude will produce zero crossings in the extracted attribute.

Computing the *first derivative* attribute twice will produce the same effect as executing the second derivative attribute or, i.e. a 180º phase shift. Another point of interest when applying a first derivative, which will be further discussed in

[12] Low frequency will produce more penetration and less vertical resolution while high frequencies result in less penetration but higher vertical resolution.

Section IV.3.2, is that *Petrel* 2008.1 uses the same algorithm to calculate the Hilbert Transform, for complex seismic trace analysis.

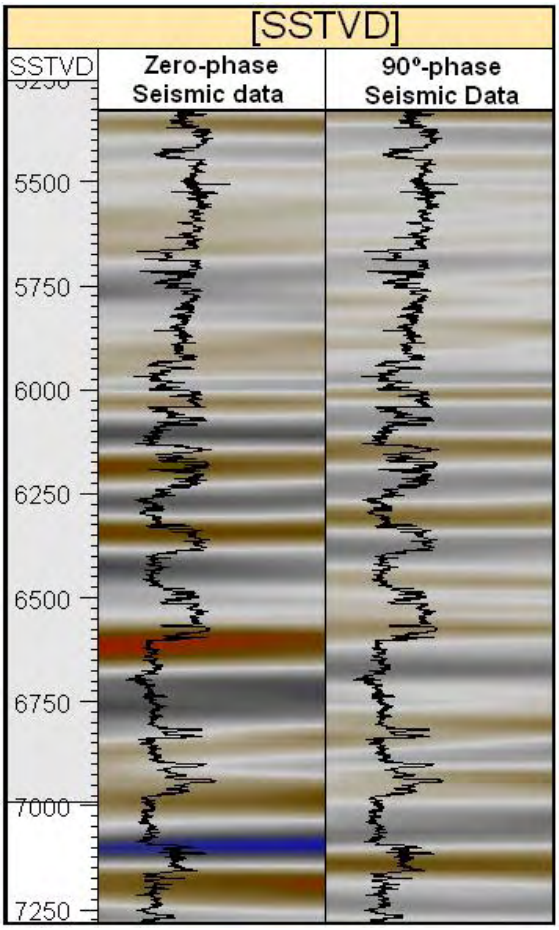

Figure 36 - Porosity log (DPHI)[13] superimposed with nearly zero-phase seismic data, on the left, and superimposed with 90º-phase wavelet (on the right). A generalized better match between seismic data and well log data is achieved when a 90º-phase seismic data is used.

IV.3.1.2. Second Derivative

Mathematically this attribute is defined as the second time derivative of the original seismic trace. Similar to the calculation of the *first derivative*, *Petrel* uses an approximation algorithm to extract this attribute from the original seismic data, Equation 6.

$$SecondDerivative(t) = \frac{d^2 f(t)}{dt^2} \qquad \text{Eq. (5)}$$

[13] DPHI is a density porosity well log data used to estimate the porosity from a formation density measurement.

$$\frac{d^2 f(t)}{dt^2} = f(t-1) - f(t+1) - f(t) * 2 \qquad \text{Eq. (6)}$$

Similarly to the *first derivate*, where a 90º-phase shift of the seismic data is calculated, the *second derivative* attribute performs a 180º-phase shift. Visually, the output volume attribute will have traces with inverted polarity; peaks will become troughs and troughs become peaks (Figure 37). As such, this attribute can be used to match seismic data from the same area which that has been recorded with inverted polarities. Another potentiality of this attribute is to check the consistency of the signal. Computing the *second derivative* twice to the same collection of traces should result in an output cube with the same polarity and consistency as the original seismic data.

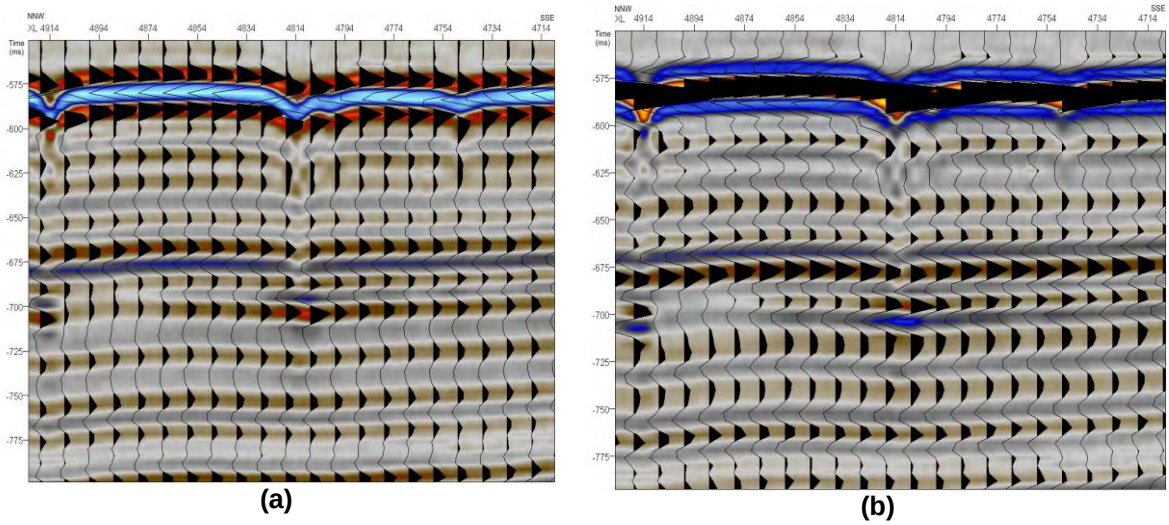

Figure 37 – (a) Original seismic data and **(b)** computed second derivative attribute. The attribute shows inverted polarity when compared to the original seismic section. Seismic data is displayed in variable density superimposed by wiggle variable area display.

Second derivative also improves reflectors continuity and sharpness in areas where reflections are poorly resolved on the raw amplitudes (Figure 38). However, the interpreter should be cautious as lateral amplitude variations will be diminished, which difficult applying automatic picking tools to interpret regional events.

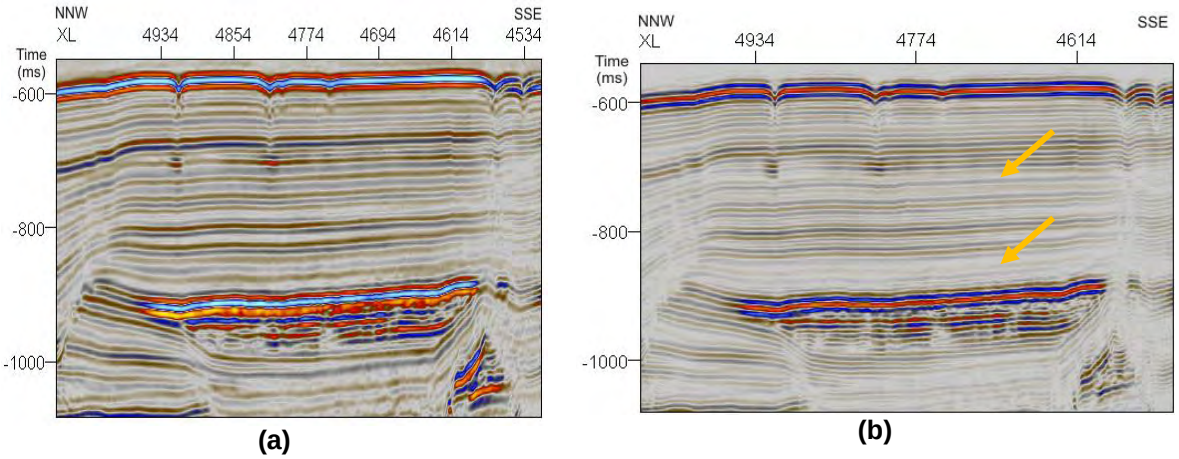

Figure 38 – (a) Original seismic data and **(b)** extracted *second derivative* attribute. Orange arrows show enhanced reflectors continuity for a small area. On the other hand at a larger scale seismic reflectores become more blury.

IV.3.1.3. Phase Shift (Phase Rotation)

The *phase shift* attribute is a user-defined variable phase rotation (or shift) of the original seismic trace in the frequency domain.

This attribute is mainly used to match different vintages of seismic data which have been recorded in different phases. As described before, performing a 90^{o}-phase shift is the same as computing the *first derivative* attribute (see Section IV.3.1.1), and choosing an angle of 180^{o} is the same as generating the *second derivative* attribute (see IV.3.1.2).

IV.3.1.4. Graphic Equalizer

The *graphic equalizer* attribute is as a user-defined frequency band-pass filter that can be applied to attenuate or enhance specific frequencies, or interval of frequencies, in order to improve the signal-to-noise ratio and the reflectors continuity.

In *Petrel* this filtering is executed in the frequency domain by Equation 7.

$$F(\omega) = W(\omega) * |A_{\omega}| e^{i\phi(\omega)} \qquad \text{Eq. (7)}$$

Where $W(\omega)$ is a linearly interpolated frequency sampled weighting function based on user-defined settings. In Equation 7 the frequency signal is represented by its coefficients expressed as magnitude and phase angle (ϕ). ω is the radian frequency.

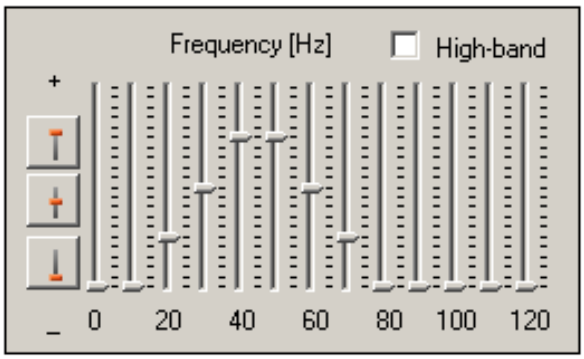

Figure 39 - *Graphic equalizer* attribute sliding control in *Petrel*. Toggling *High-band* on, the frequency range is extended to 250 Hz. The figure shows the parameters used to compute the output result shown in Figure 40.

This weighting function is created interactively in *Petrel* by sliding a control for each tenth frequency on *graphic equalizer* attribute dialog box (Figure 39). The slider position will attenuate, boost or leave the frequencies as they are originally. If the slider is over a value between 0 and 1, frequencies will be attenuated; if the slider is over a value between 1 and 2 the selected frequency will be boosted; at zero, frequencies will be deleted.

Seismic data is usually processed all-in-one with the same processing flow, which sometimes leads to areas less resolved then others. Some of these poorly resolved areas can have interesting features for the interpretation process. The *graphic equalizer* attribute allows the interpreter to filter out some frequencies, increasing the signal-to-noise ratio and improving data quality within those areas. Several band-pass filters with different parameters can easily be created almost on-the-fly, in *Petrel,* and combined in the interpretation process to show different aspects of the same data.

Figure 40 shows an example in which the *graphic equalizer* has been tested. The output seismic section has enhanced reflectors continuity solving ambiguous situations in the interpretation process.

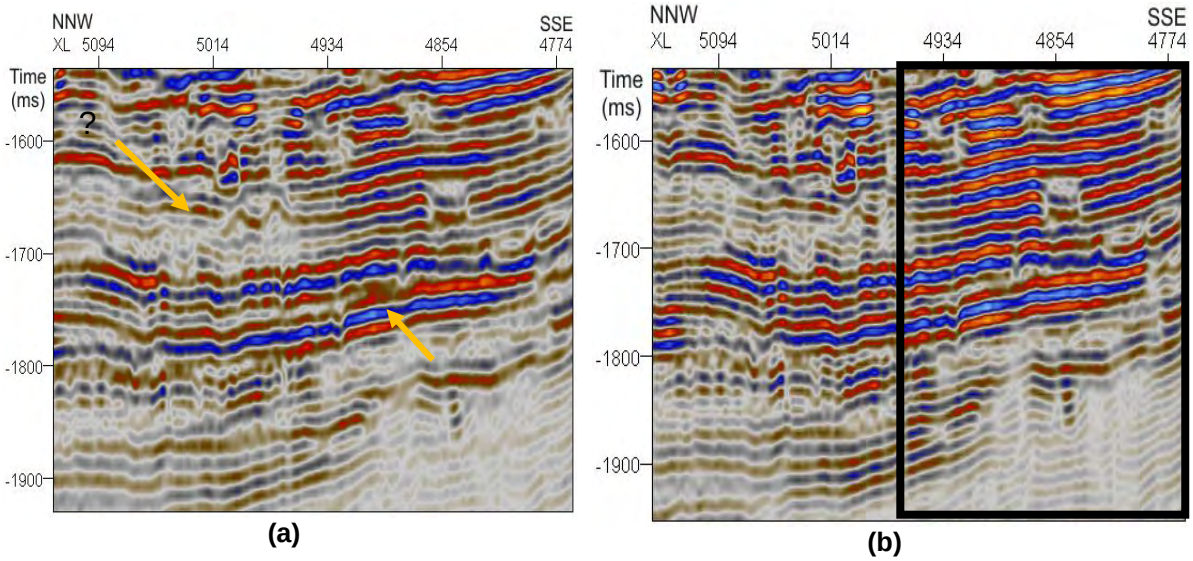

Figure 40 – (a) Original seismic data and **(b)** *graphic equalizer* attribute, computed with settings from Figure 39. Orange arrows point to unresolved seismic reflectors which are better identified after band-pass filtering. Black box is shown in Figure 41.

Highlighting reflectors that are consistent at different frequencies is the proposed workflow to solve ambiguous situations in seismic reflectors terminations (Figure 41).

In a nutshell, the *graphic equalizer* attribute is an extremely useful attribute in *Petrel* 2008.1. It applies different band-pass filters with user-defined frequencies, on-the-fly, allowing the user to test different filtered frequency intervals in order to adjust the data to his needs.

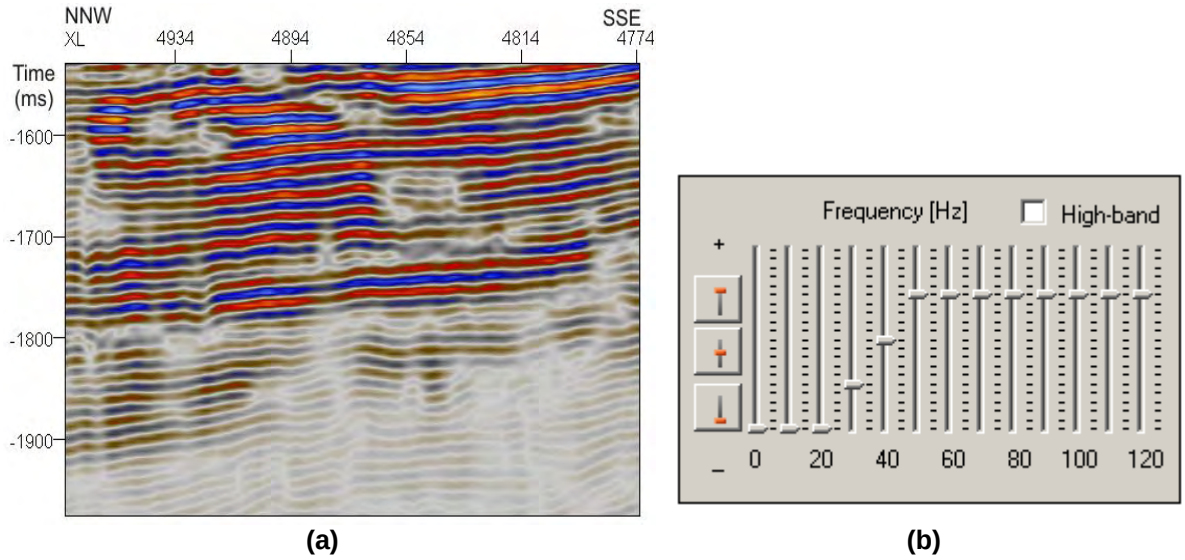

Figure 41 – (a) Seismic section with *graphic equalizer* attribute computed as a high-pass filter, with the settings shown in **(b)**, for the same area shown inside the rectangle of Figure 40b. There is an effective enhancement of seismic reflectors termination.

IV.3.1.5. Time Gain

During the propagation of the seismic energy inside the Earth its amplitude is attenuated with time. Sometimes errors during the seismic acquisition can origin time dependent variation in the seismic amplitudes. These effects are normally compensated with the introduction of a spherical divergence correction in the seismic processing stage. The *time gain* attribute is applied when specific time-dependent corrections are necessary for interpretation.Mathematically the balance of amplitudes with time is computed by the following equation, where α is a user-defined parameter:

$$TimeGain = f(t) * t^{\alpha} \qquad \text{Eq. (8)}$$

Values of *α* bigger than one will produce an increase of amplitudes with time while values of *α* smaller than one will produce a decrease of amplitudes with time (Figure 42).

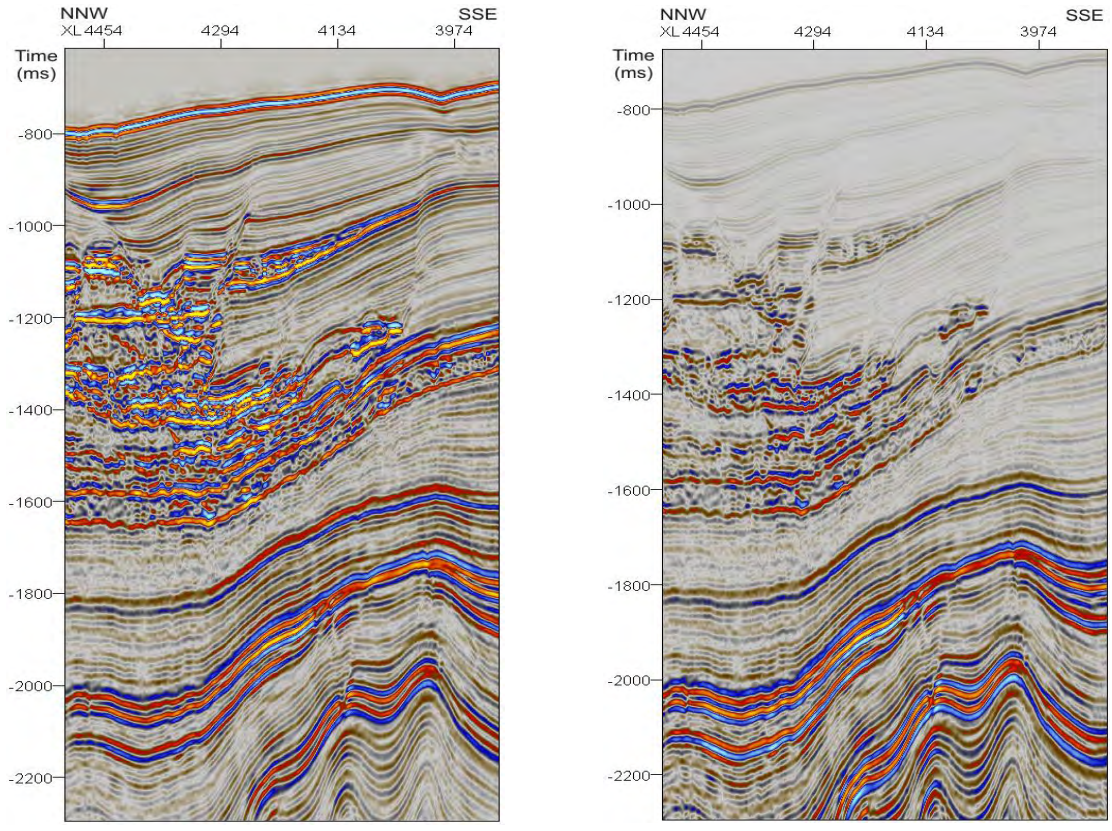

Figure 42 – Seismic sections comparing **(a)** the original seismic section with **(b)** time gain attribute in. Time gain was computed with α equal to 5. The amplitude gain was increased as function of time and amplitudes below the -1800 ms are boosted, relative to the shallower reflections.

IV.3.1.6. Trace AGC

Trace AGC attribute applies the traditional *Automatic Gain Control* (AGC), which was intensively used in the past and directly recorded during the acquisition of seismic data or applied during processing. AGC aims to provide mild amplitudes to all the data, reducing the signal amplitude where it is too strong or increasing it when it is weak (en.wikipedia.org (a)).

The use of AGC should be cautious in particular if the data is too noisy, because amplitudes related to the noise content will also be boosted in order to match the larger amplitudes of the signal. To minimize this effect, it is more adequate to use a seismic volume previously filtered (e.g. a *structurally smoothed* attribute volume; see IV.3.3.4) as an input to compute the *Trace AGC* attribute. This practice produces most of times a good result.

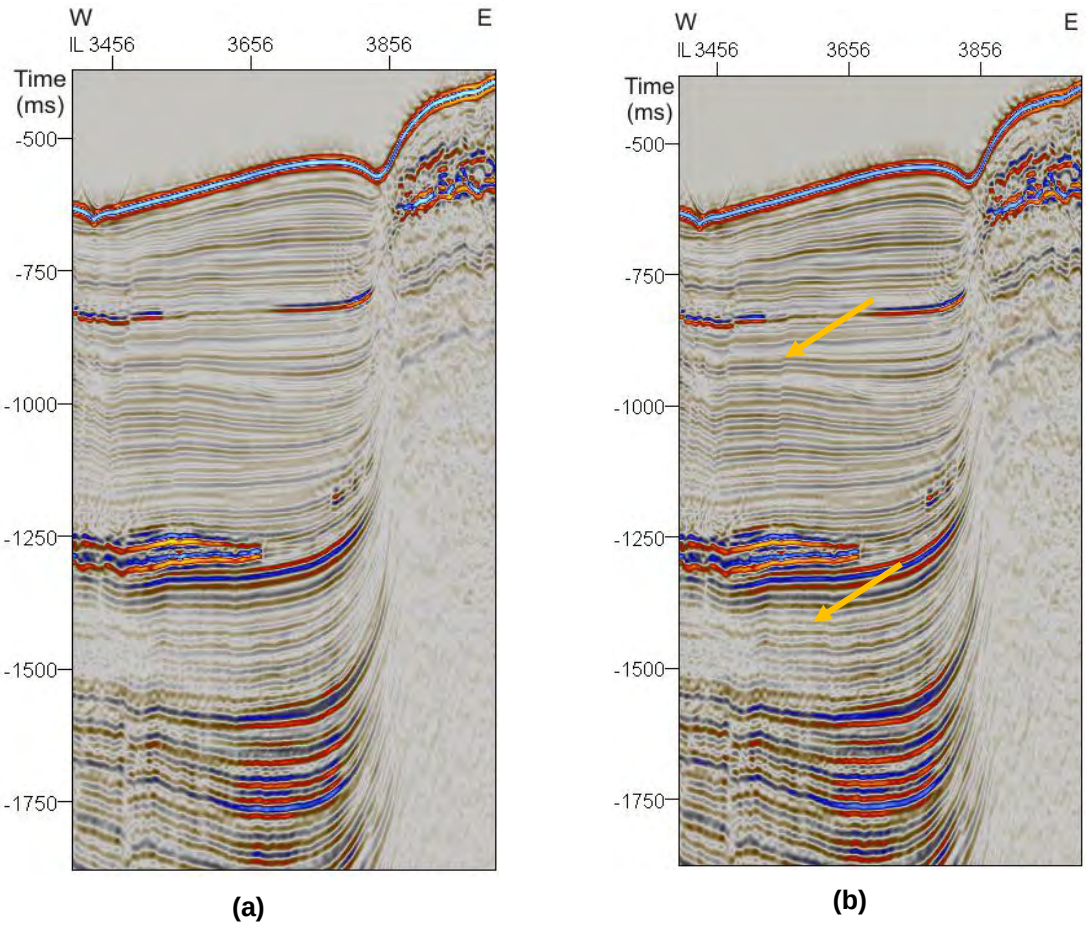

Figure 43 – (a) Seismic section in original amplitudes, and **(b)** respective *trace AGC* output computed within a window of size 9. Orange arrows show reflectors with improved coherency in **(b)**, A general boost of amplitudes is also achieved throughout all seismic section.

Petrel 2008.1 computes *trace AGC* by balancing the RMS[14] level on a moving window with a user-defined length. Mathematically speaking, the t*race AGC* is calculated as:

$$TraceAGC = f(t) * \left[\frac{1.5 - A_{RMS}(t)}{S_{max}}\right] \quad \text{Eq. (9)}$$

Where S_{max} is defined as the maximum amplitude value of the entire survey. The correspondent output data are the amplitude values, scaled with the RMS amplitude over a fixed-size window.

The *trace AGC* output attribute volume often shows improvements in the coherency and continuity of seismic reflectors especially for areas with weak seismic events (Figure 43).

IV.3.1.7. Trace Gradient

The *trace gradient* attribute computes the gradient along a trace between consecutive samples.

$$TraceGradient = f(t + K) - f(t - K) \quad \text{Eq. (10)}$$

Where *K* is the user-defined number of samples.

High values of trace gradient are related with consecutive points having great changes in amplitudes. This attribute is useful to distinguish between seismic units and can be correlated with areas with abrupt changes in lithologies, related to differences in acoustic impedance (Figure 44b).

Displaying together the original seismic data (Figure 44a) superimposed with trace gradient attribute (Figure 44c), with an adjusted transparency curve (on the lower left corner of Figure 44c), produces a sensation of relief of the seismic events. This effect is the same which is experienced when seismic data is displayed with *Petrel*'s "*bump illumination*" option activated (Schlumberger, 2007b).

[14] RMS Amplitude is defined as the "*Root Mean Square*" of amplitude. For further description it is suggested Section IV.3.1.8.

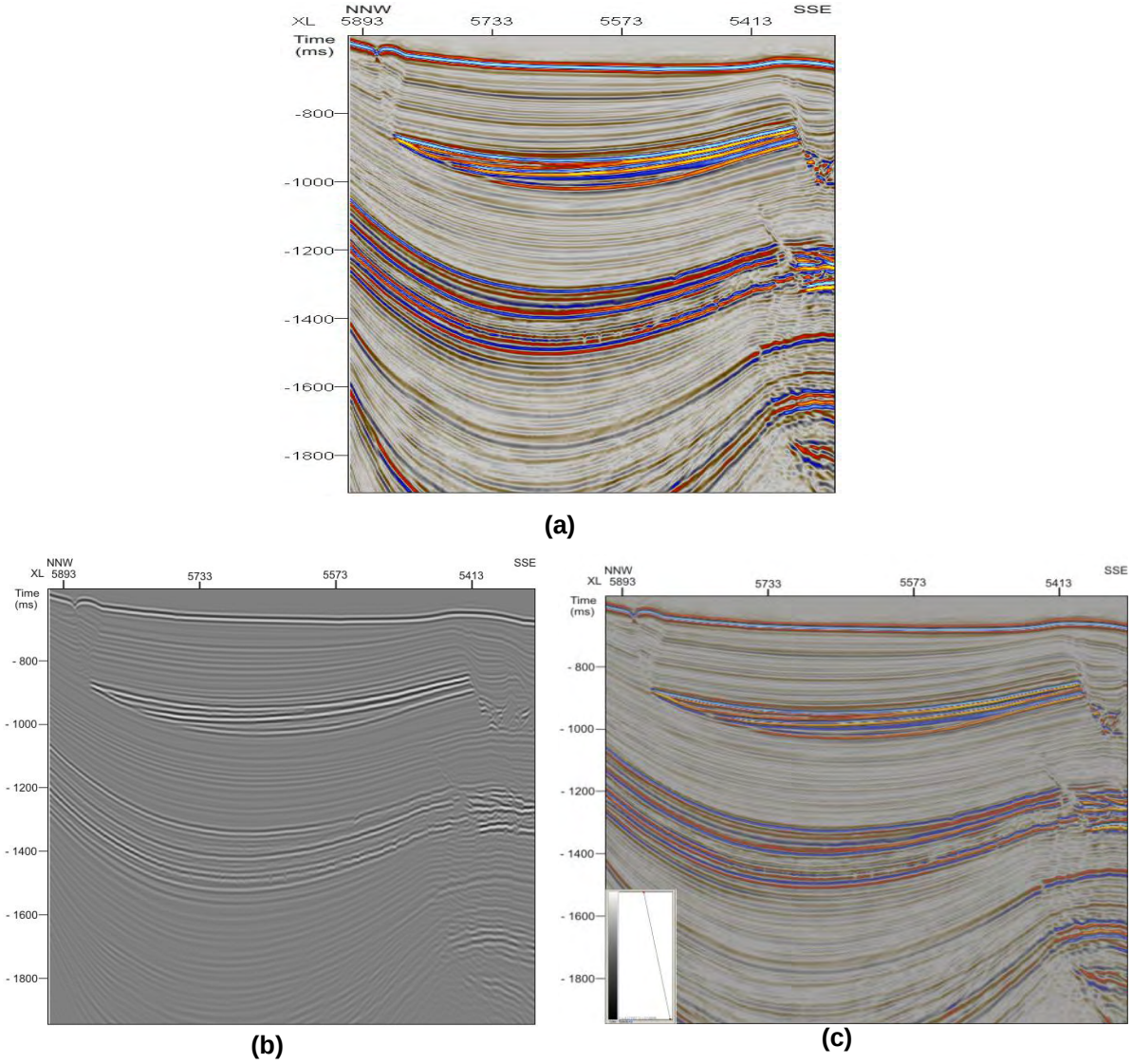

Figure 44 – (a) Seismic line in original amplitude and **(b)** extracted *trace gradient* attribute alone. **(c)** Shows the t*race gradient* attribute superimposed in the original seismic data. The opacity curve used to blend the two attributes is on the lower left corner of **(c)**. *Trace Gradient* is displayed by default in a black-grey-white scale where white represents the maximum value and black the lowest value.

IV.3.1.8. RMS Amplitude

"*Root Mean Square*" (RMS) amplitude is perhaps the most known attribute in the seismic world and by definition it is the "*root mean square*" of the original seismic trace amplitude. The *RMS amplitude* (A_{RMS}) attribute is extracted from the seismic trace within a user-defined moving window with a width of N samples (Equation 11). This attribute gives information about the energy content of the seismic data.

$$A_{RMS}(t) = \sqrt{\frac{1}{N}\sum_{k=-N/2}^{N/2}(f(t+k))^2} \qquad \text{Eq. (11)}$$

Typically, attributes related to the energy content of the seismic trace are used to distinguish different kinds of lithologies (Figure 45). High values of *RMS amplitudes* are commonly related to high porosity lithologies, such as porous sands, which are potential high quality hydrocarbon reservoirs.

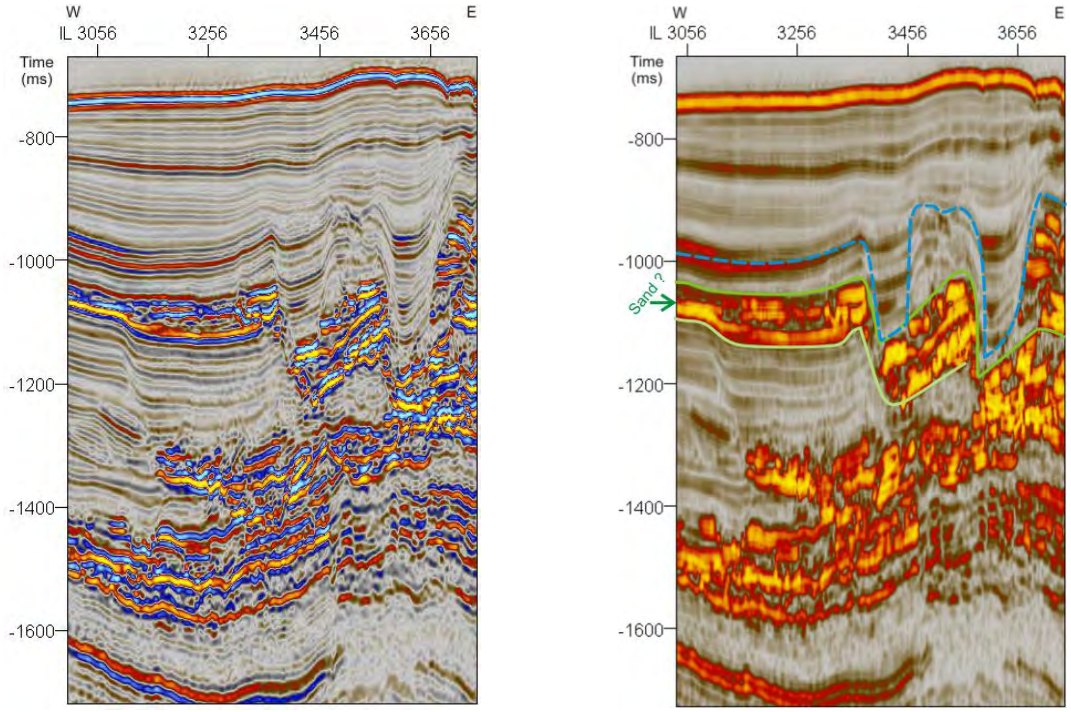

Figure 45 – (a) Seismic section displaying original seismic data and **(b)** extracted *RMS amplitude*. Based on the energy content of the seismic data, different packages of lithologies are more easily differentiated. The vertical interval bounded by the two green lines corresponds to a deep-sea channel complex.

In oil and gas industry, *RMS amplitudes* are traditionally computed as a surface attribute or in strata slices (Zeng *et al*. 1998) to build attribute maps. Computing the *RMS amplitude* attribute for an entire seismic cube enables the user to look at the data in a different perspective. Rendering a *RMS volume* attribute where only high values are displayed as in Figure 46, for example, can be used to interpret ancient channels systems and in the recognition of bright spots.

The size of the window where the attribute is extracted is a key factor in RMS amplitude attribute. Small size windows will show local geologic effects and not the

desired effect of anomalies with high values of RMS amplitude; large size windows will integrate energy from different sources and anomalies will not be distinguished.

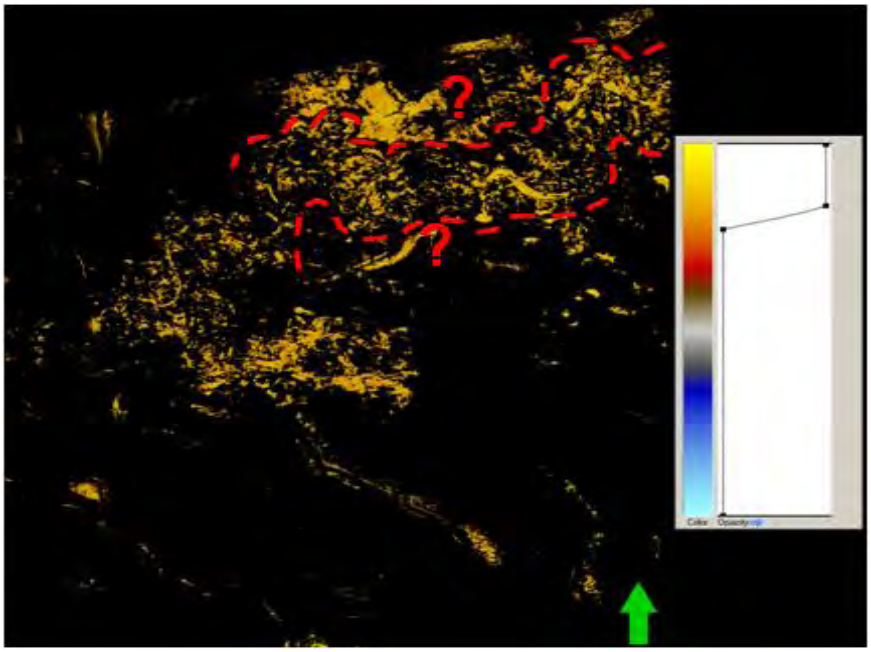

Figure 46 – High *RMS amplitudes* in the whole 3D seismic cube viewed from above (all *RMS amplitudes* below a certain threshold – see inset in figure – were hidden). High amplitudes (in yellow) define a complex of ancient meandering channels (between the two red dashed lines). Sand channels are traditionally high quality hydrocarbon reservoirs. The opacity curve used in this display is also shown on the right side of the figure.

IV.3.1.9. Reflection Intensity

The last attribute included in this library (*Seismic Processing Attribute's* library) is also related to the energy content of the seismic trace and is called r*eflection intensity* (A_{RI}). The r*eflection intensity* attribute is defined as the average amplitude over a user-defined moving window of N values multiplied by the sample interval (often assumed as 1). This attribute is similar to e*nvelope* attribute (see IV.3.2.2) but only considers the real part of the seismic trace.

$$A_{RI}(t) = \sqrt{\frac{1}{N}\sum_{K=-N/2}^{N/2} |f(t+k)|} \qquad \text{Eq. (12)}$$

This attribute is useful for the delineation of amplitude features while retaining the frequency content of the original trace (Figure 47). This *reflection intensity* attribute

can be used to distinguish different type of lithologies, and/or events that have the same amplitude but different frequency components. Conjugated with the envelope, it forms a valuable tool for AVO[15] analysis.

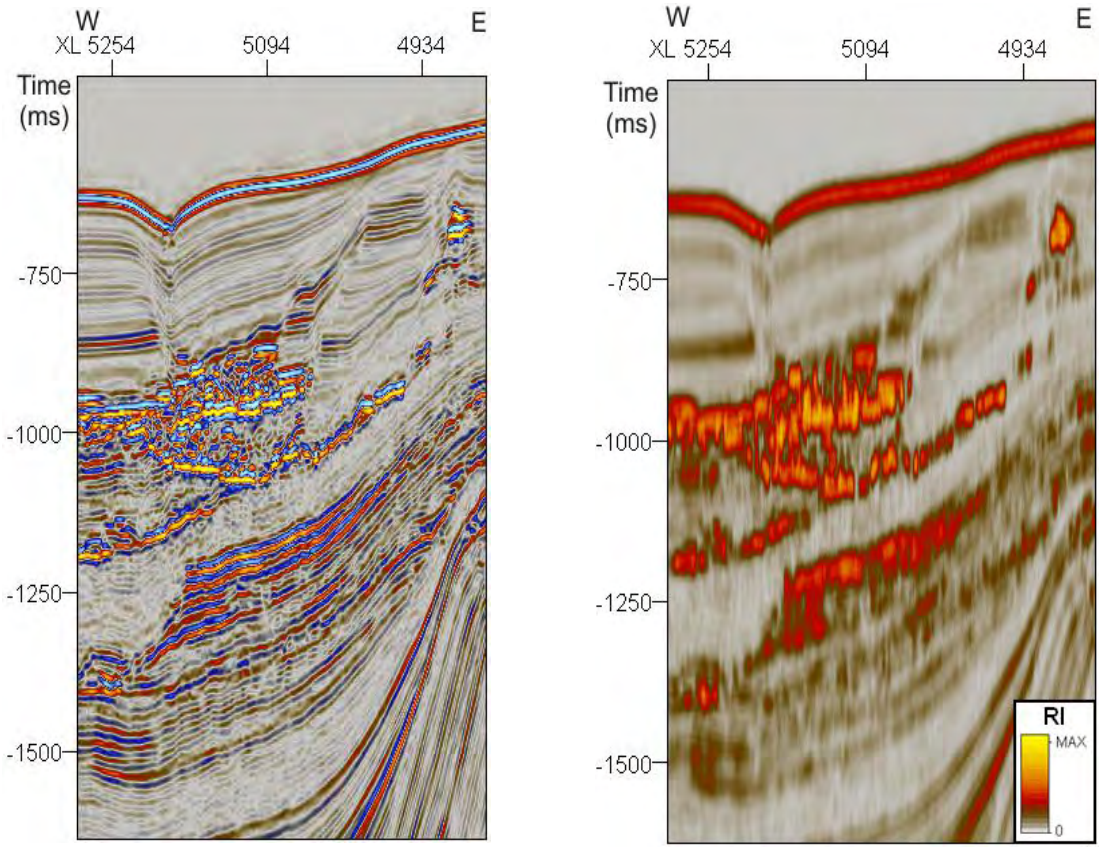

Figure 47 – (a) Original seismic plot; **(b)** *Reflection Intensity* (RI) seismic attribute. Differences in lithologies can be deduced by the differences in the value of RI and the frequency content of the data.

IV.3.2. Complex Trace Attribute Library

Seismic attributes found under the *Complex Trace Attributes* library mainly result from the work done by Taner *et al*. (1979). These authors demonstrated the benefit of thinking about the conventional seismic trace as an analytical signal having both real and imaginary parts, where the real part is the conventional seismic trace and the imaginary part can be calculated from the real part (Bracewell, 1978; Taner *et al*., 1979; Schlumberger, 2007a).

[15] Amplitude Variation with Offset (AVO) is technique widely used in the oil and gas industry to detect fluid content in the rocks from the analysis of 3D seismic data.

Visually, plotting the entire complex seismic trace (F_{HI} (t)), in the complex plane, can be thought as a vector with variable length, that is continually rotating along the time axis, tracing out an irregular helix (Figure 48). Both components of the complex seismic trace (real and imaginary), when plotted individually on the real and imaginary planes, respectively, have the same configuration with a shift of 90º (Taner *et al*, 1979).

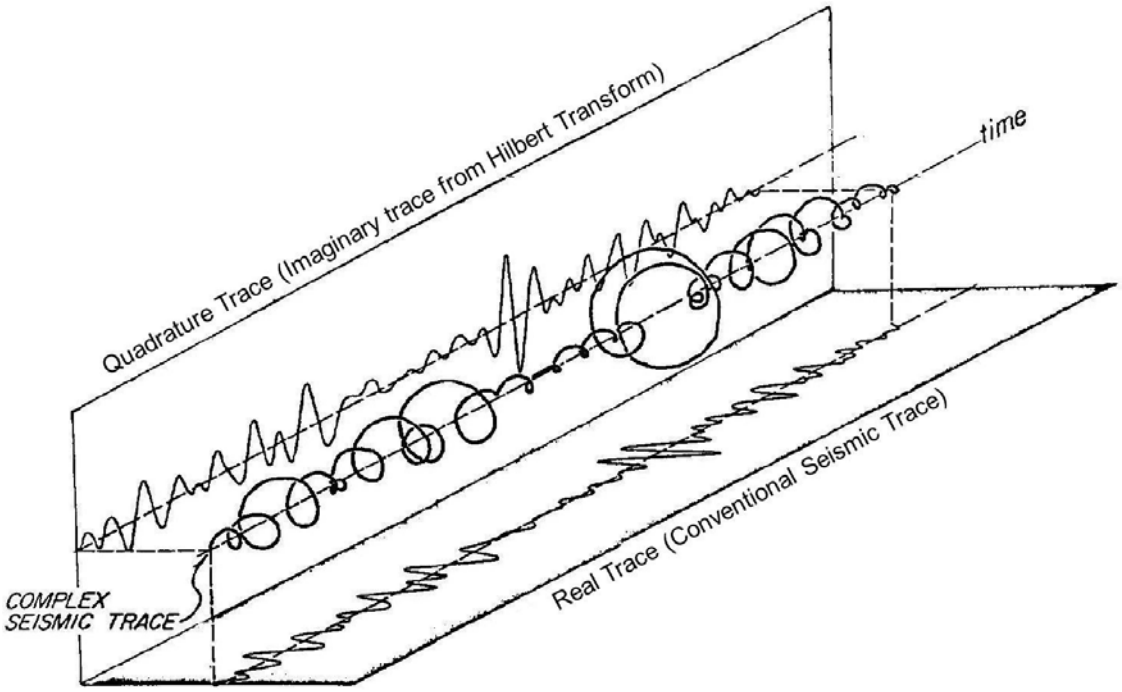

Figure 48 - Isometric diagram showing a complex seismic trace having both real and imaginary part. The real and the imaginary part of the seismic trace have a 90º-shift between them (Taner *et al*., 1979).

Using Fourier transforms there are fully implemented processes to interpret and analyze seismic data in both time and frequency domain. Fourier analysis allows thinking about average properties of a large portion of the seismic trace; alternatively, complex trace analysis permits the user to think locally since this transform technique retains the local significance of the seismic data (Taner *et al*. 1979).

Mathematically the analytical signal, or complex seismic trace, F_{HI}(t) is given by:

$$F_{HI}(t) = f(t) + if^*(t) \qquad \text{Eq. (13)}$$

f(t) is the real part of the analytical seismic trace, or the conventional seismic trace, and f^*(t) represents the imaginary (or quadrature) component of the seismic trace. f^*(t) is calculated through H{f(t)}, the Hilbert Transform, Equation 14. This operator,

when applied to a complex analytical signal, introduces a phase shift of –π/2 for each positive frequency and +π/2 for each negative frequency.

$$F_{HI} = H\{f(t)\} = \left(\frac{1}{\pi}\right) PV \int_{-\infty}^{+\infty} \frac{f(\tau)}{t-\tau} d\tau \quad \text{Eq. (14)}$$

Where *PV* the Cauchy Principal Value, which allows the integration in the presence of singularities (in this case for τ=t).

The seismic signal is normally expressed in terms of time-dependent amplitude *A*(*t*), and time-dependent phase φ(*t*). The real part, *f*(*t*), can be considered as a cosine function (Equation 15); therefore, since the real and the imaginary parts are shifted 90º, the correspondent complex component, *f**(*t*), is a sine function (Equation 16).

$$f(t) = A\cos(\omega_0 t + \phi) \quad \text{Eq. (15)}$$

$$f^*(t) = A\sin(\omega_0 t + \phi) \quad \text{Eq. (16)}$$

The complex seismic trace, F_{HI}(t), can then be defined by:

$$F_{HI}(t) = Acos(\omega_0 t + \phi) + iAsin(\omega_0 t + \phi) \quad \text{Eq. (17)}$$

Complex seismic traces are normally defined in a Cartesian system. However this results in difficult and complex calculations, leading to non reliable results. Euler's method is an alternative to overcome the calculation complexities. Equation 17 can be expressed using Euler's formula, by:

$$F_{HI}(t) = Ae^{i(\omega_0 + \phi)} \quad \text{Eq. (18)}$$

Following Euler's relationships (Figure 49), using known values of *f*(t) and *f**(t), two attributes (or measurements) can be directly extracted from complex trace analysis; *Reflection Strength*, or *envelope* (Section IV.3.2.2), which is the modulus of the entire complex trace (Equation 19) and *instantaneous phase* (Section IV.3.2.3), which is the argument of a complex signal, Equation 20.

$$|F_{HI}(t)| = \sqrt{f^2(t) + f^{*2}(t)} \quad \text{Eq. (19)}$$

$$\varphi(t) = tan^{-1}\left(\frac{f^*(t)}{f(t)}\right) \quad \text{Eq. (20)}$$

The *Instantaneous frequency* (IV.3.2.5) attribute can be derived from the phase information using:

$$\omega_c(t) = \frac{d\varphi(t)}{dt} \qquad \text{Eq. (21)}$$

Complex seismic trace analysis enables a natural separation between the amplitude and the phase content of the seismic data, from which instantaneous complex attributes are generated. This new insight in seismic interpretation provides additional information, from a usually "hidden" component of the seismic data (Taner *et al*. 1979).

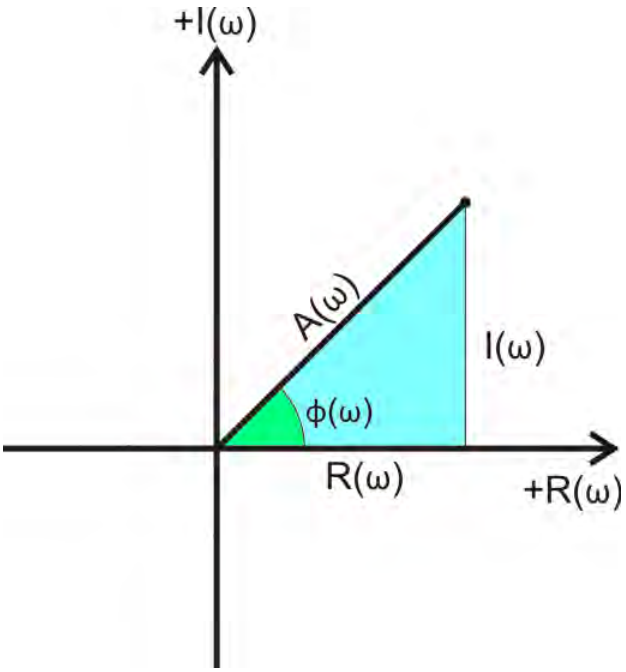

Figure 49 – Graphical representation of Euler's relationships.

In complex trace attributes analysis, the interpreted features have to be consistent in the various components of the analytical seismic trace: amplitude, energy (*envelope*), frequency (*instantaneous frequency*), and phase (*instantaneous phase*). Complex attributes, more than any other seismic attributes have to be displayed with a proper colour scale range (Taner *et al*. 1979).

Complex seismic attributes are instantaneous attributes computed trace-by-trace.

IV.3.2.1. Apparent Polarity

Apparent polarity is the sign of *f*(*t*), the real part of the complex trace, at a local maximum of the e*nvelope* (see Section IV.3.2.2; Figure 50), over a window with a

user-defined length. Depending on the sign of *f*(t) at the local maximum of the *envelope*, a colour is assigned, traditionally blue for negative values and red for positive. Variations on the value of the *envelope* will produce a gradation between blue and red.

Theoretically, the polarity of the seismic trace reveals the sign of the reflection coefficient whenever the received signal is from a single reflection of a zero-phase wavelet. However, most reflection events correspond to more than one single reflection; this will reduce the correlation between the signal of the reflection coefficient and the wave polarity. Due to this non-correlation effect, this attribute was created (Taner *et al*., 1979).

The *apparent polarity* attribute is particularly used to enhance event continuity, improving seismic reflectors interpretation through automatic tools. Lateral variations of *apparent polarity* along a reflector may indicate lateral variations in lithology (Figure 51). Thick beds can be easier detected with apparent polarity interpretation since the data is not affected by waveform effects.

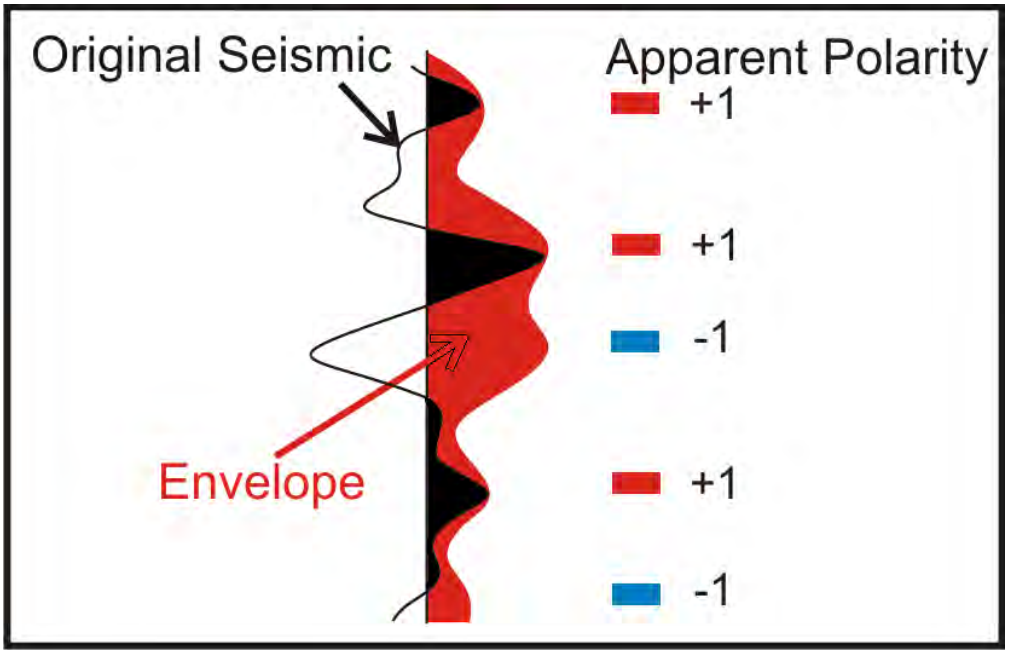

Figure 50 – Schematic representation of how *apparent polarity* is computed and its relationship with the original seismic trace and the envelope attribute (Schlumberger, 2007a).

This attribute is highly effective for quality seismic data with little noise content. For data with considerable noise, and using *Petrel* 2008.1, it is suggested to compute

apparent polarity from a *structural smoothing* (see IV.3.3.4) seismic cube, where the spatial noise is reduced to the minimum.

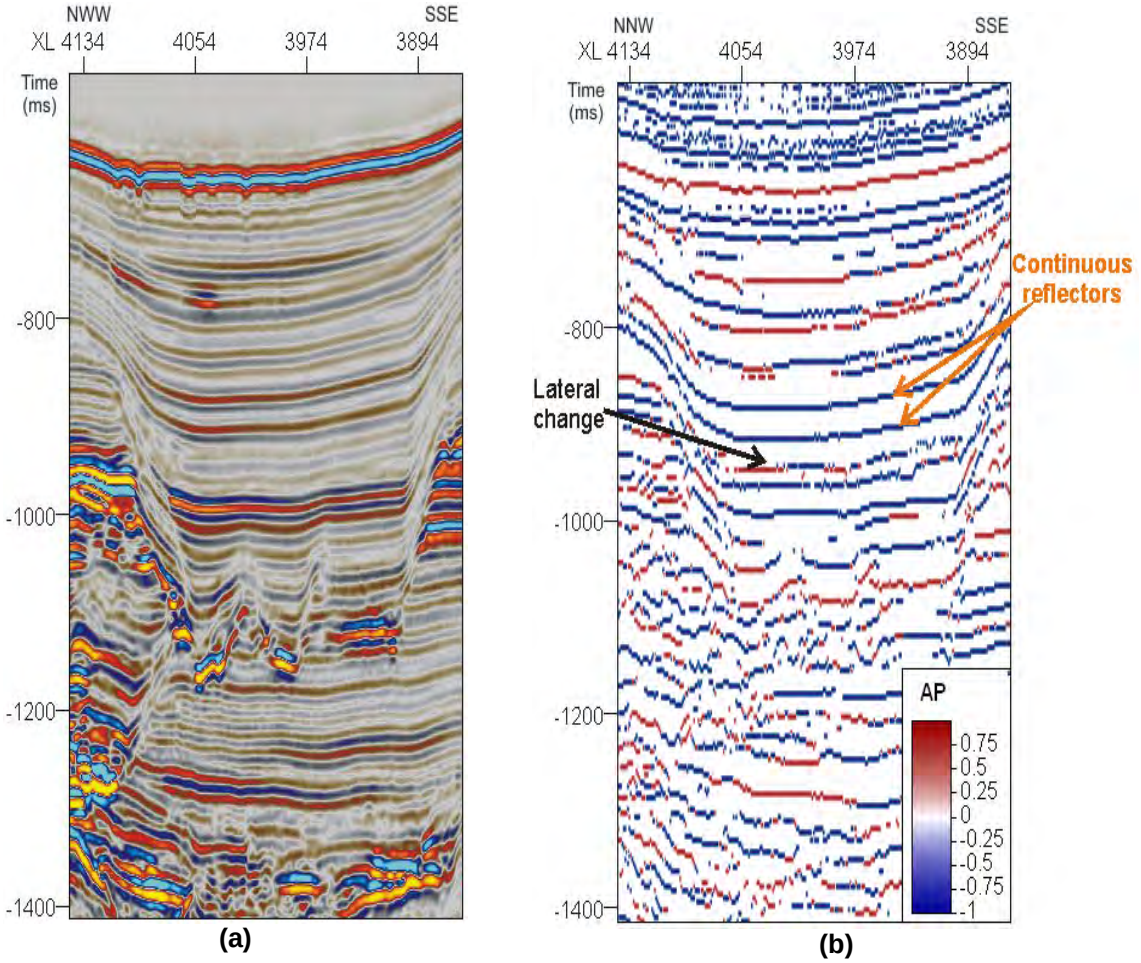

Figure 51 – (a) Seismic section with original amplitude and **(b)** extracted *apparent polarity* attribute. *Apparent polarity* enhances reflectors' continuity and lateral changes of lithology. *Apparent polarity* volumes are good for input into automatically picking interpretation tools.

When displayed with *envelope* and *instantaneous frequency* attributes apparent polarity can be used to distinguish different kinds of bright spots. Bright spots associated with gas accumulations generally show negative polarity, while positive polarity often appears associated to gas-oil and gas-water interface (Taner *et al*. 1979).

IV.3.2.2. Envelope (Reflection Strength)

The *envelope* attribute, or *Reflection Strength* as designated by Taner *et al*. (1979), was probably the first attribute calculated with Complex Trace Analysis. It

is defined as the total instantaneous energy of the entire analytical trace, both real and imaginary parts (Figure 52). In other words, the envelope is the modulus of the analytical seismic trace, computed following the Equation 19 over a user-defined window.

Envelope is a phase-independent attribute. This means that maximum values of the *envelope* may not be at the same position of maximum peaks, or troughs, when compared with the input seismic data (Taner *et al*., 1979). The *envelope* attribute can be used to compare different seismic vintages, with different phases, since both should have the peak energy always aligned.

As an attribute related to the energy content of the seismic trace, it is useful to detect major and subtle lithological changes that may be difficult to interpret from the original seismic input. High values of the *envelope* can appear due to major lithological changes and sedimentary sequences boundaries as well as related to bright spots caused by gas accumulations. Gradual lateral changes of *envelope* values are often correlated with lateral variations in lithologies (Taner *et*., 1979).

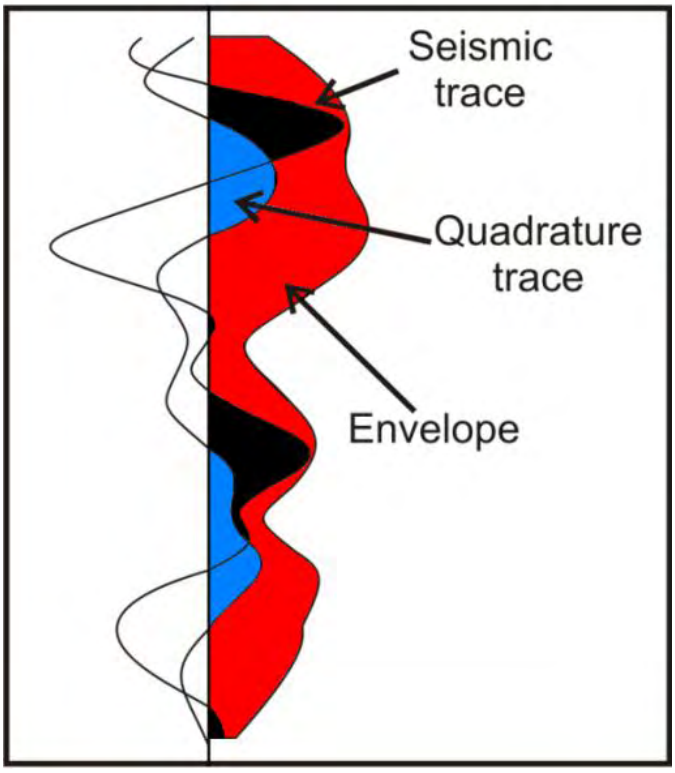

Figure 52 – Schematic representation of how *envelope* attribute is computed and its relationship with the real seismic trace and the imaginary seismic trace (Schlumberger 2007a).

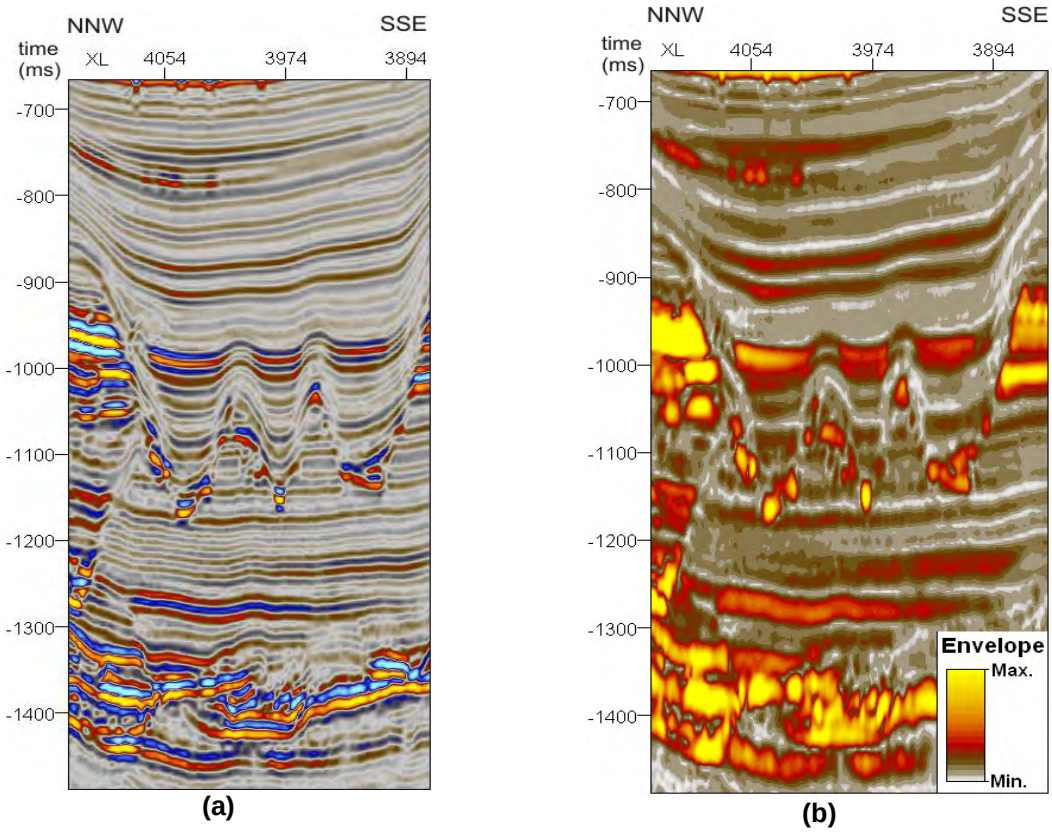

Figure 53 – (a) Original seismic section and **(b)** correspondent *envelope* attribute. Major and subtle lithologic changes are enhanced by the *envelope* attribute when compared to the original seismic section. Rather than for interpreting individual reflectors, the *envelope* is be used to identify related seismic units through their energy content.

Interpretation of thin-beds, especially those inside a hydrocarbon reservoir, can be very difficult in original amplitudes due to interference effects. Using the *envelope* attribute with the right parameters, calibrated to the formation thickness, can help to distinguish features which are not always detectable, by their energy content.

IV.3.2.3. Instantaneous Phase

The *instantaneous phase* attribute is computed from the argument of the complex seismic trace (φ) Equation (20) in a user-defined window.

Instantaneous phase enhances both weak and strong seismic events due to the invariant nature of the attribute in terms of amplitudes. This attribute has proven results enhancing reflectors continuity, discontinuities, faults and pinch-outs. Seismic stratigraphy patterns (e.g. onlaps and offlaps) are easily identified with this attribute allowing the interpreter to deduce more easily the sedimentary

processes that affected the area (Taner *et al*., 1979). Thin-bed hydrocarbon reservoirs often cause local phasing due to the presence of hydrocarbon accumulations, which explains classifying *instantaneous phase* as a DHI, a potential Direct Hydrocarbon Indicator (Chen *et al*., 1997).

The proper display for instantaneous phase should take into account that phase varies between -180º to 180º. The associated template should therefore consider a circular colour scale bar where the two extreme angles should have the same colour, since they correspond to the same phase angle (Figure 54).

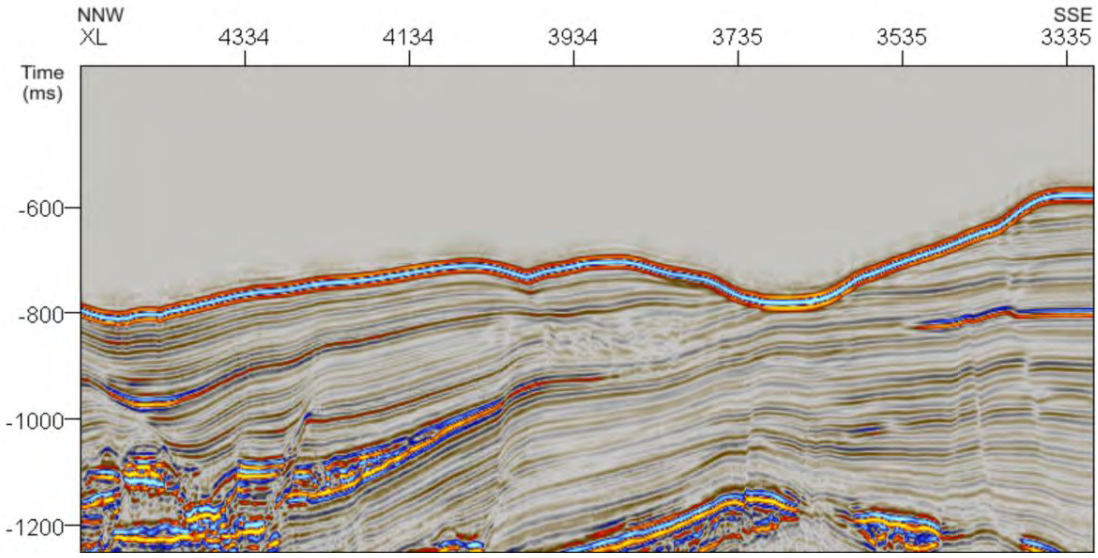

(a)

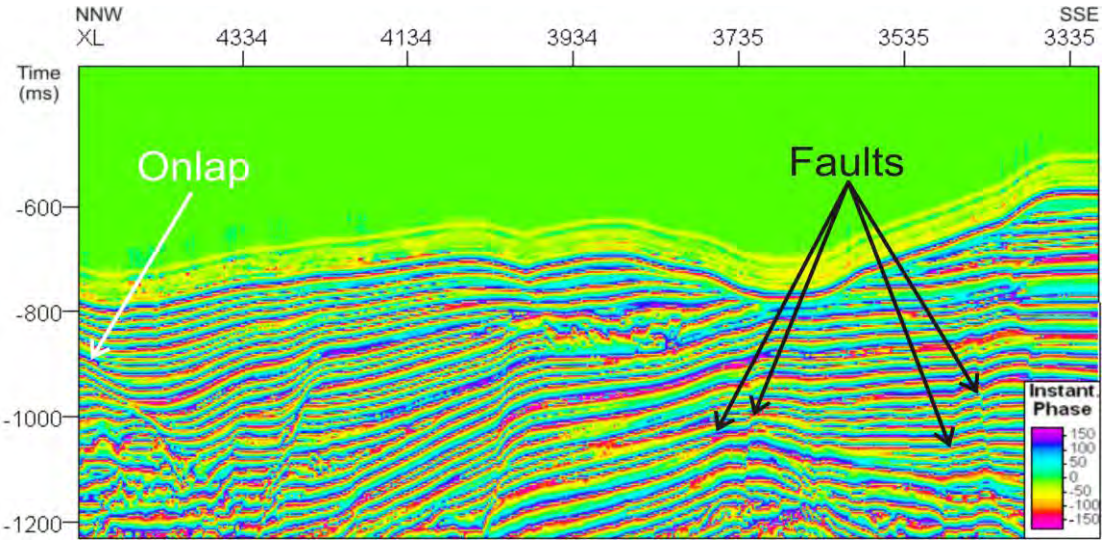

(b)

Figure 54 - (a) Seismic section displayed in original amplitude and **(b)** corresponding *instantaneous phase* attribute where reflectors have enhanced continuity. Faults and seismic stratigraphy patterns (reflectors terminations) are better interpreted.

IV.3.2.4. Cosine of Instantaneous Phase

The *Cosine of instantaneous phase*, or normalized amplitude, is the cosine of the instantaneous phase angle (φ; see Section IV.3.2.3). Amplitude peaks and troughs will remain at the same position but strong and weak events will exhibit equal strength (Partika, 2000). It should be displayed with a colour scale range between -1.0, in black, and 1.0, in white.

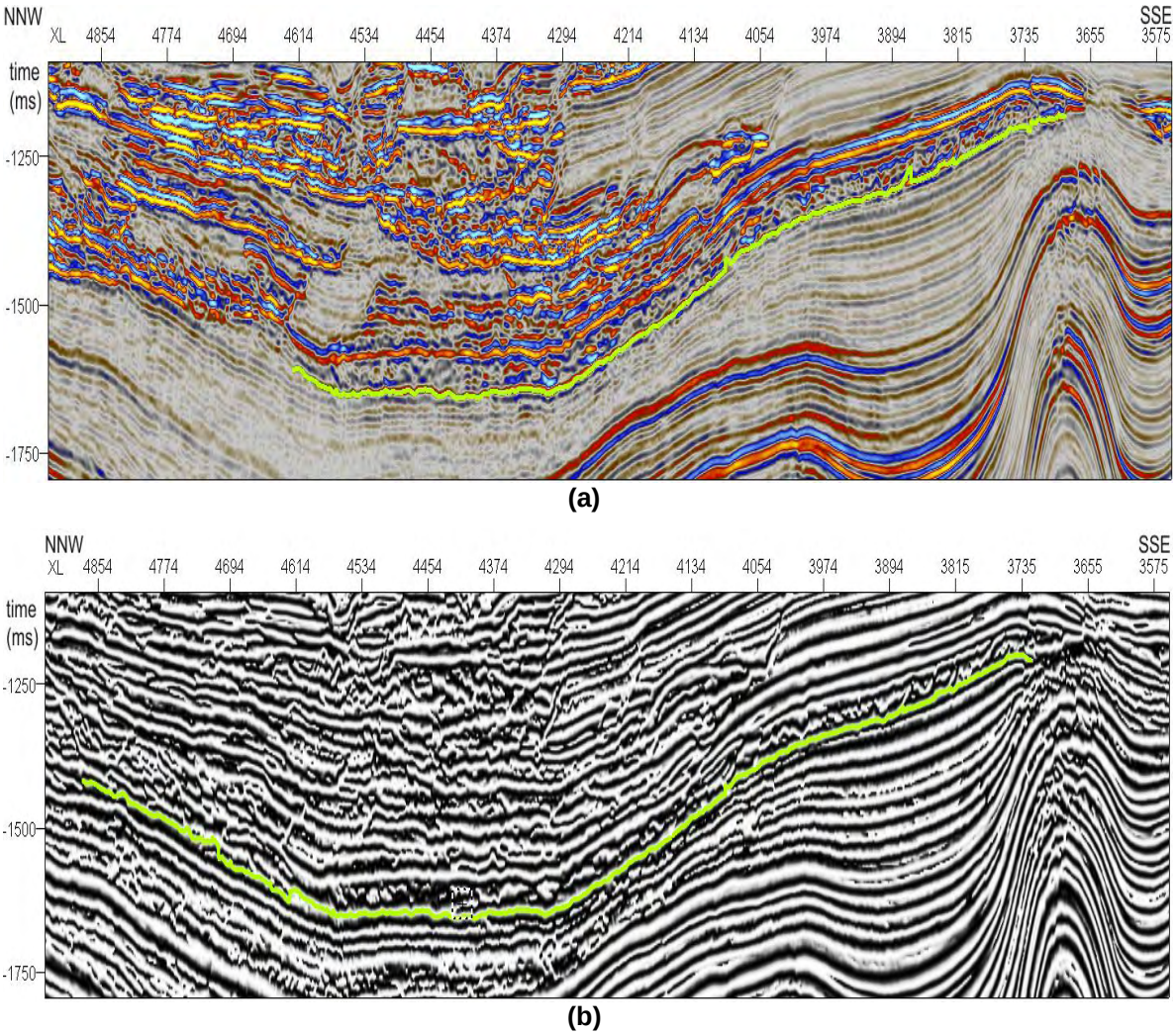

Figure 55 – (a) Original seismic section and **(b)** extracted *cosine of instantaneous phase*. The green line represents a seismic reflector interpretation using *Petrel*'s "*Seeded 2D Autotracking*" tool. It is clearly that in **(b)** the interpretation is more consistent in space and close to what should be a manual interpretation.

The *cosine of instantaneous phase* improves reflectors' continuity and enhances the visual appearance of edges, such as faults and stratigraphic boundaries. It is an indicative attribute about stratigraphic terminations, lateral variations and

seismic facies variations. Due to the improved reflectors continuity it is an excellent attribute to constrain automatic interpretation tools (Figure 55) since poorly resolved seismic reflectors, which often lead to missinterpretations, become more consistent.

The stratigraphic analysis and seismic pattern recognition is one of the hardest tasks to the interpreter but also one of the most important to infer the depositional regime which affected a sedimentary basin. Stratigraphic analysis is often based on interpretation of reflectors terminations, which are more easily identified with *cosine of instantaneous phase* volume (Figure 56).

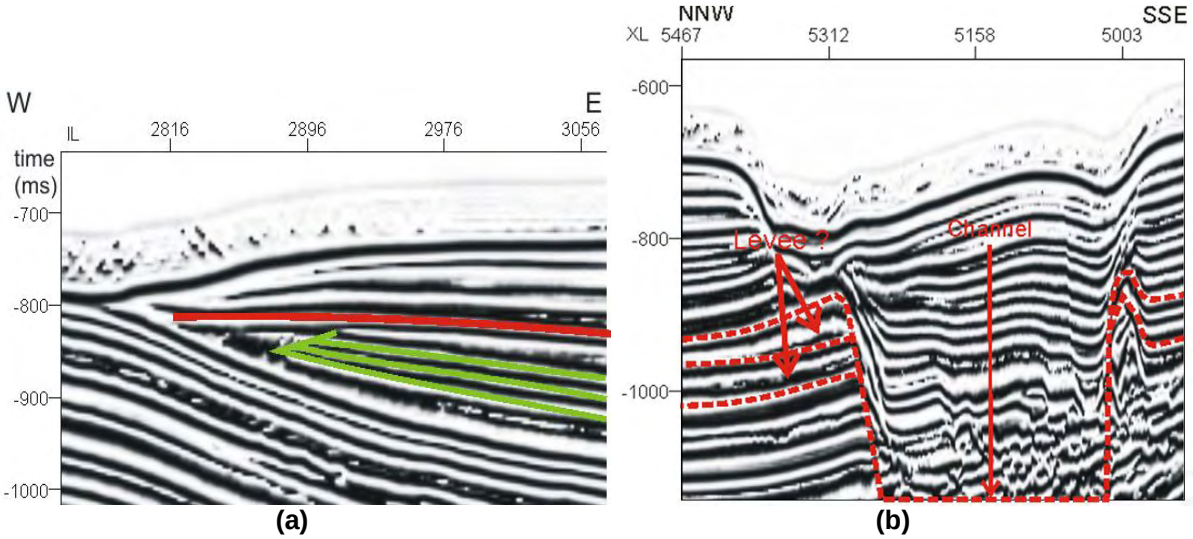

Figure 56 – Seismic stratigraphic analysis becomes easier with the *cosine of instantaneous phase* attribute. **(a)** Green lines are interpreted reflectors which are being truncated by the red one. **(b)** Shows a typical turbidite system feature, the "seagull wing", corresponding to flood events of the interpreted channel.

IV.3.2.5. Instantaneous Frequency

Instantaneous frequency is described as the rate of change in time of instantaneous phase (Equation 21) over a user-defined window. It is an attribute independent of amplitude and phase information and represents the instantaneous centered frequency, or mean frequency of the frequency spectrum (Taner *et al.*, 1979).

Negative values of *instantaneous frequency* are related to phase angle reversals, which automatically are transformed into zero values, by the algorithm which computes this attribute in *Petrel* 2008.1 (Schlumberger, 2007a).

Most of the recorded reflections in seismic data are not produced from a single geological reflection but they are the sum of reflections from closely spaced reflectors. These closely spaced reflectors have little differences in acoustic impedance between themselves and then the superimposition of individual reflections produce a frequency pattern which characterizes the composite reflection. Lateral and vertical variations in lithology can be identified by the change of the composite pattern (Taner *et al*. 1979, Chen *et al*. 1997).

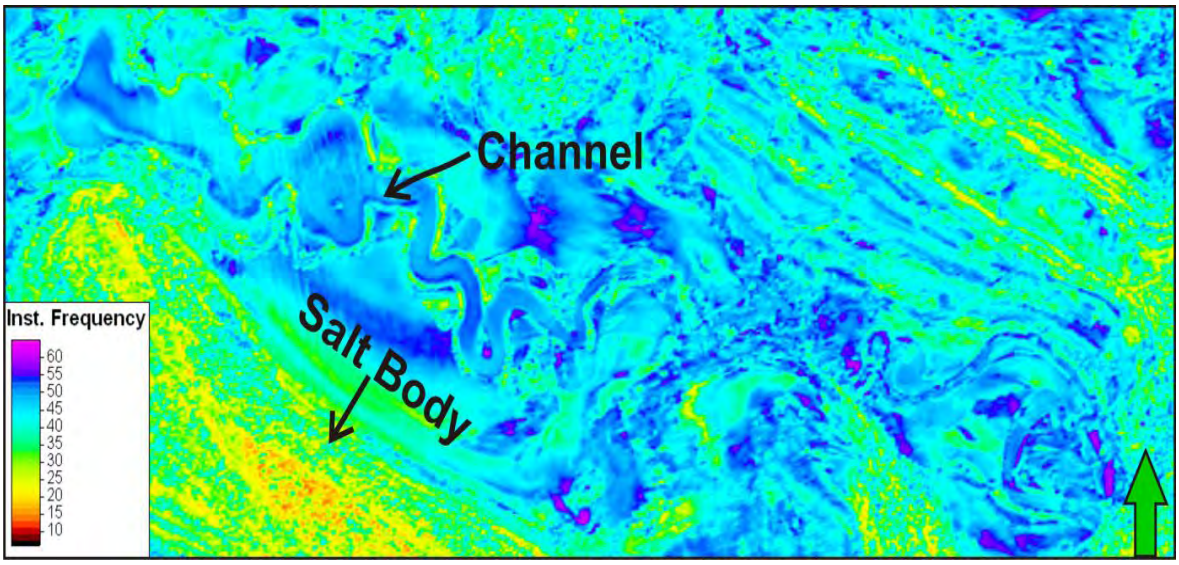

Figure 57 – Time slice of an *instantaneous frequency* cube. In the central part, an E-W channel which extends to the right part of the figure is clearly distinguished, by constant values of *instantaneous frequency*. Part of a salt body orientated NW-SE can also be identified in the lower left corner.

Instantaneous frequency is typically used to enhance vertical and lateral variations of lithologies. Channels are easier to identify in *instantaneous frequency* time slices because this attribute tends to be constant in value inside the potential hydrocarbon reservoir when compared to the surrounding environment (Figure 57). This effect happens when there are no major lithological variations inside the channel, contrasting to the abrupt lithological variations outside the channel borders. This method is also useful to detect fracture zones and as a Direct Hydrocarbon Indicator (DHI). Faults and fractures also often cause absorption

effects causing low values of instantaneous frequency, just like salt bodies (Figure 58). Sands with gas or oil content within the pores also usually cause drop-off high frequencies just below the hydrocarbon reservoir – this effect is frequently called "*low-frequency shadow*" (Taner *et al*., 1979; Chen and Sidney, 1997).

To correctly interpret *Instantaneous Fequency* attribute volumes the colour scale range to display this attribute should be adjusted from zero to a maximum value close to 65 Hz, depending on frequency component of the seismic data.

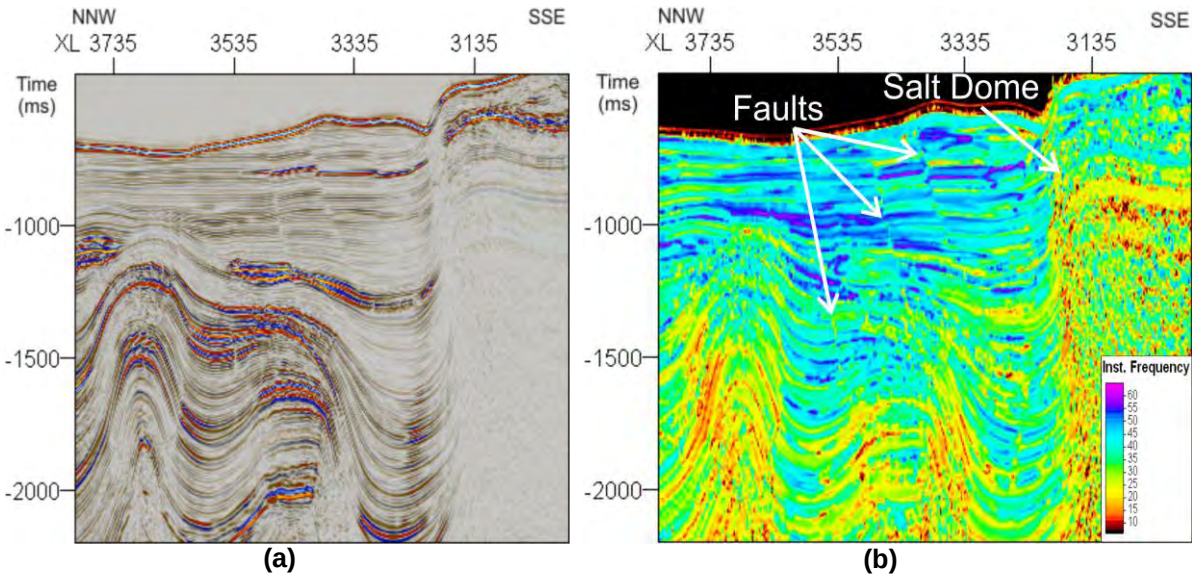

Figure 58 – (a) Seismic sections with original amplitude and **(b)** extracted *instantaneous frequency* attribute. *Instantaneous frequency* enhances faults and better delineates salt bodies, due to the characteristic low values of *instantaneous frequency*. Colour scale bar is shown in the lower left corner of **(b)**.

IV.3.2.6. Instantaneous Bandwidth

Instantaneous bandwidth, expressed in *Hertz*, by Equation 22, is mathematically described as the absolute value of the derivative of the envelope with time divided by the envelope, over a user-defined window. This attribute symbolizes the standard deviation of the instantaneous power spectrum about its mean.

$$\omega_B = \left| \frac{d\left[\frac{(env(t))}{dt}\right]}{env(t)} \right| \qquad \text{Eq. (22)}$$

Where d[(env(t)/dt) is called the decay factor.

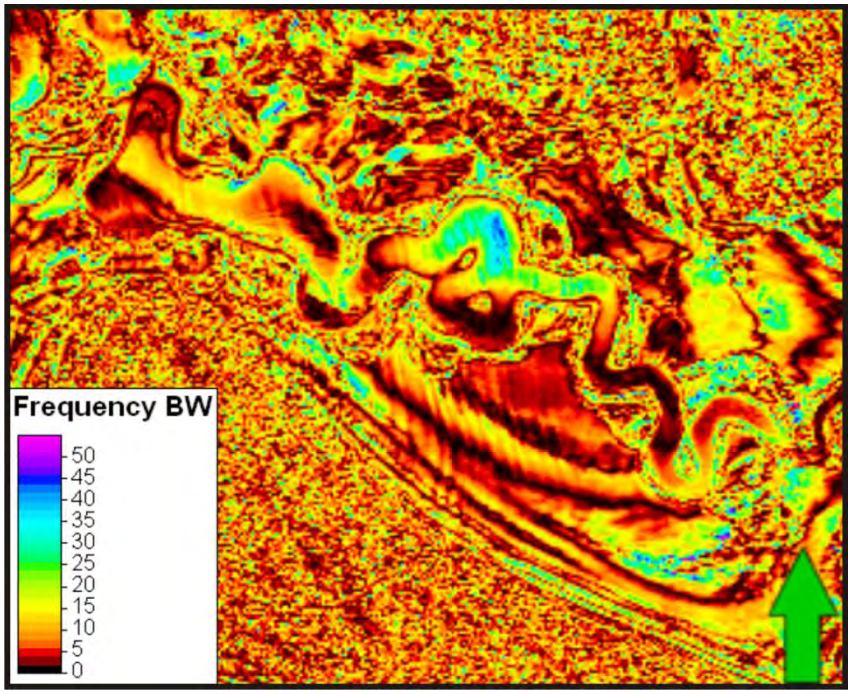

Figure 59 – Time slice from an *instantaneous bandwidth* attribute volume, same time position of the time slice displayed for instantaneous frequency (Figure 57) focused in the E-W channel. The central part of the channel is now better imaged as well as the lateral lithological variations inside the channel, that can be correlated with abrupt changes in *instantaneous bandwidth* values.

This attribute should be interpreted combined with the *dominant frequency* (see Section IV.3.2.7) and the *instantaneous frequency* attributes. Compared to the *instantaneous frequency* attribute, *instantaneous bandwidth* commonly gives lower frequency values. The output attribute cube has enhanced features related to absorption effects and changes in the seismic character, which are directly related to changes in lithology (Figure 59). This attribute is also useful to correlate seismic units from both sides of a fault.

The maximum value of the colour scale bar should be adjusted in order to achieve a convenient display, depending on the acquisition frequency.

IV.3.2.7. Dominant Frequency

Dominant frequency is the last attribute which combined with *instantaneous frequency* and *instantaneous bandwidth* characterizes the time varying spectral properties of seismic data.

The algorithm used to compute this attribute sums the square of the *instantaneous frequency* with the square of *instantaneous bandwidth* and calculates the square root of the sum (Equation 23) over a user-defined window. This represents the RMS frequency of the amplitude spectrum.

$$\omega_{RMS} = \sqrt{{\omega_B}^2 + {\omega_c}^2} \qquad \text{Eq. (23)}$$

Combining the three attributes related to the instantaneous power spectrum is the best way to look for low frequency shadows which can indicate a potential oil and gas reservoir, and distinguish channels and salt bodies from the seismic background (Figure 60).

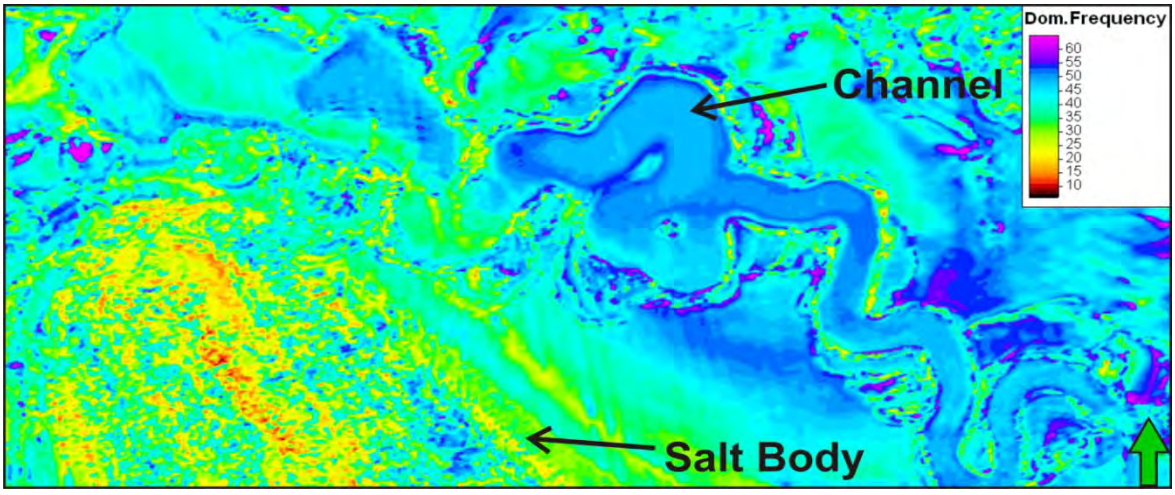

Figure 60 - Time slice from dominant frequency cube, same time position as shown in instantaneous frequency and bandwidth. Comparing the three attributes lateral changes in geology inside the channel are better characterized, as well as the seismic signature for a salt body.

Once again the colour bar should be adjusted with the frequency component of the input seismic data. When combined to instantaneous frequency and bandwidth attributes the same coulour scale should be used for the three attributes; otherwise the desired result will not be achieved, causing missinterpretation.

IV.3.2.8. Quadrature Amplitude

This attribute calculates the imaginary part, *f**(t), of the original seismic trace *f*(t). The imaginary part is computed through the Hilbert transformation by phase shifting the original seismic trace by 90º, in a clockwise direction. For further information, see Section IV.3.1.1.

IV.3.3. Structural Attributes Library

The *Structural Attributes* library contains a collection of attributes to help the structural geology interpretation process. They are mainly used to isolate and enhance local structural variations in the seismic reflection patterns. In other words, structural attributes detect edges, compute the local orientation and dip of seismic reflectors and enhance seismic event continuity parallel to the estimated bedding orientation. In structural attributes, an edge is defined as a discontinuity in the horizontal amplitude continuity within the seismic data, that can correspond to real faults and/or fractures.

Unlike attributes from the *Complex Trace* library, most of the algorithms used to compute structural attributes are computed using a collection of traces, by the multi-trace method described in Section IV.3.

The main attributes available in this library are described below: *Dip Deviation*; *Local Structural Azimuth*; *Local Structural Dip*; *Structural Smoothing*; *Variance*; *Ant Tracking* and *Gradient Magnitude*.

IV.3.3.1. Dip Deviation

Dip deviation is a multi-trace-based seismic attribute that tracks rapid changes in the local orientation of seismic reflectors; these rapid changes can be interpreted as edges. The dip deviation algorithm considers the difference between the dip trend and the instantaneous dip. Dip estimates are computed from the local maxima of the input seismic data and from the maxima of the derivative of the input data, which are then smoothed by a Gaussian smoothing operator.

This method has proven results in passive margins and soft rocks where the downthrown side of a fault typically shows significant dip into the fault. It has also been found to work successfully for low-angle illumination.
In *Petrel*, the user has the possibility to control the minimum dip difference to display trough a slider control, reducing the number of undesirable features.

Figure 61b shows a seismic section of *dip deviation* attribute volume. Major high angle faults can be identified and more easily interpreted, in the central part of the figure, minor faults, also became clearer and easy to interpret when combined with the original seismic data (Figure 61a). Since most of the fault features contain high angles the slider control was positioned to ignore dip deviations values less than 10º.

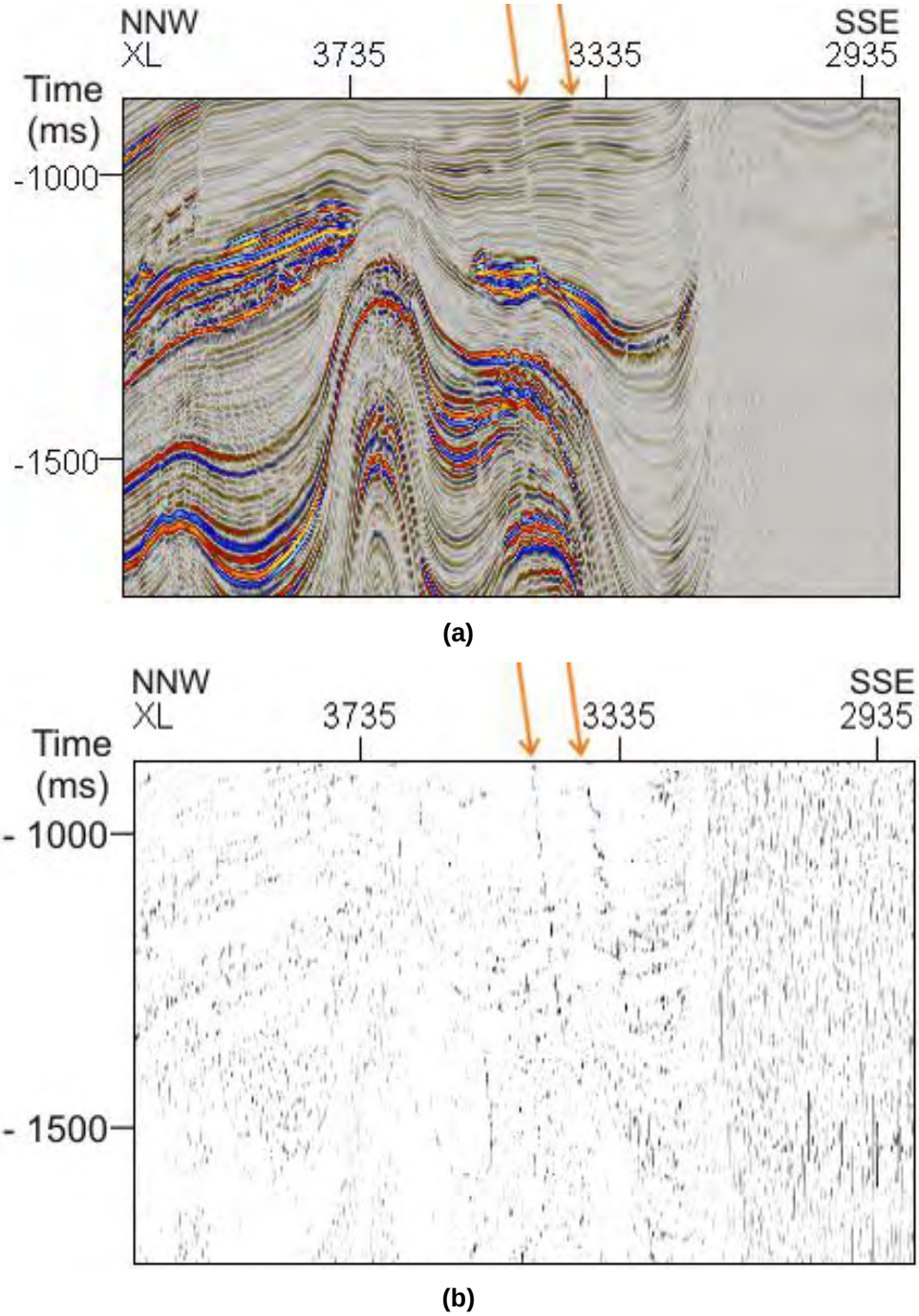

Figure 61- Comparison between original seismic data and *dip deviation* attribute. **(a)** Seismic section in original amplitude. **(b)** Seismic section from a *dip deviation* cube displaying only dip differences bigger than 10º. Orange arrows point towards two big faults perfectly identified by the attribute.

IV.3.3.2. Local Structural Azimuth and Dip

In stratigraphic hydrocarbon reservoirs one of the challenges of today is the interpretation of upper and lower unit boundaries of a hydrocarbon indicator and their correlation with seismic reflectors configuration. The internal configuration, or seismic texture, is another challenge which new seismic attributes are trying to identify and interpret automatically, especially after the introduction of 3D seismic data and volume attributes (Randen *et al*., 2000).

Local structural azimuth and *dip* are more than simply attributes to estimate the azimuth and dip of coherent seismic events. They are also used in *Petrel* as internal algorithms to compute other seismic attributes which honor the orientation of the seismic reflectors. Seismic attributes are normally extracted vertically along the seismic trace; this traditional approach can, in many cases, introduce artifacts. The two attributes described here are part of a class of attributes to avoid these artifacts and ensure that the extracted seismic attributes are invariant to dip and azimuth (Randen *et al*., 2000).

Geologically, in terms of atitude, strike is defined as the compass bearing of a horizontal line on a dipping layer, and dip is the angle of the inclination of the bed measured perpendicular to the strike direction. In *Petrel*, dip has the same definition, but azimuth is generally used rather than strike. Azimuth is a perpendicular measure to the strike, and is the compass direction (0-360º) of the normal to the plane (Figure 62).

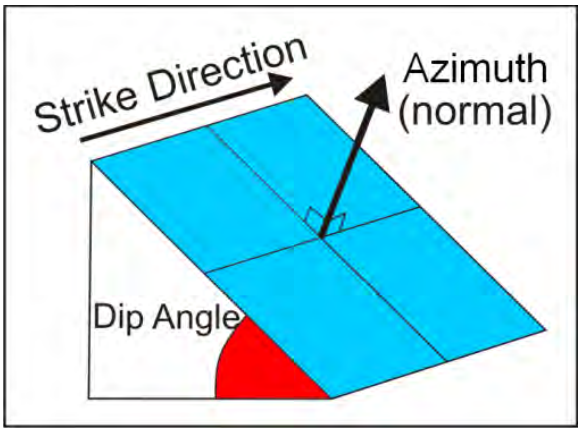

Figure 62 - How dip and azimuth are measured in *Petrel* 2008.1 (Schlumberger, 2007a).

Local structural azimuth and dip can be computed following three different computation methods with different complexities: (1) *Gradient*; (2); *Event* (3) *Principal Component* (Figure 64).

(1) *Gradient* is the instantaneous azimuth/dip in the sample neighborhood and it is the simplest method to estimate local structural azimuth and dip. It consists in calculating the gradient vector using a different operator for each of the three dimensions of space (inline and crossline directions, and vertically in time) by the same approximation of the first derivative attribute defined in Section IV.3.1.1. The calculated gradient vector is normal to the considered seismic event; in other words, it is its tangent. Dip is measured from the z-axis to the gradient vector, and the azimuth is the angle of the vertical projection of the gradient vector measured clockwise from the inline axis. Local structural azimuth ranges from 0º to 360º and dip from -90º to 90º.

(2) *Event* method computes the downslope azimuth and dip of the estimated event. Numerically it calculates the gradient, using the same approximation of the *gradient* method (see previous point) but, by convention, the event normal, or gradient vector, should always point upwards. In comparison to the gradient method, and using the positive z downwards, if the gradient vector has a negative z-component, then dip and azimuth are equal to dip and azimuth computed by the *gradient* method. On the other hand, if the computed gradient has a z-component positive (pointing downwards) then it should be reversed by multiplying by zero all the components, before measuring the angles. This explains the fact that azimuth ranges over 360º and dip from 0º to 90º.

(3) *Principal component* is a three step method which consists first in the estimation of the gradient vector, the local gradient covariance matrix and a *principal component analysis*. Dip/azimuth vectors should behave like the *event* method: the principal vector should point upwards before measuring the angles; azimuth and dip ranges from 0º to 360º and 0º to 90º, respectively.
In discrete data there are several derivative approximations in gradient computation. In the *principal component* method the derivative of Gaussian is

used due to joint optimum resolution in time and frequency of Gaussian filters and nice scalability properties.

For 3D datasets, in order to obtain the derivative of each dimension, a three-dimensional gradient, the derivative of Gaussian is applied to achieve a gradient vector with one partial derivative component for each dimension (Equation 24).

$$\nabla x(t_1, t_2, t_3) = \begin{bmatrix} \frac{\partial x(t_1, t_2, t_3)}{dt_1} \\ \frac{\partial x(t_1, t_2, t_3)}{dt_2} \\ \frac{\partial x(t_1, t_2, t_3)}{dt_3} \end{bmatrix} \quad \text{Eq. (24)}$$

The gradient vector computed from this step represents the local azimuth and dip of the seismic event but can be contaminated by noise and other artifacts. The local gradient covariance matrix estimation, $\mathbf{C}(t_1,t_2,t_3)$, is computed instead to smooth and eliminate artificial features within the gradient estimate. Smoothing wraparound effects (slightly changes in angles, but abrupt changes in its representation, changing from -180º to +180º) in dip and azimuth estimates are non-trivial. The used approximation is to estimate the covariance matrix of the gradient vectors and determine the dip as the direction of the principal eigenvector of the matrix (Figure 63; Randen, 2000). For further details and mathematical descriptions about this method it is suggested Iske and Randen (2005).

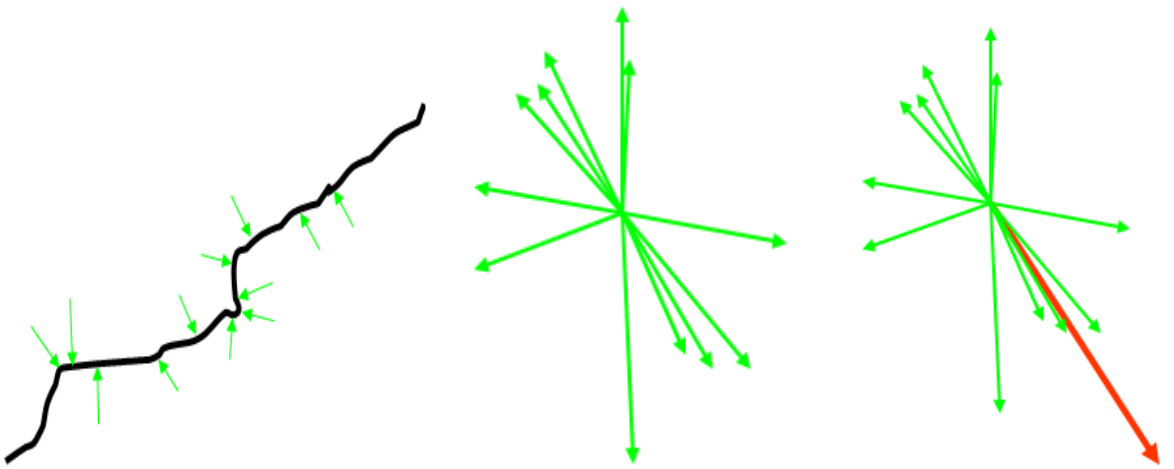

Figure 63 – Principle component steps: **(a)** calculates local gradient **(b)** estimates the covariance matrix of the gradient vectors **(c)** perform principal component analysis: Dominating orientation (in red; Schlumberger, personal communication).

Dip and azimuth estimations, by the *principal component* method, are powerful tools not only in the estimation itself, as an attribute, but also to compensate for dip and azimuth in other seismic attributes algorithms.

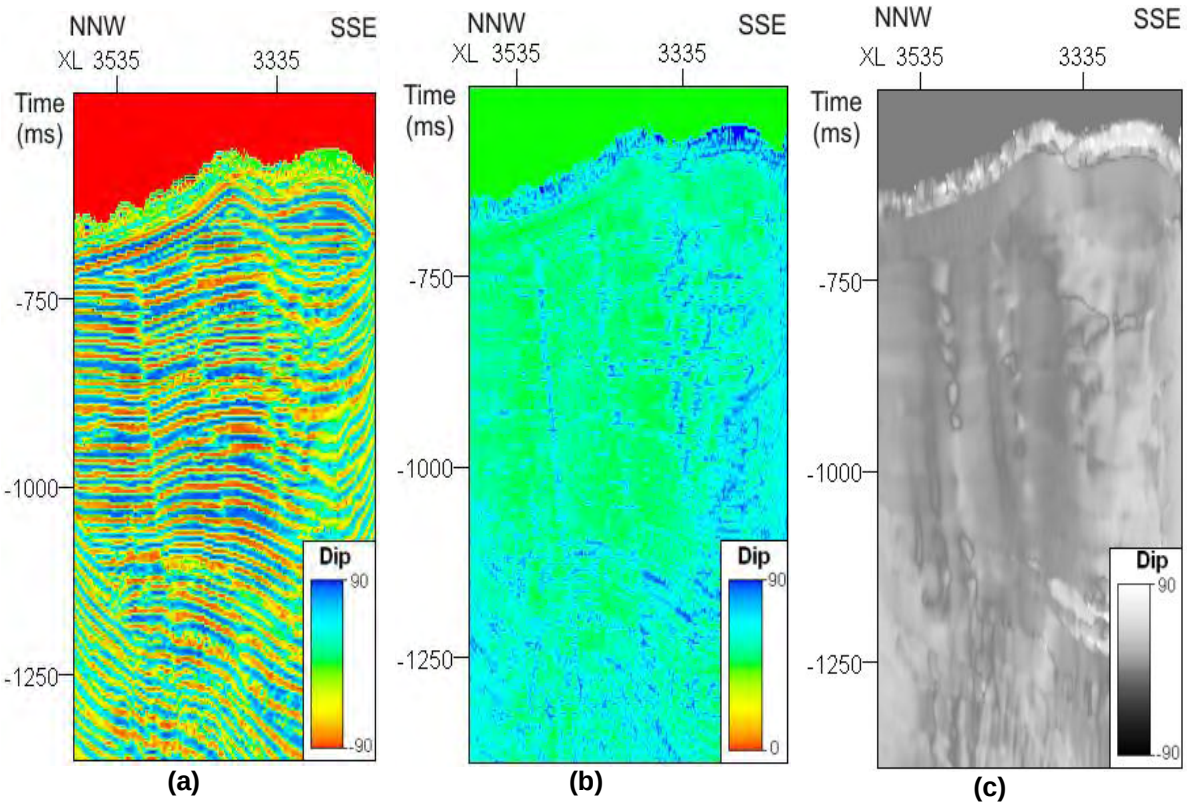

Figure 64 – Estimated *local structural dip* by the three computation methods described above: **(a)** *gradient* method; **(b)** *event* method and **(c)** *principal component* method.

IV.3.3.3. Gradient Magnitude

By definition, *gradient magnitude* is the square root of the sum of the squared first derivatives, computed following the mathematical expression given by Equation 25, in the three dimensions of space (inline, crossline and vertical directions).

$$GradientMagnitude = \sqrt{f'(x)^2 + f'(y)^2 + f'(z)^2} \qquad \text{Eq. (25)}$$

Gradient magnitude is an amplitude-sensitive attribute; therefore it can be useful to discriminate areas of weak signal from those with significant reflectivity. Based on the coherency of the signal, and the attribute value, it can be used to distinguish different lithologies (Figure 65). Interpreting time slices with this attribute can add valuable clues on fault systems and depositional regimes (Figure 66).

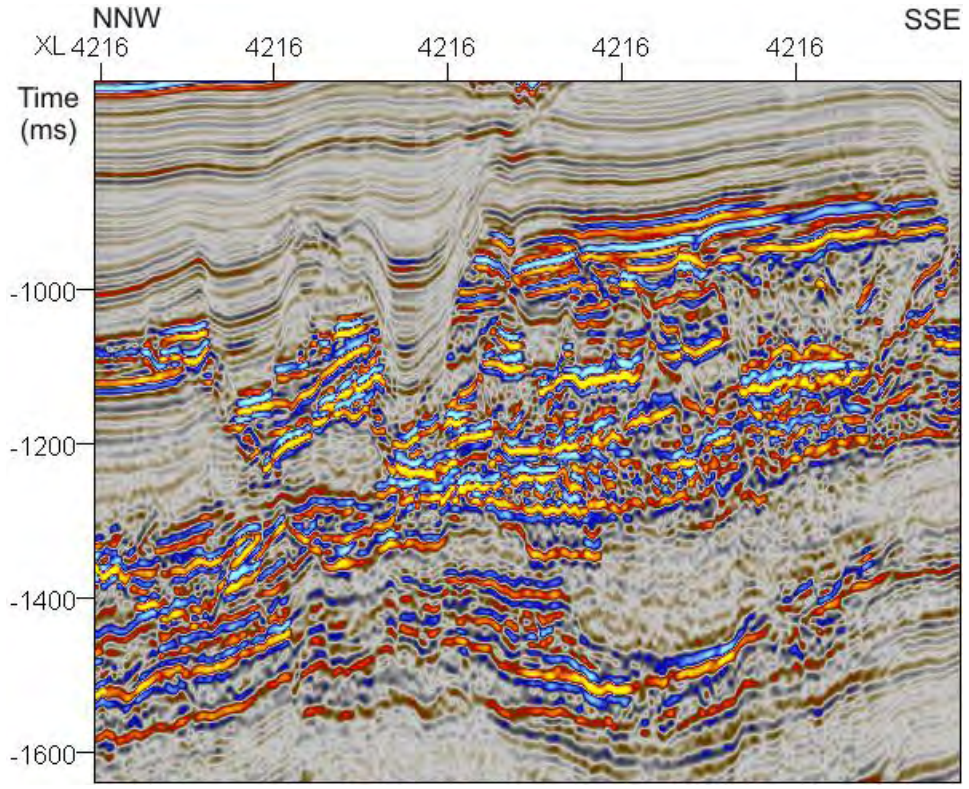

(a)

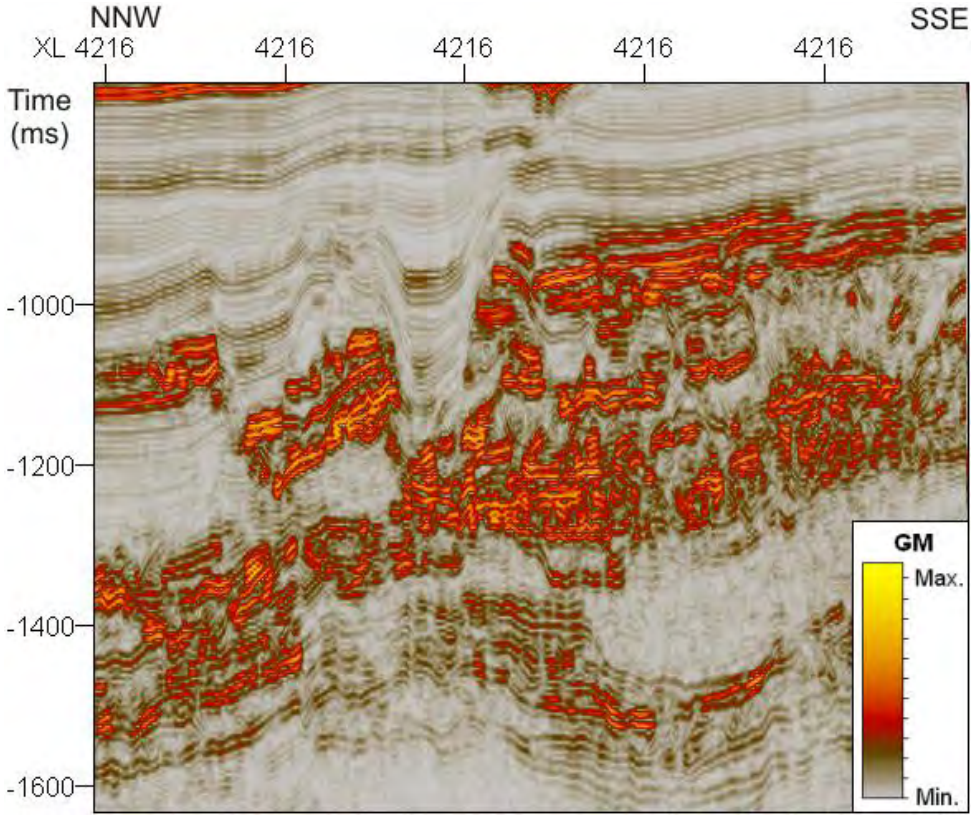

(b)

Figure 65 - Comparison between **(a)** original seismic and **(b)** *gradient magnitude* attribute. *Gradient magnitude* attribute produces sharper features and distinguish regions with signal strength from those with weak signal content. The noise content is also reduced in the output attribute volume.

Gradient magnitude does not accept user-defined parameters. In order to adjust the attribute with the data, the interpreter should use a template with two colours associated with the extreme values, and limit the colour scale range. This best practice can bring out different features from seismic data.

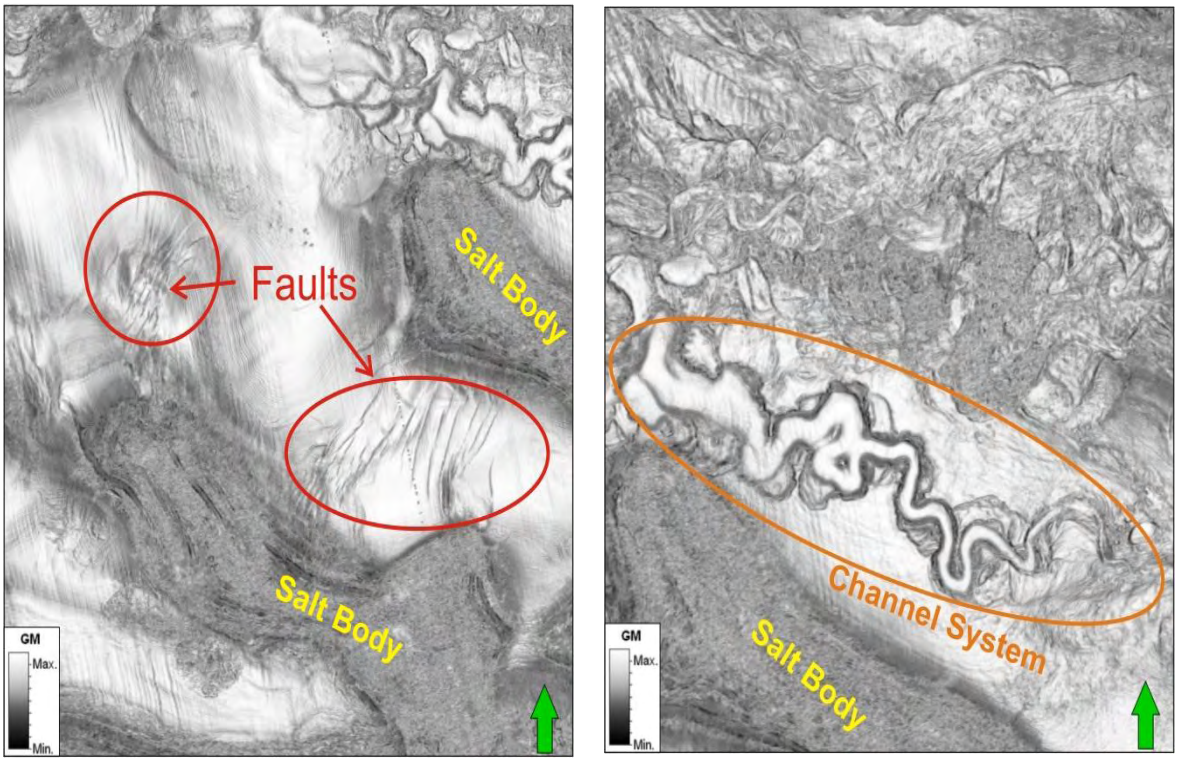

(a) **(b)**

Figure 66 - Same time slice from *gradient magnitude* attribute cube in both figures. In **(a)** it is shown the potential of this attribute in fault enhancement and detection, **(b)** shows a system of ancient channels related to a deep-sea turbidite system. Salt bodies are also identified, although their boundaries are not well defined.

IV.3.3.4. Structural Smoothing

Structural smoothing is a fast volumetric signal processing method that applies a 3D Gaussian filter to reduce the noise content of the input data. This attribute performs a structure-orientated filtering since it takes into account bed estimated orientations, by the *principal component estimation* method (see Section IV.3.3.2). A structure-orientated filter reduces the noise content without loosing information related to edges within the data.

Nowadays, the time spent in seismic data interpretation is considerably reduced when compared to the past. Costumers want fast responses with robust

interpretations and reliable geological models which best fit the seismic data with the less time-consumption possible. In addition, if in the past most of the interpreters were geophysicists they have been mostly replaced by geologists that, if by one hand are able to build best geological models, by the other hand have more difficulties in distinguishing noise from real data, and have little knowledge of seismic data processing and artifacts (Fehmers and Hocker, 2003). Fast volumetric signal processing attributes, and the ones described in IV.3.1, are part of the available tools in *Petrel* 2008.1 to help the geoscientist to improve the signal-to-noise ratio and make the interpretation easier.

The Gaussian filter can be applied with different settings to reduce spatial noise and improve reflectors continuity. In *Petrel* 2008.1, the *structural smoothing* dialog box allows the user to active the checkboxes "*Dip-guide*", "*Enhance Edges*" and select the multi-trace window size within which the attribute is computed. "*Dip-guide*" computes the local orientation of the reflector and applies the filter considering the estimated orientation (bedding orientation is estimated following the method described in Section IV.3.3.2). This option will improve both vertical and horizontal resolution (Randen *et al*., 2003). "*Enhance edges"* enhance and sharpen the presence of edges, detected by computing the instability of the structure, through the *chaos* attribute (Section IV.3.4.1).

In *Petrel* 2008.1, the Gaussian smoothing operator has the following expression (Iske and Randen (2005) in Schlumberger, 2007a):

$$h_G(k) = \frac{1}{\sqrt{2\pi\sigma}} exp\left(-\frac{1}{2}\frac{k^2}{\sigma^2}\right) \quad \text{Eq. (26)}$$

σ determines the width of the smoothing filter; the size of the smoothing window (σ) is a user-defined parameter which can be adjustable to the data in inline, crossline and time directions independently through a slider control. σ has an allowable range of 0.0 – 5.0 and can be converted easily to an approximate value in number of traces or vertical samples by:

$$Number\ of\ traces(samples) = (2\sigma) + 1 \quad \text{Eq. (27)}$$

The *structural smoothing* cube is perfectly to condition seismic data to use in automatic interpretation tools, since the reflectors' continuity is enhanced leading

to increased picking stability. "*Dip-guide*" and "*Enhance edge*" options, when activated, highlight faults and other vertical linear anomalies within the data facilitating the structural interpretation process (Figure 67).

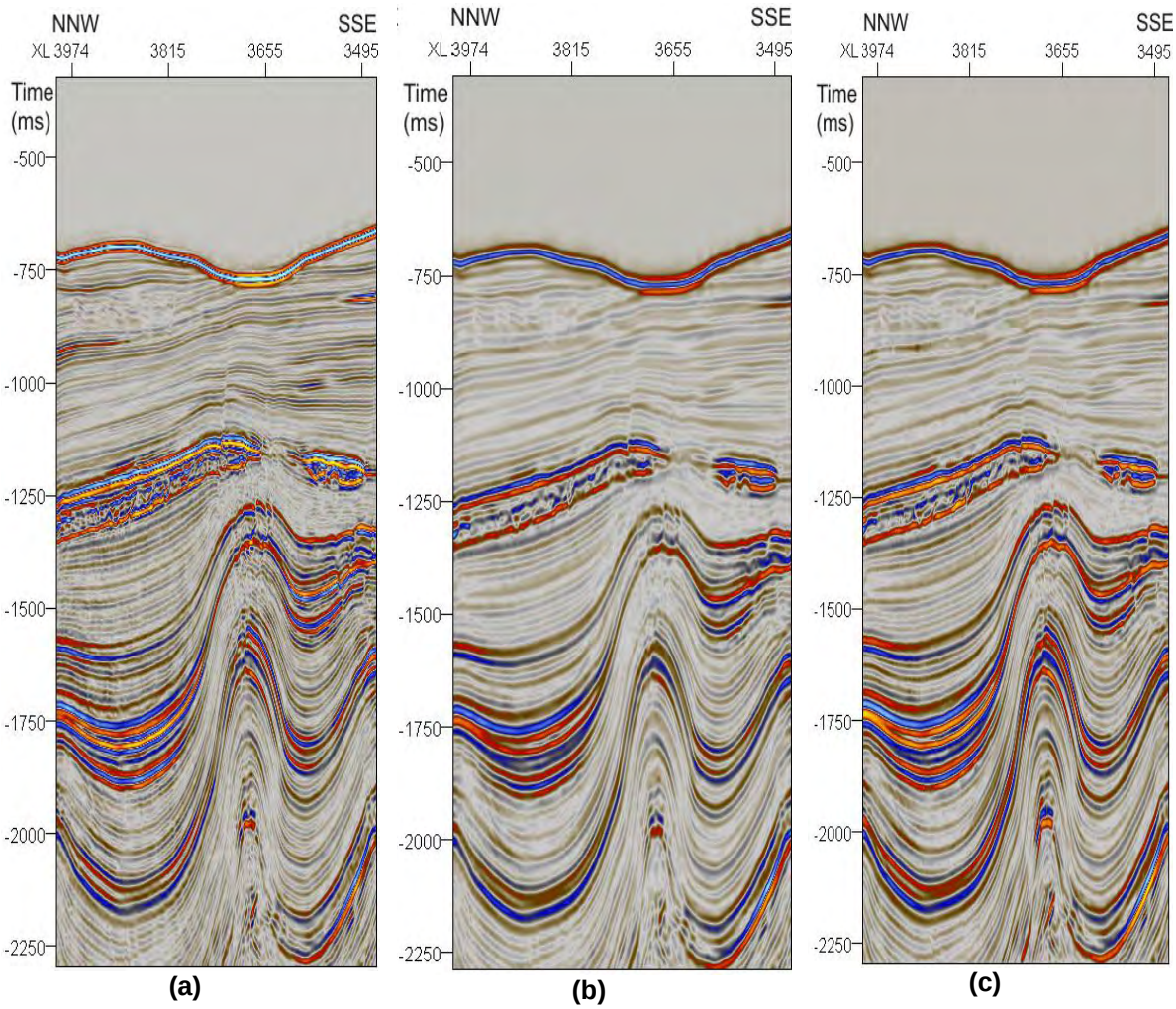

Figure 67 – Seismic section in: **(a)** original amplitude; **(b)** *structural smoothing* attribute without "*Dip*-guide" checkbox selected, same effect as applying a 3D Gaussian smoothing filter only; **(c)** *structural smoothing* honoring estimated bed orientation and automatically detecting edges.

Due to the many advantages of structural smoothing, this is the best choice to use as part of *Ant Tracking* workflow (see Section IV.3.3.6) during the seismic conditioning step.

IV.3.3.5. Variance

In probabilistic analysis, variance is the measure of how spread is the dataset around the mean value Equation 28

$$\sigma^2 = \sum_{i=1}^{l} (x_i - \bar{x})^2 \qquad \text{Eq. (28)}$$

Based on this statistical definition, *Petrel* 2008.1 uses the patented algorithm introduced by van Bemmel *et al.* (2000) to compute a normalized population variance with an optional weighted vertical smoothing. The *variance* attribute uses an algorithm which computes the local variance of the input signal through a multi-trace window with user-defined size.

$$\sigma_t^2 = \frac{\sum_{j=t-\frac{L}{2}}^{j=t+\frac{L}{2}} w_{j-t} \sum_{i=1}^{I} \left(x_{ij} - \overline{x}_j\right)^2}{\sum_{j=t-L/2}^{j=t+L/2} w_{j-t} \sum_{i=1}^{I} {x_{ij}}^2} \qquad \text{Eq. (29)}$$

Where x_{ij} is the sample value at horizontal position, i, and j is the vertical time sample. $w_{j\text{-}t}$ is the vertical smoothing term over a window of length L.

"*The Semblance Cube*" and "*The Coherency Cube*", the later introduced by Bahorich and Farmer (1995), are common attributes in the oil and gas industry to map discontinuities. The algorithm of variance is innovative because it measures directly, without the need of an intermediate step, differences from a mean value. The direct measurement produces sharper results, when compared to other edge detection methods.

The *variance* attribute is an edge imaging and detection method. The window size is the critical parameter to obtain discontinuities as sharp as possible. Long vertical windows produce vertical stripping while short window lengths produce horizontal stripping when *variance* is displayed in cross-sections (Figure 68). The size of the window can be adjusted in inline/crossline and vertical directions independently. Different values for each of the first two directions can really bring out depositional features which have a preferential directions in space (e.g. non-meandering channels).

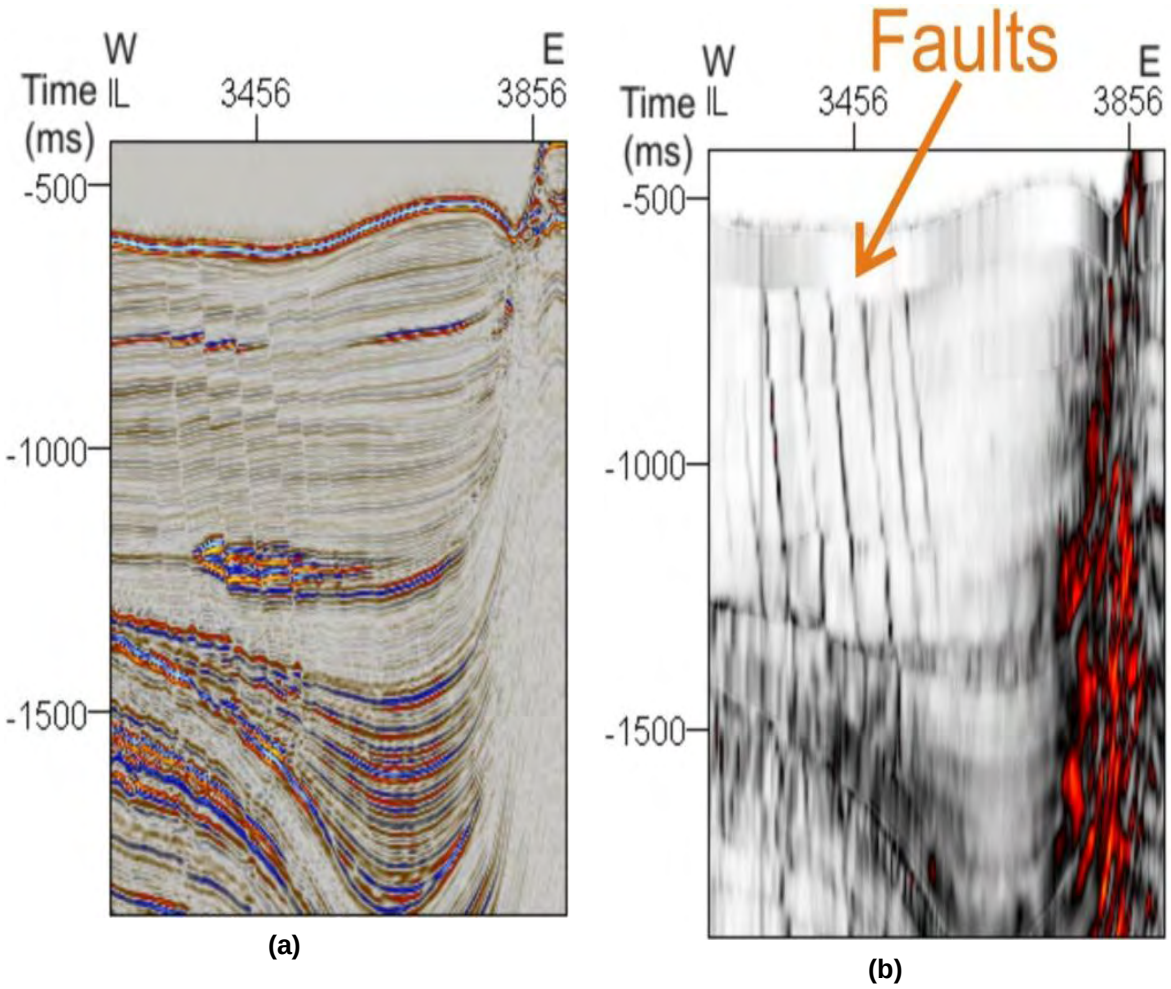

Figure 68 – (a) Seismic section in original amplitude and **(b)** *variance* attribute computed over a window of 3x3 traces in inline/crossline directions and 15 ms in time. The horizontal stripping on **(b)** is due to the short vertical window.

Short vertical time windows transform the *variance* attribute from a simply structural attribute into a good stratigraphic attribute, where depositional features, such as reefs, channels and splays, are enhanced (Figure 69). The interpretation of *variance* should be done preferentially in time slices along the attribute cube. This spatial visualization allows the interpreter to better understand the distribution of faults, channels and other geological features of interest that can be an active part in a possible petroleum system.

Values of variance equal to 1 mean discontinuities within a continuous seismic event represented by value of 0.

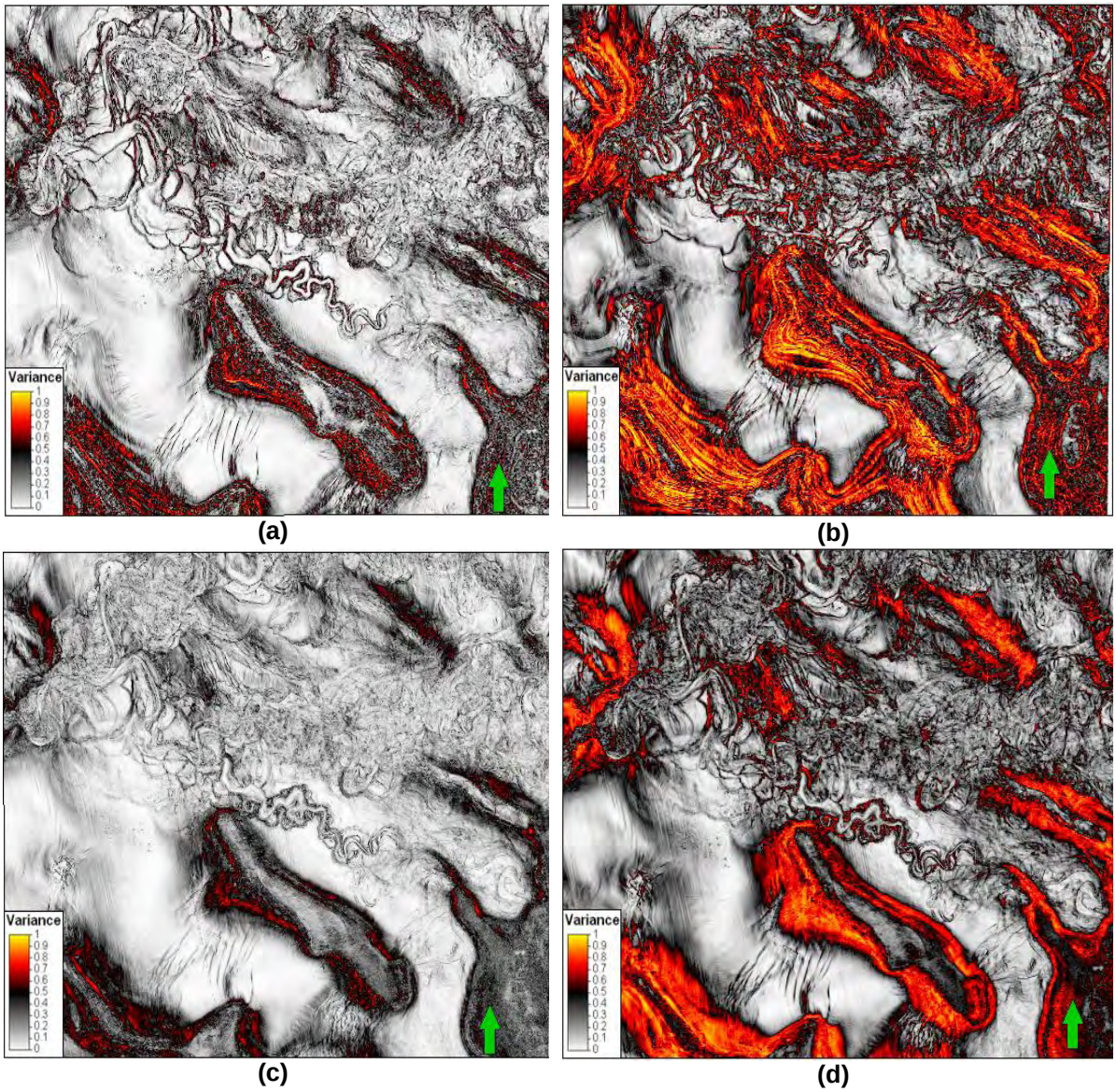

Figure 69 – Comparison between the same time slice from different variance cubes computed with different windows: **(a)** Window of 3x3 traces in inline/crossline directions and 15 ms of vertical length. For this data is the best window to have clear and sharp defined depositional features; **(b)** window of 5x5 traces in inline/crossline directions and 15 ms of vertical length. Features boundaries are less sharp when compared to (a); **(c)** window of 3x3 traces in inline/crossline directions and 65 ms of vertical length. Larger vertical windows blurry the limits of depositional features; **(d)** window of 5x5 traces in inline/crossline directions and 65 ms of vertical length show imprecise depositional feature boundaries and less defined faults.

IV.3.3.6. Ant Tracking

The *Ant Tracking* attribute is a patent-protected algorithm from *Schlumberger* that introduces a new paradigm in fault interpretation. Fault interpretation is still a manual, time consuming and very subjective task to the interpreter, and consequently difficult to perform accurately. With this new technique, edges

(faults, fractures and other linear anomalies) are automatically enhanced, following a standard workflow. The enhanced edges are then automatically or manually interpreted (or extracted; Pedersen *et al*., 2002).

An *Ant Tracking* attribute volume is generated using swarm intelligent concepts where real ants colonies looking for food are mimicked. Real ants use pheromones to mark their paths in order to optimize the search for food (Figure 70). In comparison, *Ant Tracking* uses a high number of agents (virtual ants) which are deployed over a seismic discontinuity volume to look for fault zones. "Virtual pheromones" are deployed by these agents when they find a fault zone, resulting in an attribute volume that shows fault zones in sharp detail. This high level of detail is achieved because virtual ants deployed over noisy areas or where there is a surface that does not fulfill the conditions for a fault (e.g. remains of a reflector) are terminated shortly or immediately, not deploying "virtual pheromones" (Schlumberger, 2007b).

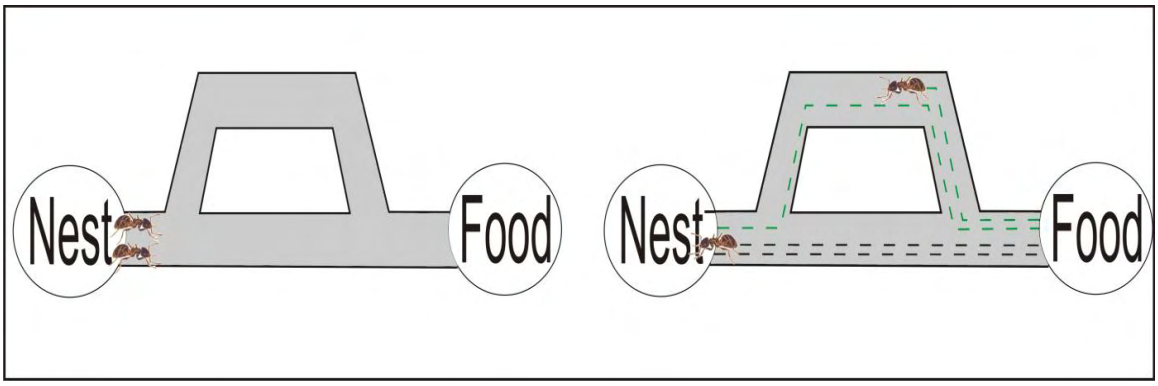

(a) **(b)**

Figure 70 – **(a)** Diagram showing two ants starting at the same time at the nest looking for food. **(b)** The ant which chooses the shortest path, the straight one (black dashed line), will arrive before the ant choosing the longest path (green dashed line). Therefore, the shorter path will be marked with more pheromones than the longer one, hence the next ant is more likely to choose the shortest path (modified from Pedersen, 2002).

In order to produce the fault seismic cube there are several volume seismic attributes which need to be computed in a chain, where the output from each one will be the input for the next process. Generally speaking, the required steps in *Ant Tracking* are: (1) seismic conditioning, to reduce the spatial noise present in the original data; (2) generation of an edge detection cube; (3) calculation of an edge enhancement volume, which is the *Ant Tracking* cube itself (Figure 71).

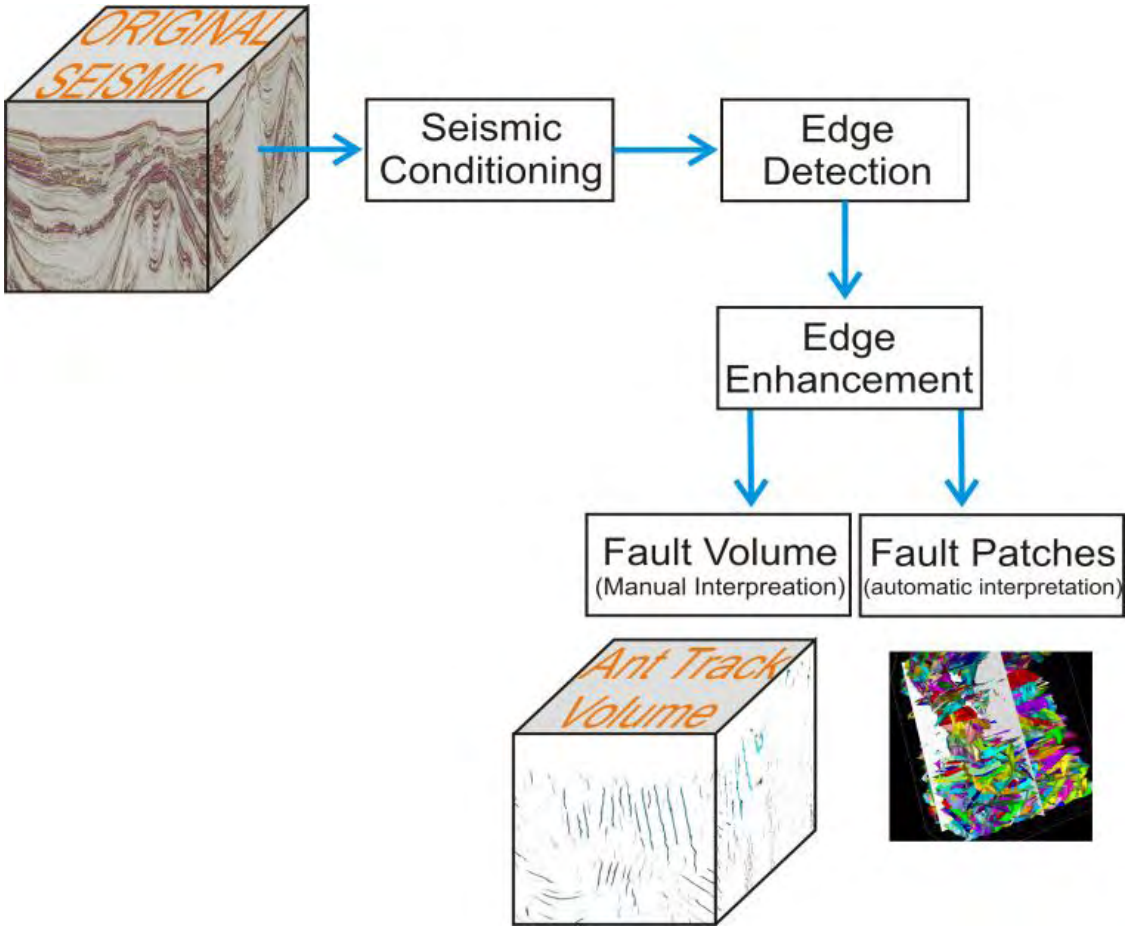

Figure 71 - *Ant tracking* general workflow (modified from Schlumberger, 2007a).

From the *Ant Tracking* cube, faults can be automatic extracted through *Petrel*'s "*Automatic Fault Extraction*" process, manually interpreted by the traditional way, or by seeding points to build patches with the *Petrel*'s "*Automatic Fault Extraction*" process active; these patches can be later transformed into fault interpretations in order to be inserted in the hydrocarbon reservoir model (Figure 72).

Seismic conditioning is used to reduce spatial noise within the data, enhancing reflectors continuity and honoring edges. The *structural smoothing* attribute is normally the seismic attribute extracted in this step. In the edge detection stage, the *variance* cube is normally used, which is an attribute data and structural dependent; therefore, it should be extracted from seismic data with as less noise as possible, without losing information about discontinuities. Finally, the edge enhancement is performed with the realization of the *Ant Tracking* attribute. The resulting output can be combined with the original seismic data and/or an edge detection cube in fault interpretation.

There are many user-defined parameters to adjust the deployment of the ant agents. The settings should be chosen to fit the conceptual model about the structural system of the area built by the interpreter as a first approach. A brief description of these parameters are summarized in the Table I and have by default two configurations depending on the desired detail level. "*Passive* Ants" should be used as a first approach to understand the major regional structural system, since the *Ant Tacking* cube will enhance faults with a low level of detail; only strong major regional faults will be detected with low resolution in the fault extraction. "*Aggressive Ants*" are used to deploy a large number of ants in the seismic cube and capture faults in a high level of detail; in this case major and subtle faults from the data will be extracted, leading to high resolution on fault extraction.

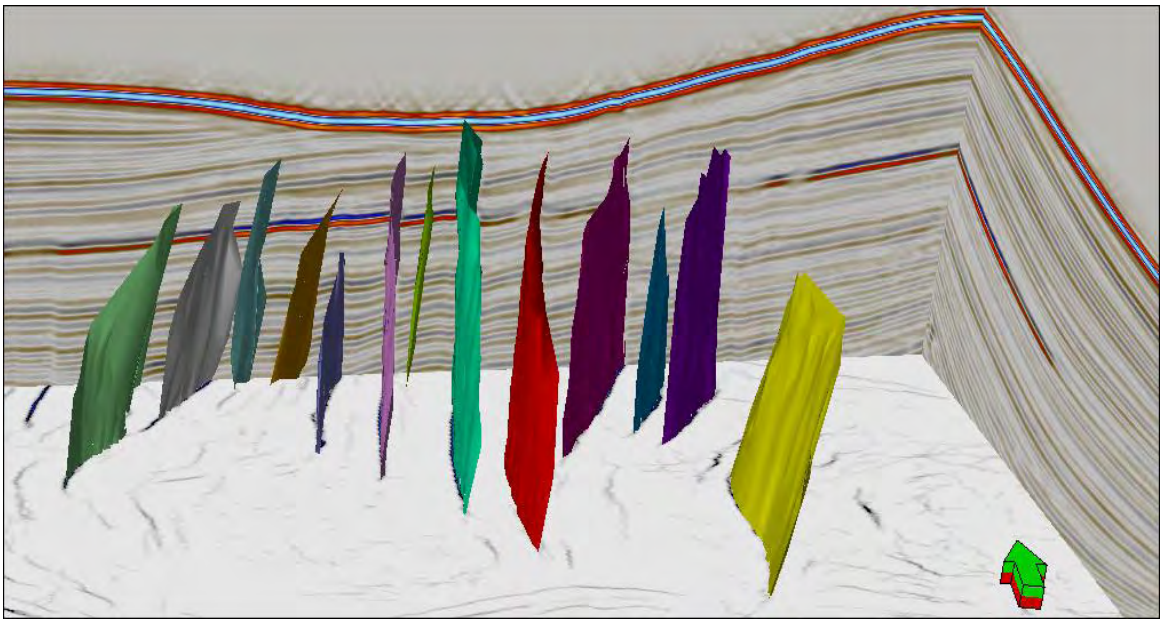

Figure 72 - *Ant Tracking* time slice combined with the original seismic data to perform the "*Automatic Fault Extraction*" using seeding points. Colour surfaces are fault patches to be used in the geological model.

Apart from these parameters, in *Petrel*, the user can also use the *Stereonet* tab. This option works as an orientation filter which allows the user to exclude specified orientations from the output volume. With this tab the interpreter can easily separate two different fault systems or eliminate footprints present within the data; since virtual ants will not be deployed within the rejected areas. The Stereonet is oriented to the inline survey direction. To reject specified dip and azimuth angles in *Petrel* (estimated using the methods described in IV.3.3.2) the user should click over the desired areas and switch them to grey (Figure 73).

Table I - Ant Tracking user-defined parameters (modified from Schlumberger, 2007b)

Parameter	Min.	Max.	Passive Ants	Aggressive Ants	Description
Initial Ant Boundary (voxels)	1	30	7	5	Defines the initial distribution and number of agents in the volume. Larger Number results in fewer ants leading to less detail.
Ant Track Deviation (voxels)	0	3	2	2	Distance to look on either side of tracking direction. Allows more connections between points.
Ant Step Size (voxels)	2	10	3	3	The amount of voxels an Ant agent advances for each increment (it is the search distance to look for discontinuity). Increasing will produce lower resolution.
Illegal Steps (voxels)	0	3	1	2	Defines how many steps an Ant can perform without finding a local maximum in one direction within its search distance.
Legal Steps (voxels)	0	3	3	2	This parameter plays with *Illegal Steps* parameter. It is the minimum number of steps that must contain a valid edge value for the agent to continue.
Stop Criteria (%)	0	50	5	10	It is the percentage of illegal steps that an Ant agent can do in its entire "life".

Since the *Ant* Tracking attribute is a heavy processing operation it should be tried first in a small cropped cube where some of the principal discontinuities are clearly shown. If these features are enhanced after the ant tracking realization then the user can apply them to the entire dataset.

Two tested workflows are proposed to compute the *Ant Tracking* cube. These two approaches differ mainly in the number of steps required and in the attribute used as edge detection method.

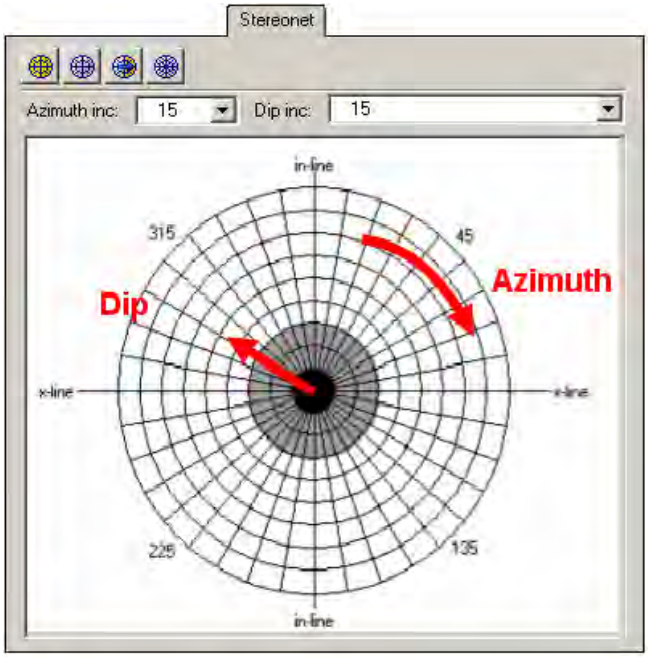

Figure 73 - Stereonet filter used to compute *Ant Tracking* cube. Red arrows represent how azimuth and dip are calculated. Grey areas represent rejected dip and azimuth ranges.

Ant Tracking proposed workflows

The first workflow discussed here is the simplest one. The first step is conditioning the original seismic data to improve the signal-to-noise ratio and enhance reflectors continuity honoring discontinuities orientation. The output attribute from this step is the *structural smoothing* cube (see Section IV.3.3.4). The user-defined size of the Gaussian filter should be enough to clean some residual noise within the data without losing information related to major discontinuities (Figure 67c).

The *structural smoothing* volume is then used as an input to the edge detection step. Several attributes available in *Petrel* 2008.1 can be used (e.g. *Chaos*, *Variance*, *Dip Deviation*). In this workflow it is suggested to compute *chaos* (see Section IV.3.4.1) volume. For less experience users this may be particular useful since there are no user-defined parameters. The *Ant Tracking* attribute is applied to the *chaos* volume with ant parameters and a stereonet filter adjustable to the original seismic data.

The second tested workflow is more complex than the first but generally achieves better results. For seismic conditioning a strong *structural smoothing* filter is used (e.g. with window of size 3x3x1.5), which will eliminate spatial noise, improving

continuity without lost of edges information. This strong Gaussian smoothing filter, in *Petrel*, should honor seismic reflectors orientation and enhance edges, with the "*Dip-guide*" and "*Enhance Edges*" checkboxes selected. For the edge detection process it is suggested to use a *variance* cube (see IV.3.3.5) with tested parameters to best fit the data. This variance cube should define faults and other discontinuities with a high level of detail.

The realized *variance* cube computed is now going to be used as an input to another *structural smoothing* attribute. This second smoothing is just a large 3D Gaussian smoothing filter realized with soft user-defined parameters without selecting the "*Dip*-guide" option. This step will eliminate possible noise created during the execution of the variance attribute.

The data is then ready to be used as an input to the *Ant Tracking* attribute. This last step is repeated several times until the output cube has little noise content. The first *Ant Tracking* pass should be computed with parameters which reflect more aggressive ants. These first run should detect both major and minor fault systems. The output cube will have enhanced real faults and other linear discontinuities with less detail. The *Ant Tracking* cube is then used as an input to another *Ant Tracking* algorithm extraction, this time with less aggressive ants. Computing the *Ant Tracking* attribute over the same attribute cube will detect only real faults associated to strong signals, thereby eliminating noisy features. If in the final the output is good enough to extract the faults in a precise way the workflow is terminated; if not, more *Ant Tracking* passes should be used. This cascade edge enhancement reinforces strong features in the volume and reduces the contribution of minor features, leading to better final results for fault interpretation.

The figure below shows a comparison of the two workflows for a random seismic intersection. The figure from the right was computed using the longer workflow. Faults are more consistent in space and well defined improving the inpterpretablity.

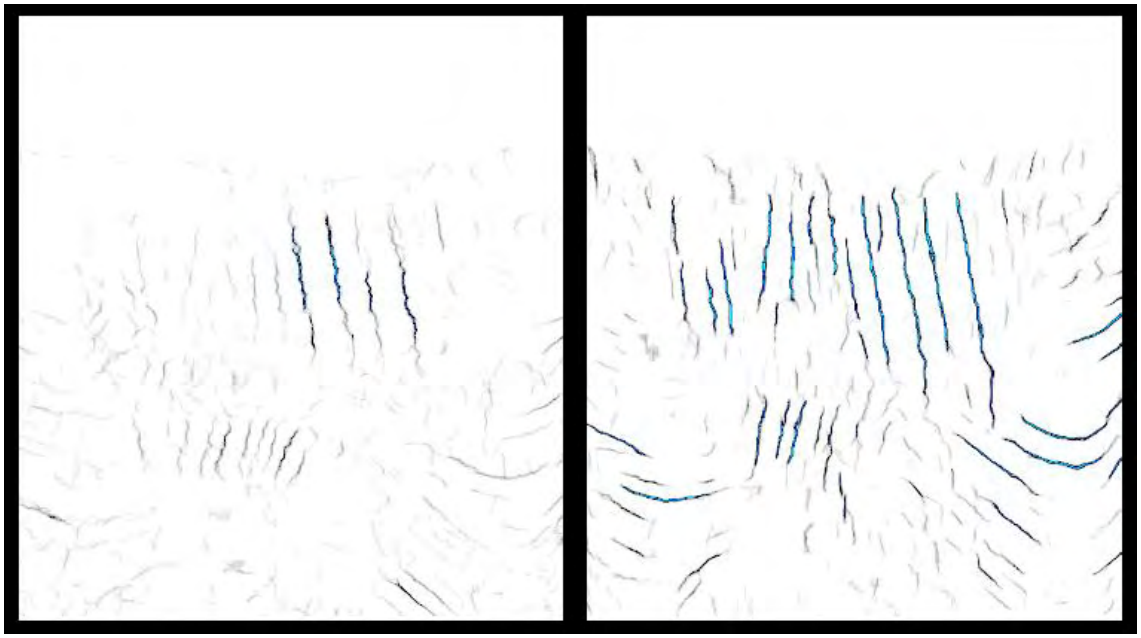

Figure 74 - Comparison between two proposed workflows to compute the *Ant Tracking* cube. The shorter workflow using the *chaos* attribute (on the left) shows less coherent faults when compared to the one on the right computed following the more complex workflow.

IV.3.4. Stratigraphic Attributes Library

Identifying stratigraphic features from seismic data is one of the most difficult tasks in the design of a reliable geological model. Furthermore, the study of stratigraphic events is important to understand how the petroleum system of an oil and/or gas reservoir works. *Stratigraphic Attributes* comprise attributes related to the identification of stratigraphic sequences, lateral and vertical variations of lithologies, structural orientation measurements, frequency decomposition and facies distribution.

IV.3.4.1. Chaos

As the name suggests, the *chaos* attribute is related to the “lack of organization” within a 3D window. This attribute measures how consistent is the dip and azimuth orientation estimated using the *principal component method* (described in IV.3.3.2; Schlumberger, 2007b). Estimated measurements with low consistency are related to a chaotic signal pattern. Chaotic patterns are used to enhance faults,

discontinuities, salt bodies, and reflectors with chaotic texture which are often associated with channel infill or reef textures (Figure 75).

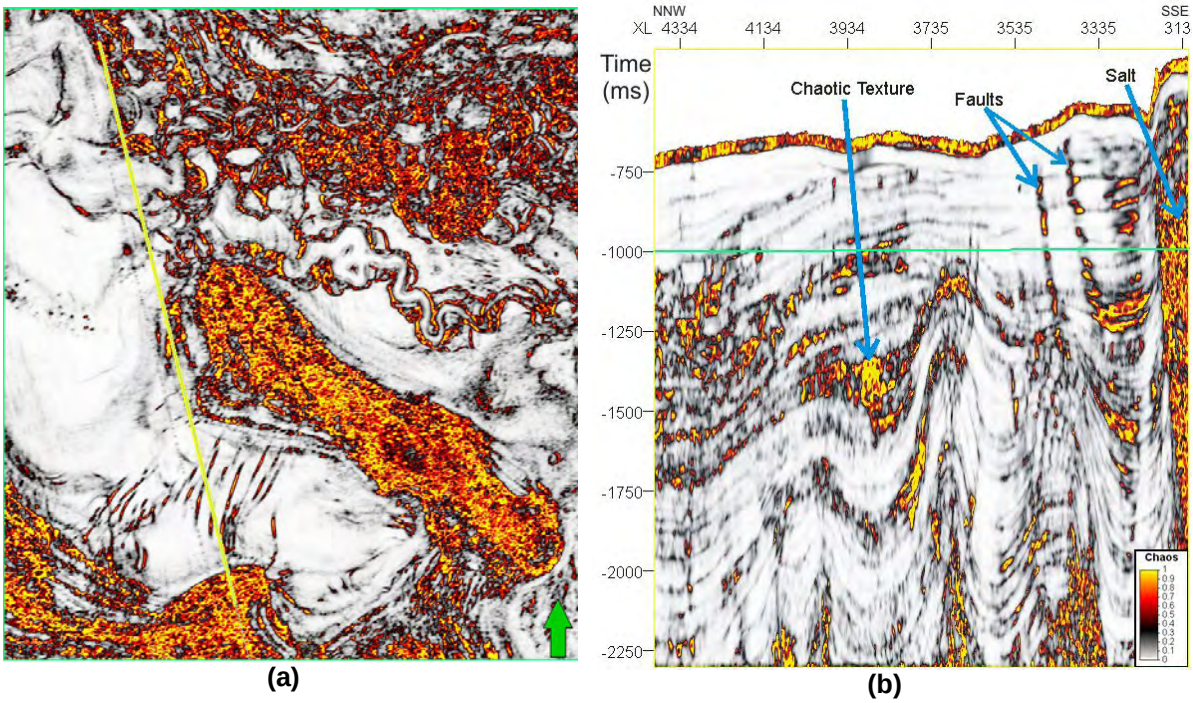

Figure 75 - (a) *Chaos* attribute in a time slice and **(b)** in a seismic section. In **(a)** the yellow line represents the position of the seismic vertical intersection. The light green line represents the position of the time slice shown in **(b)**. In the time slice can be identified; a well defined channel system and a clear salt dome delineation can be observed. In **(b)** the three major features that *chaos* attribute is able to enhance can be identified: faults/discontinuities, salt bodies and chaotic texture within reflectors.

Another important characteristic of the *chaos* attribute is that it is invariant with amplitude and orientation; therefore it will produce consistent results in areas with high or low amplitudes, and dipping or non-dipping events. The output data range is scaled between 0, corresponding to non-consistent areas, and 1, for consistent areas.

Due to the potential of *chaos* for edge detection, it is commonly used as part of the simple *Ant Tracking* workflow already discussed in Section IV.3.3.6.

IV.3.4.2. Local Flatness

The *local flatness* attribute is at the same time a stratigraphic (related to seismic textures) and a structural attribute, it is also used to enhance faults and other

vertical anomalies (Figure 76). This attribute gives information about the flatness of the local seismic signal, within a 3D window of user-defined size; the size of the window is defined by adjusting the same σ parameter of the *structural smoothing* attribute (see Section IV.3.3.4).

This attribute is a two step algorithm. First, it measures the local orientation by the *principal component method* (see Section IV.3.3.2); then it computes the normalized *variance* on the estimated orientation vector, following the method described in Section IV.3.3.5. *Flatness* does not refer to horizontal and non-dipping seismic events; it is the degree to which the local estimation is planar. If it is planar there are no discontinuities; if not an edge is detected. The output cube is scaled between 0 to 1, meaning locally planar and non-planar, respectively.

To transform the *local flatness* attribute invariant with amplitude, showing high reflectivity seismic events such as low reflectivity features, local flatness should be computed using an invariant attribute volume (e.g. *cosine of instantaneous phase*) as an input.

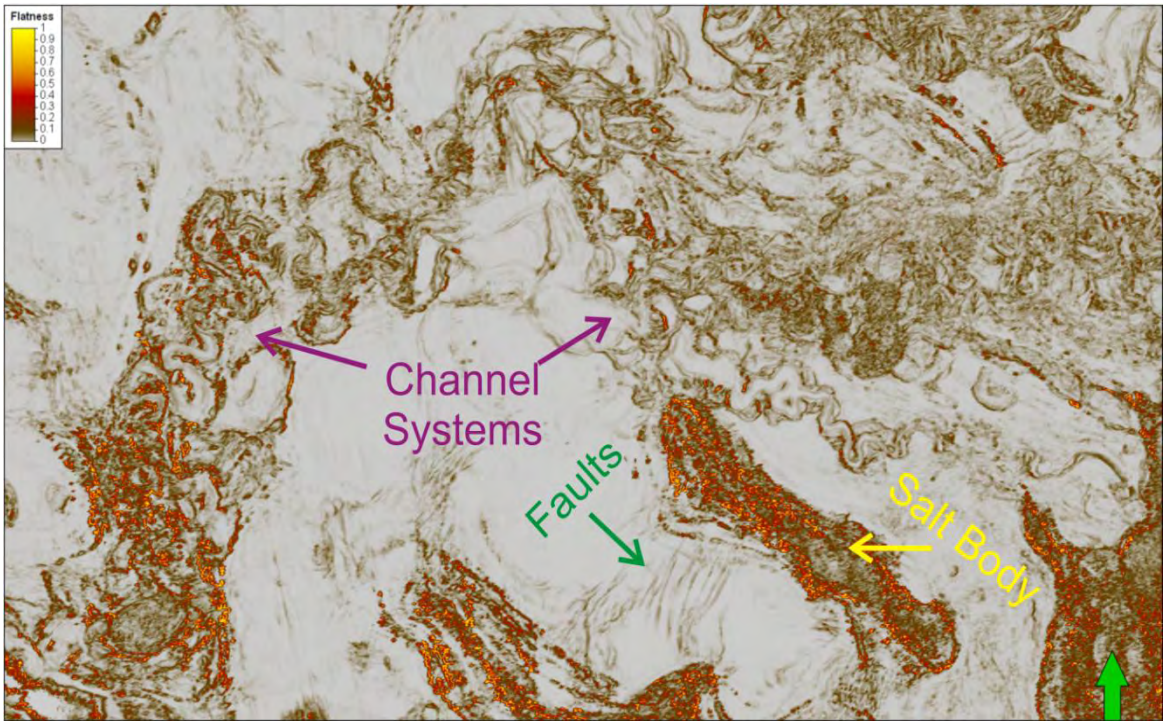

Figure 76 - Time slice from a *local flatness* attribute volume. This attribute can be considered both a stratigraphic and a structural attribute. It should be interpreted in time slices rather than seismic sections and enhances not only features related to seismic texture and channels infill, but also structural events such as faults and salt bodies.

IV.3.4.3. Iso-Frequency

The *Iso-Frequency Component* generates a volume attribute through a patented seismic decomposition method for user-defined frequencies (Pepper and van Bemmel (2001), in Schlumberger, 2007a).

The spectral decomposition is performed locally and consists first in generating an autocorrelation function of the seismic data on a short time window. The autocorrelation function is insensitive to the phase content of the original seismic data, thus aligning the seismic energy at zero lag. The second step is a cross-correlation between a cosine wave (*cosine correlation transform* (CCT) method), with a user-defined number of cycles, and the auto-correlation function generated before, to determine the numeric similarity of the auto-correlation function and the cosine wave. The cross-correlation algorithm is defined by:

$$\phi_{GH}(\tau) = \frac{\sum_{k=-N}^{N} G(k)H(k+\tau)}{\left[\sum_{k=-N}^{N} G^2(k) \sum_{k=-N}^{N} H^2(k)\right]^{1/2}} \qquad \text{Eq. (30)}$$

Where G(k) and H(k) are the two signals being correlated: either the windowed original seismic data to build the auto-correlation function, or the cosine function and the auto-correlation function.

The CCT method output value is a correlation coefficient which measures the correlation between a known cosine wave signature of a specific frequency and the auto-correlation seismic data. The output attribute cube is scaled between -1 to 1. Zero values mean uncorrelated functions. 1 is for identical signal and negative values have the same meaning as positive values but indicates inverted polarities.

Besides the cosine frequency, in *Petrel*, the user has also the option to select a desired "*Number of cycles*"; this option defines the window length where the attribute is extracted. The window length depends both on the relative frequency of the cosine function and the frequency content of the original seismic data.

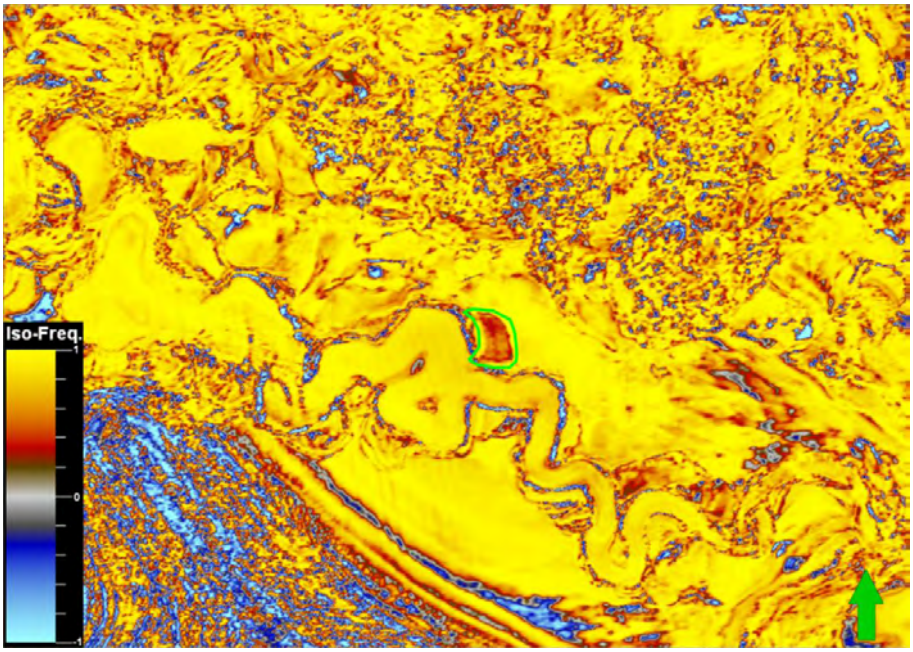

(a)

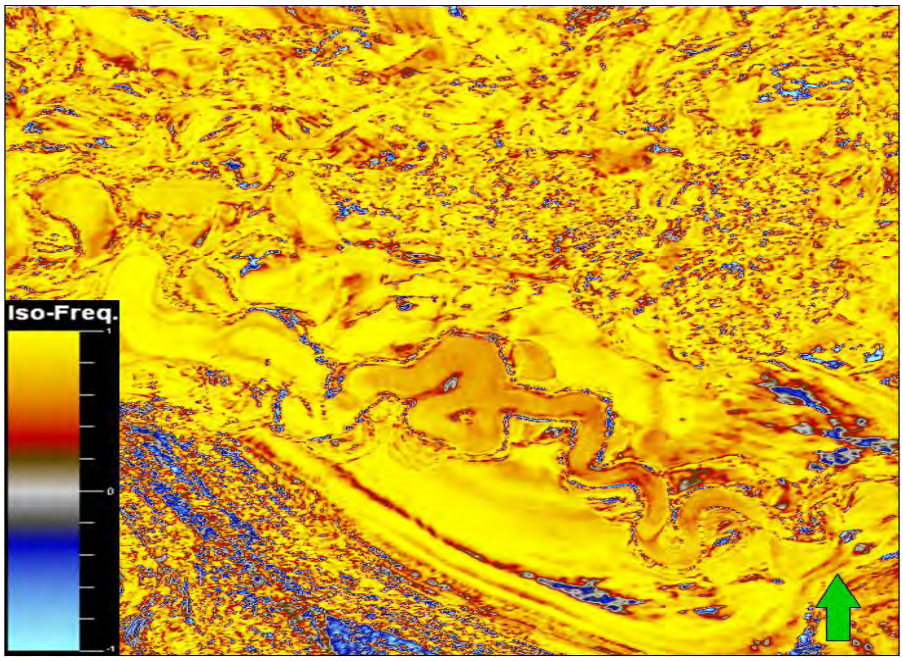

(b)

Figure 77 – Same time slice position for two *Iso-Frequency* volumes computed with a cosine wave of **(a)** 25 Hz and **(b)** 45 Hz. When **(a)** and **(b)** are compared, it is clear that inside the meandering channel there are different values for the correlation, which may indicate changes in lithology inside it. In **(a),** inside the green polygon, it is inferred that the value close to 0 is related to an abrupt change in lithology when compared to the lithology inside the channel. This feature will be interpreted further in this work, in Chapter V.

Short windows will not focus the correlation energy to illuminate anomalies, while too long windows will show local geologic effects and not tuning effects. There is also the option "*Spectral Normalization*" which performs a spectral whitening and attempts to remove the signature of the seismic wavelet from the results.

The *Iso-Frequency* attribute volume may reveal subtle variations in lithology that may indicate stratigraphic traps for hydrocarbons. If an interesting feature is identified at a designated frequency the resulting cube may represent similar features with the same frequency signature that may not be identified in the original seismic data. The *Iso-Frequency* cube helps to identify similar features/facies already correlated to potential hydrocarbon reservoir features in other areas within the data. Similar methods of spectral decomposition are becoming standard available attributes in most of the interpretation software suites.

IV.3.4.4. Relative Acoustic Impedance

Acoustic impedance (Z) is an intrinsic physical property of rocks, defined as the density of the geologic formation multiplied by the propagation velocity of p-waves through that formation (Equation 31).

$$Z = \rho . V \qquad \text{Eq. (31)}$$

To measure the real value for acoustic impedance it is necessary to use seismic inversion methods. However, in 1992, Taner demonstrated that *Relative Acoustic Impedance* (RAI) can be expressed and computed integrating the real part of the seismic trace (Equation 33). This method assumes that the input seismic data has been processed to have reduced noise and multiple contamination, and also that it contains zero phase and large bandwidth. Based on this assumption the seismic trace represents the band limited reflective series Equation 32. The integration of the seismic trace will provide a band-limited estimate of the natural log of the acoustic impedance. Since the integration is band-limited, the impedance will not have absolute magnitude values, and consequently is only relative.

$$f(t) = \frac{1}{2}\frac{\Delta\rho V}{\rho V} \qquad \text{Eq. (32)}$$

$$\ln(\rho V) = 2\int_{t=0}^{t=T} f(T)dt \qquad \text{Eq. (33)}$$

A Butterworth filter is then applied to remove long wavelength trends originated from the integration process (Schlumberger, 2007a).

$$BL(f) = \frac{1}{1 + (f/f_H)^{2N}} \qquad \text{Eq. (34)}$$

Petrel 2008.1 uses a filter with the following parameters: BL(*f)* is the band-limited signal in frequency; f_H is the frequency cutoff and has a value of 10Hz and the filter order (*N*) is 3.

RAI is not an exhaustive inversion process, since the output volume only reflects the apparent acoustic impedance contrasts, or physical property contrasts. *Relative acoustic impedance* is used in many calibration procedures since it mimics the natural log of the acoustic impedance. In interpretation, it is combined with the original seismic data to indicate sequences boundaries, associated with high contrasts in Z values, unconformity surfaces and discontinuities (Figure 78). It may be also related with porosity within the formations and the presence of fluid content inside a hydrocarbon reservoir.

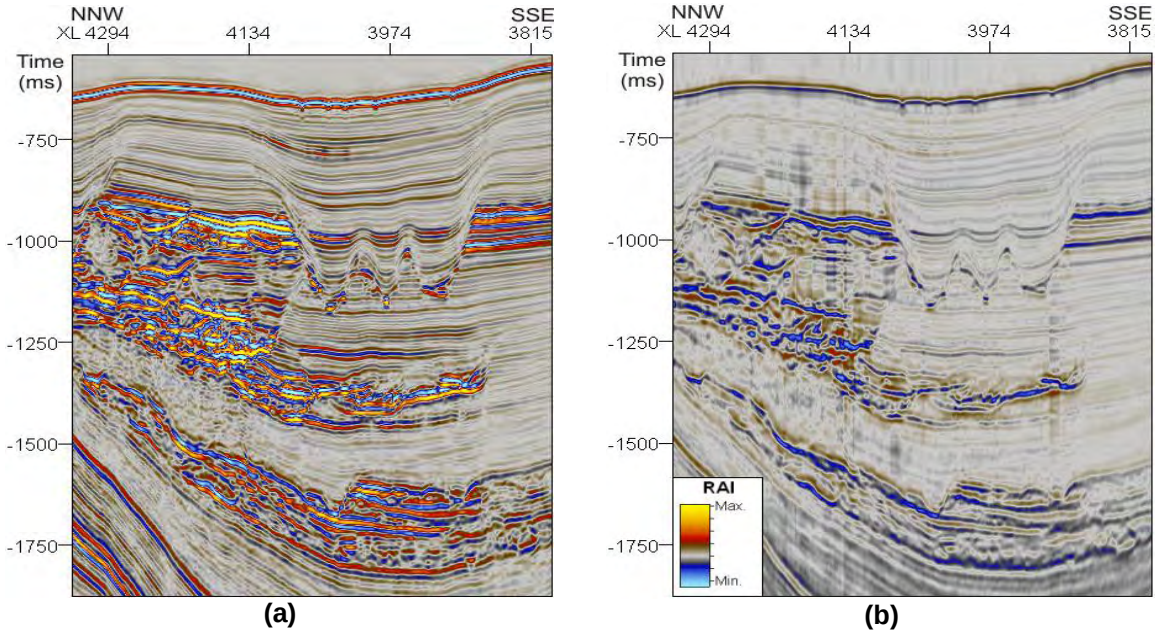

Figure 78 – (a) Input seismic data and **(b)** computed relative acoustic impedance attribute. High contrasts between values of RAI highlights sequences boundaries. Here too, the bottom of some ancient channels are better interpreted in **(b)**.

IV.3.4.5. Neural Network

The *Neural network* attribute allows the creation of an attribute classification volume based on a pre-conceived estimation model, created by *Petrel*'s "*Train*

Estimation Model" process found under "*Utilities*" (Schlumberger, 2007b). In this work an unsupervised estimation model for facies classification was tested using as input the original seismic cube and derived seismic volume attributes.

Artificial Neural Networks (ANN) can be defined as information processing algorithms that try to mimic the human brain. Unlike conventional computation algorithms that always follow the same programmed steps independently of the input data, neural networks learn by trial, using a set of inputs, and so are not programmed to perform a specific task (http://www.doc.ic.ac.uk).

Biological neural networks are made of billions of neurons interconnected, building extremely complex information networks. Many processes of how information is processed within the human brain are still a "*black box*" to the science community, although it is known that neurons are the main components of the human brain. A neuron is a specialized cell with the ability to propagate an electrical signal and has a well known basic structure and operation method. Human neurons are composed of four parts: the nucleus, the dendrites, the axon, and the synapse (Figure 79). Dendrites are fine structures which receive electrical signals from other neurons transmitting the signal into the cell body, acting like a branching input. The axon is the output connection for electrical pulses emitted by the neuron which splits into thousands of branches. At the end of each branch the synapses are the connections between neurons. Synapses receive the activity from the axon and convert it into an electrical effect that inhibits or excites the activity in the next connected neuron. If the neuron receives excitatory input sufficiently large when compared with its inhibitory input, it sends a spike of electrical activity down its axon. The human learning process occurs by changes in the effectiveness response of the synapses, i.e. changes in the influence of one neuron on another (Schlumberger personal communication, www.statsoft.com, www.doc.ic.ac.uk).

ANN use the same principle described in the previous paragraph based on artificial neurons, with simpler configuration. Artificial neurons are processing units interconnected in a complex communication network working together to solve a specific task. They receive a set of inputs, which can be fed from multiple sources,

which are then multiplied by a weight. The weighting result is summed and is passed through a transfer function returning one or more outputs.

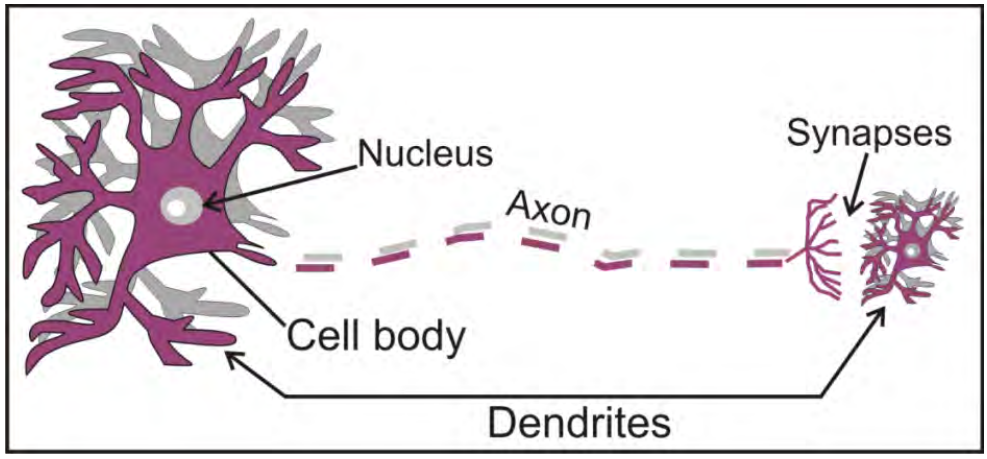

Figure 79 - Diagram of a human neuron and its components: Nucleus; Axon; Dendrites and synapse (modified from www.doc.ic.ac.uk).

Petrel 2008.1 uses feed-forward networks ANN, the output of any processor unit is not an input to other processor unit. Each input (X(n)) is received by artificial neurons similar to dendrites. Then a weighted sum of the inputs from all the units is computed. The importance of the input (X(n)) is measured by the weight of the connection (W(n)). The output is 1 or 0 according to whether the weighted sum is above or below a certain threshold. The neuron is adapted to a particular situation adjusting the values of the weights and the threshold value (Figure 80; Schlumberger personal communication; www.doc.is.ac.uk).

The learning process method is another key factor to achieve the best possible result. *Petrel* uses adaptive networks, since ANN are able to change their weights depending on the input (www.doc.is.ac.uk). There are two ways of adaptive training: supervised and unsupervised. Training supervised neural networks is only possible when there are available training data. The training data combined with the input data are used to optimize the weights for each input. The computed data from the neural network is constantly compared with the training data to give the error of the estimation. This method is normally used in facies estimation using well log data as training data and seismic attributes as input data.

Unsupervised trained neural networks are those where there are not available training data. The output is given in terms of classification, based on a probabilistic

analysis of the input data. The input points are plotted in "*n*" dimensions, where "*n*" is the number of pieces of input data. Using the *Competitive Learning Algorithm* the centre of points of each class are first distributed randomly then adjusted to fit the input data. The process subdivides the input data into a number of user-defined classes and it self-organizes it, detecting collective properties between them. This method is normally used with the purpose of discovering the underlying structure of the data, encode, compress or transform the data (Schlumberger, 2007b; www. www.doc.ic.ac.uk).

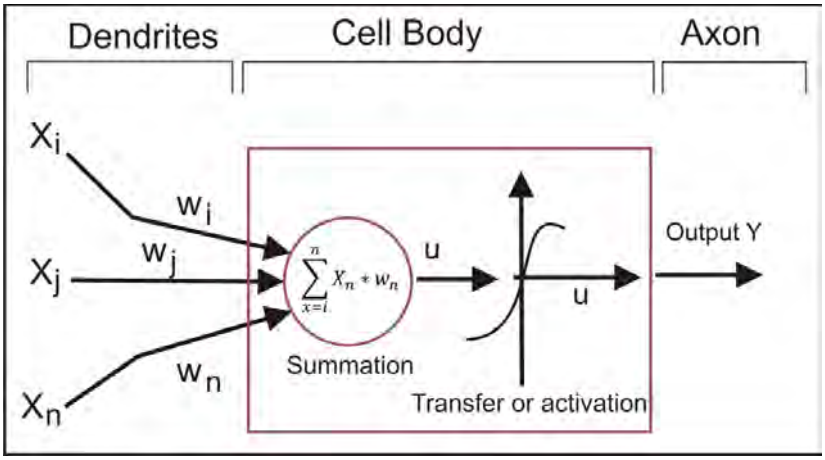

Figure 80 - Schematic representation of how a virtual neuron used by *Petrel* 2008.1 works (modified from www.doc.is.ac.uk).

Using neural networks has particular benefits when the final goal is the recognition of seismic patterns and data classification.

Workflow to compute an unsupervised Neural Network in Petrel 2008.1

Before computing the neural network attribute it is necessary to build an estimation model using the "*Train Estimation Model*" process. This process takes the input data points with the associated seismic attributes and calculates an additional attribute, a seismic classification cube. The input data should be carefully chosen in order to increase the chances of success, reducing the processing time. To compute the facies classification cube pre-selected attribute volumes, extracted from the original seismic cube, were used as input data. The attribute selection can be done by two methods: (1) the correlation between attributes; (2) Principal Components Analysis (PCA).

(1) Before computing the estimation model, in order to classify seismic data into facies, it is first necessary to build an idea about which attributes are related to lithologies and seismic textures. From the previously described seismic attributes along this chapter there are a lot of potential cubes that can be selected. Attributes related to the energy and frequency content of the data, which give information about the distribution of the acoustic impedance along the cube, and finally spectral decomposition attributes are the natural choice of an expert user in a first approach.

As stated before, a high number of input data can have the opposite effect of what one would assume, leading in most of the cases to an unsatisfactory final output. The input data should be cross-plotted against each other and should not have either a perfect correlation (Figure 81) or being uncorrelated. The plot should have a constant spatial distribution with points which can be group into families (Figure 82). The attributes that exhibit this correlation rules are the ones that should be accepted.

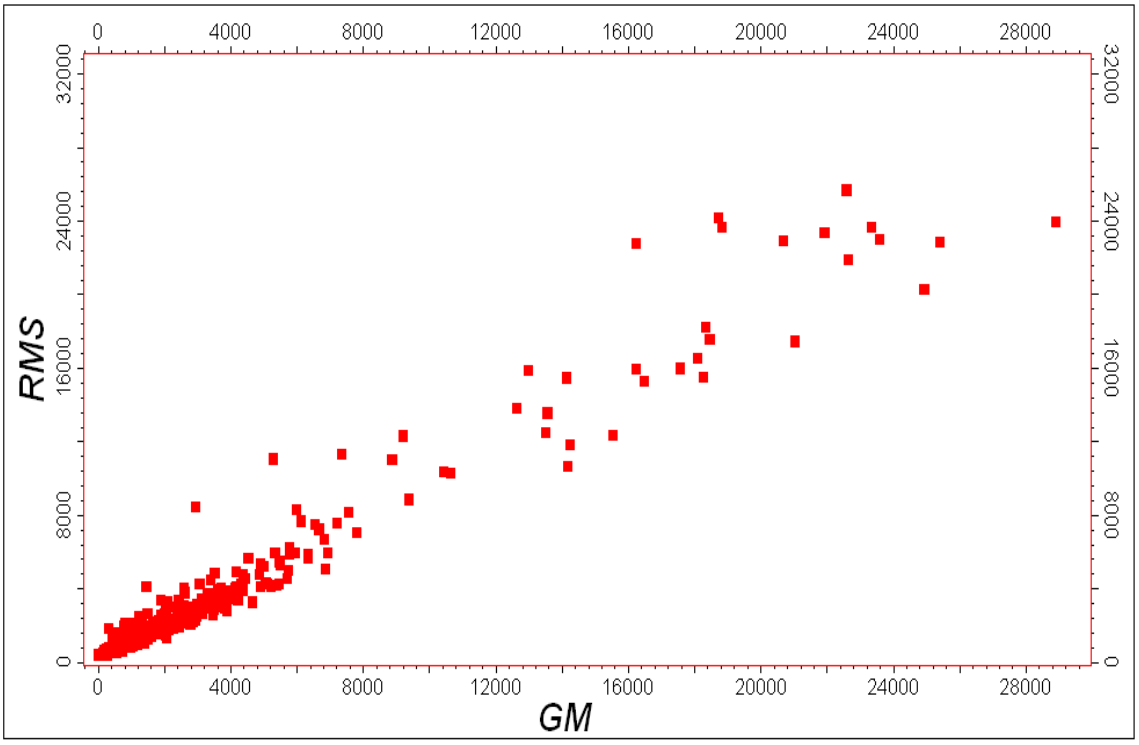

Figure 81 - Cross-plots of seismic attributes whit potential use in a neural network to create a facies classification cube. *RMS amplitude* Vs. *Gradient magnitude* attributes. The correlation between the two is perfect; therefore just one of these attributes should be used.

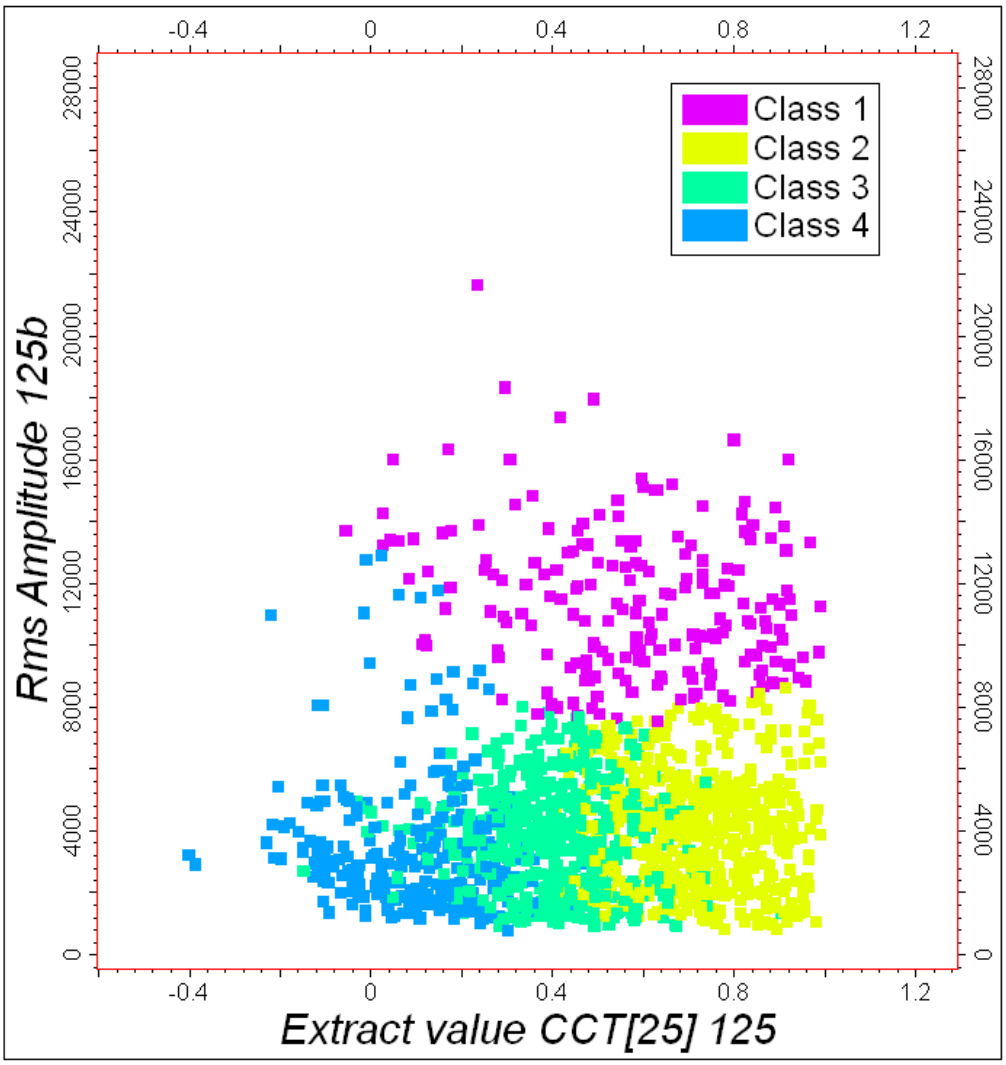

Figure 82 - Shows a cross-plot between *RMS amplitude* and *Iso-Frequency* with 25 Hz. The correlation is optimal to use into an estimation model. The data correlation is distributed and can be grouped by classes, represented here by the four different colours.

After the first trial of seismic attributes, the ones that show an acceptable behavior in the cross-plots should be selected in the "*Train Estimation Model*" process. They should be next passed through a correlation analysis for quality control, that is accessed in the process dialog box (Figure 84b). The analyzed attributes should have a correlation between 0.3 – 0.5 and present a cell box coloursed with green or light yellow in the correlation table (Figure 83). In Figure 83 blue cell boxes represent correlation values between 0 – 0.3, which means that the seismic attributes are not correlated; consequently they should not be used together in the "*Train Estimation Model*". Red cell boxes symbolize seismic attributes highly correlated. As stated before too correlated attributes should not be used to train the *neural network*. Highly correlated seismic attributes enhance the same

characteristic of the original seismic data; therefore just one of the correlated attributes should be used.

	Channel [CCT] 35	Channel [CCT] 30	Channel [Env] 50	Channel [Var] 1
Channel [CCT] 35	1.0000	0.8788	0.4277	0.3720
Channel [CCT] 30	0.8788	1.0000	0.3705	0.4463
Channel [Env] 50	0.4277	0.3705	1.0000	0.0062
Channel [Var]	0.3720	0.4463	0.0062	1.0000
Total	0.8856	0.8883	0.4596	0.4781

Figure 83 - Example of a correlation table from a correlation analysis between *Iso-Frequency* attributes, *Envelope* and *Variance*. Red and blue cell boxes are not desired in the "*Train Estimation Model*". Green and light yellow represent acceptable correlation values.

(2) *Principal Component Analysis* is a linear multivariable technique used to reduce the dimensionality of the input vectors helping to separate the necessary from the accessory in the input data before applying it into the estimation model. This method of data analysis overcomes the problems related to the graphically representation of *n* seismic attributes in *n* dimensions. In this case, it is not possible to analyze trends, highlight similarities and differences in the input data. PCA is a powerful tool to analyze the data and reduce the number of dimensions without loosing important information. Reducing the number of dimensions of the input data, using the PCA method, is a reliable solution to reduce the time-consumption of the process, and help the *neural network* to reach a solution with less associated error. An example of PCA is shown in the in table Figure 84a, where Eigenvalues, ordered from the highest to the lowest value, give an indication of the relative importance of the Principal Components. Understanding the correlation between attributes and the contribution of each input data, Principal Components (PC) which contains less or less important information should be excluded. The PCs that have been passed through the quality control are then selected.

The facies classification cube, computed by a neural network which has been trained by an estimation model build following the rules described above, is

presented in Section V.2.2, Figure 121. More details about which attributes were used in this case and how they were selected are also discussed in that Section.

Correlation Coefficients	PC1	PC2	PC3	PC4
Seismic Channel CCT	0.8624	0.0233	0.0167	0.5054
Seismic Channel GM	0.7556	-0.3415	0.3499	-0.4360
seismic Variance	0.4264	0.6604	-0.5658	-0.2490
seismic RAI	-0.0577	0.7569	0.6510	0.0050
Eigenvalue	1.4998	1.1261	0.8666	0.5075
Contribution (%)	37.49	28.15	21.66	12.69
Cumulative Contribution (%)	37.49	65.65	87.31	100.00

(a)

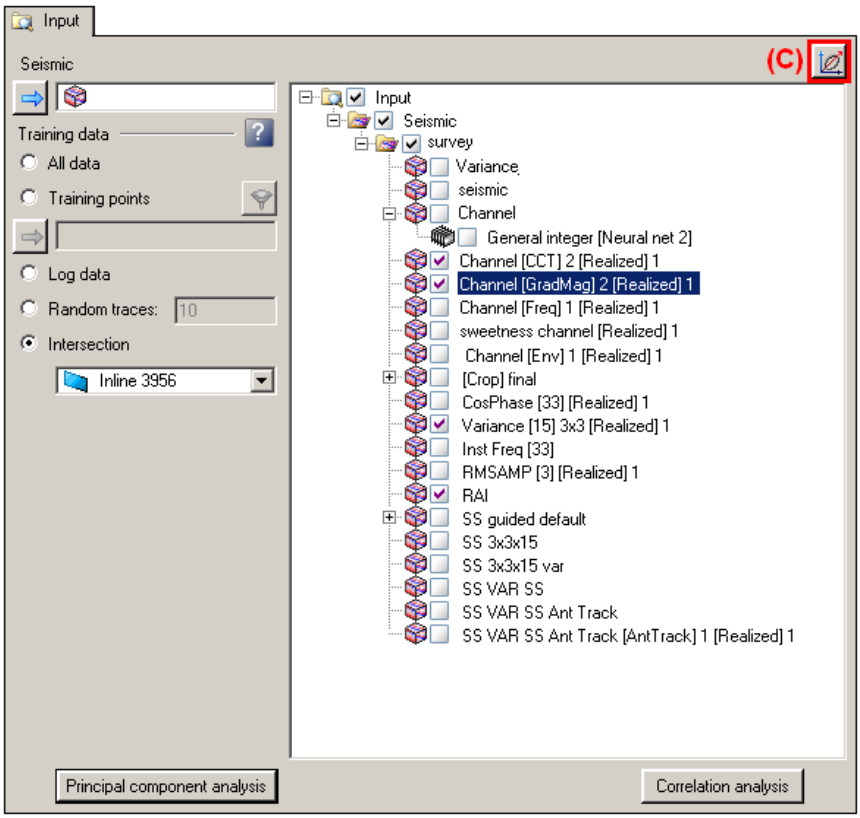

(b)

Figure 84 - (a) Principal Component Analysis table. **(b)** "*Train Estimation Model*" process dialog box and **(c)** method to calculate the Principal Components to use in the training of the neural network.

IV.4. Surface Attributes

A surface attribute is the value of an attribute relative to a single horizon and an interval window, between two horizons or within a constant time window. It can be

computed in *Petrel* using the "*Surface Attributes*" processes under "*Geophysics*". Petrel 2008.1 has fifty surface attributes divided into four areas depending on the applied algorithm: *Amplitude*; *Statistical*; *Signal Shape* and *Measurable Interval*.

In *Petrel,* surface attributes can only be computed in surfaces built from horizon interpretation. The process dialog box is divided into seven areas and the user can chose as many options to withdraw the maximum potential from the extensive list of available attributes. An example of the attributes dialog box to compute surface attributes is shown in Figure 85: (1) from the attribute library the user should choose the desired seismic attribute; (2) a seismic cube from where the attribute will be extracted needs to be set as input; (3) the attribute can be generated from three types of window specification: a) between a surface and a time window, "*Single Horizon*"; b) between two horizons, "*Horizon-Horizon*"; and c) inside a constant time window, "*Z-Z*". After the window specification, a surface should be set as the input; 4) besides the type of window, the attribute can run above or below a user-defined length from a user-defined event. These events are "*None*", "*Largest Peak*", "*Closest Peak*", "*Largest Trough*", "*Closest Trough*", "*Zero Crossing +/-* ", or "*Zero Crossing -/+*". If needed, a second surface, window specification, type of event and special parameters should be set up.

Surface attributes are much more dependent on the user interpretation, and consequently dependent on the user picking of a horizon, than volume attributes computed with user-defined parameters. The subjective percentage related to this process can lead to misunderstood interpretations and the creation of artifacts in map attributes which are directly related to the picking interpretation (Figure 86).

Depending on the hydrocarbon reservoir, surface attributes have different values in depositional regimes interpretation as they are computed from zero-phase seismic data or RAI data. For "top heavy" reservoirs, when there is a coarsening upward sequence from the bottom to the top, the more useful zero-phase attribute will be; on the other hand, the less "top heavy" is the hydrocarbon reservoir, the more RAI attributes will be useful (Schlumberger, 2007a).

In this thesis only three surface attributes, all related to energy content of the seismic data, are described.

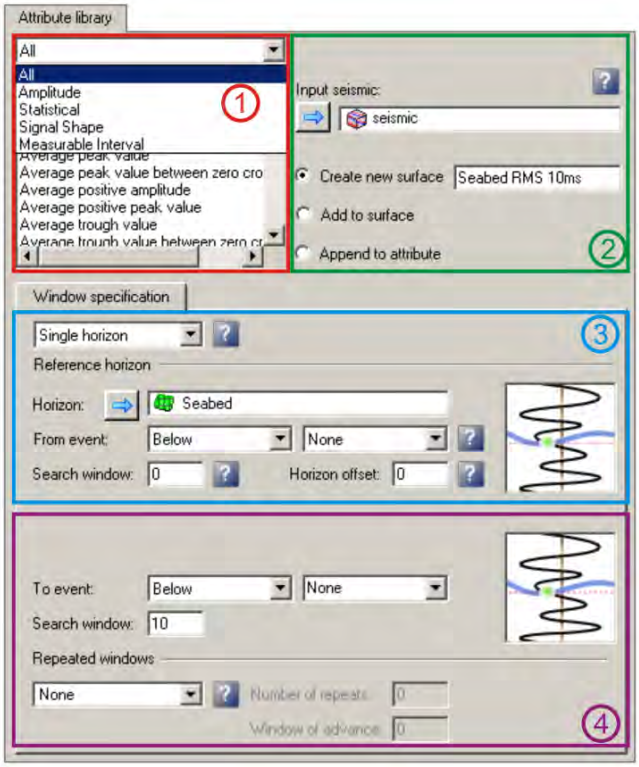

Figure 85 – *Petrel*'s Surface Attributes process dialog box.

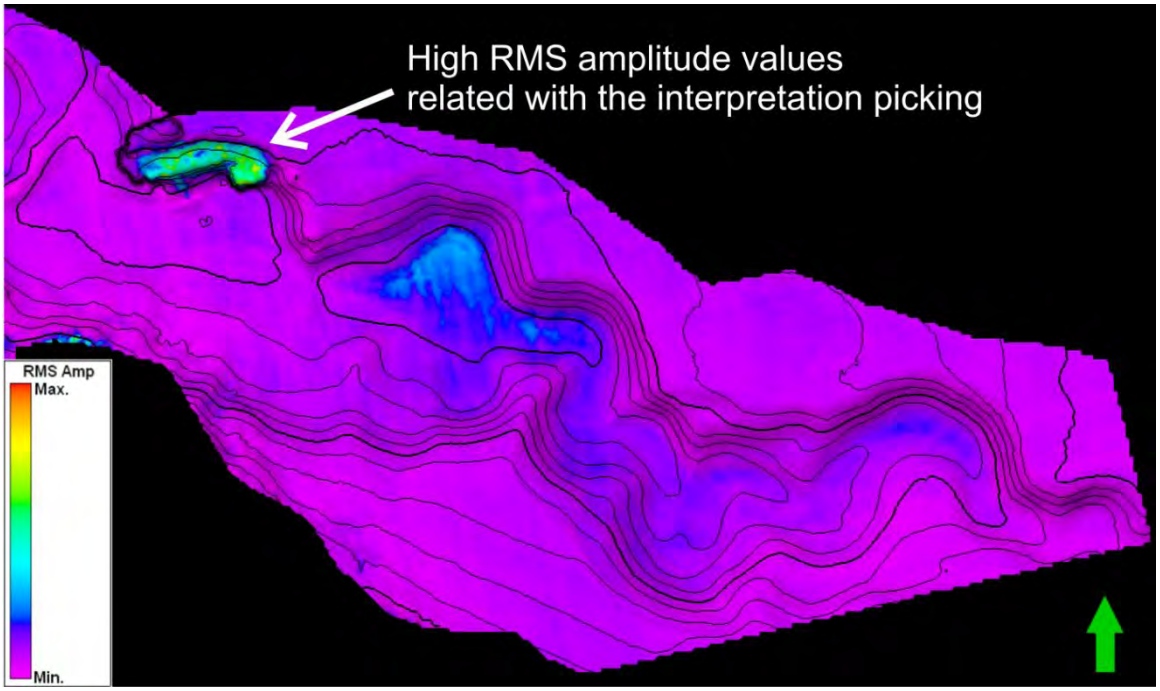

Figure 86 - Interpreted horizon and *RMS amplitude* attribute computed over a window of 5 ms below the horizon. Comparing with another horizon interpretations, very high values of *RMS amplitude* are interpreted as artifacts related to a poor picking stability. High Values in the center of the horizon can be interpreted as high porosity sands.

IV.4.1. RMS Amplitude

RMS amplitude is the same attribute described in Section IV.3.1.8 but computed relative to a surface with all the user-defined settings as discussed before. Attributes maps of *RMS amplitude* may isolate amplitude response features from the background (Figure 86), or act as a direct hydrocarbon indicator.

IV.4.2. Extract Value

The *extract value* attribute is more like a valuable utility than a seismic attribute in the truly meaning of the word. This attribute allows the user to extract the value of a seismic attribute volume relative to a single surface. It allows the production of surface attribute maps of attributes that are not available in the surface attributes library.

IV.4.3. Half Energy

The *half energy* attribute computes the time or depth required for the energy within a window to reach one-half of the total energy of the entire window, throughout (Equation 35).

$$HalfEnergy = \frac{\sum_i^n amp^2}{2} \qquad \text{Eq. (35)}$$

Attribute maps of half energy are used to infer possible asymmetric changes in lithology or porosity (Figure 87).

In this work, more attention was given to volume attributes in *Petrel* 2008.1 than to surface attributes. This is due to the high potential of visualization and application of the former. In fact, seismic attribute volumes are creating a new paradigm in 3D seismic interpretation.

More attributes can be computed using *Petrel*'s tool "*Seismic Calculation*". This tool allows not only to directly extract new information from seismic data but also

allows combining available seismic attributes with each other, or to compute their derivatives in respect to time or space.

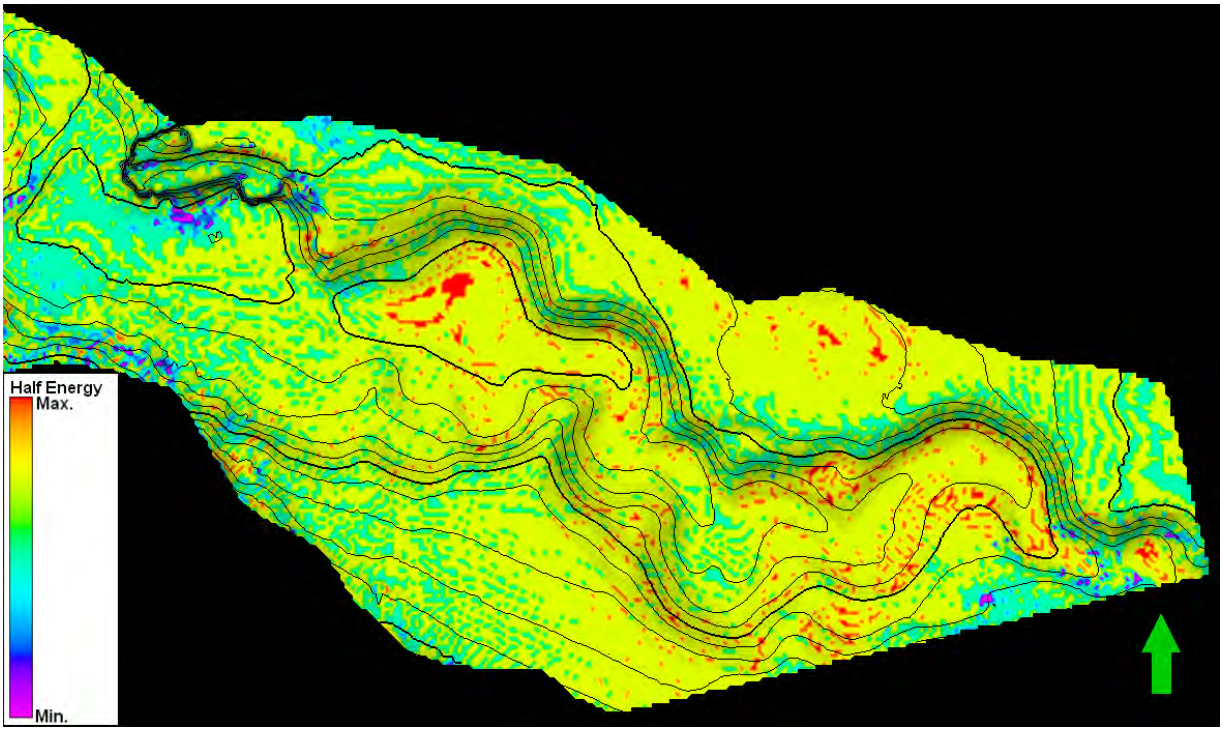

Figure 87 - Interpreted horizon and half energy attribute computed over a window of 5 ms below the horizon. Abrupt changes in the attribute value may indicate lithological changes.

Chapter V. The Role of Seismic Attributes in 3D Seismic Interpretation: A Case Study Offshore West Africa

In the previous chapter, a brief introduction was given to the standard seismic attributes available in *Petrel* 2008.1. In this chapter, seismic attributes are applied to the recognition and characterization of a potential area of hydrocarbon accumulation, from an area offshore W. Africa, where information from well log data is not available.

The interpretation process was divided into two different stages, following the standard method of 3D seismic data interpretation applied by most oil and gas companies: (1) "*Prospect Generation*" - during this stage, a raw interpretation of the original seismic data is carried out, and volume attributes are computed to identify structures that may correspond to potential hydrocarbon reservoirs; this can be followed by *geobody* extraction for inclusion into reservoir geological models; (2) "*Advanced Interpretation*" – this corresponds to the interpretation of key seismic reflectors and derived surface attributes (or attribute maps) inside the target area(s) delineated in (1). A first approach to *facies* classification, based on an artificial neural network method, was also performed on the seismic data.

V.1. Prospect Generation

The "*prospect generation*" started with the interpretation of the seabed surface (Figure 2). The seabed was automatically tracked along the seismic cube, based on the interpretation of a coarse grid of inline/crosslines, constrained by a *structural smoothing* cube. This is particularly important for this study area because the seabed surface is intensely affected by the underlying salt bodies, preferentially orientated NNW-SSE, sinuous channel complexes roughly orientated

E-W, and regional faults with NNE-SSW and NNW-SSE direction trends (Figure 88). The orientation of the sinuous channels complexes is mainly constrained by the subcrop of the salt bodies.

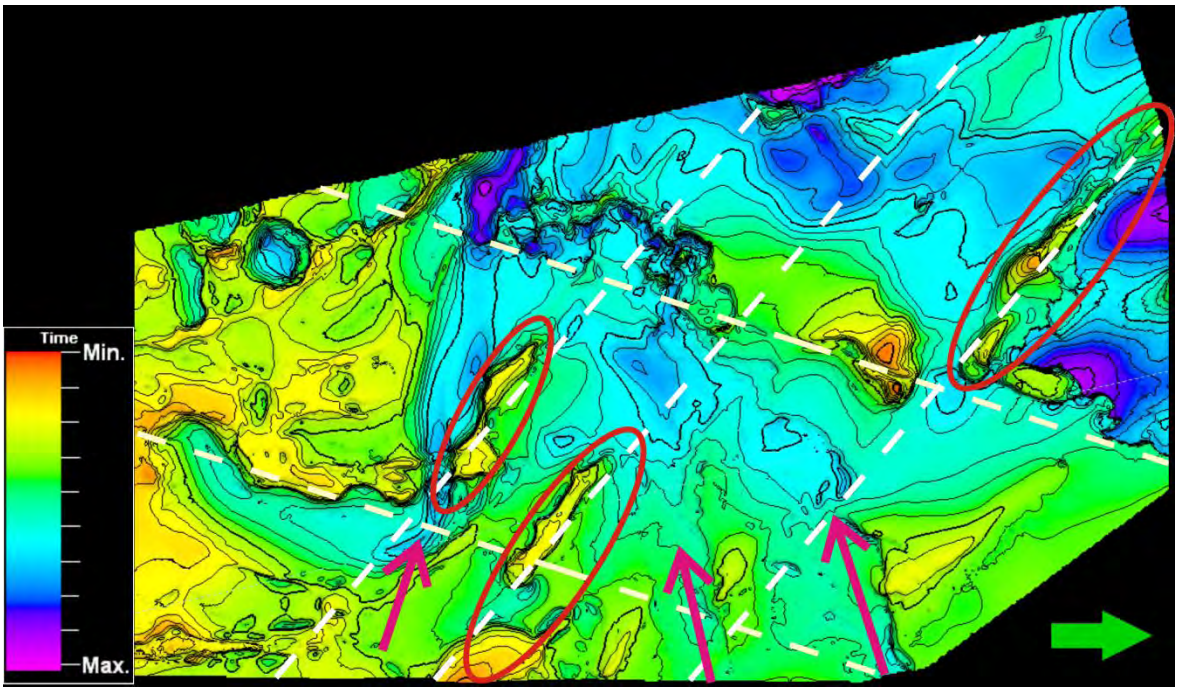

Figure 88 – Preliminary interpretation of the seabed at a regional scale. Red elipses represent elongated salt bodies. Arrows show the direction of the main channels and white dashed lines indicate the main trend of regional faults.

A detailed analysis of the seabed surface is also useful to detect the potential presence of any gas related features.

V.1.1. Identification of Gas Related Features

A detailed interpretation of the sea bottom surface for the study area, combined with the interpretation of vertical seismic sections, allowed the identification of several alignments of round depressions, interpreted as *pockmarks* (Figure 89). *Pockmarks* are seafloor depressions caused by the escape of gas or fluids from the subsurface; escape paths usually exploit faults or zones of weakness (Evans, 2003). *Pockmarks* are important structures because they reveal the presence of hydrocarbons at depth. Therefore, in the study area, the identification and interpretation of *pockmarks* at the seabed surface was used as a first approach to

evaluate its hydrocarbon potential. Following the gas escape path in depth, using vertical seismic sections, allows the interpretation of hydrocarbon accumulations. Aligned *pockmarks* reveal the presence of faults, which most of the times follow a regional trend. Buried *pockmarks* indicate ancient periods of gas escape, and were also identified in some vertical seismic sections (Figure 90).

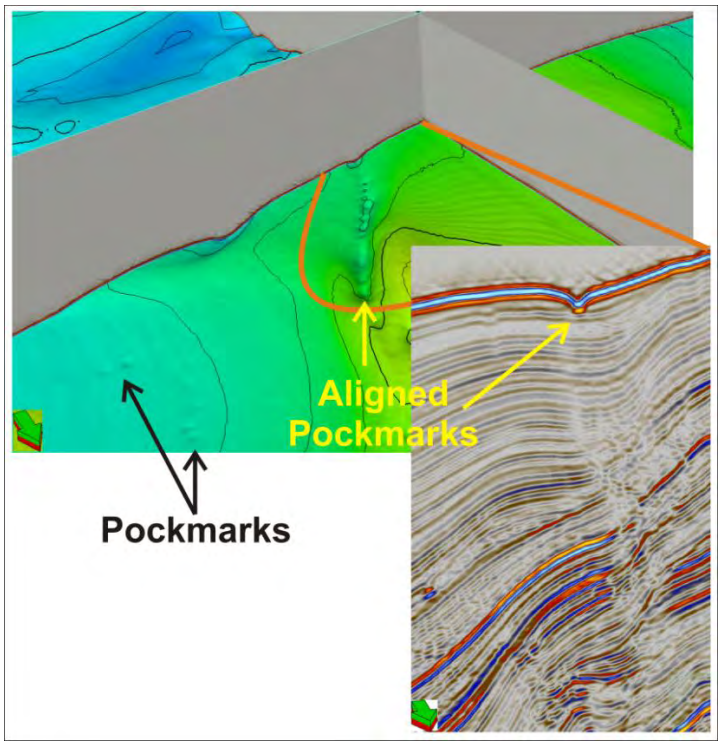

Figure 89 – Aligned *pockmarks* identified at the sea-bottom and followed at depth along vertical seismic sections. The relationship with the underlying fault that acted as the fluid conduit is evident.

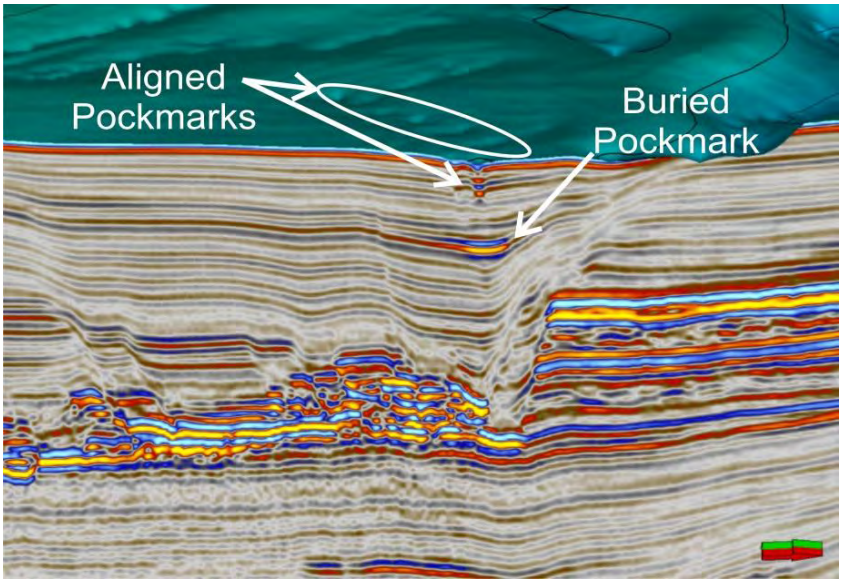

Figure 90 – Buried *pockmarks* below an active *pockmark*. Note the underlying bright reflection that represents either an old *pockmark* or a small gas accumulation related to the same escape pathway.

V.1.2. Analysis of Deep-Sea Channel Complexes

Deep-sea channel complexes have seen their importance grow in the oil and gas exploration industry as proven hydrocarbon reservoirs. These depositional features are of particular interest offshore Angola, Brazil, Guinea, Gulf of Mexico and India (Kolla *et al*., 2007). Published seismic sections from deep-sea sinuous channel complexes (or channel-levee systems) often show high amplitude reflections from their erosional bases, which are flanked by low seismic amplitude overbank deposits (or *levees;* Kolla *et al*., 2007). In these depositional environments, low amplitudes can be correlated with shales and/or mudstones, while high amplitudes are lithology-indicative of sands (Evans, 2003). The availability of recent 3D seismic datasets with high horizontal and vertical resolution, which are easily handled by leading edge seismic interpretation software, combined with the advances in the exploration and production technology from submarine channels, allow a better understanding about the geometry, architecture, and the spatial/temporal distribution of deep-sea channel complexes (Posamentier, 2003; Wynn *et al*., 2007).

In the last few decades highly sinuous channel complexes are understood as common depositional features of modern deep-sea fans. Deep-sea fans are thick sedimentary features associated with gravitationally driven mass movement deposits. These movements include turbidite deposits, mass movement debries and pelagic drapes (strata.geol.sc.edu). These sediments can be later reworked by bottom currents, creating in this way complex systems of sinuous channels (Kolla *et al*., 2007). The presence of stacked and amalgamated channels interpreted in the seismic dataset (Figure 91) suggest that the study area corresponds to the "*upper fan*" section of a deep-sea fan morphologic model (Figure 92; strata.geol.sc.edu).

Channel-levee systems can be interpreted on vertical seismic sections by their large erosional bases associated with high amplitude reflections. Often, several cuts, also with high amplitude reflections, can be interpreted above the main erosional base. Each cut corresponds to a new position of the channel in time.

Channels can also migrate laterally or suffer vertical aggradation processes (Figure 91a; Figure 93).

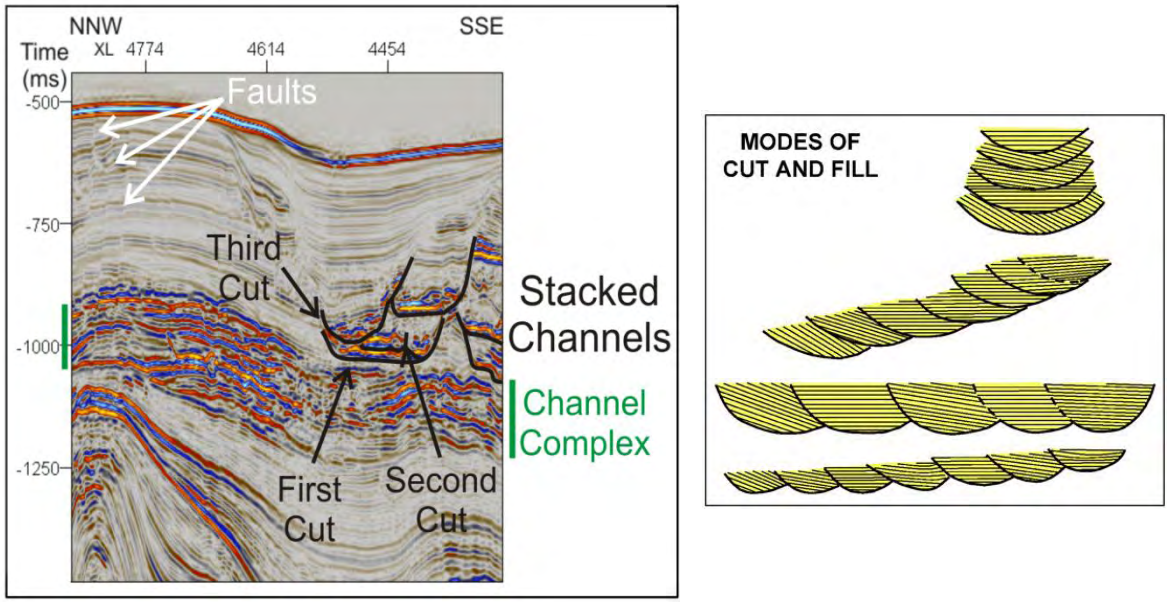

(a) **(b)**

Figure 91 – (a) Typical vertical seismic section with interpreted stacked channels commonly found throughout the seismic cube under investigation. Around the 1000ms ancient channel complexes can also be identified, but it is very difficult to interpret each channel independently. **(b)** Schematic representation of the evolution of the channel along time (Kolla *et al*., 2007). The channels interpreted in **(a)** can be correlated with the geometries represented in **(b)**. Both lateral migration and vertical aggradation are observed.

The architecture and geometry of the submarine channels can be correlated to conceptual models which describe the relative position of the channel, the mode of the cuts and the fill with the temporal evolution (Figure 91b).

Strong analogies between deep-water sinuous channel complexes and fluvial systems have been recently done in order to understand more about how deep-water complexes work. In fact, there are many similarities between both systems; however, the analogy should be done carefully since there are substantial differences in the internal architecture and the mode of evolution of deep-water channel complexes (Kolla *et al*., 2007; Wynn *et al*., 2007). Submarine channel normally have smoother bottoms with low angle overbanks and a highly vertical aggradation nature (Wynn *et al*., 2007). These differences are related to density

contrasts of flows relative to ambient fluids, the effect of centrifugal and Coriolis[16] forces on flows, modes of sediment transport, and effects of sea level changes (Kolla *et al*., 2007).

Figure 92 - Schematic representation of a deep-sea fan complex morphology. The interpretation of stacked and amalgamated sinuous channels shown in this Chapter, places the study area somewhere in the "*upper fan*" section of the deep-sea fan (from Christopher and Kendal (2006) in strata.geol.sc.edu).

In the oil and gas exploration industry the recognition of a channel system in vertical seismic sections is important, but tracking it in space is the key factor to fully evaluate the depositional feature as a possible hydrocarbon reservoir. Unfortunately, using standard horizontal time slices along the seismic cube is not enough to carry a good interpretation of the channel complexes. Submarine

[16] Coriolis force is an apparent deflection of the centrifugal force produced by the Earth. Due to this effect, moving particles in Earth's surface suffer a displacement to the right in the northern hemisphere, and to the left in the southern.

channels are not perfectly horizontal because they follow the regional dip of the area; consequently, horizontal time slices are not generally parallel to the channels' surface, originating misinterpretations or difficulties in the correlation between the vertical seismic sections and the time slices.

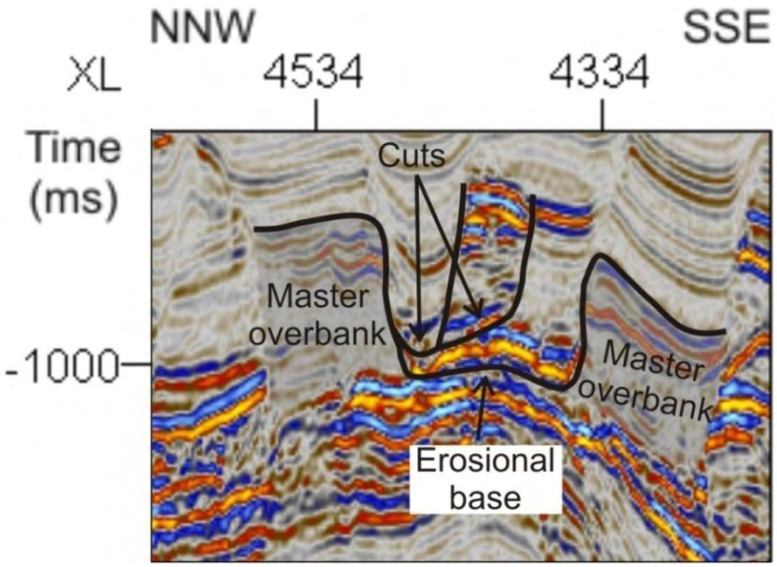

Figure 93 - Example of a sinuous channel system with lateral continuous channel migration as well as some aggradation. The sinuous channel complex, and associated overbank deposits, are housed in a larger master valley, bounded by master overbanks.

An example of a horizontal time slice extracted from the original amplitude seismic cube of the study area is shown in Figure 94. Here, high amplitudes do not define, on their own, channel-levee systems associated with deep-sea sinuous channel complexes. This happens because the horizontal slicing is not parallel to the dip of the channel complexes. In order to overcome this drawback there are three possible best practices: (1) to combine vertical and horizontal seismic intersections in a 3D view in order to follow a channel (see, for example Figure 95); this is an effective method if there is a channel which can be identified and isolated in horizontal time slices; (2) by using seismic attributes, in particular the ones that enhance edges (e.g. *variance* IV.3.3.5), to distinguish between different channel systems, isolate depositional features and correlate them with the original seismic (Figure 96); (3) by using the strata slicing method described in Zeng (1998a; b), which is generally the best approach.

In this work, considering its main objectives and due to time constraints, only the first and the second methods were used.

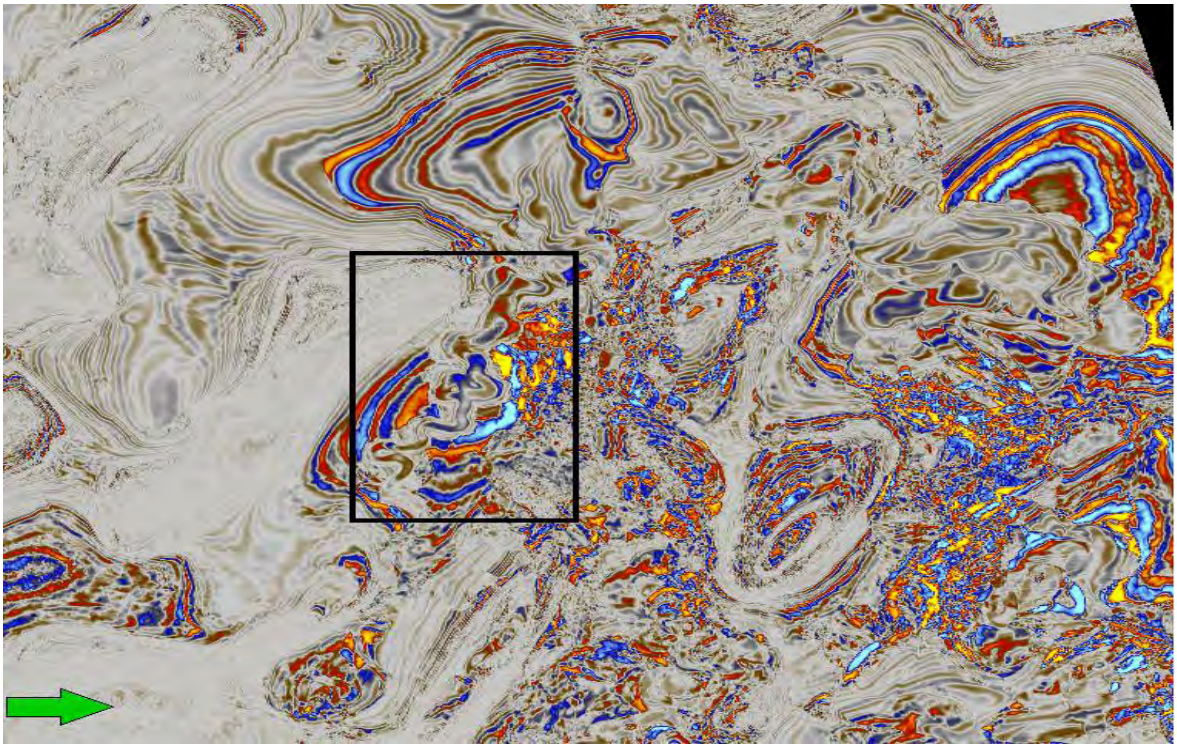

Figure 94 - Example of a time slice extracted from the original seismic cube. The identification of the sinuous channel complexes (one such system is highlighted inside the black box) is not immediate because the channels' surfaces and the time slice are not parallel.

A channel system can be observed in time slices along the original seismic volume (see Figure 94 and Figure 95). In order to enhance it for easier interpretation, seismic attributes (e.g. *variance*, *gradient magnitude*, *chaos*) were computed.

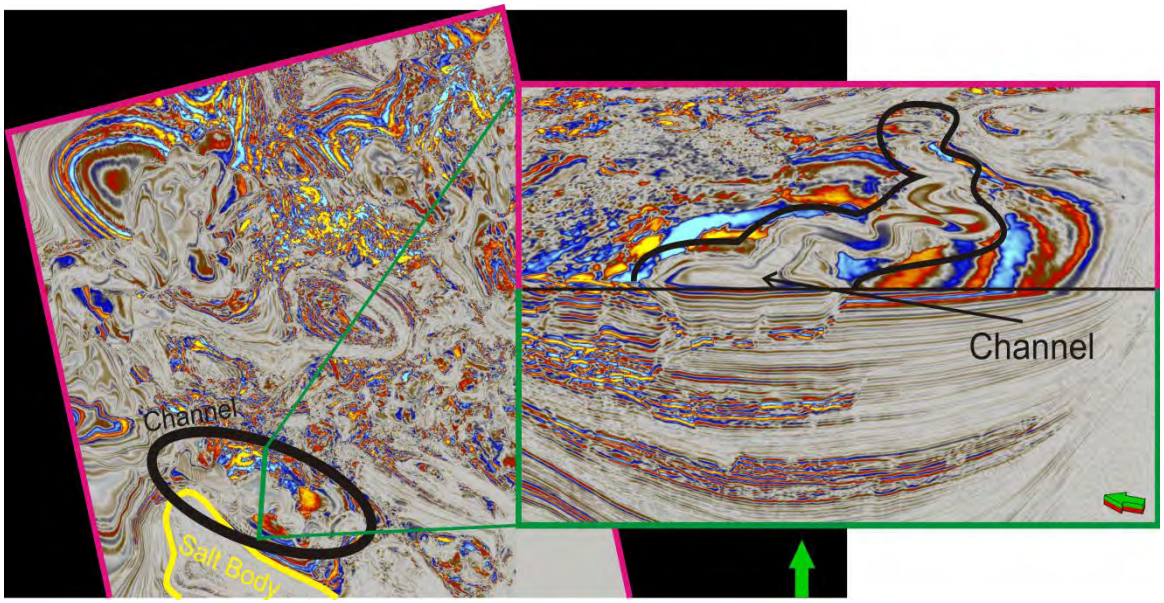

Figure 95 – Interpretation of a horizontal time slice from the original amplitude cube which allowed the identification of the target channel system (on the left). Also shown (on the right) a composite 3D view of a horizontal time slice and a vertical seismic section focusing on the target sinuous channel system.

The *variance* seismic volume was the most useful attribute volume to use in the interpretation of this depositional system. Its interpretation, combined with the original seismic data, allowed the definition of: (1) an area of several sinuous channel-levee complexes, which can be considered a "*minor unit*" of a submarine fan (Figure 96a; Wynn *et al*., 2007); (2) a well defined channel-levee system, elongated NNW-SSE, with potential to be a hydrocarbon reservoir; for this reason, most of the seismic attributes were tested at this site (henceforth, this target will be referred to as the *target channel system*; Figure 66b; Figure 96b).

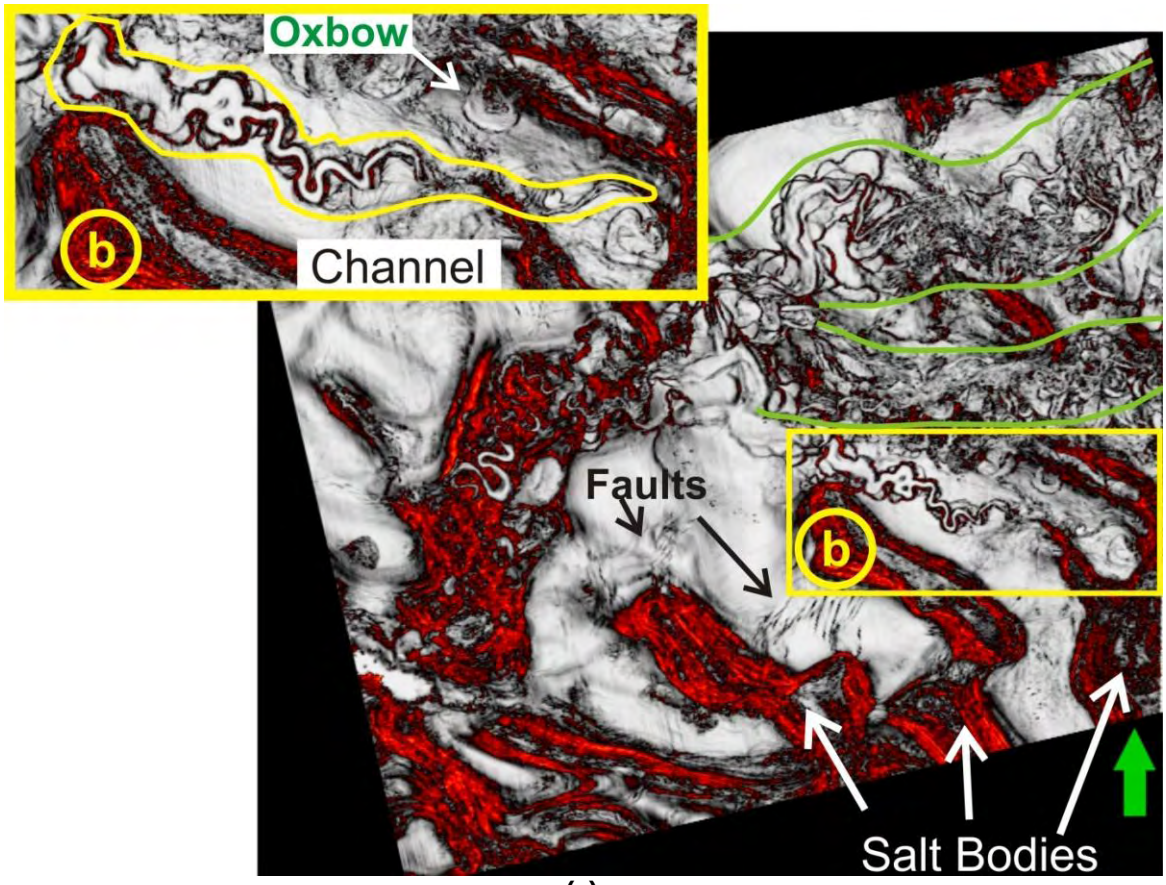

(a)

Figure 96 – (a) *Variance* time slice showing several salt bodies (in red), faults and sinuous channel complexes belts (inside the green lines). **(b)** close up to the target channel system, where an oxbow from a near channel complex can be identified. Note the much superior quality of the attribute map for interpretation, compared with the original seismic section (Figure 95).

The interpretation of several time slices along the *variance* attribute cube allowed a preliminary characterization of the depositional elements that belong to the target channel system. This system comprises a well defined sinuous channel, with levees and cutoff loops (or oxbows), within a larger channel belt (Figure 96; Figure 97). The channel-levee system is seismically characterized by high

amplitudes at the bottom, a low-amplitude fill and a thin bed with high amplitudes in the central part of the channel which may indicate a sand fill (Figure 98).

The presence of loop cutoffs (Figure 96; Figure 97) highlights the dynamic nature of these systems and is evidence of turbidity flows with high erosive power (Posamentier, 2003). A detailed examination of meander loops illustrates both the *swing* and *sweep* effects. *Swing* is the lateral loop migration and/or expansion of the channel system; *sweep* is a down-system sinuous loop migration (Figure 99; Posamentier, 2003; Wynn *et al*., 2007).

The levees associated with the target channel system have variable height and the same configuration as the ones from another channel system in the study area, illustrated in Figure 93. Levees are part of the so called *master* and *secondary overbanks*, and are often related to floodplains (term used in analogy with land fluvial systems).

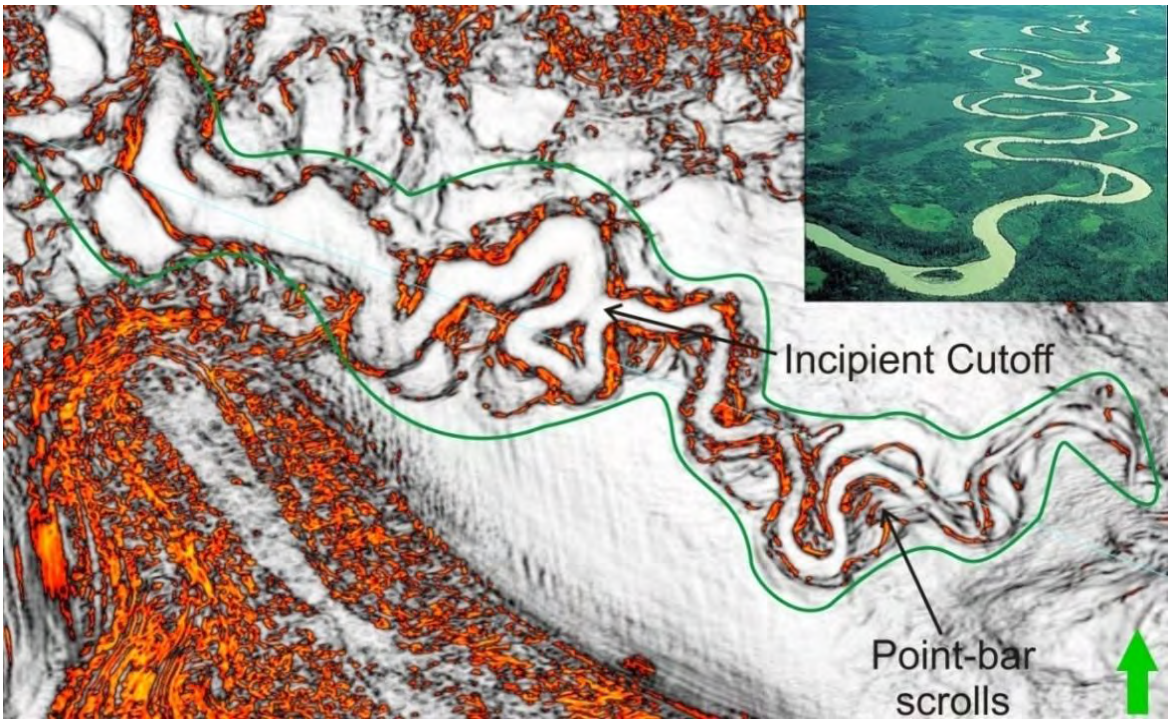

Figure 97 - *Variance* time slice highlighting the target channel system. The green line represents the limit of the sinuous channel belt. At this “depth” (TWT) along this time slice, an incipient cutoff and several point-bar scrolls can be interpreted (compare also with Figure 66b). The inset in the upper right corner shows a fluvial meandering system; there is a clear analogy in the overall morphology of the two systems.

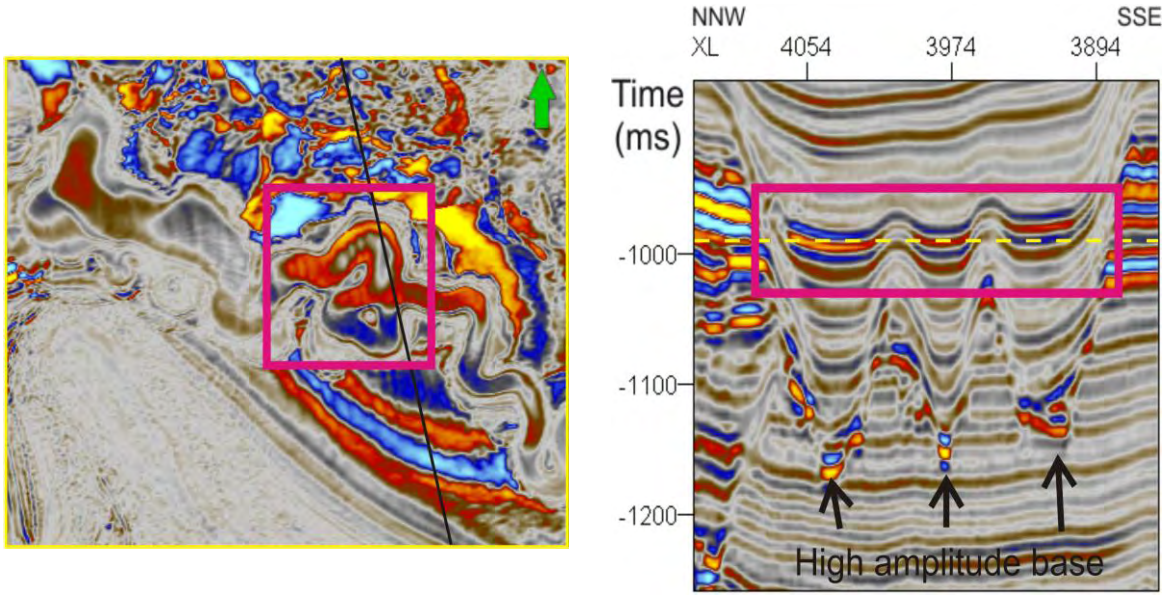

(a) **(b)**

Figure 98 – (a) Horizontal time slice showing the target channel system. **(b)** Vertical seimic section along the black line. The yellow dashed line in **(b)** represents the position of the horizontal time slice. The pink box shows the high amplitude thin layers indicative of a sand prone fill.

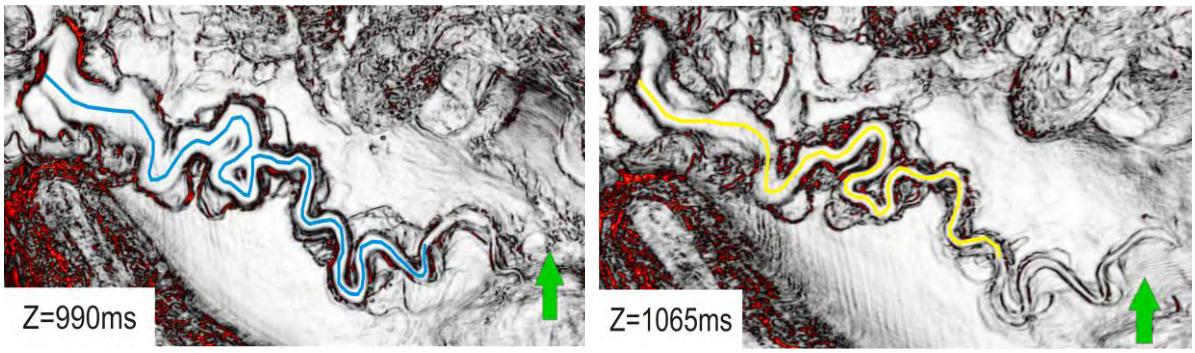

(a) **(b)**

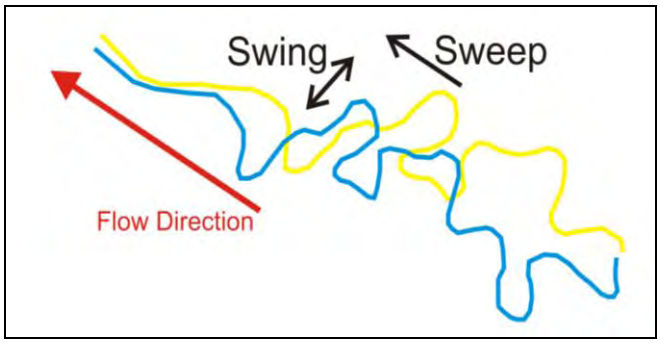

(c)

Figure 99 – Two horizontal time slices at different "depths" (TWT) within the *variance* attribute volume, showing lateral and vertical variability in the channel system. The interpreted axis of the target channel system is shown in blue **(a)** and in yellow **(b)**, for the upper and lower slices, respectively. **(c)** shows the migration with time of the channel system. Both the effects of *swing* and *sweep* were identified.

In addition, a depositional element interpreted as a crevasse splay was also identified. The interpretation was based on both the *variance* and the *Iso-Frequency* (see Section IV.3.4.3) attributes. A crevasse splay is a depositional feature, associated with highly energetic turbidity currents, which often appears at sharp bends that break the outer levee leading to the development of an unconfined lobate or tongue-shaped deposit in the overbank area (Figure 100b; Posamentier, 2003). This depositional element was first identified in the study area on *variance* time slices (Figure 100a) as an isolate body that does not correspond to an ancient location of the channel system. Using the *Iso-Frequency* attribute and comparing different cosine frequencies (Figure 77a; b) it has been shown that the feature inside the green polygon is different from the lithology inside the target channel system (the correlation value is different for the same cosine frequency). This feature has been interpreted as a crevasse splay, based on its morphology, the interpretation of indicative-lithology seismic attributes, the interpretation of the surrounding environment and the analogy with modern fluvial systems.

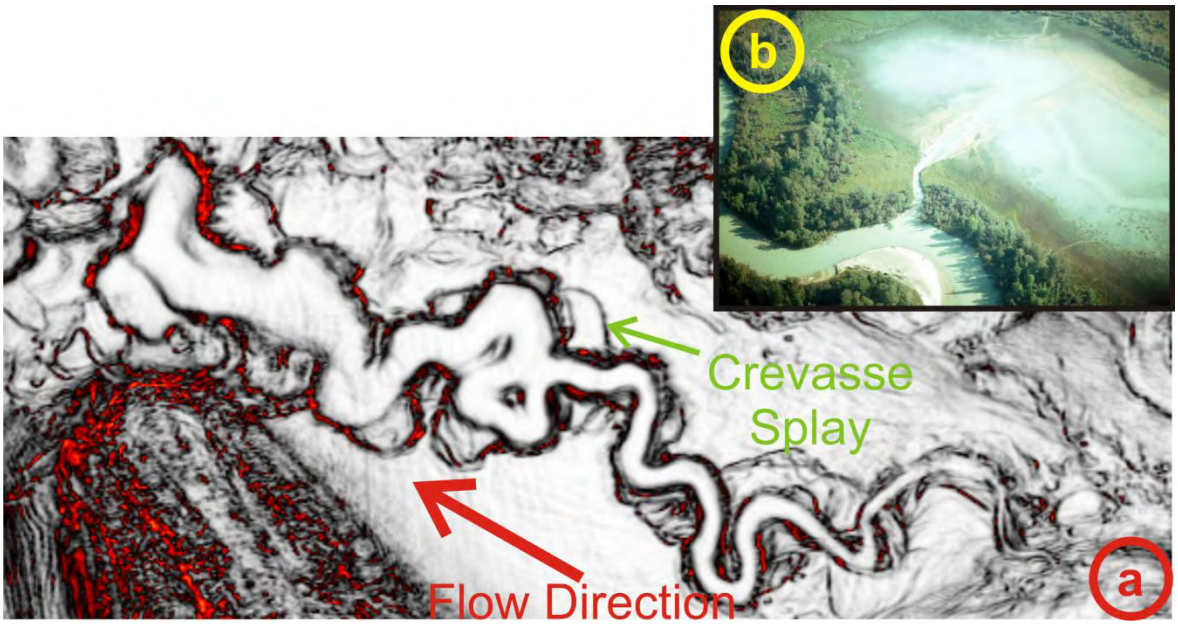

Figure 100 – Horizontal time slice of the *variance* attribute showing a depositional feature interpreted as a crevasse splay, combining *variance* with *Iso-Frequency* attribute. **(b)** Is an aerial photo of a crevasse slay in a fluvial system.

Edge detection attributes such as *variance* and *gradient magnitude* can also be extremely useful to understand the behavior of sinuous channels that cannot be tracked on time slices from the original seismic cube. In particular, the interpretation of channel complexes in vertical seismic sections is often very

difficult and ambiguous. The example below shows a vertical seismic section where three channels can be identified (Figure 101a), based on their morphology and character. However, a combined display of the vertical seismic section with a *variance* time slice (which, as discussed above, is good for highlighting features such as these) allows unraveling the fact that, instead of three separate channels, we are dealing with just one channel which is meandering in the direction perpendicular to the vertical seismic section (Figure 101b).

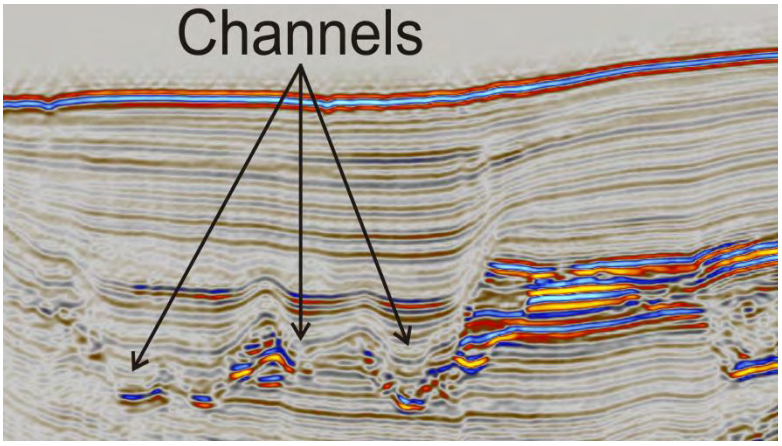

(a)

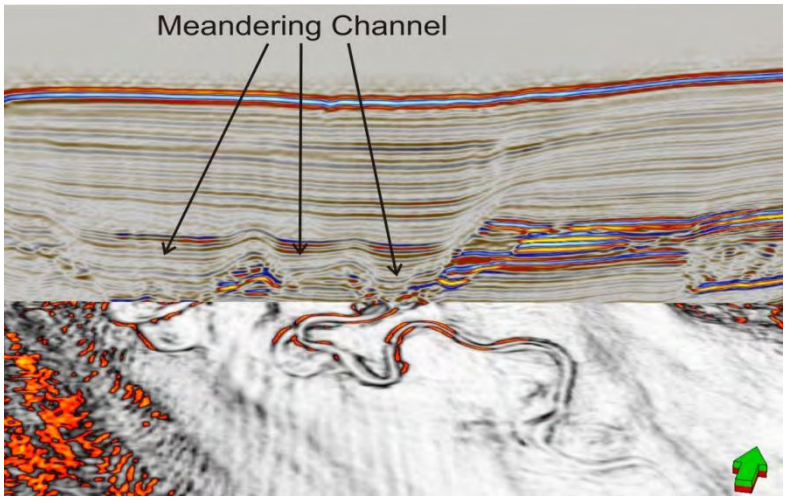

(b)

Figure 101 – (a) Seismic inline where high amplitude and erosive seismic reflectors are interpreted as individual channels bottom. **(b)** The combined interpretation of the same seismic line with a *variance* time slice highlights the channel system, in high resolution, and allows the correct interpretation of a single meandering channel.

Fully understanding the depositional systems associated with deep-sea channel complexes is still a recent branch in 3D seismic interpretation. 3D seismic datasets allow nevertheless a much better knowledge about these systems. The

introduction of seismic volume attributes to enhance depositional elements, in particular stratigraphic and structural attributes, has brought a new reality to the interpretation of deep-sea channel complexes. Combined visualizations in three-dimensions, for example (Figure 102), allow the recognition and correlation of seismic patterns with depositional features interpreted from seismic intersections of the volume attribute. Tracking 3D depositional events in space using seismic attributes is now a much easier task and contributes to a better understanding of the architectural relationship of the various depositional elements and their position and evolution in time.

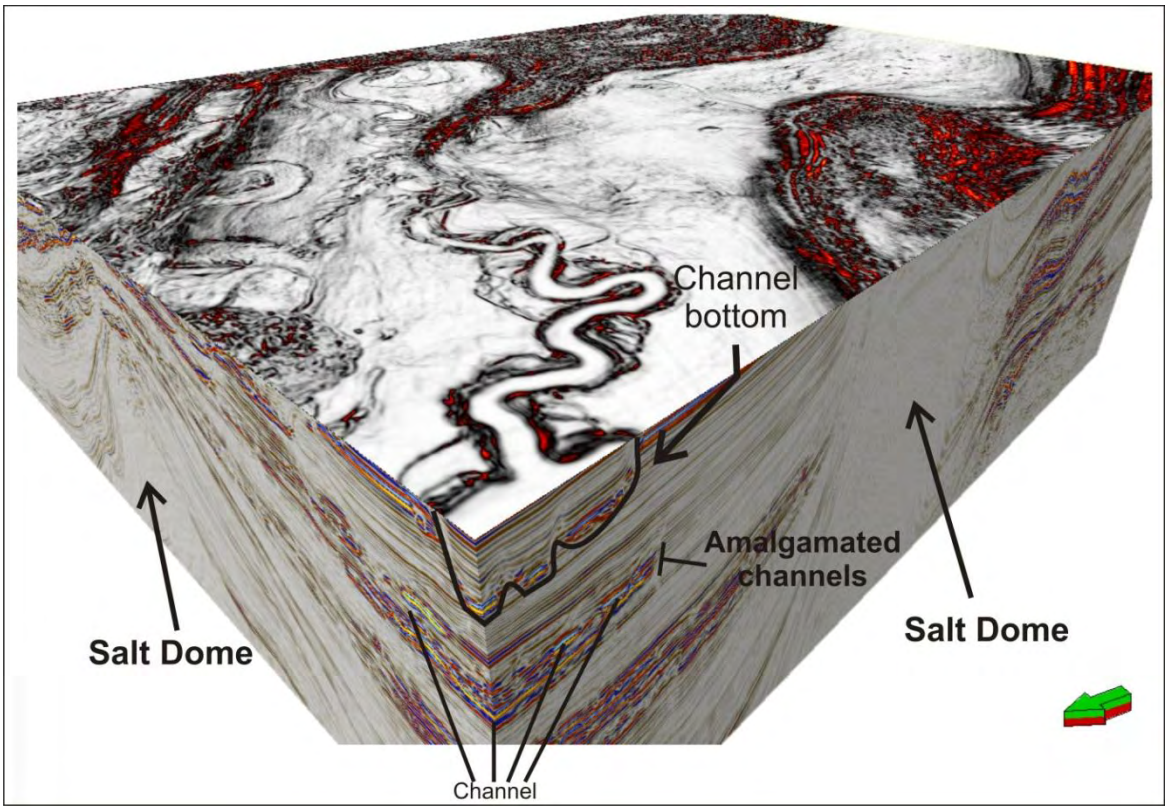

Figure 102 - Variance attribute along a time slice, combined with the original seismic data. This type of display allows the correlation between seismic patterns and depositional events and makes tracking depositional elements much easier.

V.1.3. Salt Tectonics

Salt tectonics played a very important role in the structural development of the marginal sedimentary basins off West Africa. In fact, this process allowed the

creation of many structural oil traps which are nowadays major hydrocarbon plays within the study area.

The salt is an evaporite with unique properties and behavior: it is uncompressible, it has low density (~2.2g/c^3), a high seismic velocity, a high level of plasticity and zero porosity. Therefore, it is impermeable and can act as a seal.

When compared to other sediments, the salt has higher densities until approximately the 1000m depth (Figure 103). Since the salt is uncompressible its density remains the same with the increase in depth; on the other hand, sediments, which are compressible, become denser than salt with the increase in depth (Figure 103).

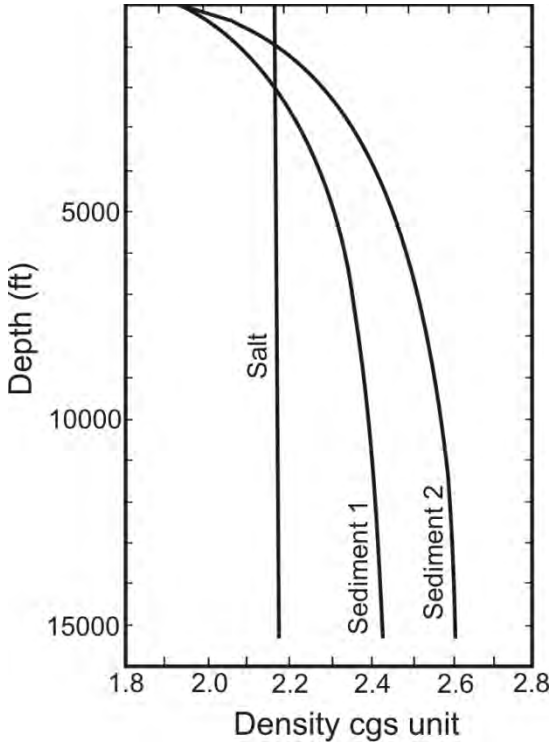

Figure 103 - Diagram of salt's density *vs*. depth. At approximately 1000m the salt starts to be less dense than the sediments surrounding (modified from Dobrin and Savit, 1988).

The salt is deposited in layers with constant thickness, but due to its mechanical properties and the weight of the sediments above, it moves upwards creating intrusive bodies with different shapes and configurations. Traditional shapes of salt bodies are: diapirs, salt domes, salt walls, massif salt, allochthonous salt, salt pillows, and salt canopies (Figure 104; Figure 108).

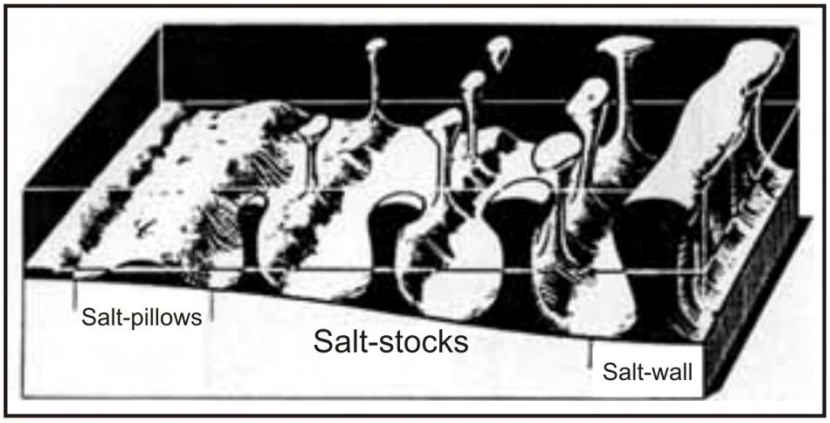

Figure 104 - Different salt bodies morphology (modified from Trusheim, 1960).

Buoyancy and differential compaction are the two main processes which trigger the salt movement to produce the salt bodies previously mentioned. The buoyancy phenomenon acts due to the weight of denser sediments above the salt layer. The salt moves laterally to an area of weakness of the overlying bed, creating a thinning below the denser sediments (Figure 105).

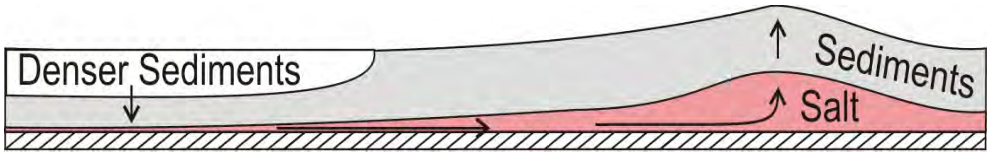

Figure 105 – Buoyancy phenomenon (modified from Garcia, 2008).

The differential compaction occurs by two reasons: (1) when there are sediments with variable densities above a salt layer (Figure 106); (2) when there is a local difference of sediment volumes above the salt layer. The lateral variations of density, or volumes, cause a thinning of the salt layer below the denser sediments. These density differences are translated in a movement of the salt to areas with lower densities, creating a rising in the sedimentary layer above.

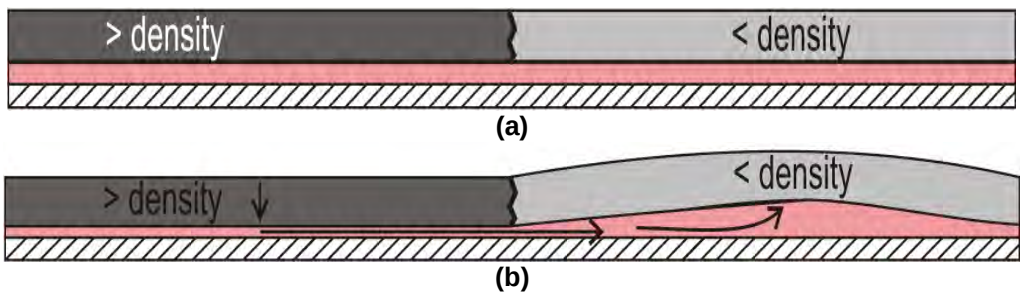

Figure 106 – Differential compaction (modified from Garcia, 2008).

Salt tectonics was a key process in the configuration of the sedimentary basins off West Central Africa. The movement of the salt to upper stratigraphic levels changed the configuration of sedimentary sequences allowing the creation of hydrocarbon traps (Figure 107).

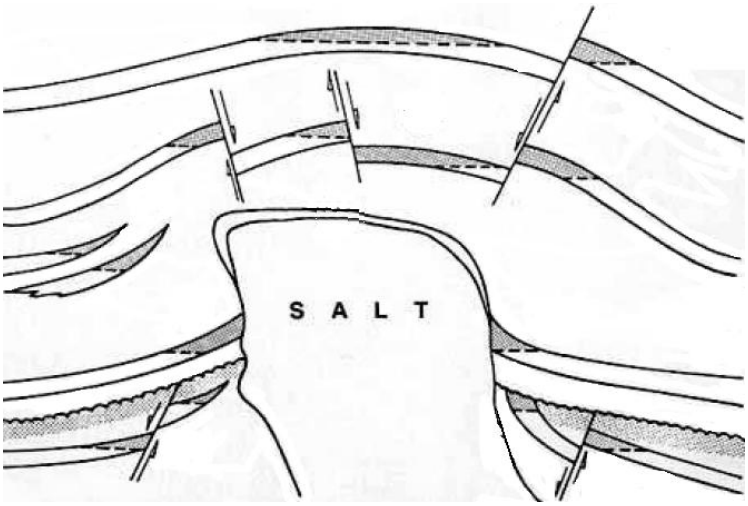

Figure 107 - Common types of hydrocarbon traps associated with the movement of salt bodies (from www.geo.wvu.edu).

In seismic data with original amplitudes, salt bodies exhibit a chaotic texture and are generally easily identified (Figure 108). However, in order to be able to isolate and enhance the salt bodies, high resolution *variance* (see Section IV.3.3.5; Figure 96) and *instantaneous frequency* (see Section IV.3.2.5; Figure 58) attributes should be used, as shown earlier in this Chapter.

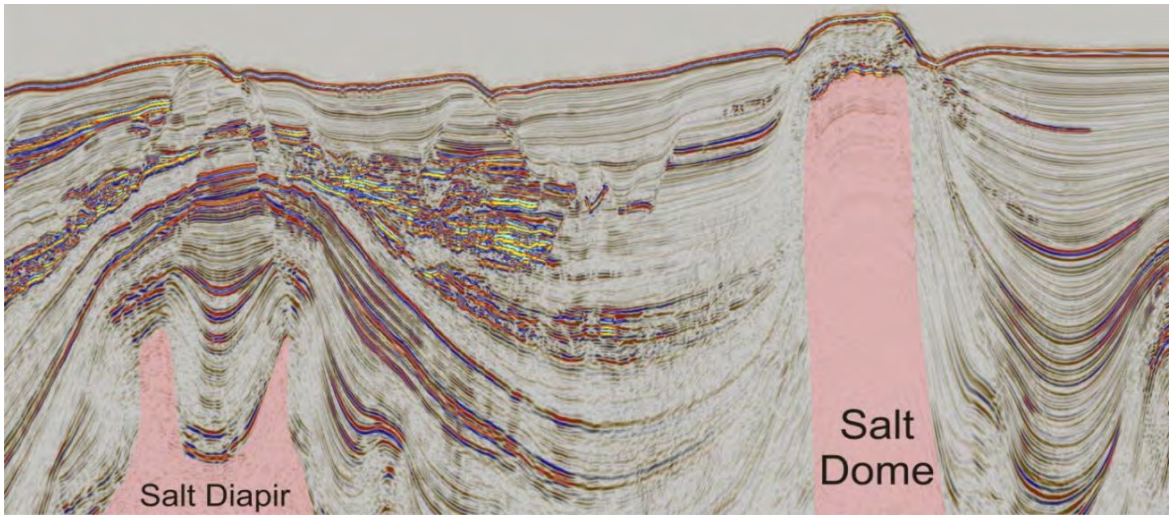

Figure 108 - Example of a vertical seismic line within the study area, showing a salt diapir and a salt dome.

V.1.4. Structural Control in the Study Area

A preliminary characterization of the principal types of faulting in the study area was performed, by identifying faults in the original seismic cube, and also using automatic detection algorithms, such as *Ant Tracking* (see Section IV.3.3.6) on the *variance* (see Section IV.3.3.5) cubes.

The main trends of the principal regional faults were interpreted both by their expression on the seafloor morphology and by the alignments directions of *pockmarks* and salt bodies (Figure 88). The interpreted regional faulting trend is mainly NNE- SSW and NNW-SSE. The two principal types of faults identified in the study area are: (1) steep normal and strike-slip faults; (2) small faults with a radial geometry immediately above the salt bodies.

(1) The steep faults are characterized by their extension from deep in the section to the seafloor, and normally follow the two main faulting direction trends mentioned above (Figure 109). At several locations, these faults act as conduits for the salt intrusions, as described in Section V.1.3.

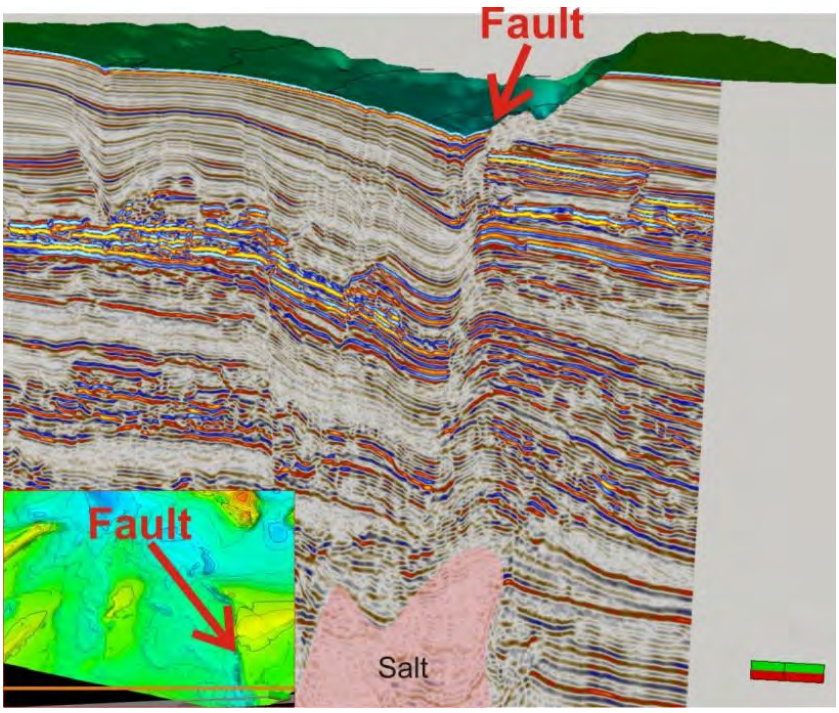

Figure 109 - Vertical seismic section showing a regional steep fault with expression at the seabed (see inset at the lower left corner). The salt body probably moved along the fault in depth.

Interpreting these faults at “depth” (TWT) is also important since oil migration paths from the sub-salt to above the salt can also be identified. Most of the proven active petroleum systems in the study area have their source rock below the salt layer and high quality reservoirs in the upper stratigraphic sequences.

(2) Small faults with radial geometry (Figure 110) can be interpreted as faults associated with the intrusion of salt in the layers above.

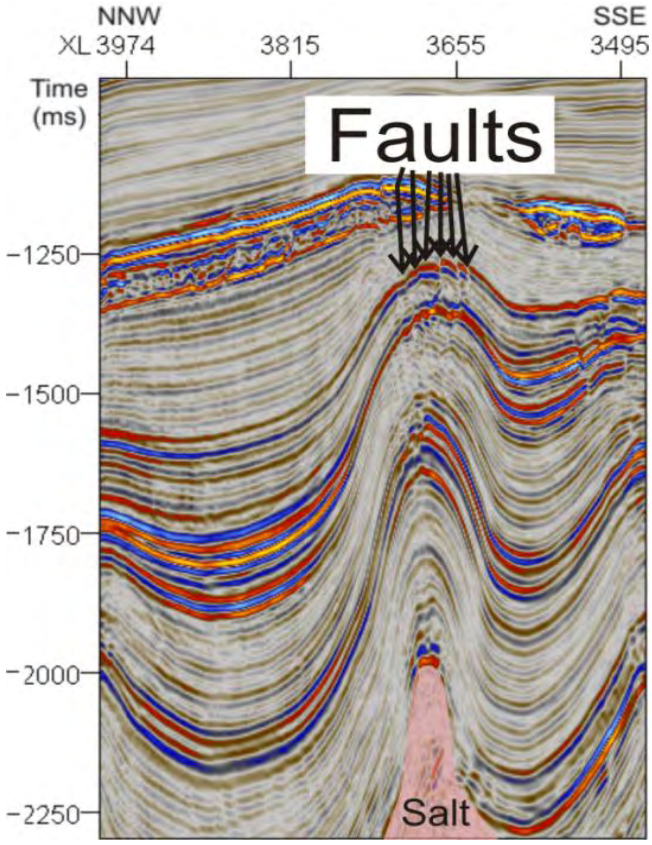

Figure 110 - Small faults created by the salt intrusion.

A detailed interpretation of the different faults system, both at large and small scales, along the target area should always be performed in order to identify possible reservoir areas. Conjugate faults with the right geometry, can act as structural hydrocarbon traps due to the closure of high porous lithologies against faults which do not allow fluid circulation along them. Fault closure is often observed in vertical seismic sections by abrupt termination of bright reflections against interpreted faults (Figure 111). Seismic attributes can be useful in the fault interpretation and characterization processes.

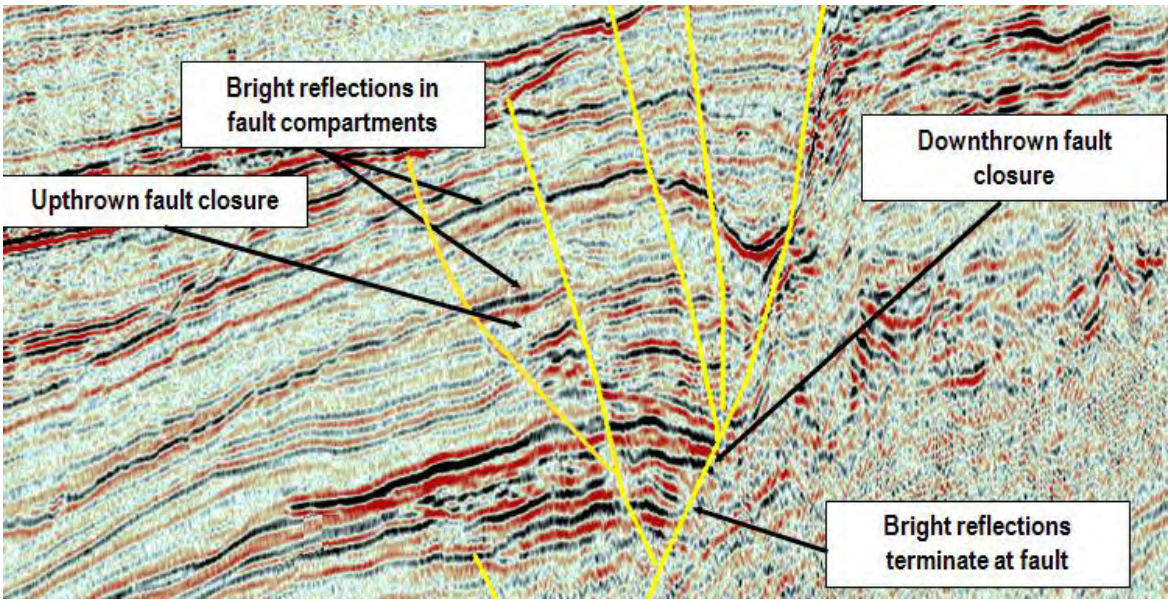

Figure 111 - Example of a fault trap system. Enhanced reflectors terminate abruptly against faults giving the needed closure to trap the hydrocarbons (Schlumberger, personal communication).

V.1.5. Geobody Extraction

Geobody Extraction is a leading edge utility, in *Petrel*, that allows extracting visually and interactively features of interest from the seismic data. Each feature is isolated blending several seismic volumes with user-defined settings. The isolated seismic feature is then extracted into a discrete object, the *geobody* itself, by a simple mouse click using the method "*what you see is what you pick*". The *geobody* can then be used for different purposes: essentially, it can be sampled into a geological model grid to be populated with properties (e.g. porosity, permeability), or its boundaries or middle surfaces converted in horizon interpretation points. These interpretation points can be used to help the traditional interpretation process or can be inserted into a hydrocarbon model after being converted into surfaces. Channels and salt domes are typical features which have proven results in *geobody* extractions. The "*Geobody Extraction*" process, in *Petrel*, can be found under *Geophysics* (*Schlumberger*, personal communication).

The first step of the extraction process is the introduction of a probe. A probe can be defined as a cropped rendering of one or more blended seismic volumes, in which the seismic feature will become isolated. Seismic volumes used to create the probe should allow the isolation of the feature through a contrast in colours

between the target feature and the background data; the isolation is achieved using the opacity curve of each seismic cube. The probe should also have enough size to cover the area of the feature to be extracted. Since the *geobody extraction* process is a very intensive process, it is suggested to draw a polygon around the seismic feature and clip the probe outside it. This last step will reduce the rendered probe volume, increasing the speed of visualization and manipulation.

Features are isolated by accessing the "*Opacity Tab*" in the probe settings. This tab shows the colour scale bar and a histogram of colours amplitudes for each seismic volume that were used to create the probe (Figure 112).

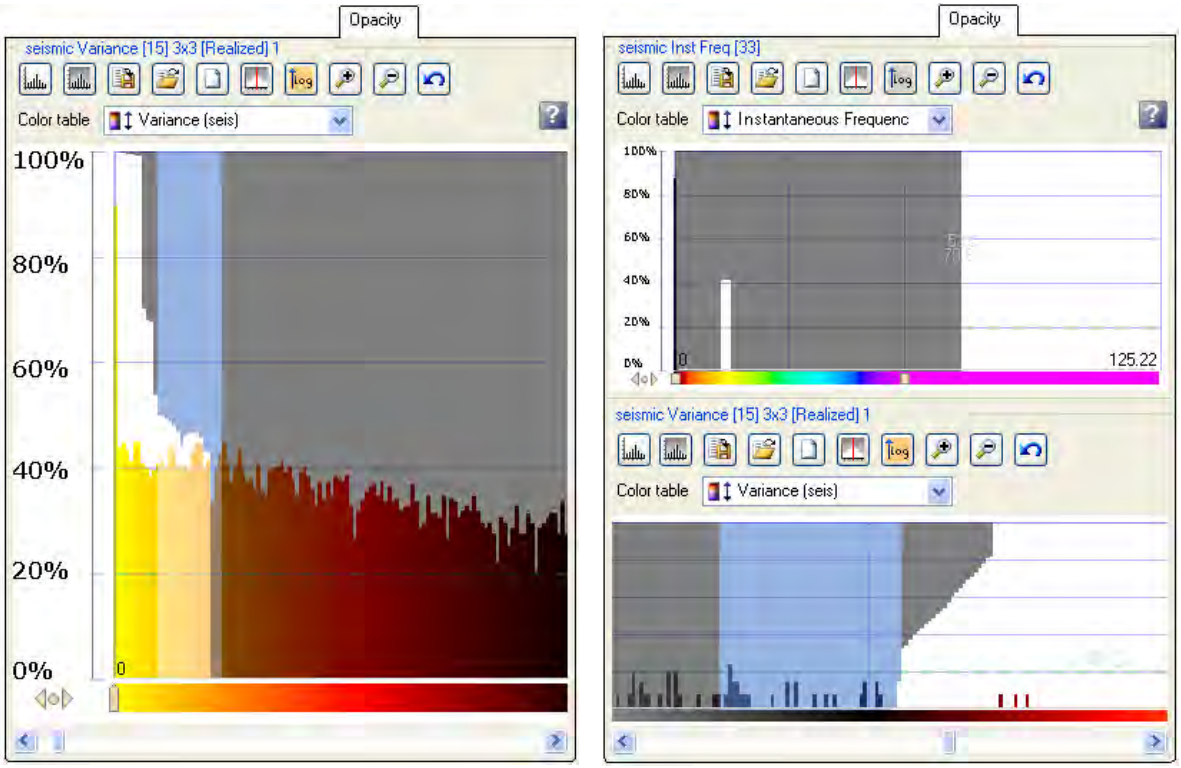

(a) **(b)**

Figure 112 – Example of two probes' "*Opacity Tab*", used in the "*Extract Geobody*" process, to extract: **(a)** a channel using a *variance* cube. Values of *variance* meaning discontinuities have been removed from the display (grey area); and **(b)** a salt body, using a blend of *variance* and *instantaneous frequency* cubes. Only a small interval of *instantaneous frequency* values is typical of a salt body signature, the rest of the values are not displayed in the probe (grey area). As a complement to isolate the salt body, the values of *variance* meaning continuity were hidden (grey area).

Colour intervals which are not part of the desired feature can be filtered and removed from the probe visualization, interactively, by turning their correspondent areas into grey, inside the histogram display. Grey areas are not displayed in the

probe visualization, isolating the feature to be extracted from the background data (Figure 113; Figure 114).

To extract the isolated feature into a *geobody*, *Petrel*'s "*Extract Geobody*" function needs to be activated. Then, the interpreter just needs to click on the isolated feature. The *geobody* will be automatically created and converted into a discrete object based on a user-defined threshold opacity value. If a cell has an opacity value below the user-defined threshold value, the area will not be sampled into the object; on the other hand, if the cell has an opacity value above the threshold, it will be inserted into the *geobody*.

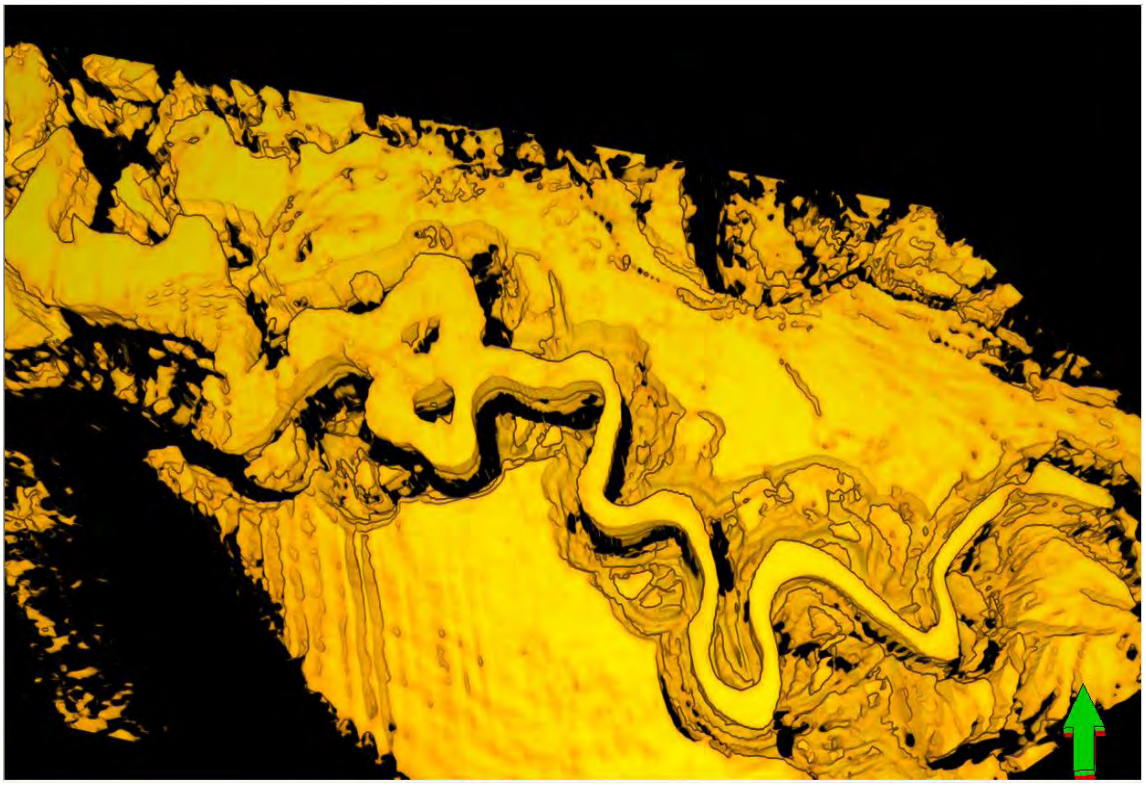

Figure 113 - Isolated target channel system using a *variance* probe and the opacity curve shown in the Figure 112a. The probe is now ready to the "*extract geobody*" process, since it is isolated from the background. Figure 115, in blue, shows the extracted channel system as a *geobody.*

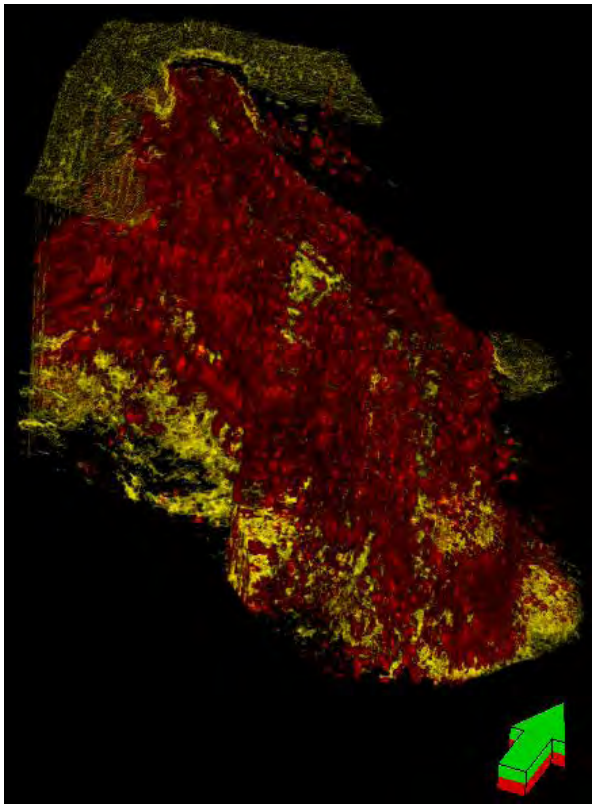

Figure 114 - Isolated salt dome using a blend of instantaneous frequency and variance probes. The opacity curve for each attribute is shown in Figure 112b. The *geobody* representing this salt dome is shown on Figure 115, in light green.

Two geological features have been extracted as a *geobody* in the scope of this work: the turbidite target channel system; and a nearby salt dome. The channel was isolated using a probe representative of the *variance* attribute, where values related to discontinuities were hidden, using the "*Opacity Tab*" shown in Figure 112a. The *variance* attribute is the adequate choice to isolate channels since normally, inside the channel, there are many continuous reflectors with values of *variance* close to 0. On the other hand, the border of the channel often appears as discontinuities in the *variance* attribute, with values of *variance* equal to 1 (Figure 113). This contrast in continuity allows a perfect isolation and extraction of the channel as a *geobody* (Figure 115).

The salt dome was extracted using two attribute volumes at the same time: the *instantaneous frequency* and the *variance* cubes. These two attributes were chosen because the former is good to fill the inside of the salt body (salt bodies show low *instantaneous frequency* values), while the *variance* attribute enhances its boundaries. With the adjusted opacity curve for both attributes (Figure 112b)

the visual isolation of the salt dome became very good (Figure 114). The extracted *geobody* from the salt dome is shown on Figure 115 (in green).

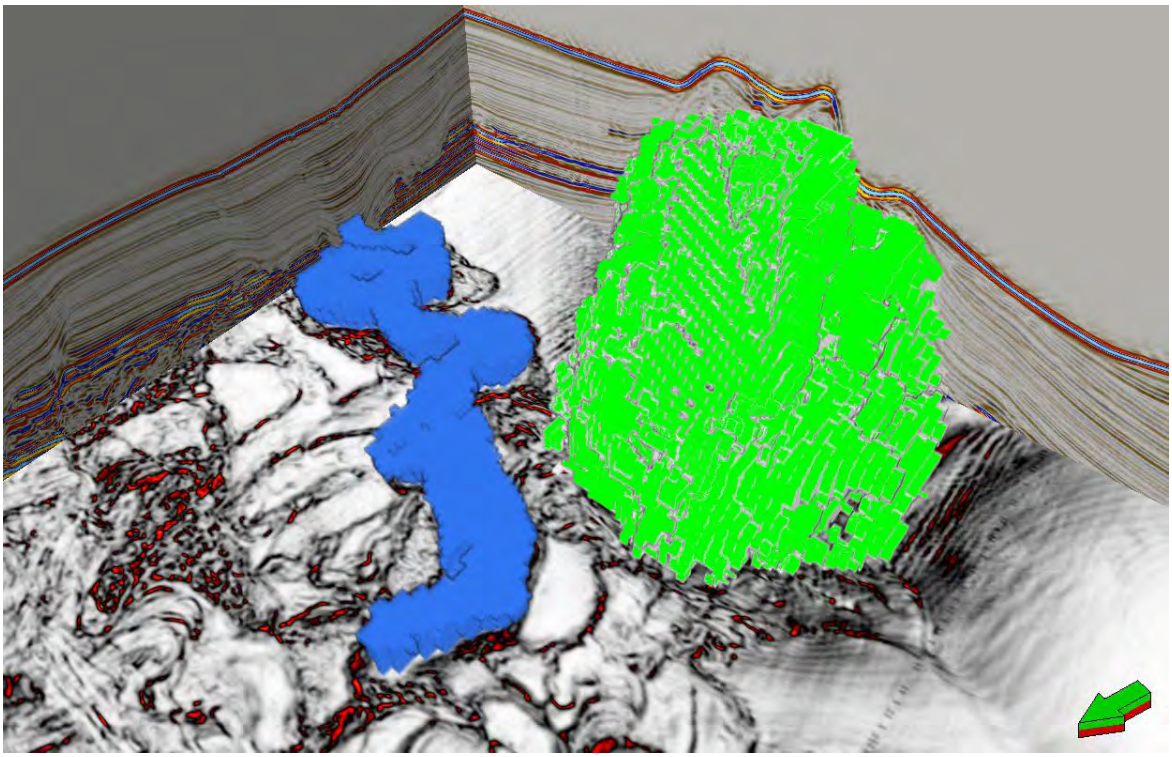

Figure 115 - G*eobody* of the target channel system (in blue) and a salt dome (in green), above a time slice of the *variance* cube. The *variance* time slice can be used to compare the level of detail that can be achieved using *Petrel*'s *"extract geobody*" process.

V.2. Advanced Interpretation and Facies Classification

Generally, at the *advanced interpretation* stage the main objective is the characterization of potential geological features, identified in the *prospect generation* stage, which may act as hydrocarbon reservoirs. The target channel system, identified in Section V.1.2, is a potential stratigraphic hydrocarbon reservoir, and consequently was used here as a testing area for *advanced interpretation*.

At this stage, the standard procedure of an oil and gas company is the interpretation of the key seismic reflectors that define the potential hydrocarbon reservoirs, and the analysis of attribute maps using surfaces provided by the *advanced interpretation* process.

V.2.1. Surface Attributes Interpretation

In this work, an interpretation of the upper and lower boundaries of the target channel system (Figure 116) was attempted, using a manual interpretation picking, guided by the interpretation points provided by the extracted *geobody* (see Section V.1.5.). A middle horizon, within the manually interpreted upper and lower boundaries of the target, was interpreted by automatically converting the middle surface of the *geobody* into interpretation points.

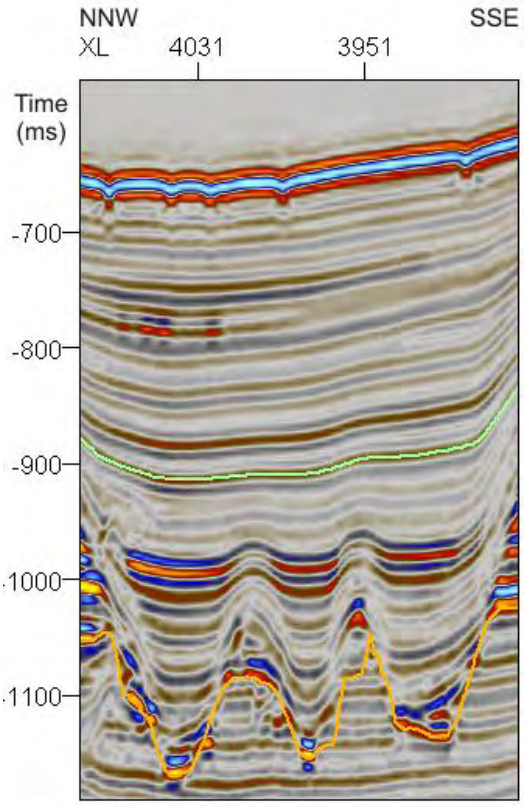

Figure 116 - Interpretation of the upper (in green) and lower (in orange) boudaries of the target channel system in a vertical seismic section.

The interpretation of the boundary surfaces of the target channel system was divided in two phases: (1) the manual interpretation of closely spaced inlines/crosslines, in order to create a tight interpretation (Figure 117a); (2) the spatial extrapolation of the interpretation grid picks, applying the *Petrel*'s "*3D Autotracking*" function constrained by a *structural smoothed* cube (see Section IV.3.3.4; Figure 117b). Using a seismic cube with reduced spatial noise and enhanced seismic reflectors continuity to extrapolate a dense interpretation grid,

was the best approach to create reliable surfaces on such a complex sinuous channel system.

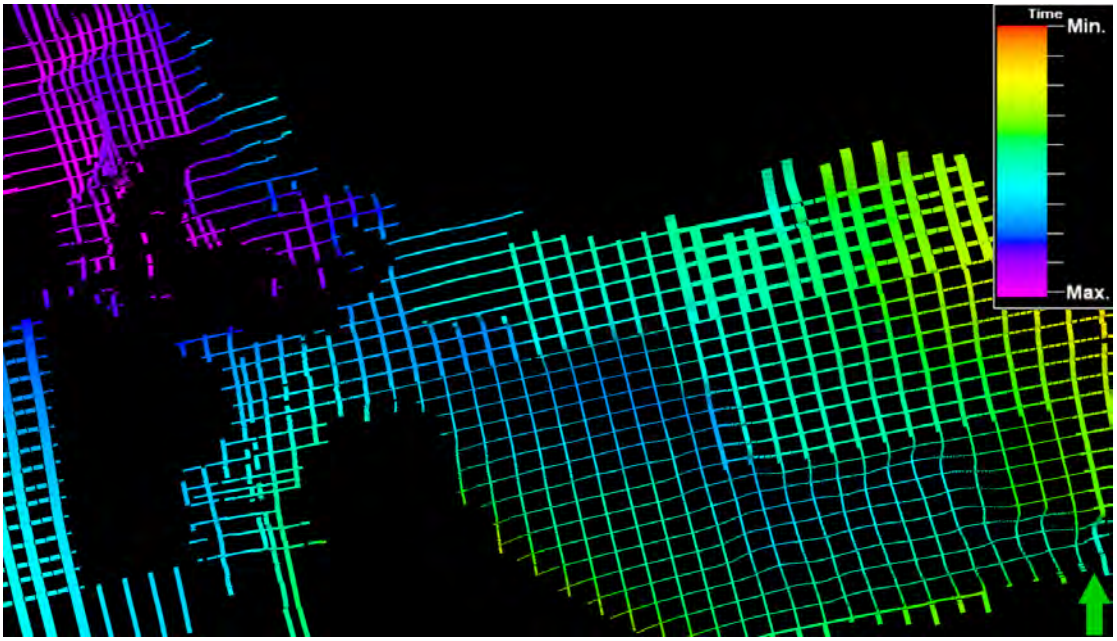

(a)

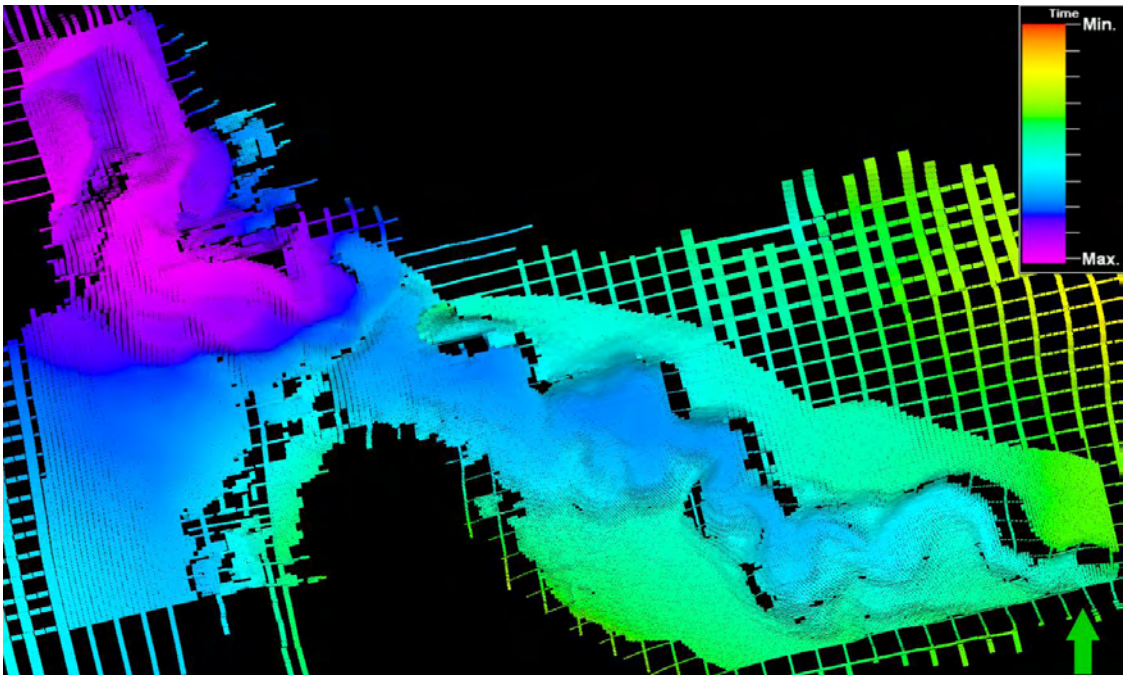

(b)

Figure 117 – (a) Interpretation grid of the upper horizon boundary; **(b)** the result of applying the *Petrel*'s "*3D Autotracking*" function in **(a)** to extend spatially the interpretation. A polygon around the channel was used to constrain the *autotracked* interpretation.

In order to characterize the target area, the interpretation of attribute maps is necessary. Attribute maps, or *surface* attributes in *Petrel*, are extracted from

surfaces and not from interpretation points (*Petrel*'s "*Make Surface*" process, found under *Utilities*, allows the conversion of the interpretations points into surfaces).

Several *surface attributes*, with different parameters were extracted from the interpreted surfaces of the target channel system. *RMS amplitude* and *Iso-Frequency* (using different cosine frequencies) were the most promising attributes, using a search window of 100ms below the upper boundary surface.

The *RMS amplitude* (see Section IV.3.1.8) attribute was the first *surface* attribute generated since it can easily detect porous lithologies, which normally have the potential to form high quality hydrocarbon reservoirs. The generated attribute map (Figure 118) shows a well defined area of high *RMS amplitude* values inside the target channel area (Figure 118, inside the white circle). This area is interpreted as corresponding to high porosity lithologies (sand-like). This *RMS amplitude* anomaly become more interesting since it is consistent in depth using different search windows lengths (e.g. in Figure 86, the same anomaly was also observed in a *surface* attribute extracted with a shorter window length).

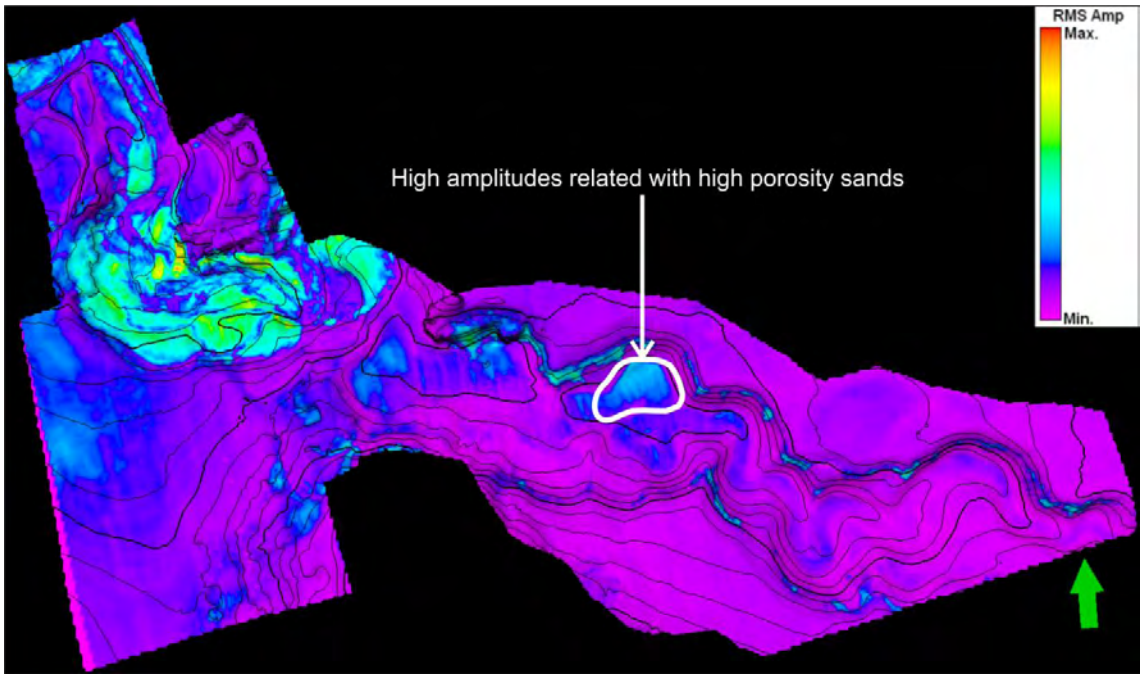

Figure 118 - *RMS amplitude* extracted below the top surface with a search window of 100ms. A small area with high *RMS amplitude* values, inside the with circle, can be indentified. This high values are probaly related to porous sands, and may indicate a potential hydrocarbon reservoir. High vaules in the flank of the channel are artifacts induced by the horizon picking.

High *RMS amplitude* values in such a small area can be indicative of a potential site for hydrocarbon accumulation. To test this assumption, *Iso-Frequency* attribute maps were computed.

Surface attributes with different *Iso-Frequencies* (Section IV.3.4.3) were extracted from the upper boundary surface. The interpretation of these attribute maps was complemented with the information given by the *RMS amplitude* attribute maps, already discussed above. The interpretation of the attribute map shown in Figure 119, extracted with a cosine frequency of 25Hz, allows a much better delineation of the same area already identified in *RMS amplitude surface* attributes. The area of interest, when compared to the surrounding areas, shows a constant value of *Iso-Frequency* allowing a better spatial delineation of the interpreted high porosity area.

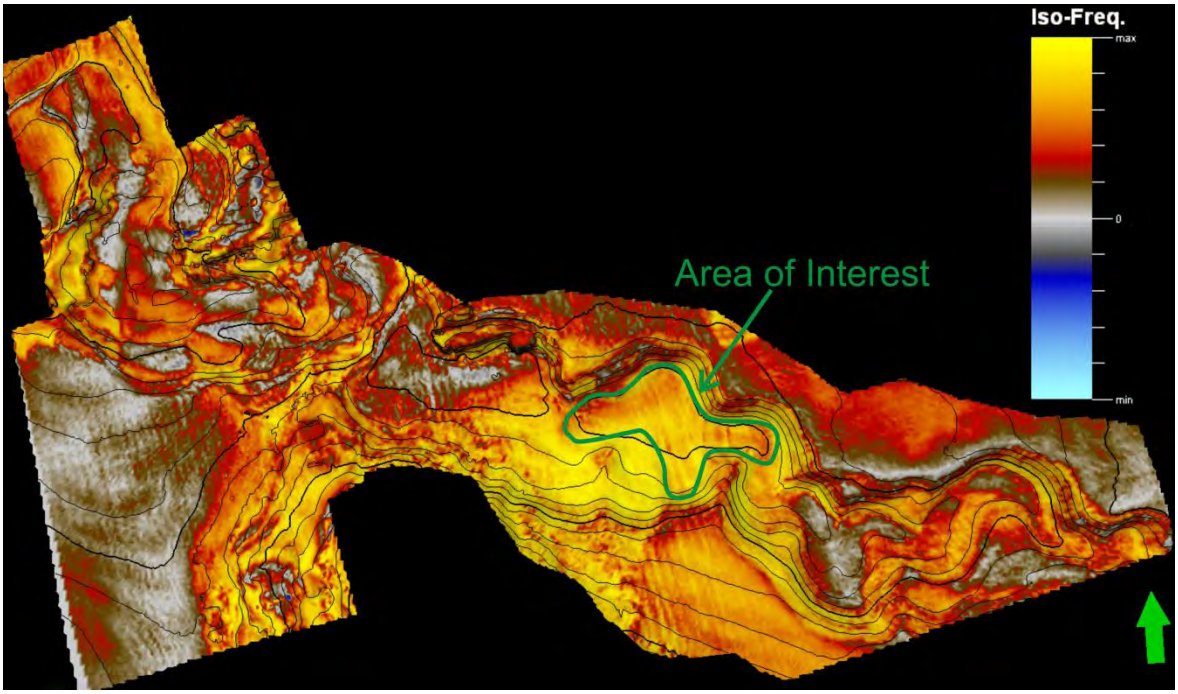

Figure 119 – *Iso-Frequency surface* attribute extracted with a cosine frequency of 25Hz, 100ms below the upper surface of the target channel system. It is possible to interpret an area of interest (inside the green circle) with different lithology when compared to other areas inside the channel system. Compare with Figure 118.

Due to time limitations, other *surface* attributes were not extracted in the scope of this work and the characterization of the area of interest was complemented, using horizontal time slices from several volume attributes. Although, as previously discussed, the target channel system is not parallel to horizontal time slices, if only

a small area inside the channel system is considered, a horizontal time slice extracted at the same two-way-time of the target area is a good approximation.

V.2.2. Facies Classification Cube

At the end of the interpretation process, a facies classification cube was computed using an unsupervised *artificial neural network* (see Section V.2.2), using seismic attributes volumes as training data. This *artificial neural network* facies classification was computed with the objective of mapping lithological variations inside the target channel.

Four attribute cubes, two *Iso-Frequency* (see Section IV.3.4.3) volumes, with frequencies at 30 and 35Hz, one *envelope* (see Section IV.3.2.2), and one *variance* (see Section IV.3.3.5) cube, were used as input to train the estimation model of the *neural network*.

These attributes were found to be the best input to train the *neural network*, in *Petrel* 2008.1, because each of these attributes enhances different features in the seismic data, but in all of them, the output attribute volume is lithologically dependent. In addition, they all showed a good behavior in the (1) correlation and (2) in the principal component analysis.

(1) The correlation table computed between the chosen attributes (Figure 83) does not follow the requirements described in Section IV.3.4.5. There are high correlation values between the 30Hz and 35Hz *Iso-Frequency* volumes (red cells), and low correlation values between the *variance* and the *envelope* attributes (blue cells). However, the correlation rules should not be followed blindly, and seismic attributes should also be selected by their potential output information, if they are suitable for the original dataset and what answers the user requires from the *neural network* process. In this case, in spite of the high correlations observed between the two *Iso-Frequency* cubes, they have proven, nonetheless useful to infer variations in lithology and therefore both were used. The *variance* cube was used since it enhances discontinuities and the main objective of computing the

facies cube was the delineation of the target channel system and its lithological variations. The *variance* cube also shows good correlation values with the *Iso-Frequency* cubes. The *envelope* cube has good correlation values with all the other attributes and, since it is an attribute related to the energy content of the data, it is useful to distinguish lithological variations. From a general point of view, the correlation table shows acceptable values between the selected attributes to train the *neural network* (Figure 83).

(2) The *principal component analysis* (PCA; Figure 120) allowed reducing the dimensionality of the input vectors, due to the low value of the *Eigenvalue* relative to the *principal component* PC4. As a result, only the three first PCs were used, accelerating the classification process and reducing the uncertainty associated with the neural network process.

Correlation Coefficients	PC1	PC2	PC3	PC4
Seismic Channel CCT [30]	0.9312	0.0533	0.2719	0.2369
Seismic Channel CCT [35]	0.9354	-0.0524	0.2538	-0.2405
seismic Envelope	0.5521	0.7085	-0.4394	-0.0142
seismic Variance	0.5598	-0.6999	-0.4431	0.0217
Eigenvalue	2.3603	0.9974	0.5277	0.1146
Contribution (%)	59.01	24.93	13.19	12.87
Cumulative Contribution (%)	59.01	83.94	97.13	100.00

Figure 120 - *Principal component analysis* table used to select the input to train the *neural network*.

Petrel's unsupervised *neural networks* allow grouping the information provided by the several inputs in a user-defined number of classes. In this case, 4 classes were used as a starting point. The *Competitive Learning Algorithm* in the "*train estimation model*" ran until the 100th interaction and the input data was placed in the most probable class every time the probabilistic value was greater than 0.10.

The output facies volume, computed in this way, shows each user-defined class with a different colour, that can ideally be assigned to different lithologies (Figure 121). From the combined interpretation of the facies classification cube, the original seismic data, and the seismic attributes used to train the estimation model, a preliminary correspondence between the class, the original seismic texture and

the lithology is proposed: *Class 1*, in purple, was interpreted as corresponding to high amplitudes in the original seismic data and can be related to high porosity lithologies, such as sands; *Class 2*, in yellow, was interpreted as corresponding to chaotic patterns in the seismic data such as those associated with salt bodies; *Class 3*, in orange, was interpreted as corresponding to low amplitude seismic reflectors, which may indicate the presence of mudstones or shales; *Class 4*, in grey, was interpreted as corresponding to discontinuities, such as borders of salt bodies, channels and channels systems.

From the interpretation of horizontal time slices along the facies classification cube following the target channel system (Figure 122) it was possible to interpret lateral changes in lithology inside the turbidite channel and to define an area of interest. This area was already identified in many seismic attributes, particularly *surface* attributes (see Section IV.4) and, following the correspondence between class and lithology, it was interpreted as high porosity sands.

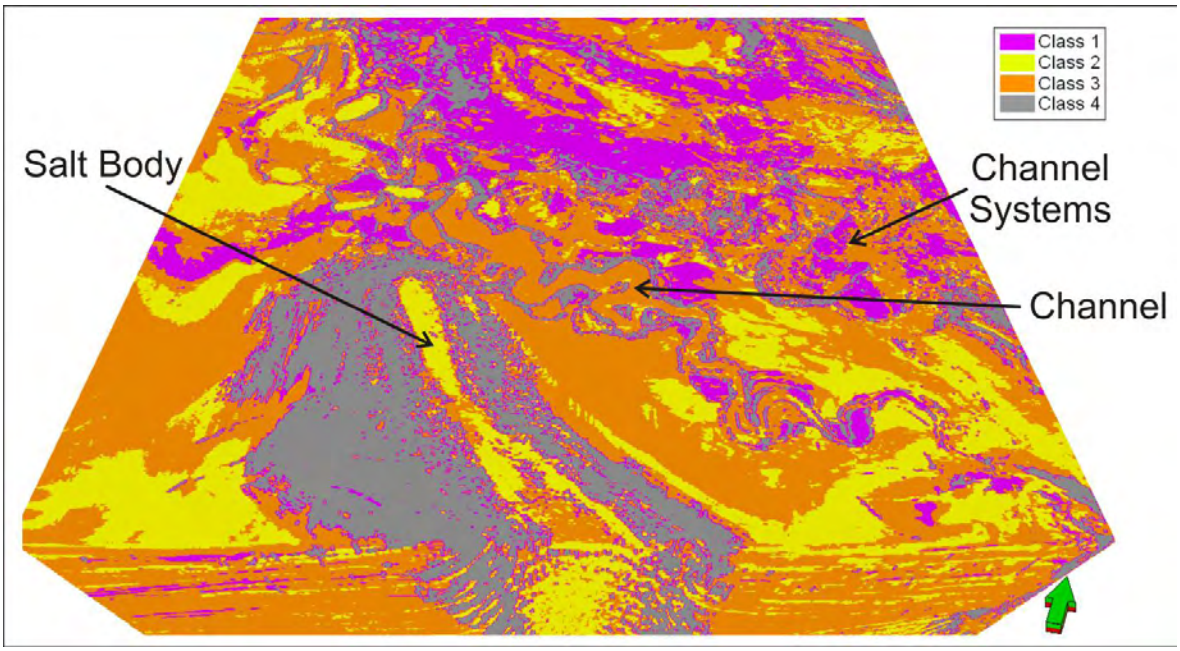

Figure 121 – Facies classification cube computed using an *artificial neural network*. As training data two *Iso-Frequency* cubes with 30 and 35Hz, an *envelope* and a *variance* cube were used. In this horizontal section a salt dome and several channel complexes including the target channel system can be distinguished.

This facies classification cube presented here is considered a first approach to infer about the subsurface lithology in the survey area. However, unsupervised

neural networks have limitations since there are no real parameters to constrain the model and therefore the results should be interpreted with caution. When well log data is available well constrained results can be achieved since the output of the *neural network* is constantly compared with the real data in order to achieve a convergence between the estimated facies and the well log data, resulting a more reliable model.

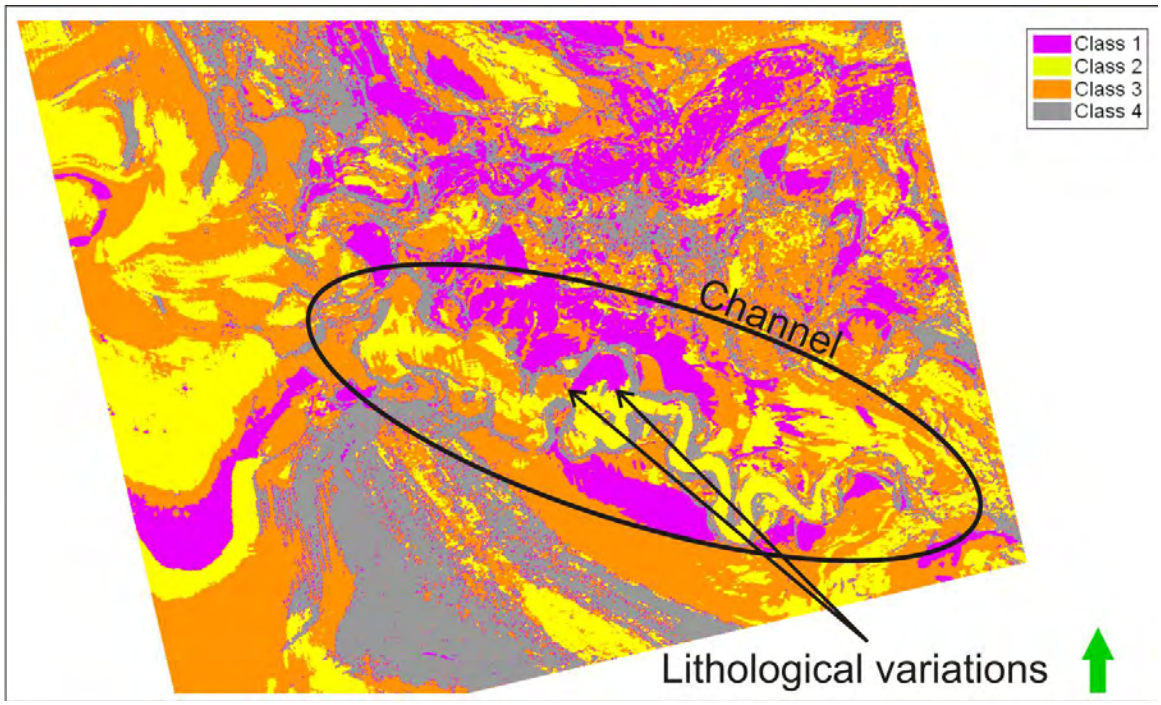

Figure 122 - Time slice from the facies classification volume. Based on the interpretation of each class it may be inferred that the area of interest in the central part of the target channel systems (in purple) is possibly related with highly porous sands and therefore a potential hydrocarbon reservoir.

V.2.3. Preliminary Characterization of a Hydrocarbon Reservoir

The delineated area, inside the target channel system, was identified from the interpretation of the *surface* attributes (Section V.2.1), and it was characterized using a combination of several seismic attributes.

Structural attributes, with a highlight for the *variance* cube, showed and allowed the identification and morphological characterization of the turbidite channel

system. From the geological background of the study area, turbidite channels are often proven and high quality hydrocarbon reservoirs. Consequently, further interpretation, based on other seismic attributes, was also carried out to delineate the area with more potential to contain hydrocarbon accumulations and therefore with more likelihood to be a hydrocarbon reservoir.

A potential hydrocarbon area was identified inside the target channel system (Figure 123). This area was identified by its response to well known seismic attributes which are indicative of the presence of hydrocarbon accumulations: (1) high values of original amplitudes (Figure 98) were the first clue; (2) the *envelope* attribute showed a limited area with high values (Figure 123), which are often indicative of porous lithologies, such as sands; (3) the *instantaneous frequency* attribute was interpreted in time slices immediately below the time slices where the *envelope* attribute was interpreted and it showed, for the same area of high values of *envelope*, low frequency values, when compared to the rest of the channel (Figure 123); this is a common signature of sands filled with gas; (4) the *RMS amplitude* attribute map (Figure 118) showed the same behavior of the *envelope* time slice, reinforcing the interpretation idea of a hydrocarbon area; (5) finally, the *Iso-Frequency* attribute, together with the *Relative Acoustic Impedance*, allows a better correlation of these hydrocarbon evidences with the spatial facies distribution (Figure 119; Figure 124).

The faulting pattern is another important factor to characterize a hydrocarbon reservoir. For this case, the *Ant Tracking* cube did not show any major faulting along this potential hydrocarbon reservoir.

In conclusion, a careful interpretation of the extracted seismic attributes, available in *Petrel* 2008.1, over the study area allowed: (1) the identification of the depositional systems in the study area and the consequent identification and characterization of stacked turbidite channel systems which can be potential high quality hydrocarbon reservoirs; (2) the recognition of what may be a hydrocarbon reservoir inside the target channel system, by its response to energy, frequency and spectral decomposition attributes; (3) the confirmation that the target section of the turbidite channel is possibly filled with sands, in contrast to the rest of the

channel, based on the seismic classification cube (V.2.2), computed from seismic attributes.

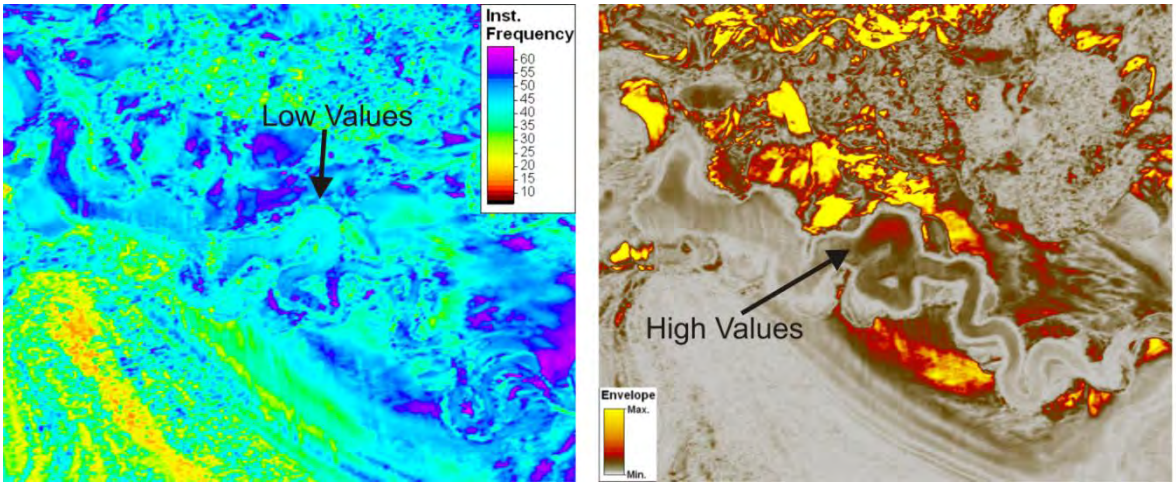

Figure 123 – Two horizontal time slices which follow the potential hydrocarbon reservoir, showing low values of *instantaneous frequency* in a time slice computed immediately below (on the left) a time slice extracted from the *envelope* cube (on the right).

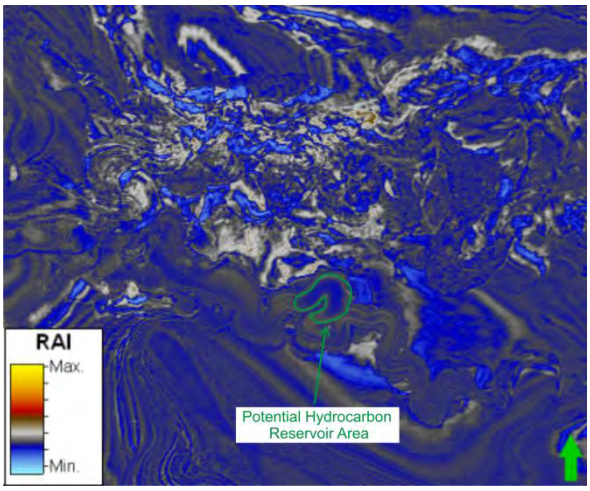

Figure 124 - Time slice of *Relative Acoustic Impedance* attribute along the potential reservoir area. Combined with the *Iso-Frequency* attribute RAI allowed to delineate the accumulation area in space

This potential reservoir area can also be delineated in the extracted *geobody* to use for further hydrocarbon modeling (Section V.1.5; Figure 125).

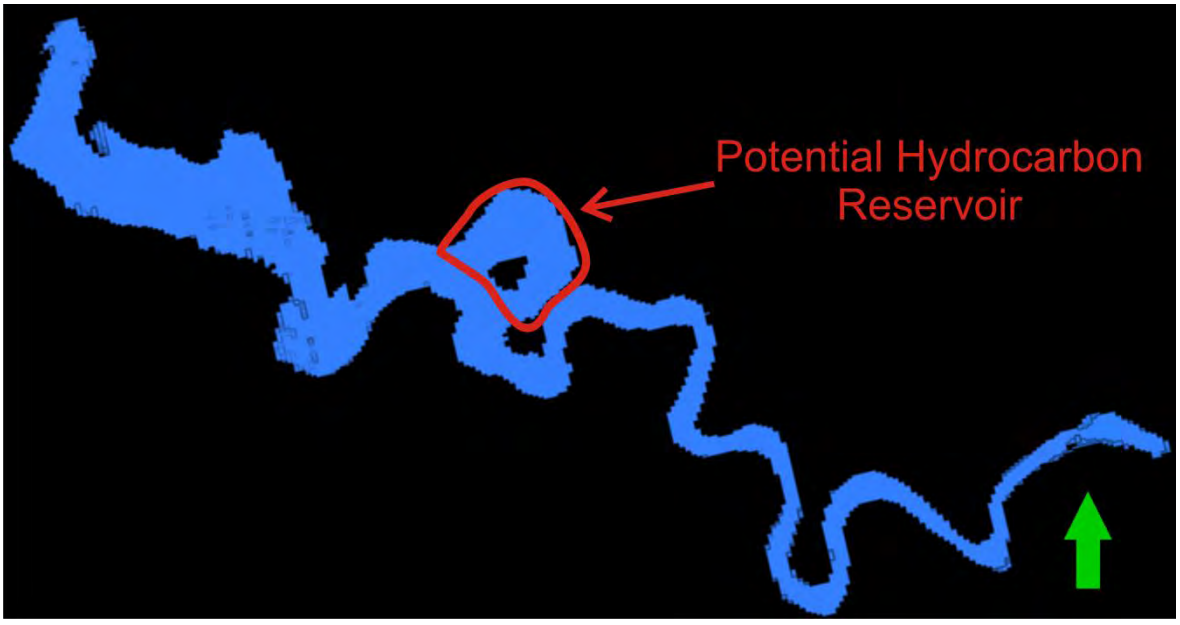

Figure 125 - Extracted *geobody* for the entire target channel system with the hydrocarbon reservoir area enhanced.

Chapter VI. Conclusions

Seismic attributes can nowadays generally be calculated in most of the modern interpretation workstations and they are powerful tools to help the seismic interpretation process. Attributes derived from seismic data try to mimic the interpreter's expertise, displaying the seismic data, which is normally plotted in amplitudes, from a new point of view. Interpreting the seismic data together with extracted seismic attributes often results in new insights into the data and the discovery of relationships between seismic events which are not always evident.

The proliferation of high quality 3D seismic data, associated with huge developments in seismic interpretation software, made seismic attributes reliable solutions to solve ambiguous situations in the seismic interpretation process. However, attributes derived from seismic data cannot be applied as a general recipe, even if there are many examples in the literature that try to correlate the attributes with the expected results. These correlations should be done with especial care, since the output volume attribute, depending on the geological background of the dataset, may produce unexpected results. As a best practice to avoid misinterpretations, the interpreter needs to first identify the feature of interest before interpreting seismic attributes, and should always refer to the original data during the attribute guided interpretation.

Seismic attributes are however extremely useful tools in the identification and characterization of hydrocarbon reservoirs since they are either directly sensitive to a reservoir property of interest or allow the user to interpret the structural and depositional systems of the study area far more easily. Identifying potential features which may act as hydrocarbon traps is the first step for a successful oil and gas exploration.

In the scope of this work, the *Petrel* "*seismic-to-simulation*" software was used to generate and interpret the studied seismic attributes. This software has an extensive list of seismic attributes to help the seismic interpretation process. In

Petrel, seismic attributes are first classified into *volume* and *surface* attributes (the equivalent to attribute maps), and then divided into different libraries according to the expected output extraction algorithm. *Petrel*'s seismic attributes which have the most potential are: all those belonging to the *Seismic Signal Processing Library* (see Section IV.3.1); *envelope* (see Section IV.3.2.2); *instantaneous frequency* (see SectionIV.3.2.5); *variance* (see Section IV.3.3.5); *structural smoothing* (see Section IV.3.3.4); *local structural azimuth and dip* (see Section IV.3.3.2); *Ant Tracking* (see Section IV.3.3.6); *chaos* (see Section IV.3.4.1); *Iso-Frequency* (see Section IV.3.4.3) and *relative acoustic impedance* (see Section IV.3.4.4).

Briefly, the seismic attributes listed above, when properly applied to seismic data can significantly increase the signal-to-noise ratio, resolve areas with low resolution, detect subtle lithological variations, enhance seismic reflectors' continuity (by increasing the interpretation picking stability with automatic algorithms), help the structural interpretation (by automatically enhancing edges), enhance depositional features and train artificial neural networks to estimate facies distribution, including reservoir properties prediction between wells, and compute a facies classification cube with new information that can help to better understand the geology of the study area. Some attributes are also direct hydrocarbon indicators (DHIs). A summary of the most used seismic attributes, in *Petrel*, with their description and applicability is given in Table II.

The interpretation of the dataset investigated in this work (see section Chapter V), and the study of the derived seismic attributes, allowed the identification of areas with pockmarks and the delineation in detail of salt intrusions and faults. In addition, a turbidite channel system with an area which may be a hydrocarbon reservoir (Figure 125) was also identified and interpreted. The *variance* attribute was successfully used for the characterization and identification of the depositional systems in the study area. Energy and frequency attributes (e.g. *RMS amplitude*, *Iso-Frequency*, *Relative Acoustic Impedance*) allowed the identification and characterization of the potential hydrocarbon reservoir.

Table II – Summary of the most promising seismic attributes available in *Petrel* 2008.1

Attribute Name	Description	Applicability
RMS Amplitude	The "*root mean square*" of the original amplitude within a user-defined window (Section IV.3.1.8).	Distinguish between lithological changes. High values of *RMS Amplitude* may indicate porous sands or sinuous channel belts. Isolated extreme values of this attribute may be a bright spot.
Apparent Polarity	The sign of *f*(t) at a local maximum of the *Envelope* attribute (Section IV.3.2.1).	Useful to track lateral changes in lithology and enhance reflectors continuity. May distinguish different kinds of bright spots.
Instantaneous Phase	Is defined as the argument of the complex seismic trace (Section IV.3.2.3).	Enhance reflectors continuity, discontinuities, faults and pinch-outs. Is useful in stratigraphic pattern interpretation. Can be used as a DHI.
Cosine of Instantaneous Phase	Is the cosine of the *instantaneous phase* attribute (Section IV.3.2.4)	Improves reflectors continuity and enhance discontinuities, faults and pinch-outs. Helps the stratigraphic interpretation process. Since it is invariant with amplitude is used conjugated with the *instantaneous phase* attribute.
Envelope	Is the modulus, or the total instantaneous energy, of the complex seismic trace (Section IV.3.2.2).	Distinguishes stratigraphic, lithologic, and fluid lateral variations inside a hydrocarbon reservoir; and major changes of lithology and sequency boundaries. It Can also be used as a DHI, it may identify bright spots.
Instantaneous Frequency	Is the rate of change in time of *instantaneous phase* attribute.	Typically used to interpret lateral and vertical changes in lithology and identify faults by absorption effects. Can also be used as a DHI, since the presence of gas often causes what so called *low-frequency shadow*, below the hydrocarbon reservoir.
Local Structural Azimuth and Dip	Uses three methods to estimate the orientation of a bed. The *gradient* method calculates the gradient in 3 directions. *The event* uses the same approximation of the *gradient* method but with a different convention. The *principal component* method uses a *principal component analysis* to estimate the orientation	Estimates the orientation, azimuth and dip, of a seismic reflector. It is also used as an internal algorithm for other seismic attributes extraction in *Petrel*.
Structural Smoothing	Fast volumetric signal processing. Apply a 3D Gaussian filter honoring, or not, the estimated bed orientation.	Reduces spatial noise within the data, improving reflectors continuity. May also enhance edges.
Variance	It computes the normalized population variance with an optional weighted vertical smoothing.	Detect edges, such as faults and discontinuities. It sharply delineates a salt body and with a short vertical window, *variance* attribute can be used to interpret depositional elements.
Ant Tracking	Uses swarm intelligent concepts where virtual "ants" are deployed into an edge detection cube (e.g. *variance*) to automatically track and enhance faults and discontinuities with high level of detail.	The enhanced faults can be automatically extracted, using *Petrel*'s "*Automatic Fault Extraction*", to be inserted in a hydrocarbon reservoir model.
Chaos	Measures how consistent is the orientation of a reflector estimated based on *local structural azimuth* attribute.	Enhances edges, salt bodies and chaotic patterns within the original seismic data.
Iso-Frequency	Is a spectral decomposition method which uses a correlation between a user-defined cosine frequency and autocorrelation function of the original seismic data.	May indicate subtle lithologic features which are not detected in original amplitude. Can also be used to interpret depositional elements.
Relative Acoustic Impedance	It tries to estimate the natural acoustic impedance log by integrating the original seismic trace and filtering it through a Butterworth filter.	High values of relative acoustic impedance are often related with unconformity surface, sequence boundaries and discontinuities. It may also be used to detect the presence of fluids within the data.

This interpreted potential hydrocarbon reservoir needs to be investigated in more detail to improve the odds of a successful exploratory drill. Horizons between the upper and lower boundaries need to be consistently picked and several attribute maps should be extracted and interpreted to achieve a better reservoir characterization and delineation.

Future work should include the development of multi-attribute analysis for the automatic prediction and correlation of seismic textures with reliable facies distribution models. Automatic faults and fractures enhancement and detection is another important aspect in which seismic attributes workflows can have high importance and could be further developed. Further studies should also be done in order to tie attributes with well log data, if available, which will enable better correlations between the attributes and the petrophysical properties of a hydrocarbon reservoir.

Lastly, the four months internship at *Schlumberger* allowed the author to become familiar with the daily routine of an employee in a support team from a service company for the oil and gas industry. It also allowed him to complement his academic background with new concepts related to seismic data processing, seismic attributes and seismic interpretation in the characterization and identification of potential hydrocarbon reservoirs.

Chapter VII. References

Adriansyah, A., McMechan, G. A. (2002). Analysis and interpretation of seismic data from thin reservoirs: Northwest Java Basin, Indonesia. Geophysics, Vol. 67; No. 1, 14-26.

Alfaro, J. C., Corcoran, C., Davies, K., Pineda, F. G., Hampson, G., Hill, D., Howard, M., Kapoor, J., Moldoveanu, N., Kragh, E. (2007). *Reducing Exploration Risk*. Oilfield Review, Spring, 26 – 43.

Amundsen, L., Landro, M. (2009). *Shooting Seismic in Linked Circles*. Geo Expro, February, 54 – 56.

Balch, A. H. (1971). *Colours sonograms: A new dimension in seismic data interpretation*. Geophysics, Vol. 36, No. 6, 1074 – 1098.

Barnes, A. E. (2001). *Seismic Attributes in your facies*. Canadian Society of Exploration Geophysicists Recorder, 26, September, 41 – 47.

Barry, K. M.,Cavers, D. A., Kneale, C. W. (1975). *Recommended Standards for Digital Tape Formats*. SEG Technical Standards Committee.

Bracewell, R. N. (1978). *The Fourier Transform and its Application*. McGraw-Hill, 2nd Edition, 444 pp..

Brown, A. R. (2001). *Understanding seismic attributes*; Geophysics, Vol. 66; No. 1, 47 – 48.

Buia, M., Hill, D., Houbiers, M., Laura, S., Menlikli, C., Moldoveanu, N., Snyder, E. (2008). *Shooting Seismic in Circles*. Oilfield Review, Autumn, 18 – 31.

Chen, Q., Sidney, S. (1997). Seismic attribute technology for reservoir forecasting and monitoring. The Leading Edge, 16, 445 – 456.

Chopra, S., Marfurt, K. J. (2005). *Seismic attributes – A historical perspective*. Geophysics, Vol.70; No.5, 3SO - 28SO.

Dobrin, M.; Savit, C. (1988). *Introduction to Geophysical Prospecting.* McGraw-Hill, 4ed., 867pp..

Duval, B., Cramez, C., Jackson, M.P.A. (1992). *Raft tectonics in the Kwanza Basin*, Angola. Marine and Petroleum Geology, 9, 389-404.

Evans, D. (2003). *Shallow Clues for Deep Exploration*. Oilfield Review, Winter, 2 – 13.

Fehmers, G., Hocker, C. (2003). *Fast structural interpretation with structure-oriented filtering*. Geophysics, Vol. 68, No. 4, 1286 – 1293.

Gaillot jr., K. (1994). *The SEG-Y Format for Geophysical Data*. Without date.

Garcia, H. (2008). *Avaliação do Potencial Petrolífero de uma Área da Bacia do Baixo Congo.* University of Aveiro, Master Thesis, 191 pp..

Gomes, J. S., Alves, F. B. (2007). *O Universo da Indústria Petrolífera – Da Pesquisa à Refinação*. Fundação Calouste Gulbenkian, 647 pp.

Kolla, V., Posamentier, H., Wood, L. (2007) *Deep-water and fluvial sinuous channels-Characteristics, similarities and dissimilarities, and modes of formation*. Marine and Petroleum Geology, vol. 24, 388 – 405.

Lynch, S., Lines, L. (2004). *Combined Attributes Displays*. 72nd Annual Internationl Meeting, SEG, Expanded Abstracts, 1953 – 1956.

McQuillin, R, Bacon, M., Barclay, W. (1984). *An Introduction to Seismic Interpretation*. Graham & Trotman Limited, 2nd Edition, 27 – 66.

Partika, G. A. (2000). Seismic attribute sensitivity to energy, bandwidth, phase and thickness. SEG Expanded Abstracts 19.

Pedersen, S., Randen, T., Sonneland, L., Steen, O. (2002). *Automatic 3D Fault Interpretation by Artificial Ants.* EAGE 64th Conference & Exhibition, Italy.

Posamentier, H. (2003). *Depositional elements associated with a basin floor channel-levee system: case study from the gulf of Mexico*. Marine and Petroleum Geology, vol. 20, 677 – 690.

Randen, T., Monsen,E., Signer, C., Abrahamsen,A., Hansen, J. O., Sæter, T., Schlaf, J., Sønneland, L. (2000). *Three-Dimensional Texture Attributes for Seismic Data Analysis*, S.E.G. Expanded Abstracts, 19.

Randen, T., Sonneland, L., Carrilat, A., Valen, T., Skov, T., Pedersen, S., Rafaelsen, B., Elvebakk, G. (2003). *Preconditioning for optimal 3D stratigraphical and structural inversion*. EAGE 65th Conference & Exhibition, Norway.

Robinson, E. A., Durrani, T. S., Peardon, L. (1986). *Geophysical Signal Processing*. Prentice – Hall, 1 – 25.

Schlumberger (2007) a. Interpreter's Guide to Seismic Attributes. 115 pp..

Schlumberger (2007) b. Seismic Visualization and Interpretation Course book. 332 pp..

Schlumberger (2008). Petrel Introduction Course book. 555 pp.

Sheline, H. E. (2005). *The Use and Abuse of Seismic Attributes*. Search and Discovery Article #40143.

Sheriff, R.E. and Geldart, L.P. (1995). Exploration Seismology, Cambridg University Press,592 pp..

Taner, M. T., Koehler, F., Sheriff, R. E. (1979). *Complex Seismic trace analysis*. Geophysics, Vol.44; No.6, 1041-1063.

Taner, M. T., Schuelke, J. S., O'Doherty, R., Baysal, E. (1994). *Seismic attributes revisited*. 64th Annual International Meeting, SEG, Expanded Abstracts, 1104 – 1106.

Taner, M. T (1997). Seismic trace attributes and their projected use in prediction of rocks properties and seismic facies. Rock Solid Images.

Taner, M. T. (2000). *Attributes Revisited*. Rock Solid Images.

Taner, M. T. (2001). *Seismic Attributes*. Canadian Society of Exploration Geophysicists Recorder, September, 49-56.

Telford, W. M.; Geldart, L. P.; Sheriff, R. E. (1990). *Applied Geophysicis*. Cambridge University Press. 2nd Edition, 136 – 280.

Trusheim, R. (1960). *Mechanism of salt migration in northern Germany*., AAPG bulletin, v. 44, no. 9, 1519 – 140.

Wynn, R. B., Cronin, B. T., Peakall, J. (2007). *Sinuous deep-water channels: Genesis, geometry and architecture*. Marine and Petroleum Geology, vol. 24, 341 – 387.

Yilmaz, O. (2001) a. *Seismic data analysis: processing, inversion, and interpretation of seismic data*. SEG, Tulsa (OK), 1 vol.

Yilmaz, O. (2001) b. *Seismic data analysis: processing, inversion, and interpretation of seismic data*. SEG, Tulsa (OK), 2 vol.

Zeng, H., Backus, M. (2005) a. *Interpretive advantages of 90^o-phase wavelets: Part 1 – Modeling*. Geophysics, Vol.7; No.3, C7 - C15.

Zeng, H., Backus, M. (2005) b. *Interpretive advantages of 90^o-phase wavelets: Part 2 – Seismic Applications*. Geophysics, Vol.7; No.3, C17 - C24.

Zeng, H., Backus, M., Barrow, K., Tyler, N. (1998) a. Stratal slicing, part I: Realistic 3-D seismic model. Geophysics, Vol. 63, 502 – 513.

Zeng, H., Backus, M., Barrow, K., Riola, J. (1998) b. Stratal slicing, part II: Real data. Geophysics, Vol. 63, 514 – 522.

Internet references

www.aug.geophys.ethz.ch:
http://www.aug.geophys.ethz.ch/teach/seismik1/06_system.pdf
commons.wikimedia.org:
http://commons.wikimedia.org/wiki/File:Airgun-array_hg.jpg
Cooper, R. (2008). The Future of Seismic Attributes. Online Webinar. http://www.rocksolidimages.com/pdf/The_Future_of_Seismic_Attributes.pdf
www.doc.ic.ac.uk:
http://www.doc.ic.ac.uk/~nd/surprise_96/journal/vol4/cs11/report.html#What%20is%20a%20Neural%20Network
en.wikipedia.org (a) - http://en.wikipedia.org/wiki/Automatic_gain_control
en.wikipedia.org (b) - http://en.wikipedia.org/wiki/Variance
www.geo.wvu.edu – http://www.geo.wvu.edu/~jtoro/Petroleum/Review%202.html
glossary.oilfield.slb.com (a)
http://www.glossary.oilfield.slb.com/Display.cfm?Term=trap
glossary.oilfield.slb.com (b)
http://www.glossary.oilfield.slb.com/Display.cfm?Term=wildcat
glossary.oilfield.slb.com (c)
http://www.glossary.oilfield.slb.com/DisplayImage.cfm?ID=230
glossary.oilfiled.slb.com (d)
http://www.glossary.oilfield.slb.com/Display.cfm?Term=normal%20moveout
glossary.oilfield.slb.com (e)
http://www.glossary.oilfield.slb.com/Display.cfm?Term=stack
www.halliburton.com
http://www.halliburton.com/ps/Default.aspx?navid=926&pageid=876&prodid=PRN%3a%3a110262578211478
hub.slb.com – Internal Schlumberger website
www.ig.utexas.edu
http://www.ig.utexas.edu/gallery/001_images/HessDeep_streamer.jpg
www.priberam.pt – http://www.priberam.pt/DLPO/default.aspx

www.seismicmicro.com

http://www.seismicmicro.com/Products/Advanced/kingdomAdvanced.html

www.slb.com (a) - http://www.slb.com/content/about/who.asp?

www.slb.com (b) - http://www.slb.com/content/about/history.asp?

www.slb.com (c) - http://www.slb.com/content/services/index_sis.asp?

www.slb.com (d)

http://www.slb.com/content/services/software/geo/Petrel/index.asp?

www-sst.unil.ch - http://www-sst.unil.ch/Research/seismic/Teaching.htm

www.statsoft.com - http://www.statsoft.com/textbook/stneunet.html#

strata.geol.sc.edu - http://strata.geol.sc.edu/

woodshole.er.usgs.gov

http://woodshole.er.usgs.gov/operations/sfmapping/airgun.htm